Understanding the role of the THIK-1 Potassium Channel in NLRP3 inflammasome activation.

A thesis submitted to the University of Manchester for the degree of Doctor of Philosophy (Ph.D.)
in the Faculty of Biology, Medicine & Health

2022

Samuel Drinkall

School of Health Sciences
Division of Pharmacy & Optometry

Table of Contents

Total word count: 30,176

List of Figures

List of Tables

Abbreviations

AD	Alzheimer's Disease
ADP	Adenosine diphosphate
AIM2	Absent in melanoma 2
ALR	Absent in melanoma 2-like receptors
APP	Amyloid precursor protein
ASC	Apoptosis-associated speck-like protein containing c-terminal caspase recruitment domain
ATP	Adenosine triphosphate
Aβ	Amyloid β
BHB	β-hydroxybuturate
BSA	Bovine serum albumin
CAPS	Cryopyrin-associated periodic syndrome
CARD	C-terminal caspase recruitment domain
CLIC	Chloride intracellular channel
CLR	C-type lectin receptors
CNS	Central nervous system
DAMP	Damage-associated molecular patterns
DFNB59	Deafness, autosomal recessive 59
DMEM	Dulbecco's Modified Eagle's Medium
DMSO	Dimethylsulfoxide
FBS	Fetal bovine serum
FISNA	Fish-specific Nacht associated domain
GSDM	Gasdermin
HMGB1	High-mobility group box 1
iBMDM	Immortalised bone marrow-derived macrophage
ICP-MS	Inductively coupled plasma mass spectrometry
IFN	Interferons
IL	Interleukin
JNK1	c-Jun N-terminal kinase 1
K2P	Two-pore domain K+ channel

KO	Knock out
LDH	Lactate dehydrogenase
LPS	Lipopolysaccharide
LRR	Leucine-rich repeat
MCAO	Middle cerebral artery occlusion
MNS	3,4-methylenedioxy-β-nitrostyrene
MSU	Monosodium urate
NBC	Novel boron compounds
NEK7	Never in mitosis gene a-related kinase 7
NF	Nuclear factor
NIMA	Never in mitosis gene a
NINJ1	Nerve injury-induced protein 1
NLR	Nucleotide-binding oligomerisation domain leucine-rich repeat receptor
NLRC4	NLR and caspase recruitment domain-containing protein 4
NLRP	NLR and pyrin domain-containing protein
NOD	Nucleotide-binding oligomerisation domain
NSAID	Non-steroidal anti-inflammatory drugs
oATP	Oxidised adenosine triphosphate
PAMP	Pathogen-associated molecular patterns
PBMC	Peripheral blood mononuclear cells
pBMDM	Primary bone marrow-derived macrophage
PD	Parkinson's disease
PenStrep	Penicillin and streptomycin
PRR	Pattern recognition receptor
PS1	Presenilin-1
PTMs	Posttranslational modifications
PYD	Pyrin domain
RIG-I	Retinoic acid-inducible gene I
RLR	RIG-I-like receptors
ROS	Reactive oxygen species

RT-qPCR	Real-time quantitative reverse transcription polymerase chain reaction
RVD	Regulatory volume decrease
TEA	Tetraethylammonium chloride
TGN	Trans-Golgi network
THIK-1	Tandem Pore Domain Halothane-Inhibited Potassium Channel 1
TLR	Toll-like receptor
TNF	Tumour necrosis factor
TNFR	Tumour necrosis factor receptor
Tpa	Tetrapentylammonium
TWIK-2	Two-pore domain Weak Inwardly rectifying K+ channel 2
UDP	Uridine diphosphate
UTP	Uridine triphosphate
VRAC	Volume-regulated anion channel
WT	Wild type

Abstract

The NLRP3 inflammasome is a multi-protein complex responsible for the activation of caspase-1 and the subsequent cleavage and activation of the potent inflammatory cytokines IL-1β and IL-18, and pyroptotic cell death. NLRP3 is implicated as a driver of inflammation in a range of diseases including neurodegenerative diseases, type 2 diabetes and atherosclerosis. A commonly reported mechanism contributing to NLRP3 inflammasome activation is potassium ion (K^+) efflux across the plasma membrane. Identification of the K^+ channels involved in NLRP3 activation remains incomplete. In this thesis, the role of the K^+ channel THIK-1 in NLRP3 activation was investigated. Pharmacological inhibitors, siRNA-induced THIK-1 gene knockdown and cells from THIK-1 knockout mice were used to assess THIK-1 contribution to macrophage, monocyte and microglial NLRP3 activation *in vitro*. Pharmacological inhibition of the THIK-1 K^+ channels inhibited caspase-1 activation in mouse bone-marrow derived macrophages (BMDMs), mixed glia, and microglia in response to NLRP3 agonists. Similarly, BMDMs and microglia from THIK-1 knockout mice had reduced NLRP3-dependent IL-1β release in response to P2X7 receptor activation with ATP. We further identified that K^+ efflux was required for caspase-1 activation, but formation of the ASC speck still occurred in the presence of K^+ channel inhibitors. In addition, THIK-1 mRNA levels were found to be elevated in post-mortem brain tissue from Alzheimer's and Parkinson's disease patients. Overall, these data suggest that the THIK-1 K^+ channel is a regulator of NLRP3 inflammasome activation in response to ATP and identify THIK-1 as a potential therapeutic target for inflammatory disease.

Declaration

No portion of the work referred to in the thesis has been submitted in support of an application for another degree or qualification of this or any other university or other institute of learning.

Copyright Statement

I. The author of this thesis (including any appendices and/or schedules to this thesis) owns certain copyright or related rights in it (the "Copyright") and he has given The University of Manchester certain rights to use such Copyright, including for administrative purposes.

II. Copies of this thesis, either in full or in extracts and whether in hard or electronic copy, may be made only in accordance with the Copyright, Designs and Patents Act 1988 (as amended) and regulations issued under it or, where appropriate, in accordance with licensing agreements which the University has from time to time. This page must form part of any such copies made.

III. The ownership of certain Copyright, patents, designs, trademarks and other intellectual property (the "Intellectual Property") and any reproductions of copyright works in the thesis, for example graphs and tables ("Reproductions"), which may be described in this thesis, may not be owned by the author and may be owned by third parties. Such Intellectual Property and Reproductions cannot and must not be made available for use without the prior written permission of the owner(s) of the relevant Intellectual Property and/or Reproductions.

IV. IV. Further information on the conditions under which disclosure, publication and commercialisation of this thesis, the Copyright and any Intellectual Property and/or Reproductions described in it may take place is available in the University IP Policy (see http://documents.manchester.ac.uk/DocuInfo.aspx?DocID=2442 0), in any relevant Thesis restriction declarations deposited in the University Library, The University Library's regulations (see http://www.library.manchester.ac.uk/about/regulations/) and in The University's policy on Presentation of Theses

Acknowledgements

First of all, I would like to thank my supervisors, Dr Michael Harte, Dr Catherine Lawrence and Prof David Brough for giving me the opportunity to complete a PhD. Together Mike, Cath and Dave provided me with everything I needed to overcome the ups and downs that accompany a PhD. Mike provided constant enthusiasm and reassured me during the most difficult times. Cath was always available to offer sound scientific and personal advice. Dave's passion for science and new data provided a fantastic driving force for my research.

I would also like to thank past and present Brough lab members. A special thanks much go to Jack Rivers-Auty, who's mentorship, support and contagious enthusiasm provided me with an exceptional role model. I would also like to thank Chris Hoyle, Jack Green and James Cook for contributing to my development and introducing me to almost every technique I know.

Thanks to all members of the Cerevance team. Not only did Cerevance provide me with a fantastic experience of industry research, they also helped push my research forward. Cerevance provided a fantastic working environment and it was a pleasure to spend 3 months with them. I would like to especially thank Dr Lee Dawson and Dr Dino Ossola for giving me the opportunity to collaborate with Cerevance. Dino went out of his way to make my trip as effective and enjoyable as possible. I am exceptionally grateful for Dino's support and friendship throughout the last year of my PhD.

Most of all, I want to acknowledge the unending support provided to me by my family and friends. My parents gave unwavering encouragement and always helped in any way they could. I have to also thank my friends Alex, Dan, George, Jordan and Tyler for reminding me that sometimes cells getting infected and dying is not the end of the world. A special thanks must go to Alice who has joined me on the final stretch of this journey and helped make this experience be the most exciting period of my life. This acknowledgment would not be complete without mentioning Darcy, who loyally sat by my side every single day during the writing of this thesis.

I also want to thank my funders the MRC.

Blank page

Chapter 1: General Introduction

1.1 Inflammation

Inflammation is the immune systems response to harmful stimuli such as pathogens, damaged cells and toxic compounds (1) and functions to remove damaging stimuli and initiate healing (2). Acute inflammatory responses initiate molecular and cellular pathways to minimize injury or infection to restore tissue homeostasis. However, uncontrolled acute inflammation can become chronic, contributing to a variety of diseases (3). Inflammation thus represents an attractive therapeutic target for limiting the pathology for a number of different diseases. Understanding the mechanisms regulating the inflammatory response is critical in order to identify novel therapeutic targets for limiting damaging inflammation.

1.2 The innate immune system

The innate immune response is the first line of defence against infection. The innate immune system functions to promote a rapid immune response against signs of infection found in the extracellular environment and subcellular compartments (4). During microbial infection, inflammation plays a key role in the clearing and containing the infection while also promoting tissue repair to restore homeostasis. Infection is a key driver of inflammation, however a diverse range of sterile stimuli such as toxins, crystals, chemicals, ischemia and mechanical trauma also trigger inflammation. Regardless of the trigger of inflammation, be that infectious or sterile the same downstream vascular and cellular mechanisms are activated. Although inflammation is extremely effective at killing microbes and fighting infection, host cells are also damaged and killed as a by-product. Since infections are typically cleared rapidly by the innate immune system, the duration of inflammation is limited resulting in minimal tissue damage. During infection, inflammation is still beneficial to the host despite tissue damage as a potential life threatening stimuli is removed (5).

However, this is not the case during sterile inflammation. The causative stimulus may offer no threat of injury to the host yet still induces the collateral tissue damage caused by inflammation. Sterile inflammation may therefore only inflict damage on healthy cells while offering no benefit to the host as there is no pathogen to kill and remove. Furthermore, if the sterile stimuli are not resolved this can lead to a chronic inflammatory response resulting in ongoing tissue damage which can

exacerbate or even cause disease. Examples in which sterile inflammation has been found to contribute to non-communicable disease pathology include atherosclerosis, Alzheimer's disease, Parkinson's disease and type-2 diabetes (6–9). Understanding the mechanisms underlying this damaging form of inflammation has become an area of intense research with the hope that greater understanding will lead to a breakthrough in therapeutic interventions.

1.3 Pattern recognition receptors

The innate immune response begins with the detection of pathogens or tissue damage via several classes of receptors termed pattern recognition receptors (PRRs) expressed by many innate immune cells including macrophages, monocytes and neutrophils. These receptors survey both the extracellular and intracellular space recognizing structures conserved among microbial species, which are called pathogen-associated molecular patterns (PAMPs) as well as endogenous agents released from damaged cells termed damage-associated molecular patterns (DAMPs).

The majority of PRRs can be classified based upon protein domain homology into one of five distinct families. The five families include Toll-like receptors (TLRs), C-type lectin receptors (CLRs), nucleotide-binding domain, leucine-rich repeat (LRR)-containing NOD-like receptors (NLRs), retinoic acid-inducible gene I (RIG-I)-like receptors (RLRs) and the absent in melanoma 2 (AIM2)-like receptors (ALRs) (10). The families can be further subdivided into two classes, membrane-bound receptors and intracellular unbound receptors. TLRs and CLRs are membrane bound receptors found within in the plasma membrane or endosomal compartments. These receptors function to detect DAMPs and PAMPs in the extracellular space and within endosomes. NLRs, RLRs and ALRs are located within the cytoplasm and detect intracellular signals. Stimulation of PRRs trigger two types of downstream signaling cascade, transcriptional and non-transcriptional. Transcriptional production of proinflammatory cytokines and interferons (IFN) are critical for initiating innate immune responses. PRRs also drive non-transcriptional responses such as phagocytosis, autophagy, cell death and cytokine processing (11–13). One critical feature of several PRRs for the processing inflammatory cytokines and induction of cell death is the formation of multi-protein complexes, termed inflammasomes. These macromolecular complexes are key drivers of inflammatory cytokine release in response to multiple DAMPs and PAMPs. However, of all the known PRRs only NLRP1, NLRP3,

NLRC4, AIM2 and pyrin have been discovered to form inflammasome complexes in response to pathogenic microorganisms and danger signals in the cytosol of cells (Figure 1.1) (14).

1.4 Inflammasomes

The inflammasome field began with a seminal paper published in 2002 which was the first to describe the inflammasome complex (15). Tschopp and colleagues identified a high molecular-weight complex present in the cytosol of stimulated immune cells that regulates inflammatory caspase activation. In the time since this discovery, our knowledge of inflammasome biology has improved substantially with a number of distinct inflammasomes having now been identified. Assembly of each inflammasome is dependent on activation of a specific PRR in response to PAMP and DAMP detection within the cytosol. In response to inflammatory stimuli, the PRRs are activated triggering oligomerization and the recruitment of the adaptor protein apoptosis-associated speck-like protein containing c-terminal caspase recruitment domain (ASC). ASC is composed of two protein-protein interaction domains: an N-terminal pyrin domain (PYD) and a C-terminal caspase recruitment domain (CARD). ASC functions via these domains to link the upstream inflammasome sensor molecules to the inflammatory caspase, caspase-1. Following recruitment of caspase-1 to ASC, proximity-induced auto processing occurs resulting in enzymatically active caspase-1 which drives the processing and release of interleukin (IL)-1 and IL-18 and induced a form of lytic cell death termed pyroptosis. Inflammasomes are now recognized to play a critical role in the host defence response against pathogens (16). However, a wide range of diseases including cancer, autoimmune, metabolic and neurodegenerative diseases are associated with dysregulated inflammasome activation.

A major advance in inflammation research came with the discovery that gain of function mutations in the NLRP3 gene resulting in constitutive NLRP3 activation cause the inherited autoinflammatory disease cryopyrin-associated periodic syndrome (CAPs) (17–19). CAPs represent a spectrum of three clinically overlapping autoinflammatory syndromes of varying severity including familial cold autoinflammatory syndrome, Muckle-Wells syndrome and neonatal-onset multisystem inflammatory disease. These findings highlighted the critical importance of NLRP3 in modulating sterile inflammation. Following findings of NLRP3's role in human monogenic autoinflammatory conditions,

NLRP3 has been shown to affect a diverse range of disease models in mice. As such NLRP3 is now the most intensely researched inflammasome due to its association with a number of both inherited and acquired inflammatory diseases. Accordingly, there is a great interest in understanding the mechanisms regulating NLRP3 in order to identify potential therapeutic targets for limiting damaging inflammation in a variety of diseases.

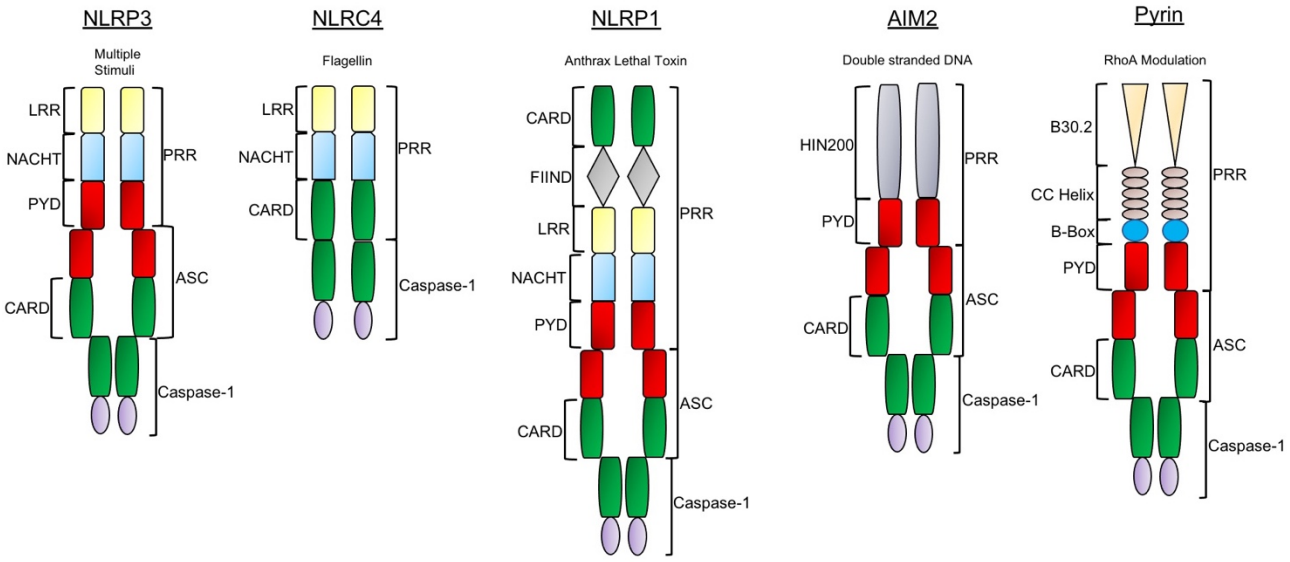

Figure 1.1 Inflammasome activators and structures.
Inflammasomes can be formed by a number of distinct PRRs. The NLRP3 inflammasome is activated by a diverse range of stimuli and is composed of a LRR domain, NACHT domain and PYD domain. Activation of NLRP3 results in the recruitment of the adaptor protein ASC which is composed of a PYD and CARD domain. ASC then recruits caspase-1 resulting in its cleavage and activation. The NLRC4 inflammasome is formed in response to detection of flagellin and is composed of an LRR, NACHT and CARD domain. The NLRP1 inflammasome is activated by anthrax lethal toxin and contains a function to find domain (FIIND), as well as CARD, LRR, NACHT and PYD domains. The AIM2 inflammasome detects double stranded DNA and is composed of a DNA-sensing HIN200 domain in addition to a PYD domain. The Pyrin inflammasome is activated by Ras homolog gene family member A (RhoA) inhibition and comprises a B30.2 domain, a central coiled-coil domain (CC), a B-box-type zinc finger domain (B-box) and a PYD domain.

1.5 NLRP3

Two separate steps are required for the activation of NLRP3 in macrophages: priming and activation (20). The initial priming step serves at least two known functions in NLRP3 inflammasome activation. Firstly, priming upregulates the expression of inflammasome components NLRP3 and pro IL-1β which are expressed at insufficient levels for inflammasome activation in resting cells. A secondary but just as important function of priming is to induce post-translational modifications of NLRP3 which stabilize NLRP3 into a state capable of activation. The secondary activation step then promotes the assembly of the NLRP3 inflammasome resulting in caspase-1 mediated IL-1β and IL-18 secretion in addition to pyroptosis. Therefore, the priming step functions to licence NLRP3 activation in the cell while the secondary step occurs in response to NLRP3 recognising an activator, inducing full activation and formation of the inflammasome generating a pro-inflammatory response.

1.5.1 NLRP3 priming

Broadly speaking, priming stimuli include any that trigger activation of the transcription factor nuclear factor (NF)-κB, such as ligands for IL-1R, TLRs, NLRs and cytokine receptors TNFR1 and TNFR2 (21, 22). For example, lipopolysaccharide (LPS) activates the cell surface receptor TLR4, which drives MyD88 and TRIF dependent signaling pathways resulting in activation of NF-κB (21). NF-κB activation is critical for upregulating the transcription of both pro IL-1β and NLRP3 (21). Pro IL-1β is not constitutively expressed and basal levels of NLRP3 are insufficient for effective signaling (23). Therefore, without transcriptional priming NLRP3 inflammasome activation would be unable to occur due to insufficient NLRP3 and pro IL-1β levels. Conversely, transcriptional upregulation is not required for other inflammasome components ASC, pro caspase-1 or pro IL-18 as they are sufficiently expressed in the steady state (21, 24, 25). In addition to pro IL-1β and NLRP3, NF-κB also induces the expression of other pro-inflammatory proteins such as IL-1α, IL-6 and tumour necrosis factor α (TNFα) (26–28). Further to this transcriptional role priming also regulates NLRP3 at the post-transcriptional level. This was first discovered by the observation that priming macrophages for only 10 minutes, which is insufficient for the induction of pro IL-1β and NLRP3 expression enhances NLRP3 inflammasome activation (25, 29). Despite transcriptional priming enhancing NLRP3 activation and being critical for IL-1β release, recent findings have shown

transcription is not required for NLRP3 activation. Co-administration of both priming and activating stimuli can activate NLRP3 independently from inducing NLRP3 protein expression (25, 29–33). Posttranslational modifications (PTMs) have been found to drive this rapid activation of NLRP3 (25, 29–33). The initial priming step licenses NLRP3 activation via ubiquination by E3 ligases and phosphorylation by c-Jun N-terminal kinase 1 (JNK1) (34, 35). These findings clearly highlight that priming facilitates NLRP3 activation through inducing expression of IL-1β and NLRP3 but also licensing actual activation of NLRP3 via PTMs.

In addition to priming induced PTMs, further modifications are also required in response to secondary activating stimuli to facilitate NLRP3 inflammasome activation. Posttranslational phosphorylation, de-ubiquination, de-SUMOylation, and acetylation are all induced by secondary stimuli and are required for inflammasome activation (35–38). Therefore, NLRP3 regulation at both the priming and activation step is extremely complicated with multiple cellular pathways tightly regulating activation. Adding further complexity, the initial priming step is dispensable for canonical NLRP3 activation in human monocytes suggesting species differences in NLRP3 activation between mouse and human myeloid cells (39). Further understanding the mechanistic differences between mouse and human NLRP3 activation will be critical in pursuing NLRP3 as a therapeutic target for human inflammatory conditions.

1.5.2 Interleukin-1

IL-1 is regarded as a master inflammatory cytokine, controlling a wide variety of innate immune responses (40). The IL-1 family consists of 11 cytokines and 10 IL-1 family receptors. More so than any other family of cytokine IL-1 family members are heavily linked with damaging inflammation (41). Two members of the IL-1 family – IL-1α and IL-1β are upregulated in response to NLRP3 priming. Both IL-1α and IL-1β signal through the major IL-1 receptor IL-1R1 and have similar biological properties (41). However, expression of IL-1β is insufficient to induce inflammatory signaling via IL-1R1 as IL-1β is expressed as an inactive precursor pro IL-1β. Cleavage and activation of pro IL-1β into its active form is dependent on inflammasome-mediated caspase-1 processing (42).

1.5.3 Canonical NLRP3 activation

The priming step of inflammasome activation licenses the cell for inflammasome activation. The secondary activation step occurs in response to recognition of NLRP3 activators inducing PTMs of NLRP3 allowing for assembly of the inflammasome and full activation. NLRP3 differs from other PRRs due to its unique ability to respond to a variety of unrelated stimuli whereas most PRRs only respond to one or a small number of related PAMPs or DAMPs. The range of stimuli capable of inducing NLRP3 activation is diverse. NLRP3 is activated by bacterial, viral and fungal infections as well as sterile stimuli. Based on the structural and chemical diversity of NLRP3 activators it is unlikely that they directly bind and activate NLRP3. A common feature shared among these stimuli is that they all result in a form of cellular stress such as mitochondrial dysfunction and reactive oxygen species production, lysosomal destabilisation, cathepsin release and potassium efflux. The mechanism by which NLRP3 senses cellular stress and which pathways are responsible for inflammasome activation remains uncertain. Research efforts have focused on trying to identify a unifying molecular mechanism of NLRP3 activation.

1.5.4 Potassium efflux

Potassium (K^+) efflux is established as a common ionic event that occurs in cells in response to most NLRP3 stimuli. Initial early studies identified the importance of K^+ efflux in NLRP3 activation through showing NLRP3 stimuli adenosine tri-phosphate (ATP) and nigericin drive K^+ efflux which is required for IL-1β processing (43). The critical role of K^+ efflux was further demonstrated by findings that triggering K^+ efflux via K^+ free media is sufficient to induce NLRP3 activation (44). Moreover, K^+ efflux was comprehensively shown to be an absolute requirement for NLRP3 activation, occurring downstream of most NLRP3 stimuli suggesting K^+ efflux to be a universal trigger of NLRP3 activation (45). Interestingly, dependence on K^+ efflux is unique to the NLRP3 inflammasome, high extracellular K^+ fails to block the NLRC4 or AIM2 inflammasome (44, 45). Therefore K^+ efflux was thought to be the specific universal trigger of NLRP3 activation. Emerging research has identified NIMA (never in mitosis gene a)-related kinase 7 (NEK7) to be an essential regulator of NLRP3 activation downstream of K^+ efflux (46, 47). NEK7 directly interacts with NLRP3 in a K^+ efflux dependent manner (46). Collectively these studies suggest NEK7 functions to bind and activate NLRP3 in

response to sensing low intracellular K^+ concentrations. More recent research suggests K^+ efflux triggers a conformational change in the protein structure of NLRP3 which promotes activation (48). Conformational changes to NLRP3 in response to K^+ efflux was dependent upon the N-terminal NLRP3 linker and fish-specific Nacht associated domain (FISNA). The NLRP6 inflammasome is not activated by K^+ efflux, yet construction of a chimeric NLRP6 receptor containing the linker-FISNA sequence resulted in responsiveness to K^+ efflux (48–50). These findings suggest the NLRP3 N-terminal linker and FISNA domain are critical for inducing conformation changes to NLRP3 which promote activation in response to K^+ efflux.

However, studies suggest K^+ efflux is not always required for NLRP3 activation. The small molecules imiquimod and CL097 have been found to activate NLRP3 independently from K^+ efflux (51). These findings suggest that potentially a further step occurs downstream of K^+ efflux to drive NLRP3 activation and these molecules directly activate this step and thus bypass K^+ efflux. Alternatively, K^+ efflux independent pathways may exist for NLRP3 activation. In addition, introduction of mutant NLRP3 ($NLRP3^{R258W}$) which is the gene equivalent to the human mutation in Muckle-Wells syndrome into mouse macrophages results in NLRP3 activation independently of K^+ efflux (52). These studies suggest K^+ efflux is sufficient but not necessary for activation of the NLRP3 inflammasome.

The findings that K^+ efflux is necessary and sufficient for NLRP3 activation in most cases has sparked interest in discovering the molecular mechanisms underlying K^+ efflux. Identification of the K^+ ion channels involved in K^+ efflux could potentially highlight novel therapeutic targets for dysregulated NLRP3 inflammasome activation.

1.5.4.1 Purinergic receptors

ATP was the first endogenous molecule found to induce caspase-1 activation and IL-1β cleavage (53). Later ATP activation of the purinergic receptor P2X7 was discovered to drive K+ efflux and subsequent NLRP3 activation (43, 54, 55). P2X receptors are cation selective, ionotropic receptors which respond exclusively to ATP binding. The P2X7 receptor belongs to a family of 7 P2X receptors which are all K^+ permeable. Of all P2X receptors, P2X7 displays the greatest ion conductance, facilitating an ion channel current which allows for the continuous flow of K^+ and other cations (56). Sustained activation of P2X7 is associated with the opening of hemichannels which further

permeabilize the plasma membrane resulting in significant K^+ efflux. The *In* vivo relevance of these findings was questioned *as* ATP only have a short half-life and high concentrations (mM range) are required for P2X7 activation (57). However, high levels of ATP have been observed *in vivo* to correlate with areas of inflammation suggesting ATP reaches sufficient concentrations to activate P2X7 *in vivo* (58, 59).

In addition to P2X7, P2X1 and P2X4 are also expressed by macrophages and evidence suggests P2X4 may contribute to NLPR3 activation through interaction with P2X7 (60, 61). Furthermore, additional studies suggest P2X4 activation alone is a distinct pathway of NLRP3 activation (62). In contrast, P2X4 deficiency was found to have no effect on ATP-induced NLRP3 activation (58). P2X4 deficiency results in reduced P2X7 expression which could which could explain the mechanism by which P2X7 is impacting NLRP3 activation (63).

The P2Y receptors represent an additional family of purinergic receptors associated with NLRP3 activation. P2Y receptors are metabotropic receptors within the G-protein-coupled receptor family (64). ATP in addition to several other nucleotides such as adenosine diphosphate (ADP), Uridine triphosphate (UTP) and uridine diphosphate (UDP) activate P2Y receptors. Activation of P2Y receptors triggers phospholipase c activation resulting in Ca^{2+} efflux. Pharmacological inhibition of P2Y1 interferes with NLRP3 mRNA expression in epithelial cells suggesting P2Y1 may contribute to NLRP3 priming (65). Furthermore, a P2Y1 antagonist decreased nano particle induced NLRP3 activation in response to some but not all nano particles tested (66). However, the impact of P2Y1 deficiency on NLRP3 priming or activation was not investigated within these studies. The observed effects with P2Y1 inhibitors and antagonists may be due to “off target” effects independent of P2Y1. Providing additional support to the existing data suggesting P2Y receptors regulate NLRP3 activation was the findings that ADP and UTP trigger NLRP3 activation via P2Y receptor activation (67). Although the data suggests P2Y receptors play a role in NLRP3 activation, the mechanism by which P2Y regulates NLRP3 activation remains inconclusive. A potential mechanism of P2Y receptor mediated activation of NLRP3 activation is through the gating of K^+ channels and thus regulation of K^+ currents. A recent study identified ADP to activate P2Y12 which in turn promotes the opening of the two-pore domain K^+ channel (K2P) THIK-1 which induces K^+ efflux and subsequent IL-1β release

in hippocampal slices (68). P2Y receptors may therefore regulate NLRP3 activation indirectly via modulating the activity of K^+ channels such as K2P and therefore regulating K^+ efflux.

1.5.4.2 Two pore domain potassium channels

K2P channels represent a superfamily of 15 members which are broadly divided into six different subfamilies based upon their biophysical, pharmacological and functional properties (69–73). The families are composed of TWIK-1, TWIK-2 and TWIK-3 (weak inward rectifying channels), THIK-1 and THIK-2 (halothane inhibited channels), TALK-1, TALK-2 and TASK-2 (alkaline sensitive channels) and TRESK (fatty acid inhibited calcium activated channel). K2P channels are spontaneously active and facilitate outwardly rectifying 'leak' background K^+ currents which maintain cellular resting potential (69, 74). K2P channels are activated by a range of biophysical stimuli such as pH, temperature and mechanical pressure in addition to being modulated by G protein signaling pathways and second messenger systems (69–72, 75, 76). K2P channels play a prominent role in many physiological processes and have been implicated in a number of diseases including autoimmune and degenerative diseases (77). Recent studies suggest K2P channels play a role in NLRP3 and innate immunity (68, 78).

TWIK-2 is a channel highly expressed in the immune system in addition to the gastrointestinal tract and blood vessels (79). Despite this its physiological function remains poorly characterised (80). However, a recent study identified a novel role for TWIK-2 in the regulation of NLRP3 activation (78). Pharmacological inhibition and genetic knockdown of TWIK-2 reduced ATP-induced NLRP3 activation and subsequent IL-1β release in macrophages. The study suggests TWIK-2 functions in cooperation with P2X7 to induce NLRP3 activation, with TWIK-2 facilitating K^+ efflux downstream of P2X7 activation by ATP. TWIK-2 did not regulate NLRP3 activation in response to P2X7 independent stimuli imiquimod and nigericin suggesting TWIK-2's function is specifically tied to activation of P2X7. In addition to TWIK-2, THIK-1 another K2P channel is also associated with ATP-induced IL-1β release in hippocampal brain slices (68). Genetic knockdown of THIK-1 resulted in depolarisation of microglia, decreased microglial ramification, reduced microglia surveillance and reduced IL-1β release in response to ATP. The authors hypothesize P2Y12 is activated in response to ADP which is converted extracellularly from ATP by the ecto-ATPase CD39. They propose P2Y12

then enhances THIK-1 channel activity resulting in K^+ efflux and NLRP3 activation. Whether THIK-1 also regulates NLRP3 activation in response to purinergic independent stimuli or is required for activation of NLRP3 in peripheral immune cells remains unknown. However, both of these findings suggest K2P channels specifically play a role in ATP-induced NLRP3 activation by facilitating K^+ efflux in response to purinergic receptor activation.

1.5.5 Chloride efflux

The role of chloride (Cl^-) in NLRP3 activation was first proposed by the findings that decreasing extracellular Cl^- enhances ATP-induced IL-1β release (81). Following on from this finding multiple studies demonstrate NLRP3 but not AIM2 or NLRC4 inflammasome activation can be inhibited by a range of Cl^- channel inhibitors (82–84). In support of a role of Cl^- in NLRP3 activation decreased intracellular occurs during NLRP3 activation (82, 84). Furthermore, incubation of macrophages with Cl^- free medium, which drives Cl^- efflux is sufficient to induce NLRP3 activation (82). Two types of anion channel have been found to facilitate Cl^- efflux during NLRP3 activation: volume-regulated anion channel (VRAC) (83, 85) and the chloride intracellular channel (CLIC) protein family (82, 86).

The role of volume-regulated responses was first discovered in 1996 by Perregaux and colleagues who demonstrated that hypotonic shock induced IL-1β release from LPS-primed human monocytes (87). Over a decade later it was discovered that hypotonicity induced the release of IL-1β via activation of the NLRP3 inflammasome (83). Activation was linked to a regulatory volume decrease (RVD) which reduces cell volume in response to hypo-osmolarity-induced cell swelling. NPPB, a blocker of volume activated Cl^- channels was found to prevent RVD and inflammasome activation without impacting K^+ currents suggesting a role of Cl^- efflux in NLRP3 activation during RVD (83). Further evidence to suggest a role of Cl^- channels in NLRP3 activation was the finding that fenamate non-steroidal anti-inflammatory drugs (NSAIDs) could inhibit canonical NLRP3 activation by blocking a Cl^- channel which was proposed to be VRAC (84). A more recent study found pharmacological inhibition and genetic knockout of VRAC inhibited NLRP3 activation in response to hypotonicity and not activation in response to other canonical stimuli (85). Together these studies suggest the Cl^- channel VRAC regulates NLRP3 activation in response to hypotonic shock.

In addition to VRAC, CLIC channels are also associated with NLRP3 activation (82, 86). Knockdown of several CLIC family members was found to inhibit NLRP3 activation (82). Tang and colleagues proposed a mechanism in which NLRP3 agonists induce K^+ efflux resulting in generation of mitochondrial reactive oxygen species which induce localization of CLIC channels to the plasma membrane resulting in Cl^- efflux and subsequent NLRP3 activation (82). However, an additional study demonstrated CLIC1 and CLIC4 localize to the plasma membrane after NLRP3 priming but regulate NLRP3 activation at the secondary activation step of inflammasome activation (86). Evidence therefore suggests Cl^- efflux plays an important role in NLRP3 inflammasome activation. Multiple Cl^- channels are associated with NLRP3 activation, however the specific Cl^- channels regulating NLRP3 activation depend upon the type of NLRP3 stimulus. Research suggests not just one Cl^- channel is universally responsible for Cl^- efflux in NLRP3 activation but different channels regulating Cl^- ion fluxes dependent upon the context of inflammasome activation.

1.5.6 Potassium and Chloride co-regulation of NLRP3 activation

Both K^+ and Cl^- ions have been shown to play an important role in NLRP3 inflammasome activation. Recent research suggests K^+ efflux and Cl^- efflux regulate different stages of inflammasome activation. One study investigating the impact of blocking both Cl^- and K^+ efflux independently found Cl^- efflux is required for NLRP3-dependent oligomerization of ASC (88). However, Cl^- efflux in the absence of K^+ efflux drove ASC speck formation without the downstream activation of caspase-1 and IL-1β release. K^+ efflux was required to permit activation of the NLRP3 inflammasome via inducing NEK7-NLRP3 interaction.

1.5.7 Trans-Golgi Network Dispersal and NLRP3 activation

Identification of K^+ efflux-independent mechanisms of NLRP3 activation has resulted in no currently accepted universal mechanism for NLRP3 activation in all contexts. However, a recent study found both K^+ efflux dependent and independent NLRP3 stimuli drive dispersal of the trans-Golgi network (TGN) (89). The dispersed TGN then recruits NLRP3 via interaction between the polybasic motif of NLRP3 and phosphatidylinositol-4-phosphate on the Golgi resulting in oligomerization of NLRP3 and ASC resulting in inflammasome formation. Dispersal of the TGN may therefore represent a universal

mechanism by which the diverse range of NLRP3 agonists converge, however, how stimuli induce TGN dispersal remains unclear. Understanding the cellular pathways by which both K^+ efflux dependent and independent NLRP3 stimuli induce TGN dispersal will provide useful insight into the mechanisms regulating NLRP3 activation.

The dispersed TGN therefore serves as a scaffold in which NLRP3 activation is initiated, resulting in the formation of the inflammasome complex, which serves as a platform for caspase-1 recruitment and activation. NLRP3 is made up of three domains: a pyrin death-fold domain (PYD) which is located at the N-terminus and interacts with the homologous domains of the adaptor protein ASC, a NACHT domain required for ATP hydrolysis and protein oligomerization and a C-terminal LRR-sequence which interacts with NEK7 (46). Following activation of NLRP3, ASC molecules are recruited to NLRP3 via PYD-PYD interactions. ASC recruitment induced oligomerization into filamentous structures in a prion-like manner to form an ASC speck (90–92). The ASC speck functions as a macromolecular platform in which the inactive precursor pro-caspase-1 is recruited via CARD-CARD domain interactions resulting in proximity-induced autocleavage and activation of caspase-1 (93). The major active form of caspase-1 has been identified as the transiently active dimer composed of P33/P10 subunits (93). The active p33/p10 species further undergoes self-limiting autoprocessing to a p20/p10 dimer which triggers the release of caspase-1 from the inflammasome complex and thus stopping its enzymatic activity (93).

1.5.8 Non-canonical and alternative NLRP3 activation

The term “non-canonical inflammasomes” was first used in a seminal study to describe the observation that caspase-11 in mice (caspase 4/5 orthologs in humans) is activated by a mechanism independent from the canonical pathway of inflammasome activation (94). During non-canonical signaling caspase-11 acts as a direct sensor of cytosolic LPS from Gram-negative bacteria (95). Following priming, which also induces the upregulation of caspase-11 in addition to pro-IL-1β and NLRP3, intracellular LPS can bind and activate caspase-11 in the cytosol, bypassing membrane bound TLR4 activation thus caspase-11 specifically responds to pathogens within the cytosol (96, 97). Once activated by LPS, caspase-11 cleaves gasdermin D (GSDMD) resulting in K^+ efflux from the cell through GSDMD pores which then activates the NLRP3 inflammasome and subsequent

caspase-1 activation and IL-1β secretion (98–101). K^+ efflux is therefore suggested to be a common requirement for both canonical and non-canonical NLRP3 inflammasome activation (102). Non-canonical NLRP3 activation therefore demonstrates a mechanism by which extracellular LPS can act as a priming signal and intracellular LPS a secondary NLRP3 activating stimuli.

It is well established that classical (canonical and non-canonical) NLRP3 activation requires a two-step activation mechanism. However, in human monocytes LPS alone is sufficient to induce both priming and inflammasome activation thus bypassing the need for a secondary activation stimulus (103, 104). This new type of inflammasome activation was named alternative inflammasome activation and is induced solely through the TLR4 signaling pathway (104). In alternative activation, LPS activation of TLR4 signaling via TRIF results in RIPK-1-FADD-caspase-8 signaling (105). Caspase-8 then activates NLRP3, however the exact mechanisms by which this occurs remains elusive (106). Alternative activation differs from classical activation in a number of ways including, non-dependency on K^+ efflux, absence of ASC speck formation and lack of pyroptosis. Furthermore, alternative inflammasome activation appears to be species specific as it is not observed in murine cells but is in both human and porcine monocytes (104, 107). Further studies are required to identify how caspase-8 activates NLRP3 and also the role alternative inflammasome activation plays physiologically and during disease states. A recent study found apolipoprotein C3 activates caspase-8-dependent alternative NLRP3 inflammasome activation in human monocytes, promoting organ injury in an *in vivo* model (108). This study suggests alternative NLRP3 inflammasome activation is of pathophysiological importance, contributing to damaging inflammation under certain conditions. Therefore, understanding the mechanisms underlying alternative inflammasome activation may allow for the development of specific treatments targeting conditions associated with alternative inflammasome activation.

1.6 IL-1β release and pyroptosis

In its active form caspase-1 cleaves pro-IL-1β and pro-IL-18 into their mature forms which are secreted from the cell, in addition, caspase-1 also induces a form of pyroptotic cell death (Fig. 1.2) (21). Pyroptosis is characterised by the rupturing of the plasma membrane and the release of DAMPs such as high-mobility group box 1 (HMGB1) and lactate dehydrogenase (LDH) which promote and amplify inflammatory responses (109–112). In addition to enhancing inflammatory responses through the release of DAMPs it may also serve a beneficial function to the host by removing the replicative niche of intracellular pathogens following infection therefore reducing pathogen propagation (113, 114) Furthermore, viable bacteria expelled from the intracellular space are trapped by pore-induced cellular traps created following pyroptosis which drive the recruitment and efferocytosis of pathogens by neutrophils (115) while also driving a rapid innate immune response through the secretion of proinflammatory cytokines (109). Pyroptosis thus is a critical component of the innate immune system, contributing to the removal of invading pathogens.

Despite inflammasome activation, pyroptosis and IL-1β secretion being closely associated, the mechanism of IL-1β release remained unclear until the pore-forming protein GSDMD was identified (99, 116). GSDMD is a direct substrate of caspase-1 and cleavage of GSDMD generates a N-terminal fragment which translocate to the plasma membrane and forms pores in the membrane to induce IL-1β release and eventually pyroptosis (117, 118). These initial findings suggested that GSDMD triggers both pyroptosis and IL-1β secretion. However, this paradigm was called into question through the discovery that GSDMD can mediate IL-1β release independently from inducing pyroptotic cell death suggesting GSDMD pores can form in the absence of pyroptosis to facilitate IL-1β release (119). Furthermore, in murine neutrophils NLRP3 activation and caspase-1 dependent release of IL-1β can occur in the absence of pyroptosis through GSDMD-dependent and independent mechanisms (120–122). These studies indicated pyroptosis and IL-1β may be separate and distinguishable events. Recent findings have provided more evidence to suggest GSDMD is not a direct facilitator of pyroptotic cell death. Although GSDMD is required for IL-1β and HMGB1 secretion in response to inflammasome activation, the GSDMD pore does not directly facilitate plasma membrane rupture and the secretion of HMGB1 (123). Release of HMGB1 in response to inflammasome activation is dependent upon disruption of plasma membrane integrity (124). A recent

study confirmed these findings that GSDMD is not directly responsible for plasma membrane rupture during pyroptosis by identifying nerve injury-induced protein 1 (NINJ1), a transmembrane protein found to be essential for plasma membrane rupture following induction of pyroptosis (123). Depletion of NINJ1 in macrophages inhibited the release of HMGB1 and LDH in response to inflammasome activation suggesting NINJ1 is required for pyroptosis-related plasma membrane rupture (123). This study confirms GSDMD-driven cell death and IL-1β release are distinct separate events from plasma membrane rupture and DAMP release. Supporting the hypothesis that plasma membrane rupture is an event likely to occur after cell death (125, 126).

A recent study found GSDMD pores allow the preferential passage of mature IL-1β and IL-18 over their inactive pro forms (127). GSDMD was found to be predominantly negatively charged (127), and repel IL-1 precursors which have an acidic domain (122). The acidic domain is proteolytically cleaved and removed by caspase-1 which then allows mature cytokines to pass through the GSDMD pore which suggests GSDMD mediated IL-1β release by electrostatic filtering. Together these findings suggest IL-1β release is not intrinsically linked to pyroptosis but is dependent on GSDMD pores in the membrane functioning as a conduit for release.

1.6.1 Other members of the gasdermin family

Due to GSDMD being the first executor of pyroptosis to be discovered it has received intense interest within the inflammasome field. However, the GSDM family in human is composed of 6 members: GSDMA-E and deafness, autosomal recessive 59 (DFNB59) (128). Except for DFNB59, GSDM members have an auto-inhibited two-domain architecture that consists of a cytotoxic N-terminal domain and a C-terminal repressor domain connected by a linker domain (118). However, regulation of GSDM activation is not universal, only GSDMD contains a caspase-1 cleavage site in its linker region and thus is the only GSDM regulated by caspase-1 activation (128). GSDME for example is activated through cleavage by caspase-3 during chemotherapy inducing pyroptosis in epithelial cells (129, 130). In addition to GSDMD and GSDME, the N-terminal domain of GSDMA, GSDMB and GSDMC are all associated with membrane pore formation and pyroptosis (118). Although GSDMD regulates caspase-1 mediated IL-1β release and pyroptosis, research is beginning to emerge to

suggest other members of the GSDM family play important roles in regulating inflammatory cell death.

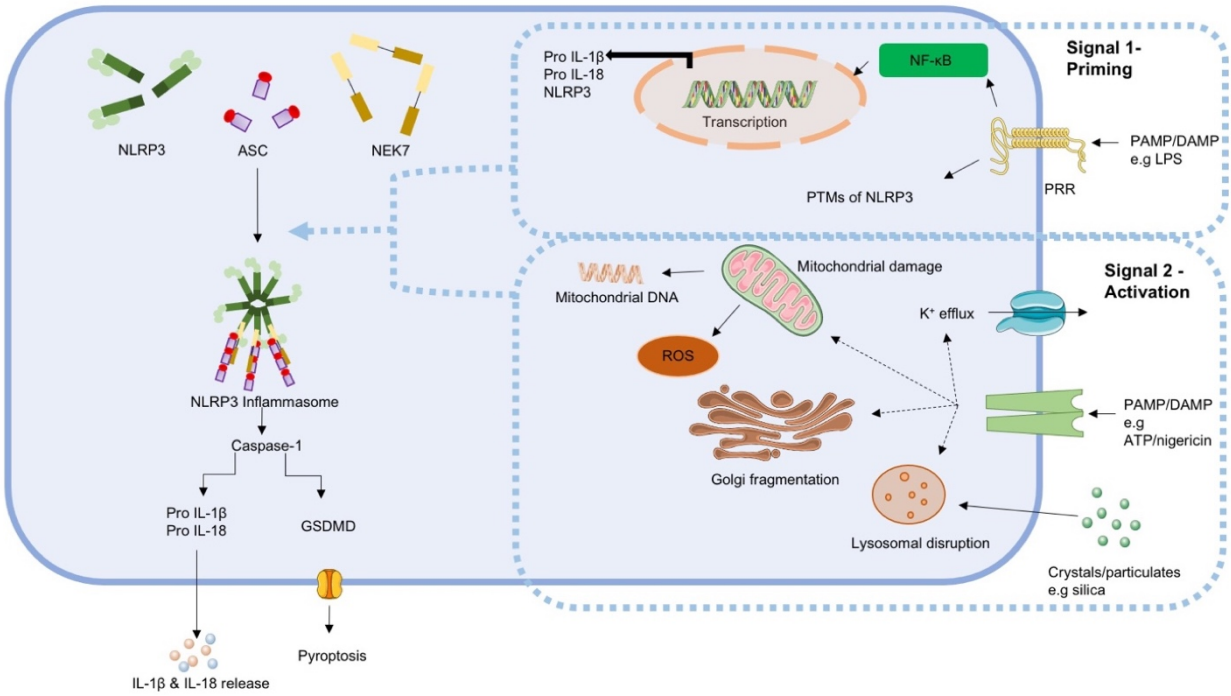

Figure 1.2 Canonical NLRP3 activation.
Activation of NLRP3 requires an initial priming step which is triggered by the binding of PAMPs and DAMPs, such as LPS to PRRs, triggering NF-κB dependent transcription of NLRP3, pro IL-1β and pro IL-18. Priming also triggers PTMs of NLRP3 enabling rapid NLRP3 regulation. Additionally, PAMPs and DAMPs such as extracellular ATP and nigericin, or crystals/particulates such as silica act as secondary NLRP3 activating signals. This triggers numerous intracellular events, including K^+ efflux, lysosomal disruption, dispersal of the trans-Golgi network and mitochondrial damage leading to the release of mitochondrial DNA and the production of reactive oxygen species (ROS). In response to priming and activation, NLRP3 undergoes oligomerization resulting in the recruitment of ASC which triggers the formation of the ASC speck and the recruitment of pro caspase-1. NEK7 is also recruited to the inflammasome complex and functions to mediate interactions between NLRP3 subunits. Pro caspase-1 then undergoes auto-catalytic self-cleavage resulting in caspase-1 activation. Active caspase-1 then cleaves pro IL-1β, pro IL-18 and GSDMD. Mature IL-1β and IL-18 are released from the cell and cleaved GSDMD inserts into the cell membrane to from pores which drive pyroptotic cell death.

1.7 NLRP3 in disease

NLRP3 is thought to provide a beneficial response to infection early in life, and when considering the diverse range of damage-related stimuli detected by NLRP3, it likely evolved to initiate immune responses to tissue damage. Although NLRP3 serves a beneficial function in the detection and removal of pathogens, it is considered a contributor to non-communicable diseases that arise in ageing populations. A common feature among many diseases associated with ageing is chronic inflammation occurring in response to the accumulation of sterile stimuli in tissue. As the primary sensor of sterile stimuli, NLRP3 is considered a key driver of damaging chronic inflammation in a diverse range of diseases and conditions.

1.7.1 CAPS

NLRP3 was first discovered following the findings that point mutations of NLRP3 which result in constitutive activation of the NLRP3 inflammasome drive CAPS as previously mentioned (17–19). Clinically CAPS are characterised by fever, chronic pain, fatigue and elevated levels of NLRP3 inflammasome components in the blood (131). CAPS symptoms are believed to occur as a consequence of elevated pro-inflammatory IL-1β and IL-18 cytokines and subsequent inflammatory responses. Isolated unstimulated monocytes and macrophages from CAPS patients have high basal levels of IL-1β secretion (132). Furthermore, expression levels of IL-1β and IL-18 have been found to correlate with tissue damage in CAPS patients, and the same pattern can be observed in mice expressing CAPS-associated mutations (133). The clinical and non-clinical research suggesting IL-1β is playing a pathogenic role in CAPS is strongly supported by the clinical effectiveness of anti-IL-1β therapies. Available effective IL-1β therapies for CAPS patients are the IL-1β antagonist anakinra (134), the IL-1β neutralising antibody, cankinumab (135) and the IL-1β decoy receptor, rilonacept (136) demonstrating the role of IL-1β signaling in CAPS disease pathology.

1.7.2 Metabolic disorders

NLRP3 was first discovered as a complex capable of detecting infection and regulating inflammation. More recently, NLRP3 has been suggested as a sensor of metabolic danger and cellular stress (137).

NLRP3 activation is now associated with multiple metabolic diseases including atherosclerosis, gout and type-2 diabetes (138).

Cardiovascular diseases which cover multiple disorders of the heart and vasculature represent the leading cause of death worldwide (139). Myocardial infarction and cerebral infarction which are responsible for the majority of cardiovascular disease deaths are caused in most cases by atherothrombic blockage of blood vessels. Atherosclerosis is characterised by the deposition of fatty substances and cholesterol resulting in the formation of plaques within the inner walls of arteries and immune cell infiltration. NLRP3 is highly expressed in human atherosclerotic plaques and multiple sterile stimuli associated with atherosclerosis drive NLRP3 priming and activation (140, 141). Cholesterol crystals which represent a hallmark of advanced atherosclerotic plaques stimulate NLRP3 inflammasome formation and subsequent IL-1β release in both human and murine macrophages via lysosomal destabilisation (6, 142). Furthermore, oxidised low-density lipoprotein cholesterol which is considered a major risk factor of atherosclerosis induced NF-κB signaling and NLRP3 inflammasome priming in macrophages (143). These studies suggest danger signals implicated in atherosclerosis development induce NLRP3 inflammasome activation. Several *in vivo* studies provide further evidence of a role of NLRP3 in atherogenisis. For example, diet-induced atherosclerosis was impaired by silencing NLRP3 expression in mice (144). In addition, it was recently reported that NLRP3 activation is triggered by a western diet during early atherogensis before plaque burden can be observed, with NLRP3 deficient mice developing significantly smaller atherosclerotic lesions (145). Epidemiology studies also provide indirect evidence for a role of NLRP3 in atherosclerosis. Patients with coronary atherosclerosis have high aortic NLRP3 expression with expression of NLRP3 found to correlate with disease severity (146). Furthermore, NLRP3, ASC, caspase-1, IL-1β and IL-18 expression is significantly higher in human atherosclerotic plague tissue (140, 141). Increasing experimental research and epidemiological studies are supporting a critical role of NLRP3 in atherosclerosis and cardiovascular disease.

Gout is a common form of inflammatory arthritis initiated by the formation of monosodium urate (MSU) crystals within joints and other tissues resulting in sudden bouts of joint inflammation and pain (147). PRRs such as TLRs bind MSU crystals triggering phagocytosis by resident macrophages

(148, 149). Intracellular MSU crystals can then activate NLRP3 *in vitro* and *in vivo* potentially via inducing lysosomal damage (150). A hallmark of a gout-induced inflammatory episode is the influx of neutrophils into joint fluid. NLRP3 deficient mice show impaired neutrophil influx in response to MSU injection, suggesting NLRP3 is a driver of MSU-induced inflammation in gout (150).

NLRP3 and IL-1β are also suggested to play a role in chronic inflammation associated with obesity and development of insulin resistance and type-2 diabetes (151–153). Obesity results in the generation of a number of DAMPs and organelle stress responses capable of inducing NLRP3 inflammasome activation such as lipotoxic lipids, mitochondrial dysfunction, generation of reactive oxygen species and ATP release from necrotic adipocytes (138). Activation of the NLRP3 inflammasome has been observed to impair adipocyte differentiation, in addition to insulin signaling, resulting in the development of insulin resistance, the hallmark of type-2 diabetes (152, 154). Furthermore, IL-1β is considered to be an important driver of pathogenesis in type-2 diabetes contributing to the loss of β cells which are responsible for insulin secretion required for regulating glucose levels in the blood (152, 155). The role of IL-1β in type-2 diabetes is further supported by clinical data showing IL-1β antagonists improve glycaemic control and increase β cell mass in type-2 diabetes patients (156).

1.7.3 Central nervous system disease

Neuroinflammation is a fundamental innate immune response of the central nervous system (CNS) by which the brain and spinal cord respond to pathogens and signals of cellular damage. Although inflammatory responses within the CNS are required for the elimination of invading pathogens, removal of damaged cells and facilitation of tissue repair (157–161) dysregulated inflammation in the CNS can exacerbate tissue damage and lead to neuronal dysfunction (162–164). Thus, neuroinflammation is known to contribute to a range of brain pathologies including neurodegenerative diseases and also psychiatric disorders. Therefore, neuroinflammation represents a promising therapeutic target for treating a diverse range of CNS diseases.

Microglia and astrocytes represent the two main cellular regulators of inflammation within the CNS (165, 166). Microglia are the resident macrophage-like innate immune cells within the CNS, derived

during early-stage embryonic development from yolk-sac myeloid progenitors (167). They continually survey and monitor their surroundings for signs of infection or tissue damage while also playing an active role in CNS development, neuroprotection and maintenance of brain homeostasis (168, 169). Microglia, like peripheral immune cells express numerous PRRs including NLRP3 and are considered the first responders to pathogenic insults within the CNS (10, 170–174). In their resting state, microglia exhibit a highly ramified appearance. However, upon detection of damaging stimuli such as brain injury, infection or protein aggregation microglia rapidly undergo activation which is characterised by transformation into an amoeboid appearance, microglial proliferation and migration of microglia to insult sight (175–177). Controlled microglia responses are generally considered beneficial to the host and serve a protective function within the CNS (178). However, overactivation can promote neuroinflammation and neuronal dysfunction via excess production of pro-inflammatory cytokines such as TNFα, IL-1β, IL-18 and IL-6 in addition to cytotoxic reactive oxygen species and nitric oxide (169, 179, 180). Consistent with the findings that microglia are key drivers of excessive neuroinflammation, microglia have been found to initiate and maintain inflammatory responses during infectious brain diseases, CNS injury and multiple neurodegenerative diseases (181–187). NLRP3 inflammasome activation appears to be an important driver of microglial inflammatory responses during pathology (188).

NLRP3 was the first inflammasome to be studied in the brain and is predominantly expressed by microglia which also exhibit strong expression of other inflammasome components ASC, caspase-1, GSDMD and IL-1β (189, 190). In microglia, similar to the peripheral immune system, activation of the NLRP3 inflammasome requires a priming step mediated by an innate immune or cytokine receptor, followed by a secondary activation signal which drives NLRP3 assembly and activation (191). Within the brain multiple different stimuli present during disease have been identified to induce NLRP3 activation including but not limited to amyloid-β (Aβ) (192), ATP (193, 194) and α-synuclein (195, 196). Although NLRP3 is the most intensively studied inflammasome in the CNS, it is important to note that other inflammasomes such as NLRP1, NLRP2, NLRC4 and AIM2 have also been associated with neurodegenerative disease (191). However, the focus of this section will be the role of NLRP3 in CNS disease.

1.7.3.1 Alzheimer's disease

Alzheimer's disease (AD) is the most prevalent neurodegenerative disease and the most prominently studied in regard to inflammasome biology, with an increasing number of studies implicating microglia driven inflammation with AD progression (197, 198). AD is characterised by the deposition of (Aβ) plaques and the presence of intraneuronal neurofibrillary tangles consisting of hyperphosphorylated tau, both of which serve as DAMPs known to induce microglial activation (199, 200). Aβ can be cleared from the brain by removal into the cerebral spinal fluid or blood vessels and microglial phagocytosis and degradation (201). However, if the rate of Aβ production exceeds the rate of removal, Aβ concentrations rise to reach a critical threshold resulting in oligomers and fibril formation which deposit into Aβ plagues within the brain.

The first evidence suggesting microglial NLRP3 is important in AD was published in 2008, when Halle *et al* observed Aβ fibrils to activate microglial NLRP3 activation, caspase-1 cleavage and IL-1β secretion *in vitro* (192). A seminal study confirmed these findings and established NLRP3 as a key driver of AD pathology (202). Amyloid precursor protein (APP)/presenilin-1 (PS1) transgenic mouse models of AD were crossed with NLRP3 deficient mice to study the impact of NLRP3 on AD pathology. The depletion of NLRP3 completely protected against AD-associated memory deficits and reduced caspase-1 activation and IL-1β release. Furthermore, removal of NLRP3 reduced Aβ plaque burden potentially through enhancing the ability of microglia to clear plaques. In addition, the same study demonstrated caspase-1 activation was increased in brain samples from human AD patients in comparison to non-demented age-matched controls. Caspase-1 activation was observed in patients displaying mild cognitive impairment early in AD progression and also early onset AD patients suggesting NLRP3 inflammasome activation occurs early in AD progression. Later work, revealed an additional mechanism by which NLRP3 activation potentially contributes to AD pathology, through promoting the seeding and spreading Aβ plaques (203). Microglial ASC specks generated in response to Aβ activation of NLRP3 are released into the extracellular space and can cross-seed Aβ plaques potentially propagating Aβ pathology. This study suggests NLRP3 activation could potentially drive AD pathology independently of IL-1β release through the generation and release of ASC specks. However, it is likely that both ASC speck seeding of plaques and IL-1β release in response to NLRP3 activation both are contributors to AD pathology.

Following the discovery that NLRP3 plays a key role in AD pathology, multiple studies have confirmed these findings through demonstrating pharmacological inhibition of NLRP3 activation is protective in AD models. Fenamate NSAIDs were found to be inhibitors of NLRP3 activation and when administered to 3xTg mouse models of AD, reversed memory deficits and reduced neuroinflammation (84). Moreover, intraperitoneal injection of APP/PS1 AD model mice with the selective NLRP3 inhibitor MCC950 (204) reduced NLRP3 activation and microglial activation while also reducing Aβ accumulation and improving cognitive function (205). Recently, OLT1177, a specific inhibitor of NLRP3, when incorporated into the diet of APP/PS1 mice improved learning and memory, restored synaptic plasticity, reduced Aβ plaque load and reduced glial cell activation (206). Together these studies strongly support a detrimental role of NLRP3 in AD pathology. Further supporting this, recent studies have identified microglial NLRP3 activation to exacerbate tau pathology, an additional hallmark of AD (207, 208). NLRP3 activation in response to Aβ within the brain of AD patients therefore appears to be an early driver of AD pathology driving damaging neuroinflammation, Aβ pathology and tau pathology ultimately leading to neuronal dysfunction and cognitive decline.

1.7.3.2 Parkinson's disease

Parkinson's disease (PD)is the second most common neurodegenerative disease behind AD and is characterised by the loss of dopaminergic neurons in the substantia nigra and presence of Lewy bodies formed from the aggregation of α-synuclein. In a similar fashion to Aβ, fibrillar α-synuclein has been found to activate NLRP3 inflammasome activation in microglia (209). Activation of NLRP3 is dependent upon phagocytosis of α-synuclein, production of reactive oxygen species, and release of cathepsin B (195, 196, 210). In post-mortem PD brain tissue and multiple animal models of PD elevated levels of activated caspase-1 and ASC were observed while NLRP3 and ASC were also upregulated in microglia (209). Earlier studies also found elevated levels of IL-1β within the cerebral spinal fluid of PD patients (211). Together these studies suggest NLRP3-induced inflammation may contribute to PD pathology.

In support of these findings a study identified a rare NLRP3 polymorphism to be statistically associated with a decreased risk of PD (212). The single nucleotide polymorphism rs7525979 associated with decreased PD risk was observed *in vitro* to impair NLRP3 translation, resulting in

the accumulation of ubiquinated, insoluble NLRP3, a protein state which is consistent with protein inactivation (213). These findings suggest reducing the activation of NLRP3 can decrease the risk of PD development therefore providing further evidence for a role of NLRP3 in PD pathology.

1.7.3.3 Stroke

Stroke is a life-threatening condition caused by a lack of blood supply to the brain. There are two clinical causes of stroke, either the occlusion of cerebral arteries (ischaemic) or rupturing of cerebral blood vessels (haemorrhagic). Both forms of stroke result in oxygen deprivation, neuronal death and the rapid production and secretion of DAMPs (214). Evidence suggests that inflammation and IL-1 play a critical role in the pathogenesis of stroke (215). IL-1 was first implicated with stroke pathology in the 1990s, when peripheral and central administration of recombinant IL-1 receptor antagonist (IL-1Ra) was found to be protective in rats following middle cerebral artery occlusion (MCAO), a model of ischaemic stroke (216, 217). In addition, intracerebroventricular injection of anti-IL-1β antibody was also observed to reduce ischaemic injury following MCAO (218). More evidence for a role for IL-1 in stroke was generated from transgenic animal models. Mice deficient in both IL-1α and IL-1β showed drastically reduced MCAO-induced injury when compared to wild type controls (219, 220).

With IL-1 established as playing an important role in stroke, studies began to look for a driver of elevated IL-1 levels in response to stoke. Studies have suggested NLRP3 may be a regulator of inflammation in response to ischaemic damage, however, conflicting data make the role of NLRP3 in stroke unclear (221). Early studies associated NLRP3 activation with stroke pathology, mice deficient in NLRP3 were found to show lessened ischaemic damage, reduced blood-brain barrier breakdown and improved neurological outcomes when subject to MCAO (222). Furthermore, inhibition of NLRP3 activation through peripheral administration of NLRP3 antibody (223) and MCC950 (224) was protective against ischaemic injury induced by MCAO. These studies together suggest NLRP3 is a contributor to tissue damage following ischaemic events. However, these studies did not investigate whether the beneficial effects of NLRP3 inhibition were due to reduction in NLRP3 activation in the periphery or within the CNS. Peripheral administration of IL-1 exacerbates neuronal death and blood brain barrier breakdown in response to experimental stroke in mice suggesting peripheral IL-1 contributes to stroke outcomes (225). The beneficial effects of inhibiting NLRP3 in

these studies could be due to peripheral lowering of IL-1 levels rather than inhibiting NLRP3 within the CNS. Future studies should investigate whether peripheral and/or CNS inhibition of NLRP3 activity is beneficial in stroke models.

However, multiple contrasting studies have also suggested NLRP3 does not contribute to stroke pathology. NLRP3 deficiency had no effect on brain injury in response to a filament model of MCAO (226). Ischaemic damage was however, found to be dependent on ASC and the AIM2 and NLRC4 inflammasomes suggesting non-NLRP3 inflammasomes may play a role in ischaemic injury. Furthermore, a more recent investigation found NLRP3 deficiency, intraperitoneal or intracerebral MCC950 administration failed to reduce ischaemic damage in a permanent stroke model (227). Although the role of NLRP3 in ischaemic damage remains controversial, as previously mentioned NLRP3 has been shown to contribute to vascular inflammation which drives atherosclerosis suggesting NLRP3 could contribute to an increased risk of stroke (228). Thus, the contribution of the NLRP3 inflammasome-induced inflammation to ischaemic stroke outcomes remains contentious however, NLRP3 may contribute to stroke via increasing the risk of ischaemic stroke.

1.8 Targeting NLRP3 therapeutically

The association of NLRP3 with a diverse range of diseases, some of which lack any effective treatments, has established NLRP3 as a promising therapeutic target. Therapies targeting IL-1β are already approved for therapeutic use, highlighting the potential of inhibiting inflammasome-dependent processing of IL-1β in the clinic (229). Although IL-1β therapies are already available, inhibition of NLRP3 may confer several advantages over targeting IL-1β directly. Firstly, targeting NLRP3 inflammasome activation should also reduce downstream pyroptotic cell death, reducing the propagation of inflammatory responses caused by the release of DAMPs. Secondly, targeting IL-1β directly impairs immune responses to both bacterial and viral infections potentially leaving patients susceptible to infection. Inhibition of NLRP3 would target only IL-1β release in response to sterile stimuli, allowing other inflammasomes to generate IL-1β in response to infection thus, avoiding leaving patients vulnerable to infection. Furthermore, due to the complex nature of the NLRP3 signaling cascade, multiple pathways upstream of activation can be targeted. Different mechanisms can be manipulated to disrupt NLRP3 activation, for example, blocking Cl^- or K^+ channels, disrupting

NLRP3-ASC interactions or directly inhibiting the activity of NLRP3 (Fig. 1.3). In addition, given the importance of PTMs in NLRP3 activation, targeting the biological components responsible for NLRP3 PTMs also represent another avenue for regulating NLRP3 activation. Given the potential of NLRP3 inhibitors and the multiple novel approaches to altering activation it is unsurprising that several companies have dedicated programs aimed at reducing NLRP3 activation. The race to develop effective NLRP3 inhibiting compounds has already led to the identification of several inhibitors of the NLRP3 inflammasome pathway.

In 2015, Coll *et al*, published a ground breaking report which identified MCC950, a compound previously known to inhibit caspase-1 dependent processing of IL-1β (230) to inhibit canonical and non-canonical NLRP3 activation (204). MCC950 was found to specifically target the NLRP3 inflammasome without inhibiting the activation of NLRP1, AIM2 or NLRC4 inflammasomes. *In vivo,* MCC950 is effective in a range of animal disease models such as CAPS, AD, PD and atherosclerosis (202, 204, 209, 231). Recently, Inzomelid, an oral, brain-penetrant derivative of MCC950 has completed phase I trials and is currently in phase II clinical trials for CAPS. In addition, a peripherally restricted derivative Somalix is currently in phase 1 clinical trials.

Although MCC950 clearly represents a promising therapeutic compound, research is continuing to identify and develop novel NLRP3 inhibitors. Given the importance of K^+ efflux in NLRP3 inflammasome activation, unsurprisingly, a number of compounds interfering with ion transport have been identified to possess NLRP3 inhibiting properties. In the late 1990s, Perregaux et al, found the anion transporter inhibitor tenidap to inhibit ATP-induced IL-1β release from macrophages (232). A year later in 1997, the approved type-2 diabetes treatment glyburide which blocks ATP-sensitive K^+ channels was observed also to inhibit macrophage IL-1β release following ATP treatment (233). Further investigation into the anti-inflammatory properties of glyburide revealed glyburide to be a selective NLRP3 inflammasome inhibitor which had no inhibitory action on NLRP1, NLRC4 or AIM2 inflammasomes (234). In addition, glyburide was effective at reducing mortality in response to LPS-induced septic shock in mice models. However, the high concentrations of glyburide required for anti-inflammatory effects limited the pharmacological potential of glyburide as a selective NLRP3 inhibitor. An additional compound β-hydroxybuturate (BHB) was also identified as a specific inhibitor

of NLRP3, potentially via its ability to block K^+ efflux from cells (235). The precise mechanism by which BHB inhibits NLRP3 does however remain unknown. One study has also provided evidence to suggest MCC950 may in part inhibit NLRP3 activation via inhibiting Cl^- efflux, however, more research is required to validate these findings (236). These compounds highlight the potential of pharmacologically manipulating ion channels/transporters upstream of NLRP3 to regulate its activation. To date, no selective ion channel/transporter inhibitors have been developed or identified as potential treatments for NLRP3-mediated inflammation in disease. Identification of specific ion channels involved in the regulation of NLRP3 inflammasome activation could reveal a novel avenue of therapeutic NLRP3 inhibitors.

Additional recently identified or synthesised compounds with demonstratable NLRP3 inhibiting properties *in vitro* include boron-based inhibitors (such as novel boron compounds (NBC)), CY-09, 3,4-methylenedioxy-β-nitrostyrene (MNS) and JC-171 (236–240). Identifying and developing NLRP3 inflammasome inhibitors is clearly an area of intense research due to their potential in treating not just one but a large number of inflammatory diseases. However, before any compounds can progress to the clinic it is critical, we must understand the pharmacological properties of the compounds *in vivo* identify any off-target effects which could be detrimental to patient health. Selectively targeting NLRP3-driven inflammation has clear potential. However, undesired disruption of innate immune pathways could have detrimental impacts on patients such as leaving patients susceptible to infection therefore given the widespread potential applications of NLRP3 inhibitors it is critical we understand exactly which cellular pathways these compounds manipulate.

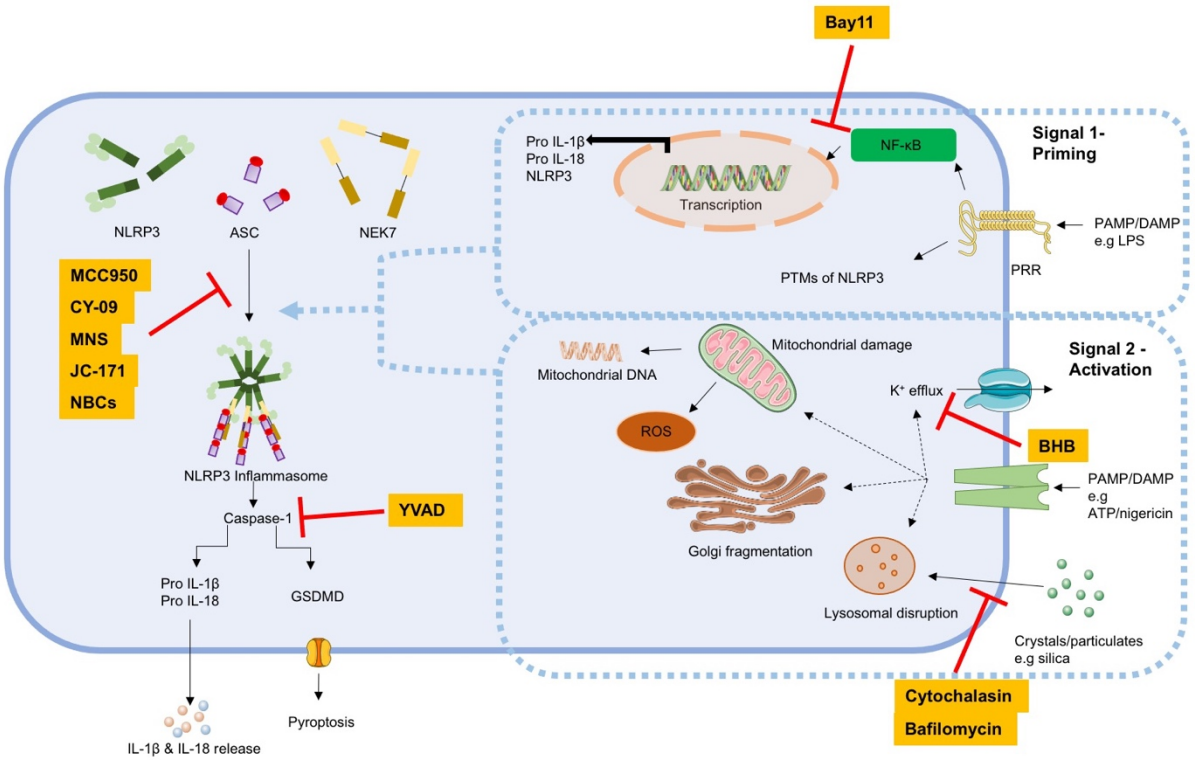

Figure 1.3 Targeting the NLRP3 inflammasome regulatory pathways.
Activation of the NLRP3 inflammasome can be targeted at a number of different stages and levels of regulation. NLRP3 itself can be directly inhibited by a number of different compounds including MCC950, CY-09, MNS, JC-171, and boron-based inhibitors such as the NBC series of compounds. Ion flux is also an additional target for NLRP3 inhibiting compounds such as BHB which inhibits NLRP3 via blocking K^+ efflux. In response to crystal and particulate stimuli which activate NLRP3, preventing phagocytosis with Cytochalasin and Bafilomycin prevents lysosomal disruption and subsequent NLRP3 activation. The effector caspase of the NLRP3 inflammasome, caspase-1 can be targeted to prevent NLRP3 mediated pro IL-1β, pro IL-18 and GSDMD cleavage via inhibitors such as YVAD. The initial priming step required for NLRP3 transcriptional upregulation of NLRP3, pro IL-1β and pro IL-18 can be targeted to inhibit NLRP3 activation. Compounds such as Bay11 inhibit NF-κB mediated priming resulting in insufficient NLRP3 and pro IL-1β protein expression required for NLRP3 activation and subsequent IL-1β release.

1.9 Summary and aims

The NLRP3 inflammasome is a multi-protein complex responsible for the cleavage and activation of the potent inflammatory cytokines IL-1β and IL-18 and pyroptotic cell death through activation of the effector protein caspase-1. NLRP3 is implicated as a driver of inflammation in a range of diseases including neurodegenerative diseases, type 2 diabetes and atherosclerosis, and as such represents a therapeutic target. A commonly reported mechanism of NLRP3 inflammasome activation is K^+ efflux across the plasma membrane. Developing a greater understanding of the mechanisms regulating NLRP3 activation such as the mechanism by which K^+ efflux occurs may reveal novel targets for therapeutic intervention.

The overall aim of this PhD was to investigate the role of K^+ channels in the regulation of the NLRP3 inflammasome to identify novel therapeutic targets for limiting NLRP3 mediated inflammation in disease. Specifically, this thesis aimed to:

1. Identify potential K^+ channels involved in the regulation of the NLRP3 inflammasome
2. Asses the effectiveness of commercial, novel, selective K^+ channel inhibitors on NLRP3 activation.
3. Validate the specific K^+ channels regulating NLRP3 activation using genetic engineering techniques.

Chapter 2: General methods

2.1 Materials

Pharmacological reagents were obtained from the following manufacturers: Sigma (ML133, quinine, tetraethylammonium chloride (TEA), tetrapentylammonium (Tpa), MCC950, LPS from *Escherichia coli* O26:B6, and ATP), AdooQ (TRAM-34 and PAP-1), Alomone Labs (guangxitoxin-1E), Tocris (dofetilide), Merck Millipore (Ac-YVAD-CMK), U.S Silica (Silica), Life Technologies (DNA (pEF/v5-His A plasmid empty vector), Lipofectamine 3000) and Invivogen (ultrapure flagellin from *Salmonella typhimurium* and imiquimod). CVN1 and CVN2 were provided by Cerevance Ltd. Specific antibodies were used targeting: mouse IL-1β (AF-401, R&D), caspase-1 p10 (EPR16883, abcam), gasdermin D (ab209845, Abcam), NLRP3 (G-20B-0014-C100, Adipogen), β-actin (Sigma) and THIK-1 (APC-121, Alamone) as detailed in Table 2.1. All other materials/reagents were obtained from Sigma unless otherwise stated.

Table 2.1 Antibodies used in western blots.

Antibody	Supplier	Dilution	Vehicle
Anti-mouse IL-1β, AF-401 (Goat)	R&D	1:800	PBS, 0.1% Tween™ 20 (ThermoFisher Scientific) and 1% (wt/vol) bovine serum albumin (BSA)
Anti-mouse caspase-1 p10, EPR16883 (Rabbit)	Abcam	1:1000	PBS, 0.1% Tween™ 20 and 1% (wt/vol) BSA
Anti-mouse gasdermin D, ab209845 (Rabbit)	Abcam	1:1000	PBS, 0.1% Tween™ 20 and 1% (wt/vol) BSA
Anti-mouse/human NLRP3, G-20B-0014-C100 (Mouse)	Adipogen	1:1000	PBS, 0.1% Tween™ 20 and 1% (wt/vol) BSA
Anti-mouse/human β-actin (Mouse)	Sigma	1:40,000	PBS, 0.1% Tween™ 20 and 1% (wt/vol) BSA
Anti-mouse THIK-1, APC-121 (Rabbit)	Alamone	1:200 – 1:1000	PBS, 0.1% Tween™ 20 and 1% (wt/vol) BSA

2.2 Pharmacological inhibitors

All inhibitors used in this thesis are detailed in the table below (Table 2.2).

Table 2.2 Details of inhibitors used.

Inhibitor	Supplier	Target
TEA	Sigma	Non-selective K^+ channel inhibitor
TRAM-34	AdooQ	KCa3.1
Tpa	Sigma	K2P channels (THIK-1/TWIK-2)
ML133	Sigma	Kir2.1
Quinine	Sigma	K2P channels (THIK-1/TWIK-2)
Guangxitoxin-1E	Alomone	Kv2.1
PAP-1	AdooQ	Kv1.3
Dofetilide	Tocris	Kv11.1
MCC950	Sigma	NLRP3
Ac-YVAD-cmk	Merck Millipore	Caspase-1
Bay11		NF-κB
CVN1	Cerevance	THIK-1
CVN2	Cerevance	THIK-1

2.3 Generation of THIK-1 knockout mice

The THIK-1 gene (*kcnk13)* was disrupted by MRC Harwell by using CRISPR/Cas9 to insert a single nucleotide into the wild-type DNA sequence (241–243). Insertion resulted in a frameshift mutation in the codon of for amino acid 14. This resulted in a premature stop codon after amino acid 68. The mice were maintained as homozygotes on a C57BL/6 background. To confirm the genotype of the mice Taqman MGB Allelic Discrimination genotyping assays were designed using Primer Express

3.0.1 (Applied Biosystems). Taqman MGB probes were purchased from ThermoFisher & primers were purchased from Sigma Aldrich. Table 2.3 below details the primers used for genotyping.

Table 2.3 Primers used for genotyping THIK-1 KO mice.

Primer/Probe Name	Sequence (5'-3')
MmKCNK13 SNP Genotyping FP	GGTCGGCAGAGCACATCCT
MmKCNK13 SNP Genotyping RP	CTGCAACTCCTGCGCTAGCT
MmKCNK13 WT SNP Genotyping Probe	FAM-CACCTGAACGAGGAC-MGB
MmKCNK13 KO SNP Genotyping Probe	VIC-CACCTGAATCGAGGAC-MGB

Lysates were prepared from ear snips using Extract-N-Amp Tissue PCR Kit from Sigma (XNAT2R). qPCR was run in 384 plates with the following thermocycler conditions: 60°C x 30 s, 95°C x 10 min, then 40 cycles at 95°C x 15 s, 60°C x 1 min, lastly one cycle at 60°C x 30 s.

2.4 Cell culture

2.4.1 Primary and immortalised murine BMDM preparation

Primary bone marrow-derived macrophage (pBMDM) cells were prepared from adult wildtype (WT, C57BL/6) and THIK-1 knockout (KO) male and female mice aged 6-12 weeks. In brief, bone marrow was flushed from femurs, red blood cells were lysed before culturing the remaining cells in Dulbecco's Modified Eagle's Medium (DMEM) (Gibco) containing 10% (vol/vol) fetal bovine serum (FBS, Thermo), 100 U mL^{-1} penicillin and 100 µg mL^{-1} streptomycin (PenStrep, Thermo), supplemented with L929 conditioned media (30% vol/vol) or M-CSF (20 ng/mL). pBMDMs were differentiated for 6-7 days, with extra L929 conditioned or M-CSF media added on day 3. pBMDMs were then re-seeded overnight at a density of $1x10^6$ cells mL^{-1} prior to experiments. pBMDMs were primed with 1 µg mL^{-1} LPS for 4h then treated with drug or vehicle (1% (vol/vol) dimethylsulfoxide (DMSO)) in serum free DMEM for 15 min. Following drug incubation, the NLRP3 inflammasome was activated by stimulation with ATP (5 mM) or nigericin (10 µM) for 1 h, imiquimod (75 µM) for 2 h or silica (300 µg mL^{-1}). Alternatively, the NLRC4 inflammasome and AIM2 inflammasome were activated by transfection with ultrapure flagellin from *Salmonella typhimurium* (1 µg mL^{-1}) or DNA

(pEF/v5-His A plasmid empty vector) (1 μg mL^{-1}) respectively for 4h. Transfections were performed using Lipofectamine 3000 according to the manufacturer's instructions. For priming experiments pBMDMs were treated with drug or vehicle (1% (vol/vol) DMSO) for 15 min prior to priming with 1 μg mL^{-1} LPS for 4h. Supernatants were removed and analysed for IL-1β, IL-6 and TNFα content by ELISA (Duoset, R&D Systems). Supernatants and lysates were collected to analyse IL-1β, caspase-1, NLRP3 and GSDMD processing by western blot.

Immortalised BMDM (iBMDM) cells were obtained from Clare Bryant (Department of Veterinary Medicine, University of Cambridge). iBMDMs were cultured in DMEM supplemented with 10% (vol/vol) FBS and 1% (vol/vol) PenStrep. Before experiments iBMDMs were seeded overnight at a density of $0.75x10^6$ cells mL^{-1} at 37°C. For priming experiments iBMDMs were treated with drug or vehicle (1% (vol/vol) DMSO) for 15 min prior to priming with LPS (1 μg mL^{-1}, 4 h). Supernatants were removed and analysed for IL-6 and TNFα content by ELISA (Duoset, R&D Systems) according to manufacturer's instructions. For inflammasome activation experiments iBMDMs were seeded overnight at a density of $0.75x10^6$ cells mL^{-1} at 37°C. Cells were primed with LPS (1 μg mL^{-1}, 4 h) then treated with drug or vehicle in serum free DMEM for 15 min or where appropriate media was changed to fresh media containing the indicated isotonic salt solution: control (145 mM NaCl/5 mM KCl), high K^+ and normal Cl^- (150 mM KCl), or high K^+ and Cl^- free solution (150 mM KGluconate) for 15 min. NLRP3 inflammasome activation was then stimulated by adding ATP (5 mM) for 1 h. Supernatants were removed and analysed for IL-1β, IL-6 and TNFα content by ELISA. Supernatants and lysates were collected to analyse IL-1β and NLRP3 protein expression by western blot.

2.4.2 Primary murine mixed glial culture preparation

Murine mixed glial cells were prepared from the brains of C57BL/6 male and female 2-4-day old mice that were sacrificed by cervical dislocation under S1. All experimental procedures were performed under Home Office UK project license in accordance with the Animals (Scientific Procedures) Act UK 1986 and approved by the University of Manchester AWERB (Animal Welfare and Ethical Review Body). The brains were isolated, followed by dissection of hemispheres and removal of meninges as previously described (244). Tissue was homogenized by trituration in DMEM supplemented with 10% FBS and 1% PenStrep. Homogenate was centrifuged at 500x*g* for 10 min and the pellet was

resuspended in fresh DMEM with 10% (vol/vol) FBS and 1 % (vol/vol) PenStrep. Cells were washed at day 5 and media replaced. Media was replaced every 2 days. Cells were seeded at $2x10^5$ cells mL^{-1} in 96 well plates and incubated for 2 days before use. Mixed glia were primed with 1 μg mL^{-1} LPS for 4 h then treated with drug or vehicle (1% DMSO (vol/vol)) in serum free DMEM for 15 min Following drug incubation NLRP3 was activated by stimulation with ATP (5 mM, 1 h), nigericin (10 μM, 1 h), imiquimod (75 μM, 2 h) or silica (300 μg mL^{-1}, 4 h). Supernatants were collected and analysed for IL-1β content by ELISA.

2.4.3 Primary murine adult microglia preparation

WT and THIK-1 KO C57BL/6 male and female mice aged 6-10 weeks were sacrificed by cervical dislocation under S1. All experimental procedures were performed under Home Office UK project license in accordance with the Animals (Scientific Procedures) Act UK 1986 and approved by the University of Manchester and University of Cambridge AWERB (Animal Welfare and Ethical Review Body). All subsequent steps, unless otherwise stated, were performed at 4°C. Brains were isolated followed by removal of cerebellum and meninges. Brains were minced with a disposable scalpel into 1-3 mm^3 chunks and digested using a Neural Tissue Dissociation Kit (Miltenyi) according to manufacturer's instructions. The resulting suspension was homogenized using a Dounce tissue grinder with 20 passes of a loose clearance pestle. Myelin was removed from the subsequent single-cell suspension by centrifuging in 33% Percoll (GE Healthcare) for 10 min at 1000x*g* with low break and aspiration of myelin layer. Cells were pelleted by diluting 1:4 in Hanks balanced salt solution without calcium or magnesium (Gibco) and centrifuged for 10 min at 500x*g*. Cells were incubated with 10 μL anti-CD11b magnetic microbeads (Miltenyi) per brain in MACs buffer (PBS without calcium or magnesium with 2 mM ethylenediaminetetraacetic acid and 0.5% (wt/vol) bovine serum albumin (BSA) for 15 min at 4°C under slow rotation followed by passing through LS columns (Miltenyi) according to manufacturer's instructions. The remaining microglia suspension was pelleted, counted and spot plated onto 96-well Cell+ plates (Sarstedt) at a density of 20,000-30,000 cells per well. The plates were left at room temperature for 10 min to allow cell attachment followed by addition of 100 μL culture medium (Dulbecco's modified Eagle's medium/F12 containing 10% (vol/vol) FBS, 1% (vol/vol) PenStrep and 2 mM glutamine supplemented with IL-34 (20 ng mL^{-1}; R&D Systems) and transforming growth factor-β_1 (50 ng mL^{-1}; Miltenyi). Cells were used at day 8. Microglia were primed

with 1 μg mL^{-1} LPS for 4h then treated with drug or vehicle (1% (vol/vol) DMSO) in serum free media for 15 min Following drug incubation NLRP3 was stimulated with ATP (5 mM, 1 h), nigericin (10 μM, 1 h), imiquimod (75 μM, 2 h) or silica (300 μg mL^{-1}, 4 h). For priming experiments microglia were treated with drug or vehicle (1% DMSO) for 15 min prior to priming with LPS (1 μg mL^{-1}, 4 h). Supernatants were removed and analysed for IL-1β, IL-6 and TNFα content by ELISA.

2.4.4 Primary human monocyte and THP-1 preparation

Fresh blood was isolated from healthy volunteers following approval from Ethics Committee 05/Q0401/108 and 2017-2551-3945 (University of Manchester). Peripheral blood mononuclear cells (PBMC) were isolated from blood using a 30% Ficoll gradient (Thermo) and centrifugation at 400xg for 40 min at room temperature. The PBMC layer was separated and washed 3 times with MACs buffer to remove platelets. Monocytes were positively selected by incubating with CD14+ magnetic microbeads (Miltenyi) for 15 min at 4°C and then passed though LS columns. Cells were pelleted and counted before seeding at $1x10^6$ cells mL^{-1} in 96 well plates for immediate use. Human WT and NLRP3 KO THP-1 cells were cultured in RPMI-1640 medium supplemented with 10% (vol/vol) FBS, 1% PenStrep, and 2 mM L-glutamine and seeded in 96 well plates for immediate use. NLRP3 deficient THP-1 cells were a gift from Prof Veit Hornung (Ludwig Maximillian University of Munich). THP-1 cells were primed with LPS (1 μg mL^{-1}, 4 h) then treated with drug or vehicle (1% DMSO) in serum free media for 15 min. Following drug incubation canonical NLRP3 activation was stimulated with silica (300 μg mL^{-1}, 4 h). For alternative NLRP3 activation primary human monocytes and THP-1 cells were treated with drug or vehicle (DMSO) in serum free media for 15 min before stimulation with LPS for 16 h. Supernatants were removed and analysed for IL-1β content by ELISA.

2.4.5 siRNA transfections

For THIK-1 knockdown in pBMDMs and iBMDMs, SMARTpool: ON-TARGETplus kcnk13 siRNA or ON- TARGETplus Non-targeting Control Pool (Dharmacon) were diluted to 20 μM in 250 μL UltraPure Distilled Water (Invitrogen). Transfections were performed using Viromer GREEN (Lipocalyx) according to manufacturer's instructions. Briefly, 2.75 M kcnk13 or control siRNA was added to 45 μL Viromer GREEN and incubated at room temperature for 15 min. For each

transfection, 25 nM of siRNA plus Viromer GREEN mixture (50 µL) was added to each well. Following 48 h incubation in siRNA mix, inflammasome activation and cell death was investigated.

2.5 Sample analysis

2.5.1 Cytokine assessment

IL-1β, IL-6 and TNFα released into culture supernatants was measured using the ELISA DuoSet™ kit (R&D Systems) following manufacturer's instructions. In brief, capture antibody was coated onto NuncTM 96-well plates (Thermo Fisher) and incubated overnight at room temperature. Plates were then washed with ELISA wash buffer (PBS, 0.05% (vol/vol) Tween 20) followed by blocking with 1% BSA in PBS. Plates were blocked for 60 min after which blocking solution was removed by washing with ELISA wash buffer. Pre-prepared samples were then added to plates followed by 120 min incubation at room temperature. Plates were then washed in wash buffer followed by addition of biotinylated detection antibody and incubated for 60 min. Excess detection antibody was removed via washing with wash buffer and horse-radish peroxidase (HRP)-conjugated streptavidin was added to samples for 20 min. Following an additional washing step with wash buffer, 3,3',5,5' – tetramethlybenzidine (TNB) substrate solution (Sigma) was added to samples for a duration of 20 min. The reaction was then stopped with H2SO4 prior to measuring absorbance at wavelength 450-590nm using a Synergy HT microplate reader with Gen5 software (Biotek). For analyses, sample absorbance was compared with IL-1β, IL-6 or TNFα standard absorbance.

2.5.2 Western blotting

IL-1β, caspase-1, and GSDMD processing in addition to NLRP3, IL-1β and THIK-1 protein expression were determined by western blotting. Both cell supernatant and cell lysates were collected together and precipitated in deoxycholate containing 20% trichloroacetic acid (Fisher) and washed with acetone followed by air drying at room temperature before concentration in 2x Laemmlii buffer. All samples were separated using Tris-glycine SDS/PAGE and then transferred using a semi-dry Transblot Turbo System (Bio-Rad) at 25V onto nitrocellulose or PVDF membranes. Membranes were blocked in 5% (wt/vol) BSA (Sigma) in PBS, 1% (vol/vol) Tween 20 (PBST). Following blocking, membranes were incubated with primary antibodies: IL-1β (1:800), caspase-1 (1:1000), GSDMD

(1:1000), NLRP3 (1:1000), THIK-1 (1:200-1:1000) or β-actin-peroxidase (1:40000) in 1% (vol/vol) BSA PBST at 4°C overnight. Membranes were then incubated and labelled with HRP-tagged secondary antibodies (1:1000) in 1% (vol/vol) PBST and visualised with Amersham ECL detection reagent (GE Healthcare). Images of western blots were captured digitally using a G-Box Chemi XX6 (Syngene).

2.5.3 Lactate dehydrogenase (LDH) assay

Cell death was quantified in pBMDMs, iBMDMs and mixed glia following treatment by measuring the release of the enzyme lactate dehydrogenase (LDH). This was achieved using the Cytotox-96 assay (Promega) according to the manufacturer's instructions. In brief, following treatment, 25 µL of cell supernatant was transferred into 96-well plates. This was followed by addition of 25 µL of CytoTox-96 Reagent to individual wells and incubation at room temperature for 20 min. The reaction was stopped via the addition of 50 µL Stop Solution (Promega) and absorbance was measured at 490 nm using a Synergy HT microplate reader with Gen5 software (Biotex).

2.5.4 ASC speck imaging

Real-time ASC speck assays were performed using iBMDMs stably expressing ASC-mCherry (ASC-mCherry iBMDMs) (84). ASC-mCherry iBMDMs were seeded out overnight into 96 well plates at a density of $0.75x10^6$ cells mL^{-1} followed by priming for 3 h with 1 µg mL^{-1} LPS. To prevent pyroptosis and loss of ASC specks iBMDMs were pre-treated with the pan-caspase inhibitor Ac-YVAD-CMK (50 µM) for 30 min prior to microscopy. After priming, cells were pre-treated with vehicle control (1% (vol/vol) DMSO), TPA (50 µM) or MCC950 (10 µM), or appropriate cells were reperfused with high K^+ and normal Cl^- or high K^+ and Cl^- free solution for 15 min. Following pre-treatment, cells were stimulated with ATP (5 mM) or reperfused with Cl^- free, K^+ free or K^+ and Cl^- free solution where indicated. Images were captured using a 20x/0.61 S Plan Fluor objective at 15-min intervals and

quantified using an Incucyte Zoom System (Essen Bioscience). Comparison of ASC speck formation was analysed after stimulation for 105, 150 or 165 mins.

2.5.5 YO-PRO-1 P2X7 assay

P2X7 receptor-dependent membrane permeability was determined using the YO-PRO-1 fluorescent dye (245). iBMDMs were seeded out overnight into 96 well plates at a density of $0.75x10^6$ cells mL^{-1} followed by priming for 4 h with 1 μg mL^{-1} LPS. After priming, cells were pretreated with vehicle control (1% (vol/vol) DMSO), TPA (50 μM) or the P2X7 inhibitor oxidised ATP (oATP, 5 mM) before stimulation with ATP (5 mM) for 30 min. Supernatant was removed and cells washed with PBS without calcium or magnesium. 200 μL of YO-PRO-1 (2 μM) staining solution (Thermofisher Scientific) was then added to cells and fluorescence measured every 5 min for 30 min.

2.6 Post-mortem human brain tissue

2.6.1 Source of human brain tissue and research ethics committee approval

Post-mortem AD brain samples from the temporal cortex (Table 2.4) and PD brain samples from the substantia nigra and frontal cortex (Table 2.5) were obtained from The Manchester Brain Bank at Salford Royal NHS Foundation Trust (University of Manchester). The Manchester Brain Bank has been approved by the Newcastle & North Tyneside 1 Research Ethics Committee on 6th May 2014 (REC reference 09/H0906/52+5).

Table 2.4 Demographic parameters for Alzheimer's disease post-mortem human brain samples.

	Control (Braak Stage 0-II)	Mild AD (Braak Stage III-IV)	Severe AD (Braak Stage V-VI)
Age of death (Years)			
All (N=120)	82.6 ± 11.5	85.5 ± 6.3	78.1 ± 8.8
- Male (N=60)	84.5 ± 9.4	84.0 ± 6.5	73.3 ± 4.7
- Female (N=60)	80.7 ± 13.3	87.1 ± 6.0	83.0 ± 9.3
Post-mortem interval (Hours)	81.2 ± 36.9	79.4 ± 38.4	86.2 ± 43.0
All (N=120)	85.7 ± 41.4	81.2 ± 37.0	82.7 ± 48.9
- Male (N=60)	76.5 ± 31.8	77.5 ± 40.6	89.6 ± 37.1
- Female (N=60)			

Table 2.5 Demographic parameters for Parkinson's disease post-mortem human brain samples.

	Control (Male N=8, Female N=7)	**PD** (Male N=6, Female N=9)
Age of death (Years)		
All (N=30)	82.6 ± 9.8	80.3±8.2
Male (N=14)	80.1 ± 8.4	78.0±8.6
Female (N=16)	85.4±11.1	81.8±8.0
Post-mortem Interval (Hours)		
All (N=30)	25.9 ± 8.0	18.1 ± 7.8*
Male (N=14)	27.8 ± 9.8	17.5 ± 7.6
Female (N=16)	23.7 ± 7.8	18.6 ± 8.4

* The post-mortem interval of the PD group was shorter than control group, but it did not correlate with any of the quantification value of mRNA or protein expression assessed in this study.

2.6.2 Reverse transcriptase semi-quantitative real-time PCR (RT-qPCR)

To determine THIK-1 mRNA levels RT-qPCR was carried out. Briefly, total RNA was extracted from AD and non-AD brain tissues using using TRIzol™ Reagent (Thermo Fisher, Cat. No. 15596018) followed by RNA clean up using RNeasy mini kit (Qiagen, Cat. No.74104). RNA purity and concentrations were assessed using a NanoDrop 2100 (Thermo Fisher). RNA concentrations ranged from 84.78-593.46 ng mL^{-1}. An optical density at wavelength 260/280 nm range of 2.01–2.11 were chosen for this study. Single-stranded cDNA was synthesized from 1 ng of total RNA using M-MLV Reverse Transcriptase (Thermo Fisher) following the manufacturer's instructions. The oligonucleotide primer pair 5'- TGGAAGCCCTCCGTGTACTA-3' (forward) and 5'- CAGCAGACACCCATGAGGAT – 3' (reverse) specific for human THIK1 were selected for qPCR amplification (Thermo Fisher). Real-time quantitative PCR was performed using Power SYBR™ Green Master Mix (Applied Biosystems) and QuantStudio™ 12K Flex Real-Time PCR System (Thermo Fisher). The thermal cycler parameters were as follows: UDG activation at 50°C for 2 min, and DNA polymerase activation at 95°C for 10 min, followed by amplification of cDNA for 40 cycles with denaturation at 95°C for 15 s and annealing/extension at 60°C for 1 min. The values were normalized using geometric mean of human _RPL13A mRNA level and human _ GAPDH mRNA level as an endogenous internal standard (specific oligonucleotide primer of RPL13A: forward 5'- AGCCTACAAGAAAGTTTGCCTAT -3', reverse 5'- TCTTCTTCCGGTAGTGGATCTTGGC-3'; GAPDH: forward 5'- CCTGCACCACCAACTGCTTA -3', reverse 5'- GTCTTCTGGGTGGCAGTGATG -3' Thermo Fisher). Data were analysed using 2(-Delta Delta Ct) Method.

2.7 Statistical analysis

Data are presented as the mean ± standard error of the mean (SEM). Levels of significance accepted were *p<0.05, **p<0.01, ***p<0.001, ****p<0.0001. Statistical significance was calculated using GraphPad Prism version 9.2.0. Data with multiple groups were analysed using a one-way ANOVA followed by Dunnet's post hoc comparison. Experiments with two independent variables were analysed using two-way ANOVA followed by Bonferroni's post hoc correct analysis.

Chapter 3: Pharmacological inhibition of two-pore domain potassium channels blocks NLRP3 inflammasome activation

3.1 Introduction

Canonical activation of NLRP3 *in vitro* typically requires a two-step activation process. The first "priming" step can be induced by stimulation of Toll-like receptors which drives the expression of pro-IL-1β and NLRP3 (23). The second step is NLRP3 inflammasome activation, which can be induced by a range of structurally unrelated stimuli such as the K^+ ionophore nigericin, extracellular ATP and crystalline/particulate matter including silica (55, 246). Several studies have proposed mechanisms to explain how such a diverse range of stimuli converge on NLRP3 activation. One proposed mechanism is a decrease in intracellular K^+ (44, 247) which is suggested to be important for multiple NLRP3 activating stimuli (45). However, the mechanism by which K^+ efflux regulates NLRP3 activation remains unclear. Recent studies have also shown small molecules such as imiquimod and CL097 can trigger canonical NLRP3 activation independently of K^+ efflux (51). K^+ efflux is therefore an important but not universal driver of canonical NLRP3 activation. Studies also suggest a potential involvement of Cl^- channels in NLRP3 activation (82, 84, 86). We have previously shown Cl^- efflux is an ASC oligomerizing signal required before K^+ efflux dependent activation of NLRP3 suggesting both Cl^- and K^+ efflux are important in NLRP3 regulation (88). In addition to this two-step activation process, an alternative K^+ independent mechanism of NLRP3 activation occurs in human monocytes (87, 104). In contrast to canonical activation, LPS alone in the absence of a secondary stimulus is sufficient to trigger NLRP3 activation by this alternative mechanism (104).

K^+ channels regulate an array of cellular and immune responses including immune cell proliferation, cell volume regulation, cytokine production and surveillance (68, 248–250). Members of the K2P channel family in particular, have recently been implicated with NLRP3 inflammasome activation (68, 78). The Two-pore domain Weak Inwardly rectifying K^+ channel 2 (TWIK2) has been suggested to facilitate ATP-induced K^+ efflux and subsequent NLRP3 activation in macrophages (78). Furthermore, a recent study identified the K^+ channel Tandem Pore Domain Halothane-Inhibited Potassium Channel 1 (THIK-1) regulates IL-1β release from hippocampal slices in response to ATP (68), suggesting that it may be important for NLRP3 activation. This chapter aimed to utilize RNA-sequencing databases and pharmacological screening processes to identify potential K^+ channels involved in NLRP3 inflammasome activation in a range of *in vitro* inflammatory systems.

3.2 Results

3.2.1 Potassium channels shared by cultured bone-marrow derived macrophages and microglia

In order to identify potential K^+ channels involved in regulating NLRP3 activation in macrophages and microglia, K^+ channel RNA expression in both cultured murine microglia and iBMDM cells from existing datasets were analysed (251). Through quantitative expression analysis of existing RNA expression databases (https://braininflammationgroup-universityofmanchester.shinyapps.io/GrapheneOxide/, https://braininflammationgroup-universityofmanchester.shinyapps.io/NLRP3KOmicroglia) eight different K^+ channels were identified to be expressed by both microglia and iBMDMs (Fig. 3.1). Channels identified included the calcium-activated K^+ channel KCa3.1, the inwardly rectifying K^+ channel Kir2.1, two-pore domain K^+ (K2P) channels TWIK-2 and THIK-1 and voltage gated K^+ channels Kv1.3, 2.1, 4.1 and 11.1.

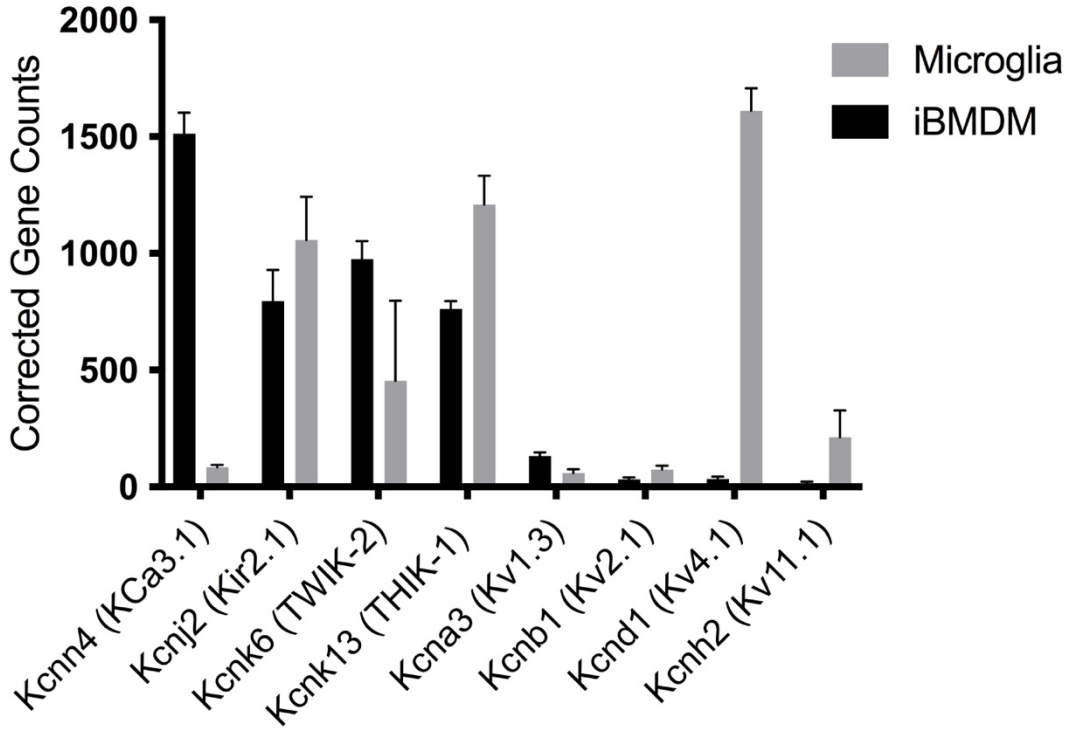

Figure 3.1 K^+ Channels Expressed in Cultured Microglia and iBMDM Cells.

Data shows K^+ channels expressed by untreated adult mouse microglia (n=6) and mouse iBMDMs following LPS treatment (1 µg mL^{-1}, 2h, n=4). Data was collected through data mining of RNA sequencing data bases collected from our research group on microglia (https://braininflammationgroup-universityofmanchester.shinyapps.io/NLRP3KOmicroglia) and iBMDMs (https://braininflammationgroup-universityofmanchester.shinyapps.io/GrapheneOxide/). Only genes with corrected counts above 80 are shown. Data is represented as mean corrected gene counts generated through normalizing raw gene counts relative to gene library sizes.

3.2.2 Pharmacological blockade of two-pore domain potassium channels inhibited NLRP3 inflammasome activation in murine macrophages

To identify K^+ channels involved in activation of the NLRP3 inflammasome, LPS-primed (1 μg mL^{-1}, 4 h) pBMDMs were incubated for 15 min with K^+ channel inhibitors TEA (non-selective K^+ inhibitor), TRAM-34 (KCa3.1 inhibitor), TPA (THIK-1 and TWIK-2 inhibitor), ML133 (Kir2.1 inhibitor), quinine hydrochloride dihydrate (THIK-1 and TWIK-2 inhibitor), Guangxitoxin-1E (Kv2.1 inhibitor), PAP-1 (Kv1.3 inhibitor), and dofetilide (Kv11.1 inhibitor). The inhibitors selected inhibited one or more of the K^+ channels identified through RNA profiling above (Fig. 3.1), in addition to the non-specific K^+ channel inhibitor TEA. The NLRP3 inhibitor MCC950 (252) was included as a positive control. Inhibitors and concentrations used were based on previously published work (68, 253–258). BMDMs were stimulated for 1h with 5mM ATP which induces NLRP3 activation via P2X7 channel activation (55). BMDMs were also stimulated for 4h with 300 μg mL^{-1} silica which stimulates NLRP3 activation via lysosome damage (246). Both ATP and silica-induced activation of the NLRP3 inflammasome are reported to depend upon K^+ efflux (45). IL-1β in the supernatant was used as a readout of NLRP3 activation.

Analysis of cell supernatant by ELISA confirmed the importance of K^+ channel activation in NLRP3 stimulation as the non-specific K^+ channel blocker TEA (50 mM) significantly inhibited IL-1β release in response to both ATP (Fig. 3.2Ai) and silica (Fig. 3.2Aii). Blocking K2P channels (including THIK-1 and TWIK-2) with Tpa (50 μM) and quinine (100 μM) (71, 259) also significantly inhibited ATP-induced IL-1β release (Fig. 3.2Ai). Likewise, Tpa and quinine significantly inhibited silica-induced IL-1β release (Fig. 3.2Aii), suggesting their effect was not due to direct inhibition of the P2X7 receptor. In contrast, the inhibitors blocking KCa3.1 (TRAM-34, 10 μM), Kir2.1 (ML133, 20 μM), Kv2.1 (Guangxitoxin-1E, 25 nM), Kv1.3 (PAP-1, 2 μM) and Kv11.1 (dofetilide, 1 μM) had no impact on IL-1β release in response to ATP or silica (Fig. 3.2Ai and Aii respectively). The Kir2.1 inhibitor ML133

did however significantly reduce cell death in response to ATP, but not silica, while no other K^+ channel inhibitor reduced cell death in response to ATP or silica (Fig. 3.2B).

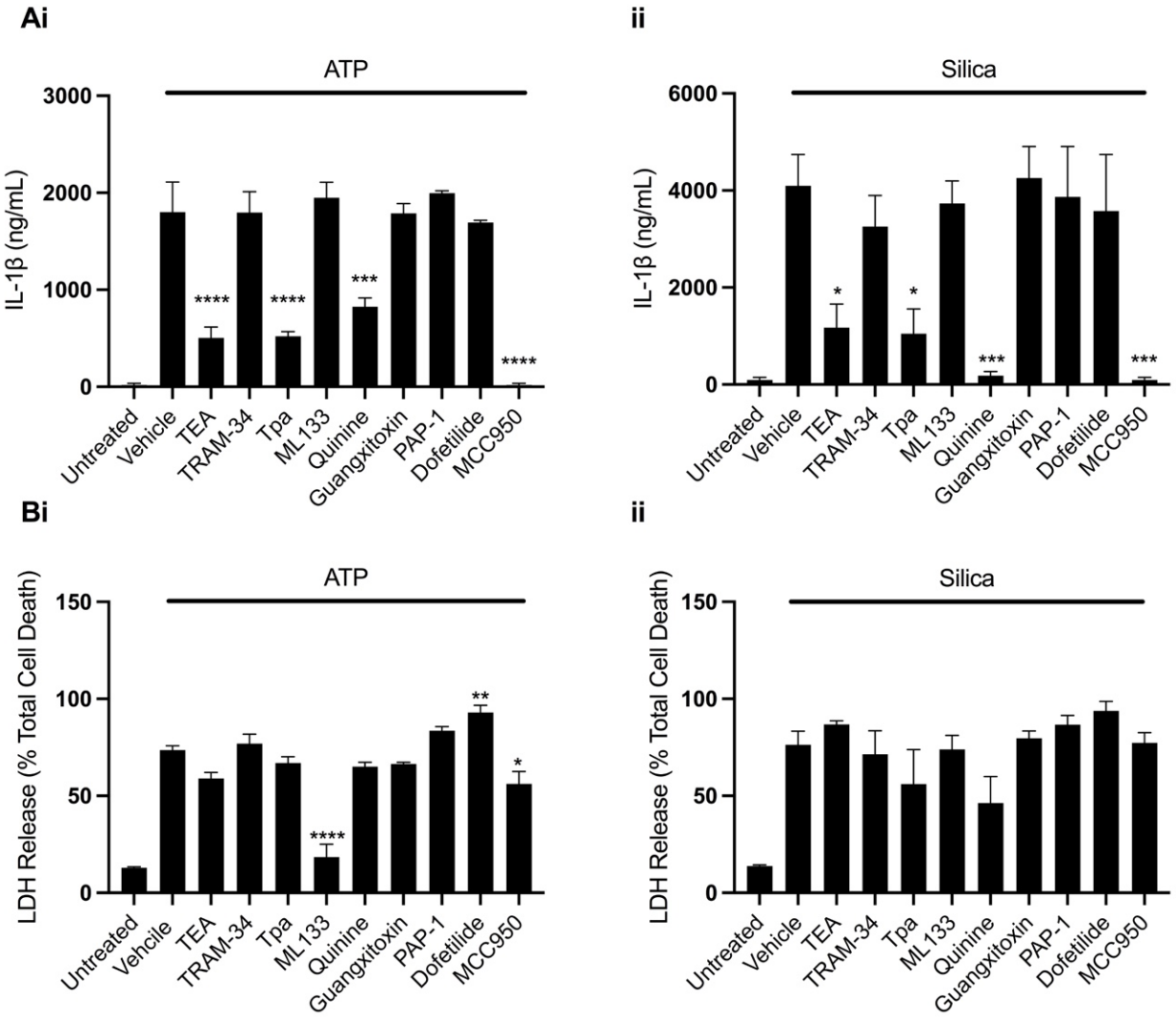

Figure 3.2 Pharmacological inhibition of two pore domain potassium channels blocks NLRP3 inflammasome activation and IL-1β release in response to ATP and silica.
A) IL-1β ELISA and **(B)** LDH release assay of the supernatant of pBMDMs primed with LPS (1 μg mL^{-1}, 4 h) followed by pretreatment with MCC950 (10 μM) or K^+ channel inhibitors TEA (50 mM), TRAM-34 (10 μM), Tpa (50 μM), ML-133 (20 μM), Quinine (100 μM), Guangitoxin-1E (25 nM), PAP-1 (2 μM) or Dofetilide (1 μM) for 15 min before stimulation with ATP (5 mM, 1 h) (n=4) or silica (300 μg mL^{-1}, 4 h). ****p<0.0001, ***p<0.001, **p<0.01, *p<0.05 determined by one-way ANOVA with Dunnett's post hoc analysis. Values shown are the mean ± SEM.

Having established K^+ channel inhibitors inhibit NLRP3 inflammasome activation in response to ATP and silica, the study next investigated whether the effects of TEA, Tpa and quinine on NLRP3 activation were due to their inhibitory action on K^+ channels and not an alternative "off target" mechanism. In order to test this, the impact of the K^+ channel inhibitors on NLRP3 activation was tested described in the protocol above using the K^+ efflux independent NLRP3 activator imiquimod (21). Stimulation of LPS-primed pBMDMs for 1h with 75 μM imiquimod induced IL-1β release which was abolished by pre-treatment with quinine (Fig. 3.3Ai). In contrast, TEA, Tpa and other inhibitors had no effect on imiquimod induced IL-1β release. Imiquimod-induced cell death was not significantly affected by treatment with any inhibitor (Fig. 3.3Bi). In addition to imiquimod, the effect of TEA, Tpa and quinine on nigericin-induced NLRP3 activation was determined. Nigericin is a K^+ ionophore which activates NLRP3 by facilitating K^+ efflux independently of K^+ channels (55). Stimulation of LPS-primed pBMDMs for 1h with 10 μM nigericin induced IL-1β release which was unaffected by pre-treatment with TEA or Tpa (Fig. 3.3Aii). Pre-treatment with quinine inhibited nigericin-induced IL-1β release suggesting quinine inhibited NLRP3 independently of specific K^+ channels (Fig. 3.3Aii). Nigericin-induced cell death was not significantly affected by treatment with Tpa, TEA or quinine (Fig. 3.3Bii). The effect of imiquimod and nigericin on IL-1β release were all NLRP3 dependent as IL-1β release was inhibited by MCC950 (Fig. 3.3A).

These data suggest K^+ channels targeted by TEA and Tpa do not play a role in imiquimod- or nigericin-induced NLRP3 activation. Furthermore, these data suggest that Tpa inhibited NLRP3 via a K^+ channel dependent manner indicating NLRP3 inhibition was a consequence of its K2P channel inhibiting properties and not an additional unidentified mechanism of action. Although only weakly, TEA also inhibits K2P channels (71). Therefore, TEA may also inhibit NLRP3 activation via inhibition of K2P channels. In contrast, quinine's ability to inhibit NLRP3 activation in response to stimuli that are reported to activate NLRP3 in the absence of K^+ efflux suggests quinine may not be inhibiting NLRP3 through blocking K^+ efflux. K2P channels selectively regulate the NLRP3 activation pathway only when K^+ efflux is required and mediated via K^+ channels.

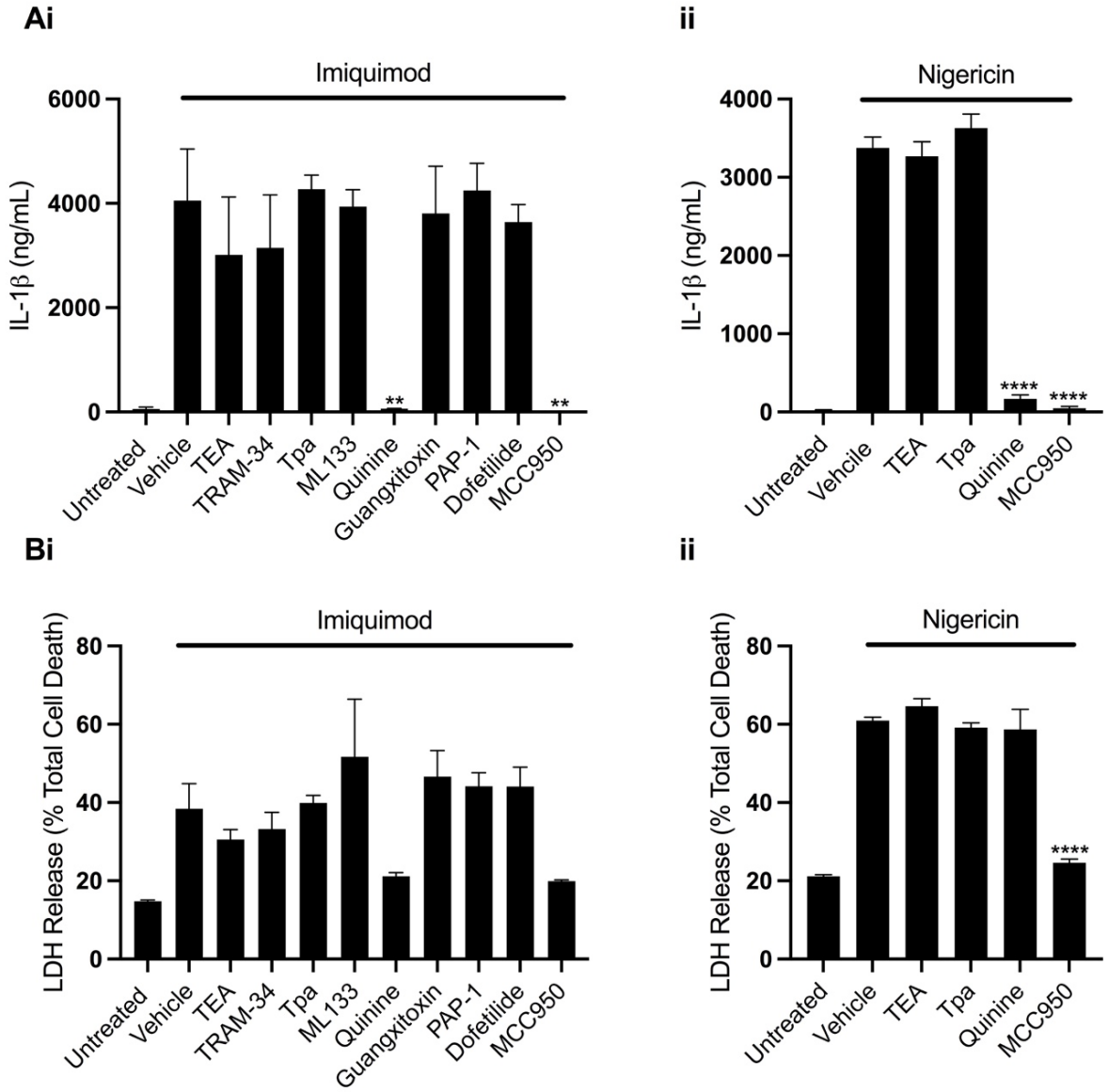

Figure 3.3 Pharmacological inhibition of two pore domain potassium channels has no effect on NLRP3 inflammasome activation and IL-1β release in response to imiquimod and nigericin.

(**A)** IL-1β ELISA and **(B)** LDH release assay of the supernatant of pBMDMs primed with LPS (1 μg mL^{-1}, 4 h) followed by pretreatment with MCC950 (10 μM) or K^+ channel inhibitors TEA (50 mM), TRAM-34 (10 μM), Tpa (50 μM), ML-133 (20 μM), Quinine (100 μM), Guangitoxin-1E (25 nM), PAP-1 (2 μM) or Dofetilide (1 μM) for 15 min before stimulation with imiquimod (75μM, 2h) (n=3) or nigericin (10 μM, 1h) (n=4). ****p<0.0001, **p<0.01 determined by one-way ANOVA with Dunnett's post hoc analysis. Values shown are the mean ± SEM.

NLRP3 inflammasome activation results in the recruitment and cleavage of caspase-1, which in turn cleaves pro-IL-1β into its active released form (90). Active caspase-1 also cleaves and activates GSDMD (116). In order to establish whether Tpa and TEA inhibit activation of downstream mediators of NLRP3 activation, western blotting was used to investigate the effect of Tpa and TEA pre-treatment on ATP-induced caspase-1, IL-1β and GSDMD cleavage. Western blot analysis showed that caspase-1, IL-1β and GSDMD processing induced by ATP was inhibited by Tpa and TEA (Fig. 3.4A) further indicating Tpa and TEA as inhibitors of NLRP3 inflammasome activation. In support of western blot experiments, caspase-1 Glo, a quantitative measure of caspase-1 activity showed Tpa and TEA inhibited caspase-1 activity in pBMDMs in response to ATP treatment (Fig. 3.4B) further confirming Tpa and TEA as inhibitors of NLRP3 activation and downstream processing of caspase-1, IL-1β and GSDMD. Tpa inhibited both ATP and silica-induced IL-1β release in a concentration dependent manner (Fig. 3.5Ai and Aii respectively) with no concentrations found to inhibit ATP (Fig. 3.5Bi) or silica-induced cell death (Fig. 3.5Bii).

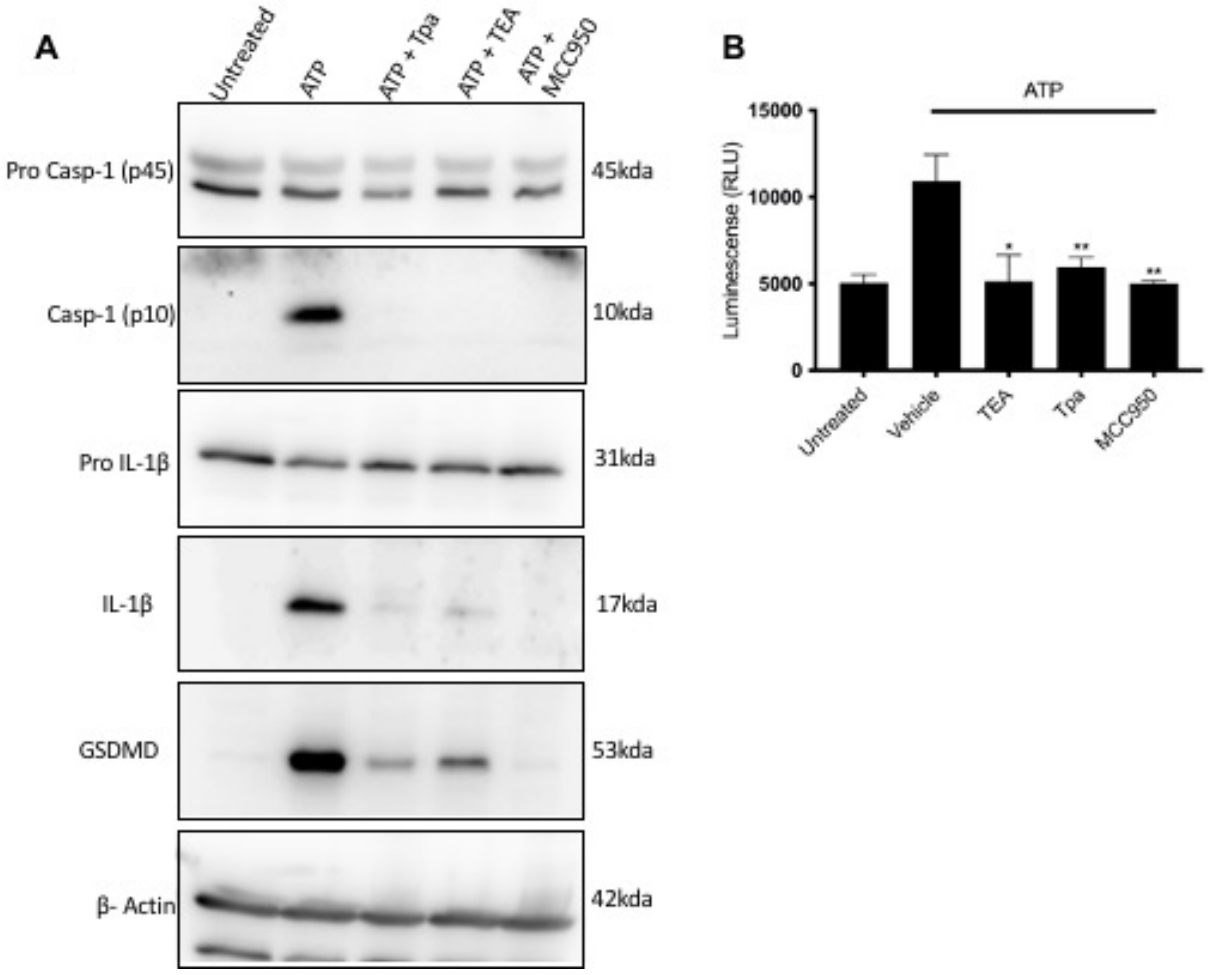

Figure 3.4 Pharmacological inhibition of two pore domain potassium channels blocks caspase-1, IL-1β and GSDMD processing in response to ATP-induced NLRP3 activation.
(A) Caspase-1, IL-1β and gasdermin D western blot of total cell lysates (cell lysate + supernatant) from LPS-primed (1μg mL^{-1}, 4 h) pBMDMs pretreated with vehicle control, TEA (50 mM), Tpa (50 μM) or MCC950 (10 μM) for 15 min then stimulated with ATP (5 mM, 1 h). **(B)** Caspase-1 Glo assay to measure caspase-1 activity of LPS-primed (1 μg mL^{-1}, 4 h) pBMDMs pretreated with vehicle control, TEA (50 mM), Tpa (50 μM) or MCC950 (10 μM) for 15 min then stimulated with ATP (5 mM, 1 h) (n=4). $^{**}p<0.01$, $^{*}p<0.05$ determined by one-way ANOVA with Dunnett's post hoc analysis. Values shown are the mean ± SEM.

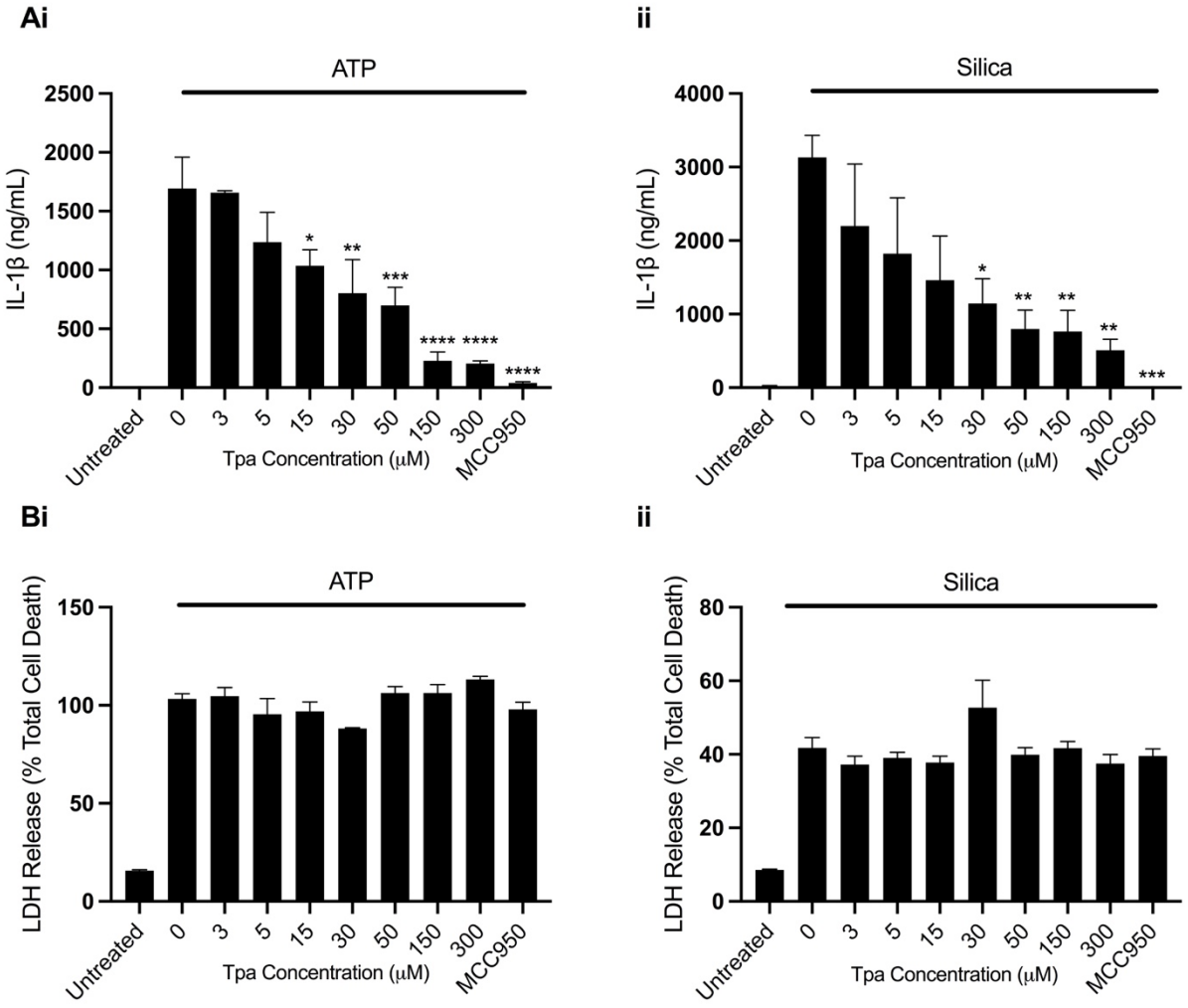

Figure 3.5 Tpa inhibits NLRP3 inflammasome activation and IL-1β in a concentration dependent manner.

(A) IL- 1β ELISA or **(B)** LDH release assay of the supernatant of pBMDMs primed with LPS (1 μg mL^{-1}, 4 h) followed by pretreatment with MCC950 (10 μM) or Tpa (3-300 μM) before stimulation with ATP (5 mM, 1 h) (n=5) or silica (300 μg mL^{-1}, 4 h) (n=3). ****p<0.0001, ***p<0.001, **p<0.01, *p<0.05 determined by one-way ANOVA with Dunnett's post hoc analysis. Values shown are the mean ± SEM.

3.2.3 Pharmacological blockade of potassium channels does not inhibit the AIM2 or NLRC4 inflammasome

In addition to NLRP3, other well characterized inflammasomes AIM2 and NLRC4 also drive caspase-1 cleavage and subsequent IL-1β release in response to cytosolic DNA and intracellular bacteria respectively (260, 261). Previous studies have shown high extracellular K^+ fails to block AIM2 and NLRC4 inflammasomes (44, 45) demonstrating dependence on K^+ efflux is a unique feature of the NLRP3 inflammasome. AIM2 and NLRC4 inflammasomes can be activated by transfection of poly(dA:dT) and flagellin respectively (237). To determine whether the effect of K2P channel inhibition on IL-1β release is selective to NLRP3 inflammasome activation, the impact of K^+ channel inhibition on AIM2 and NLRC4-dependent IL-1β release was tested.

AIM2 inflammasome activation was not inhibited by any of the K^+ channel inhibitors tested including Tpa, TEA and quinine which were previously shown to inhibit NLRP3 activation (Fig. 3.6Ai). NLRC4 inflammasome activation was enhanced by Tpa and quinine but none of the K^+ channel inhibitors tested had an inhibitory effect on NLRC4 activation (Fig. 3.6Aii). Cell death in response to AIM2 inflammasome activation was also enhanced by Tpa and quinine (Fig. 3.6Bi), with Tpa also elevating cell death in response to NLRC4 inflammasome activation (Fig. 3.6Bii). These data show TEA, Tpa and quinine selectively inhibit the NLRP3 pathway, thus suggesting K^+ channels and specifically K2P channels selectively regulate NLRP3 inflammasome activation without impacting other inflammasomes.

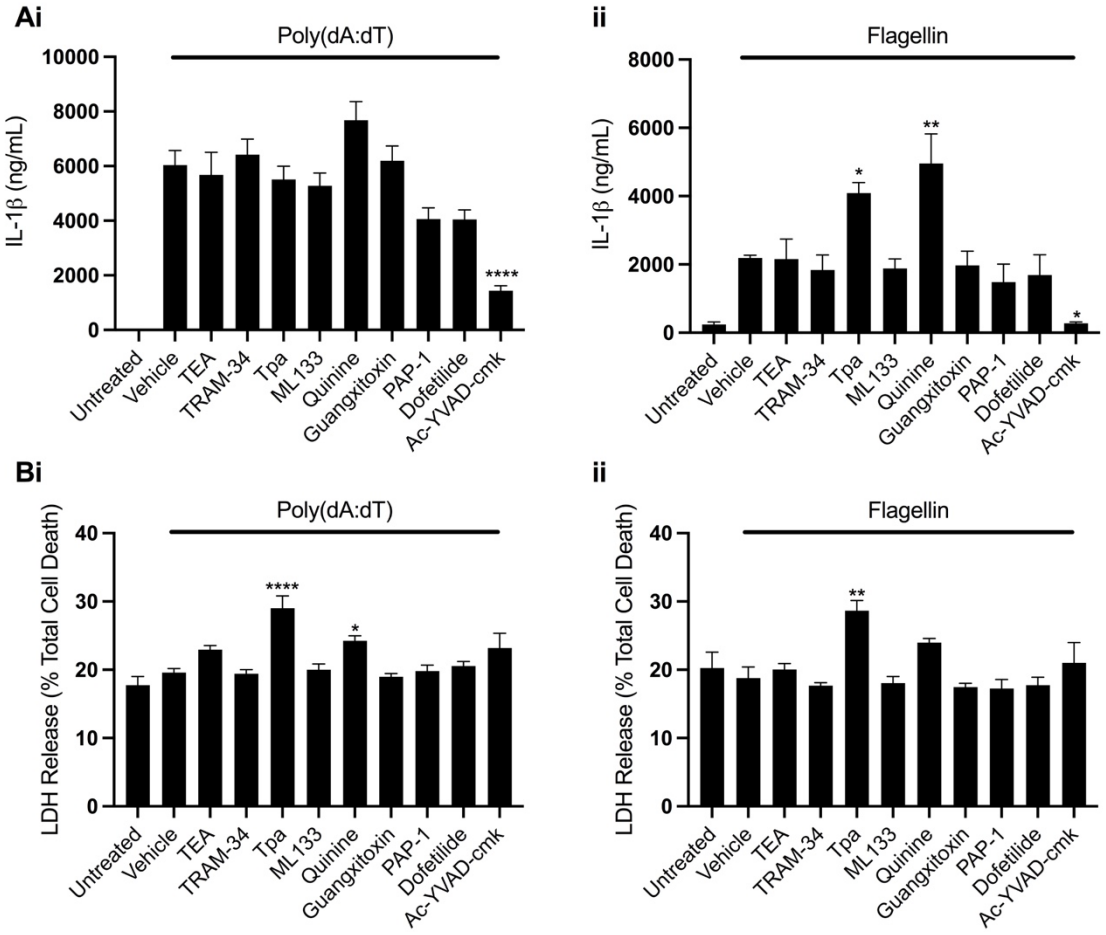

Figure 3.6 Pharmacological inhibition of two pore domain potassium channels selectively regulates the NLRP3 inflammasome.
(A) IL-1β ELISA and **(B)** LDH release assay of the supernatant of pBMDMs primed with LPS (1μg mL^{-1}, 4h) followed by pretreatment with the caspase-1 inhibitor Ac-YVAD-cmk (50 μM) or K^+ channel inhibitors TEA (50 mM), TRAM-34 (10 μM), Tpa (50 μM), ML-133 (20 μM), Quinine (100 μM), Guangitoxin-1E (25 nM), PAP-1 (2 μM) or Dofetilide (1μM) for 15 min before stimulation with transfected Poly(dA:dT) (1 μg mL^{-1}, 4 h) (n=3) or transfected ultrapure flagellin from Salmonella typhurium (1 μg mL^{-1}, 4 h) (n=3). ****p<0.0001, ***p<0.001, **p<0.01, *p<0.05 determined by one-way ANOVA with Dunnett's post hoc analysis. Values shown are the mean ± SEM.

3.2.4 Pharmacological blockade of two-pore domain potassium channels inhibits the NLRP3 priming step

Having observed inhibition of K2P channels to reduce NLRP3 activation, the impact of K^+ channel inhibition on the initial priming step of canonical NLRP3 inflammasome activation was also investigated. LPS-induced priming results in the activation of the transcription factor NF-κB, which in addition to upregulating NLRP3 and pro-IL-1β expression, also upregulates other pro inflammatory cytokines such as IL-6 and TNFα (262, 263). iBMDMs were pre-treated K^+ channel inhibitors and the NF-κB inhibitor Bay11 for 15 min prior to priming with LPS for 4 hours. TEA, Tpa and quinine significantly inhibited both IL-6 and TNFα release in response to LPS (Fig. 3.7A). None of the K^+ channel inhibitors tested had any effect on cell death (Fig. 3.7B). By western blot Tpa and TEA were found to inhibit LPS-induced protein expression of NLRP3 and pro-IL-1β (Fig. 3.7C). Together these results show Tpa, TEA and quinine inhibit both NLRP3 priming and activation suggesting K2P channels may also play a role in NLRP3 priming as well as activation.

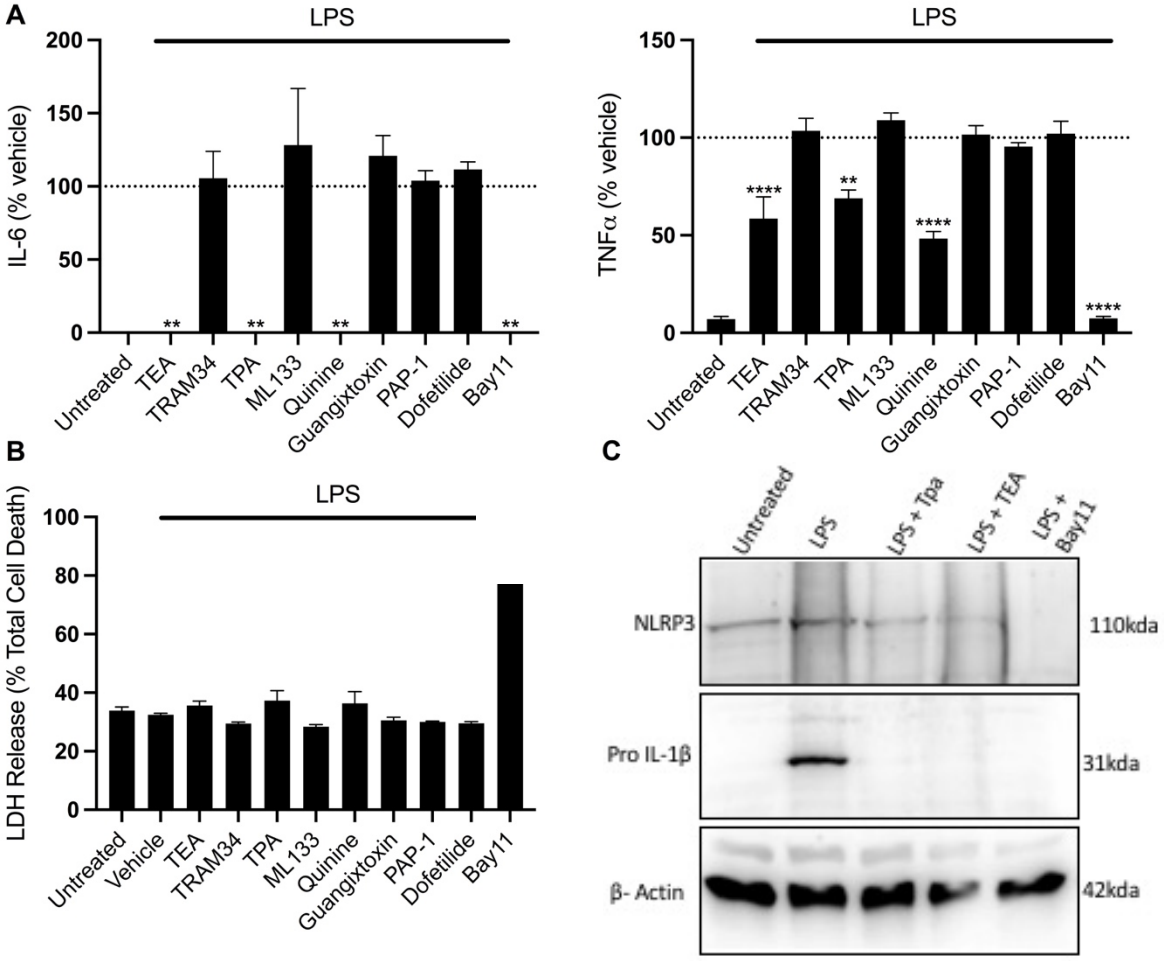

Figure 3.7 Pharmacological inhibition of two pore potassium channels blocks priming of the NLRP3 inflammasome.
(A) IL-6 and TNFα ELISA and **(B)** LDH release assay of the supernatant of iBMDMs pretreated with Bay11 (10 μM) or K^+ channel inhibitors TEA (50 mM), TRAM-34 (10 μM), Tpa (50 μM), ML-133 (20 μM), Quinine (100 μM), Guangitoxin-1E (25 nM), PAP-1 (2 μM) or Dofetilide (1 μM) for 15 min before priming with LPS (1 μg mL^{-1}, 4 h) (n=4). **(C)** NLRP3 and IL-1β western blot of the supernatant and total cell lysates respectively of iBMDMs pretreated with TEA (50 mM), Tpa (50 μM) or Bay11(10 μM) for 15 min before priming with LPS (1 μg mL^{-1}, 4 h). ****p<0.0001, **p<0.01 determined by one-way ANOVA with Dunnett's post hoc analysis. Values shown are the mean ± SEM.

3.2.5 Blocking two-pore domain potassium channels enhances ASC speck formation despite inhibiting NLRP3 inflammasome activation

Following activation, NLRP3 nucleates the oligomerization of the adaptor protein ASC. ASC itself then undergoes oligomerization into inflammasome specks which leads to caspase-1 recruitment and activation. To establish whether inhibition of K2P channels reduced NLRP3 activation via preventing ASC oligomerization, the effects of Tpa and TEA on ASC speck formation were investigated.

Using iBMDMs stably expressing ASC-mCherry (84), the effect of K^+ channel inhibition on ASC speck formation over time was tested. Incubation of LPS-primed ASC-mCherry iBMDMs with 5mM ATP induced the formation of ASC specks which were inhibited by MCC950 (204) (Fig. 3.8ai, 3.8aii). Tpa was observed to evoke a large and significant increase in the number of ASC specks formed in response to ATP (Fig. 3.8ai, 3.8aii). Furthermore, TEA had no effect on ATP-induced speck formation. These data reveal ASC speck formation occurs in the presence of concentrations of Tpa and TEA that inhibited the activation of caspase-1. ASC specks are released from the cell into extracellular space following cell death (264). To determine whether Tpa and TEA could stimulate the formation of ASC specks in the absence of an NLRP3 activating stimulus ASC-mCherry iBMDMs were treated with Tpa and TEA without ATP stimulation. Treatment with Tpa and TEA alone failed to induce ASC speck formation suggesting Tpa and TEA do not induce ASC oligomerization despite Tpa enhancing speck formation in response to ATP (Fig. 3.8aiii). The observation that Tpa enhances ASC speck formation in response to ATP yet TEA does not could potentially be due to differences in the ability of each compound to inhibit K2P channels. TEA is only a weak inhibitor of K2P channels whereas Tpa is effective at inhibiting K2P channels (68, 71). Therefore, a high degree of K2P channel inhibition with Tpa may enhance ASC speck formation but TEA may not inhibit K2P channels sufficiently to induce an increase in ASC specks in response to ATP. These data show a disassociation between ASC speck formation which resembles the oligomerization of inflammasome components from activation of the NLRP3 inflammasome into a caspase-1 activating complex. ASC oligomerization occurred in the presence of the inhibitors suggesting K^+ channel activation and specifically K2P channel activation may be required to shift inactive preformed ASC specks to active caspase-1 cleaving complexes.

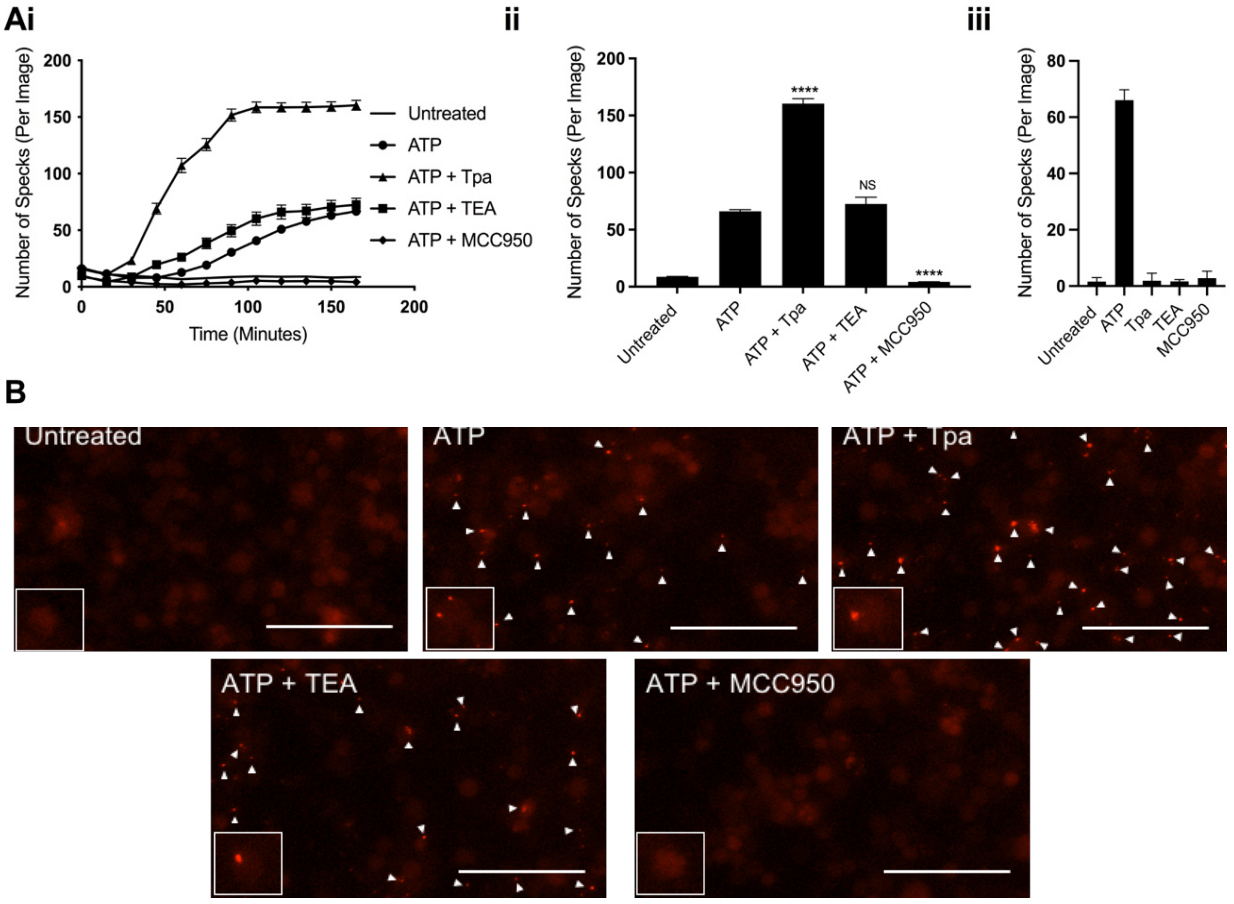

Figure 3.8 Potassium efflux is required for NLRP3 inflammasome activation but not ASC speck formation in response to ATP.
(Ai) ASC speck formation measured in real time and **(Aii)** ASC speck formation after 165 min of ATP stimulation from ASC-mCherry iBMDMs primed with LPS (1 μg mL^{-1}, 4 h) followed by pretreatment with vehicle control, TEA (50 mM), Tpa (50 μM) or MCC950 (10 μM) for 15 min before stimulation with ATP (5 mM) (n=6). **(Aiii)** ASC speck formation after 165 min from ASC-mCherry iBMDMS primed with LPS (1 μg mL^{-1}, 4 h) followed by treatment with, TEA (50 mM), Tpa (50 μM) or MCC950 (10 μM) in the absence of ATP (n=6). **(B)** Representative images of ASC-mCherry iBMDMs after 165 min ATP stimulation (Scale bar, 50 μm, arrows denote ASC specks). ASC speck experiments were performed in the presence of Ac-YVAD-CMK (50μM) to prevent pyroptosis and loss of ASC specks. ****p<0.0001, determined by one-way ANOVA with Dunnett's with Dunn's post hoc analysis. Values shown are the mean ± SEM.

3.2.6 Blocking potassium efflux enhances ASC speck formation despite inhibiting NLRP3 inflammasome activation

Our group previously reported Cl^- flux to be required for ASC oligomerization while NLRP3 activation is K^+ efflux-dependent (88). Having observed that inhibition of K2P channels with TPA increased ASC speck formation in response to ATP (Fig. 3.8) the next experiment aimed to determine whether TPA was enhancing speck formation via blocking K^+ efflux through K2P channels. The study investigated whether blocking K^+ efflux also enhances ASC speck formation in response to ATP. To understand the effect of blocking K^+ efflux on inflammasome activation we performed ion substitution experiments. LPS-primed iBMDMs were incubated in solutions with high K^+ and Cl^- free, or high K^+ and normal Cl^- to block only K^+ efflux or both K^+ and Cl^- efflux, respectively as previously reported (88). NLRP3 activation was then stimulated with ATP. Incubation with both high K^+ or high K^+ and Cl^- free completely abolished IL-1β release in response to ATP (Fig. 3.9Ai). Only incubation with high K^+ and normal Cl^- media inhibited ATP-induced cell death (3.9Aii). These data show that blocking K^+ efflux is sufficient to block activation of the NLRP3 inflammasome supporting the findings that K^+ channel inhibitors block NLRP3 activation (Fig. 3.2).

The study next aimed to investigate the impact of incubating iBMDMs in the above-mentioned isotonic salt solutions on ASC speck formation. To test the impact of isotonic salt solutions on ASC speck formation, ASC-mCherry iBMDMs were primed with LPS and incubated with a) normal K^+, normal Cl^-, b) high K^+, normal Cl^- or c) high K^+, Cl^- free solution. NLRP3 activation was stimulated with ATP and ASC formation analysed in real time. Blocking both K^+ and Cl^- efflux with high K^+ and normal Cl^- solution completely inhibited the formation of ASC-specks in response to ATP (Fig. 3.9Bi, 3.9Bii). In contrast, allowing Cl^- efflux but blocking K^+ efflux with high K^+ and Cl^- free solution enhanced ASC speck formation in response to ATP (Fig. 3Bii). These findings are consistent with our previous report that Cl^- efflux serves as an ASC oligomerizing signal while K^+ efflux is required for NLRP3 activation (88). These results show that blocking K^+ efflux directly or inhibiting K2P channels inhibits NLRP3-dependent caspase-1 activation but enhances ASC speck formation. Therefore, suggesting K2P channels and K^+ efflux are not involved in the formation of ASC specks in response to ATP.

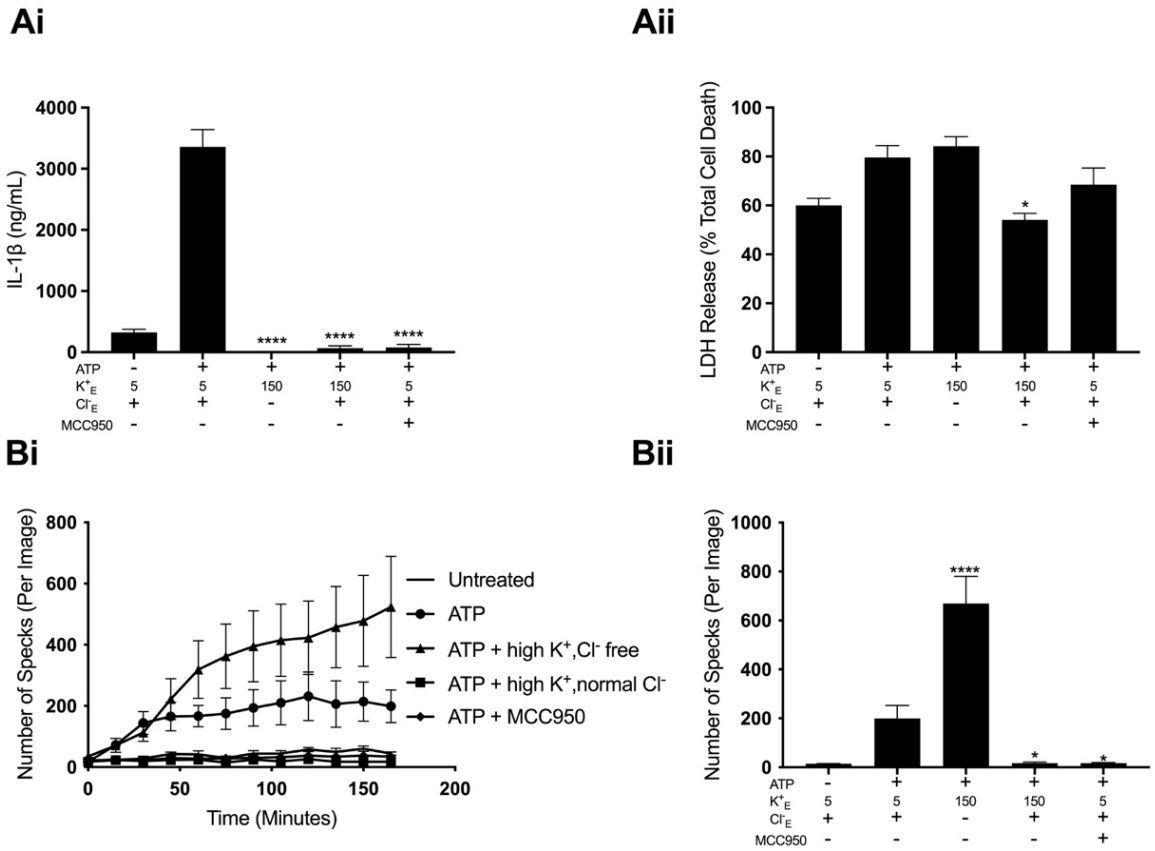

Figure 3.9 K^+ efflux is required for NLRP3 inflammasome activation but not ASC speck formation in response to ATP.
(A, i) IL-1β ELISA and **(A, i)** LDH assay of the supernatant of iBMDMs primed with LPS (1 μg mL^{-1}, 4 h) followed by incubation in a control (145 mM NaCl/ 5 mM KCl), high K^+ and normal Cl^- (150 mM KCl), high K^+ and Cl^- free (150 mM KGluconate) or control and MCC950 (10 μM) solution for 15 min before stimulation with ATP (5 mM, 1 h) (n=6). **(B, ii)** ASC speck formation measured in real time and **(B, iii)** ASC speck formation after 165 min of ATP stimulation from iBMDMs stably expressing ASC-mCherry (ASC-mCherry iBMDMs) primed with LPS (1 μg mL^{-1}, 4 h) followed by incubation in a control (145 mM NaCl/ 5 mM KCl), high K^+ and normal Cl^- (150 mM KCl), high K^+ and Cl^- free (150 mM KGluconate) or control and MCC950 (10 μM) solution for 15 min before stimulation with ATP (5 mM. 165 mins) (n=4). ****p<0.0001, *p<0.05 determined by one-way ANOVA with Dunnett's post hoc analysis. Values shown are the mean ± SEM.

3.2.7 Pharmacological inhibition of two-pore domain potassium channels reduces NLRP3 activation in murine mixed glia and microglia

Having observed Tpa to inhibit NLRP3 activation in BMDMs the study next aimed to determine whether Tpa mediated K2P inhibition could block NLRP3 in microglia, the brain resident macrophage cells. Initially, the impact of Tpa on ATP, silica, nigericin, or imiquimod-induced NLRP3 activation in primary mouse mixed glial cultures was investigated. Supporting the previous findings in BMDMs (Fig. 3.2), Tpa also inhibited NLRP3 activation in mixed glial cultures containing both microglia and astrocytes in response to ATP (Fig. 3.10Ai) and silica (Fig. 3.10Aii). TEA had no inhibitory effect on ATP or silica induced IL-1β release in mixed glia (Fig. 3.10Ai, 3.10Aii) despite inhibiting NLRP3 activation in BMDMs. Tpa and TEA had no impact on cell death in response to ATP (Fig. 3.10Bi) or silica (Fig. 3.10Bii).

Tpa and TEA failed to inhibit K^+ channel independent activation in response to nigericin and imiquimod in line with the findings in BMDMs (Fig. 3.11Ai, 3.11Aii) in addition to having no effect on imiquimod (Fig. 3.11Bi) and nigericin (Fig. 3.11Bii) induced cell death. These results show Tpa inhibits NLRP3 activation in mixed glia potentially through its ability to block K2P channels.

To confirm Tpa was inhibiting NLRP3 activation in microglial cells directly, the effect of Tpa on ATP and silica induced NLRP3 activation in isolated adult microglia was evaluated. Consistent with mixed glial culture data, ATP-induced IL-1β release was inhibited by Tpa in isolated adult microglia (Fig. 3.12A). In addition, Tpa inhibited IL-1β release from isolated microglia in response to silica (Fig. 3.12B). TEA also inhibited both ATP (Fig. 3.12A) and silica (Fig. 3.12B) induced NLRP3 activation in microglia. The observation that TEA inhibits NLRP3 activation in response to ATP and silica in adult microglia, but not neonatal mixed glial cultures could potentially be explained by age-dependent differences in microglial inflammatory responses. Neonatal microglia have been found to produce significantly more proinflammatory cytokines compared to adult cells in response to stimuli *in vitro* (265, 266). In addition, TEA is only a weak inhibitor of K2P channels (71). It is possible that greater K2P channel inhibition is required to dampen NLRP3 inflammasome activation in neonatal microglia in comparison to adult microglia. Therefore, TEA may inhibit sufficient K2P channels to attenuate NLRP3 activation in adult microglia, but in neonatal microglia greater K2P inhibition, not achieved by

TEA is required to inhibit NLRP3 activation. This study shows Tpa inhibits NLRP3 activation in response to both ATP and silica in both mixed glial and adult isolated microglial cultures. These results suggest Tpa sensitive channels are important for regulating NLRP3 activation within CNS resident microglia as well as peripheral macrophages.

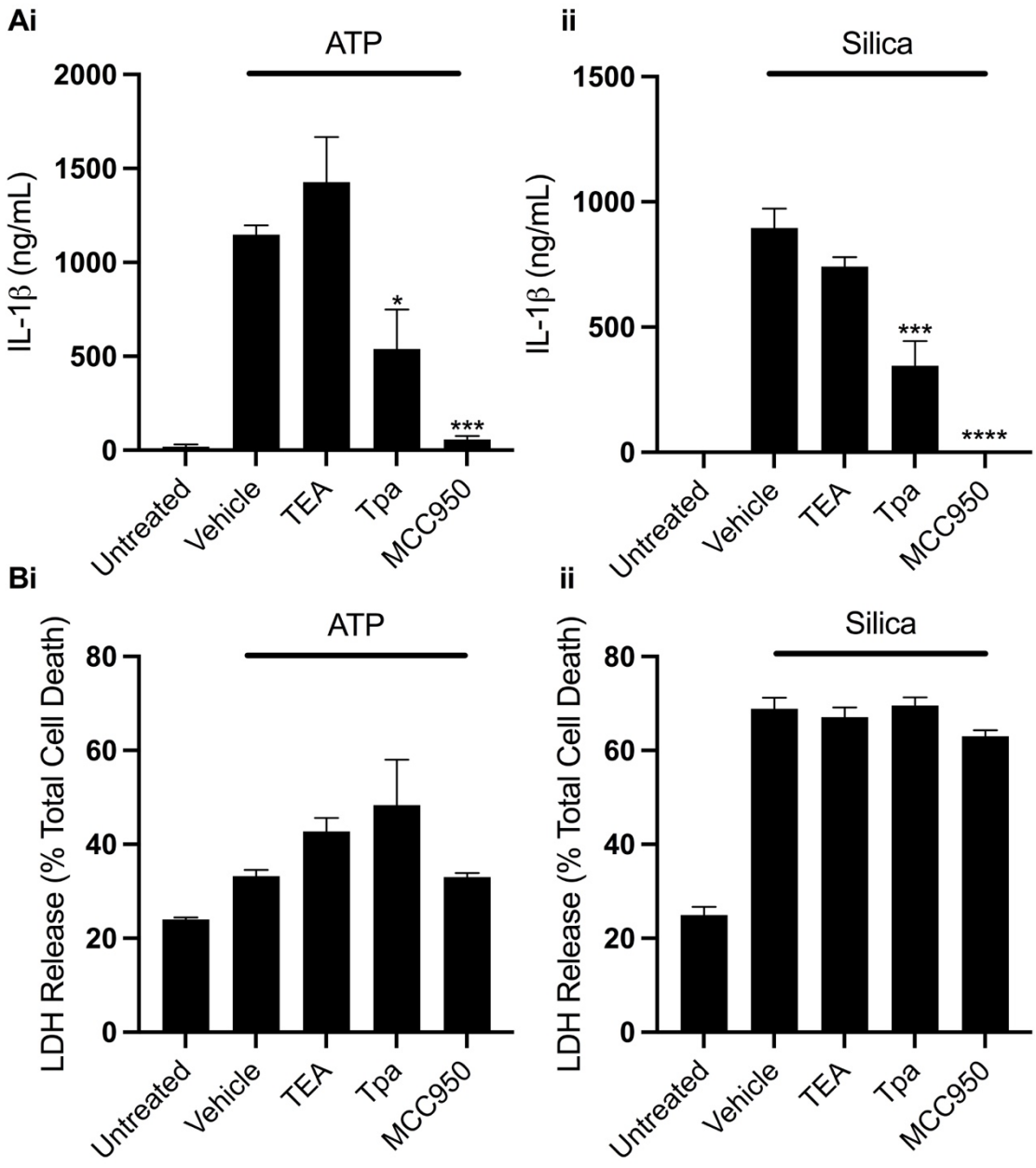

Figure 3.10 Inhibition of two pore domain potassium channels blocks ATP and silica induced NLRP3 activation in mixed glia.
(A) IL-1β ELISA and **(B)** LDH release assay of the supernatant of primary mouse mixed glia primed with LPS (1 µg mL^{-1}, 4 h) followed by pretreatment with vehicle control, TEA (50 mM), Tpa (50 µM) or MCC950 (10 µM) for 15 min before stimulation with ATP (5 mM, 1 h) (n=5) or silica (300 µg mL^{-1},4 h). ****p<0.0001, ***p<0.001, *p<0.05 determined by one-way ANOVA with Dunnett's post hoc analysis. Values shown are the mean ± SEM.

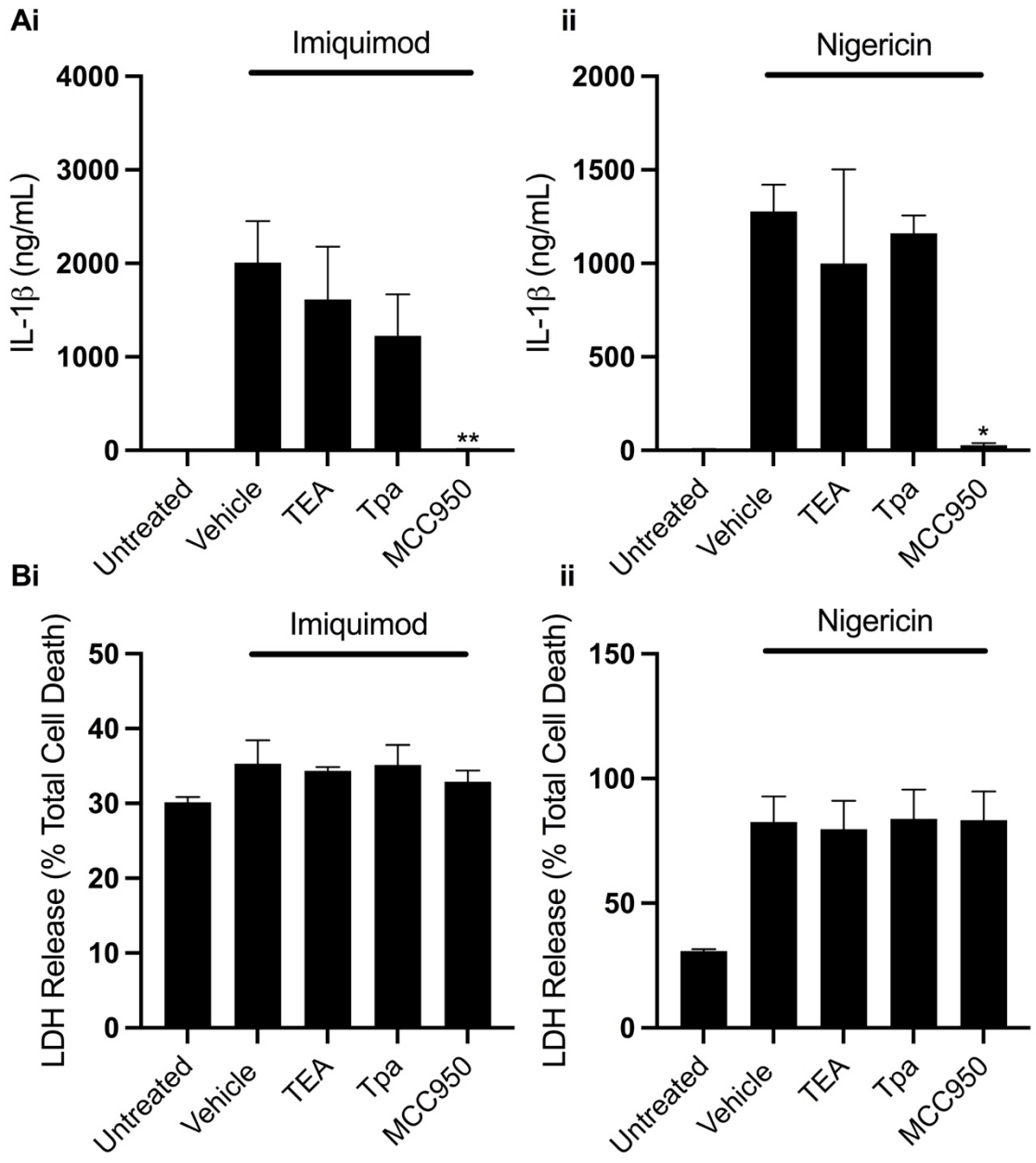

Figure 3.11 Inhibition of two pore domain potassium channels has no effect on imiquimod or nigericin induced NLRP3 activation in mixed glia.
(A) IL-1β ELISA and **(B)** LDH release assay of the supernatant of primary mouse mixed glia primed with LPS (1 μg mL^{-1}, 4 h) followed by pretreatment with vehicle control, TEA (50 mM), Tpa (50 μM) or MCC950 (10 μM) for 15 min before stimulation with imiquimod (75 μM, 2 h) (n=4) or nigericin (10 μM, 1 h) (n=3). ****p<0.0001, ***p<0.001, *p<0.05 determined by one-way ANOVA with Dunnett's post hoc analysis. Values shown are the mean ± SEM.

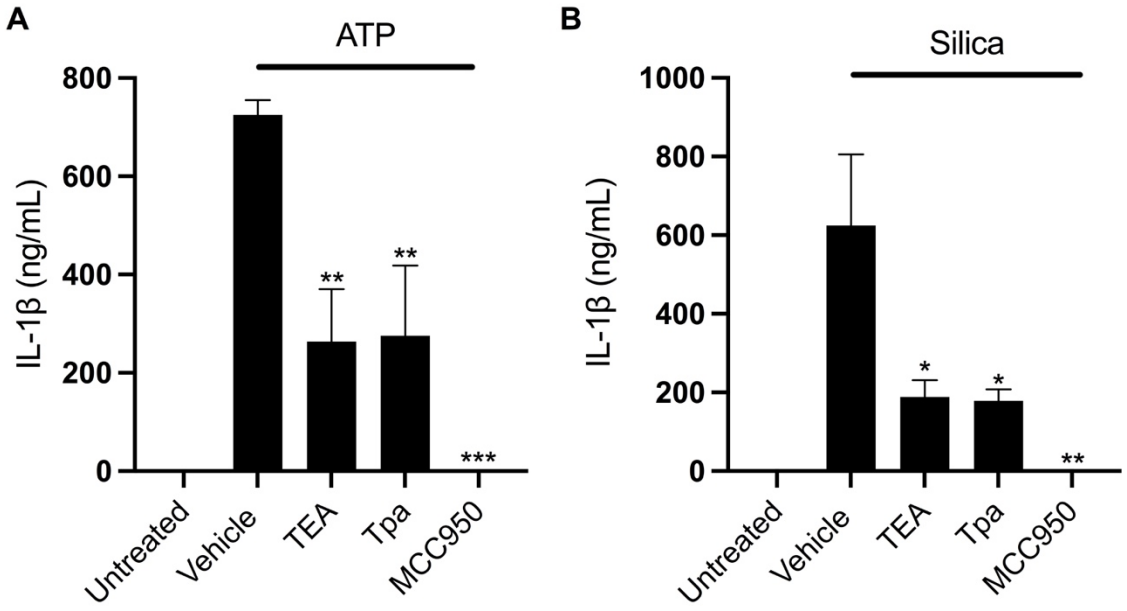

Figure 3.12 Inhibition of two pore domain potassium channels blocks ATP and silica induced NLRP3 activation in isolated microglia.
IL-1β ELISA of the supernatant of mouse primary microglia primed with LPS (1 μg mL^{-1}, 4 h) followed by pre-treatment with vehicle control, TEA (50 mM), Tpa (50 μM) or MCC950 (10 μM) for 15 min before stimulation with **(A)** ATP (5 mM, 1 h) (n=3) or **(B)** silica (300 μg mL^{-1},4 h) (n=3). ***p<0.001, **p<0.01, *p<0.05 determined by one-way ANOVA with Dunnett's post hoc analysis. Values shown are the mean ± SEM.

3.2.8 Canonical and alternative NLRP3 activation in human monocytes is inhibited by blocking two pore domain potassium channels

Previous research suggests that in addition to K^+ efflux dependent NLRP3 activation, LPS alone can stimulate caspase-1 activation and IL-1β release (87). This mechanism has been defined as alternative NLRP3 inflammasome activation and does not require K^+ efflux (104). The impact of the K2P channel inhibition on canonical and alternative NLRP3 activation in human monocyte THP-1 cell lines and also primary human CD14+ monocytes freshly isolated from healthy donors was therefore tested. Stimulation of K^+ dependent canonical NLRP3 activation via LPS priming and silica stimulation in THP-1 cells induced NLRP3 dependent IL-1β release (Fig. 3.13A). As observed in mouse BMDMs pre-treatment with Tpa and TEA inhibited IL-1β release in response to canonical activation in THP-1 cells (Fig. 3.13A). Alternative NLRP3 inflammasome activation was stimulated by treatment with LPS alone for 16 h in THP-1 cells. LPS treatment alone induced IL-1β release in a NLRP3-dependent manner which was also inhibited by Tpa and TEA (Fig. 3.13B). The impact of Tpa and TEA on alternative activation in CD14+ human monocytes was investigated following the same protocol. Following the same trend as THP-1 cells, alternative NLRP3 activation and IL1β release was inhibited by both Tpa and TEA in CD14+ monocytes (Fig. 3.13C). These results suggest K2P channels regulate both canonical and alternative mechanisms of NLRP3 activation in human monocytes.

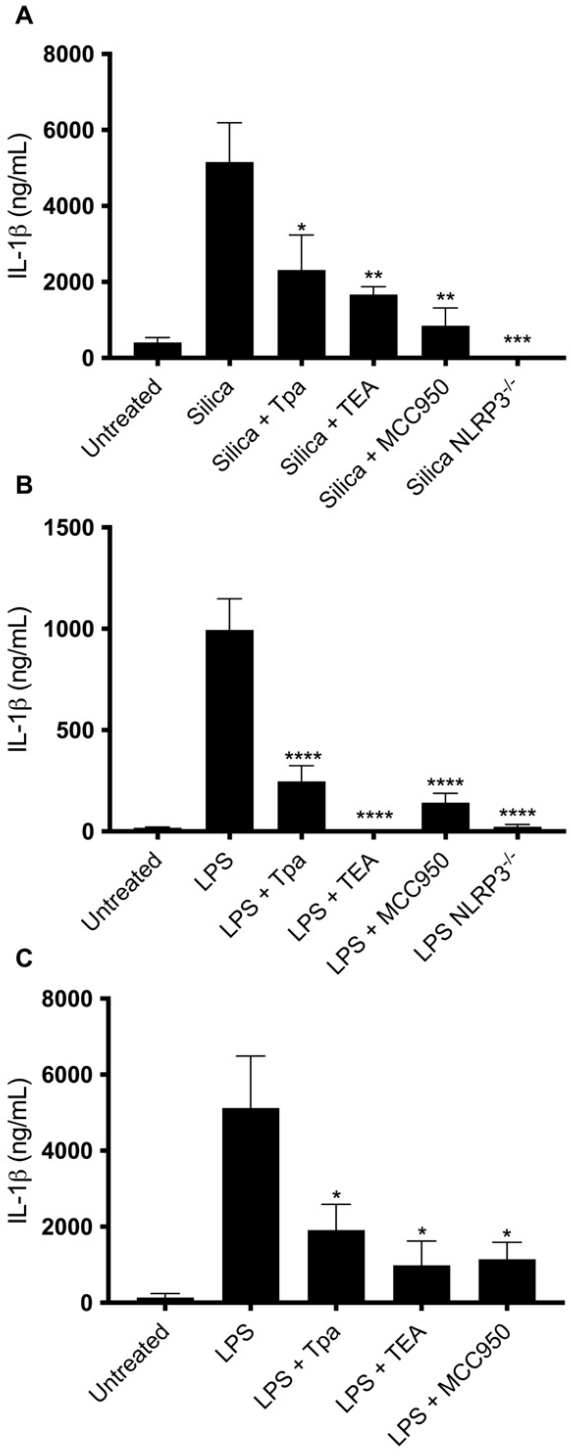

Figure 3.13 Pharmacological inhibition of two-pore domain potassium channels blocks canonical and alternative NLRP3 activation in human monocytes.
(A) IL-1β ELISA of the supernatant of WT and NLRP3 KO THP-1 monocytes primed with LPS (1 μg mL^{-1}, 4 h) followed by pre-treatment with vehicle control, Tpa (50 μM), TEA (50 mM) or MCC950 (10 μM) for 15 min before stimulation with silica (300 μg mL-1,4 h) (n=4). **(B)** IL-1β ELISA of the supernatant of WT and NLRP3 KO THP-1 monocytes pre-treated with vehicle control, Tpa (50 μM), TEA (50 mM) or MCC950 (10 μM) for 15 min before stimulation with LPS (1 μg mL^{-1}, 16 h) (n=6). **(C)** IL-1β ELISA of the supernatant of primary human monocytes pre-treated with vehicle control, Tpa (50 μM), TEA (50 mM) or MCC950 (10 μM) for 15 min before stimulation with LPS (1 μg mL^{-1}, 16 h) (n=3). ****p<0.0001, ***p<0.001, **p<0.01, *p<0.05 determined by one-way ANOVA with Dunnett's post hoc analysis. Values shown are the mean ± SEM.

3.2.9 Inhibition of two-pore potassium channels fails to inhibit potassium efflux in response to ATP treatment in murine macrophages

Previous studies have observed genetically knocking out the K2P channels THIK-1 or TWIK-2 abolished ATP-evoked K^+ current in mouse microglia and BMDMs respectively (68, 78). These findings suggest K2P channels may regulate ATP-induced NLRP3 activation via promoting K^+ efflux. To investigate whether inhibition of K^+ channels in general or K2P channels prevented K^+ efflux in response to ATP, the impact of TEA and Tpa on ATP-induced K^+ efflux was evaluated. iBMDMs were primed with LPS, then incubated with Ac-YVAD-Cmk to prevent pyroptotic cell death and loss of membrane integrity which would facilitate release of intracellular ions independently of ion channels/transporters. iBMDMs were then pretreated with Tpa, TEA and MCC950 before 15 min stimulation with ATP. Lysates were collected and cellular intracellular ion concentrations determined by inductively coupled plasma mass spectrometry (ICP-MS).

In response to ATP treatment, intracellular K^+ concentration was significantly reduced (Fig. 3.14A). Treatment with Tpa, TEA or MCC950 did not inhibit ATP-induced reduction in intracellular K^+ concentration (Fig. 3.14A). ATP also stimulated a significant reduction in intracellular magnesium (Mg^{2+}) (Fig. 3.14B), a significant increase in calcium (Ca^{2+}) (Fig. 3.14C) in addition a decrease in zinc (Zn^{2+}) however this was statistically insignificant (Fig. 3.14D). Tpa, TEA or MCC950 treatment has no effect on intracellular concentrations of Mg^{2+}, Ca^{2+} or $Zn^{2=}$ in response to ATP. These data show ATP induces a reduction in intracellular K^+ in iBMDMs which is not prevented by inhibition of K^+ channels with TEA or K2P channels with Tpa. The findings from this study suggest inhibition of K2P channels is insufficient to inhibit K^+ efflux in response to ATP.

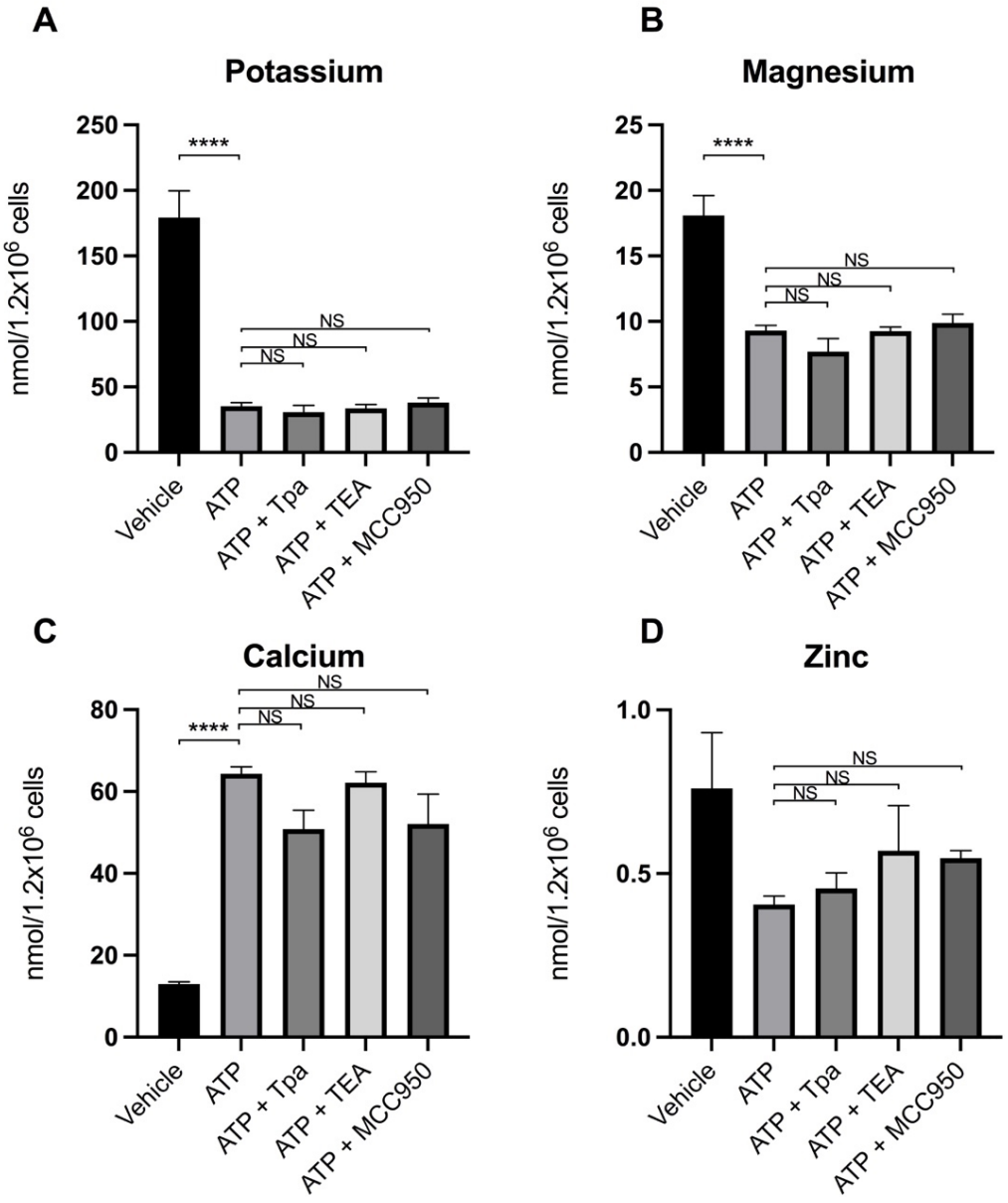

Figure 3.14 Pharmacological inhibition of two-pore domain potassium channels does not block ATP induced potassium, magnesium, calcium or zinc ion flux. Intracellular **(A)** K^+, **(B)** Mg^{2+}, **(C)** Ca^{2+} and **(D)** Zn^{2+} measurements from cell lysates of iBMDMs primed with LPS (1 µg mL^{-1}, 4 h) followed by incubation with Ac-YVAD-cmk (50 µM) to prevent cell death before pre-treatment with MCC950 (10 µM) or K^+ channel inhibitors Tpa (50 µM) or TEA (50 mM) for 15 min before stimulation with ATP (5 mM, 15 min) (n=4). ****p<0.0001 determined by one-way ANOVA with Dunnett's post hoc analysis. Values shown are the mean ± SEM.

3.3 Discussion

These data reveal K2P channels as potential regulators of ATP and silica-induced NLRP3 activation and suggest that this occurs through a mechanism independent of ASC oligomerization. These data suggest that in response to extracellular ATP and silica K2P channel activation is required for the activation of caspase-1.

Numerous studies over the years have provided evidence that K^+ efflux is a common event required for activation of NLRP3 in response to many stimuli (43–45). Recent findings have identified K2P channels TWIK-2 and THIK-1 as potential regulators of the K^+ sensitive process required for NLRP3 activation (68, 78). Knockdown of the TWIK-2 channel prevents K^+ efflux and NLRP3 activation induced by ATP while having no effect on K^+ channel independent stimuli nigericin and imiquimod (78). Furthermore, TWIK-2 was required for sepsis-induced NLRP3 inflammasome activation and inflammation *in vivo* (78). Previous research has also associated an additional K2P channel, THIK-1 with microglial function and ATP-induced IL-1β release in hippocampal slices (68). Genetic KO of THIK-1 in mice results in depolarization of microglia, decreased microglial ramification, reduced microglial surveillance and reduced IL-1β release in response to ATP (68). In support of these previous findings, this study shows, pharmacological inhibition of K2P channels with Tpa reduced NLRP3 activation in murine macrophages, monocytes and microglia. Moreover, K2P channel inhibition had no effect on activation of the AIM2 or NLRC4 inflammasomes, suggesting K2P regulation of inflammasome activation is limited to NLRP3.

In addition to reducing NLRP3 activation, K2P inhibition also dampened transcriptional NLRP3 priming demonstrated by a reduction in pro IL-1β and NLRP3 protein levels in addition to IL-6 and TNFα release in response to LPS induced TLR4 signaling. These data suggest K2P channels may also regulate NF-κB dependent priming of the NLRP3 inflammasome in addition to the secondary activation step. However, as with NLRP3 activation, Tpa inhibition of NLRP3 transcriptional priming could be driven by an off-target effect of Tpa independently of inhibiting K2P channels.

Furthermore, Tpa inhibited both canonical and K^+ independent alternative inflammasome activation in human monocytes (104). The impact of Tpa on alternative activation could be explained by the

findings that Tpa inhibited TLR4-mediated NLRP3 inflammasome priming, TLR4 signaling is also critical for alternative inflammasome activation (106). Tpa therefore, could potentially inhibit K^+ efflux independent alternative inflammasome activation via blocking TLR4 signaling pathways independently from its function as a K2P channel inhibitor.

Of the K2P channel family, RNA profiling of cultured BMDMs and microglia identified high expression of THIK-1 and TWIK-2 channels (Fig. 1). Previous research has already shown TWIK-2 to facilitate ATP-induced K^+ efflux and NLRP3 activation (78). Therefore, Tpa may inhibit NLRP3 activation through targeting TWIK-2, however, the study cannot rule out THIK-1 as a regulator of NLRP3 activation as it has been previously shown to regulate ATP-induce IL-1β release (68). This study using Tpa suggests K2P channels play a role in NLRP3 activation. However, K^+ channel modulators are known to inhibit cellular signaling pathways independently from action at K^+ ion channels (267–269). This study can therefore not rule out that the inhibitory action of Tpa on NLRP3 activation were due to off-target effects independent of K2P channel inhibition. Previous studies have used quinine as a K2P channel inhibitor, however, in this study quinine was found to inhibit K^+ efflux independent NLRP3 activation suggesting quinine can inhibit NLRP3 activation independently of its function as a K^+ channel inhibitor.

A previous study recently reported a mechanism of NLRP3 activation in which a Cl^- channel/transporter-dependent step is required to drive NLRP3-dependent ASC oligomerization (88). Although Cl^- efflux was required to form an ASC speck, K^+ efflux was required to permit activation of caspase-1 (88). These previous findings are supported by recent research which demonstrated low intracellular K^+ levels trigger a conformational change in ASC oligomer structure resulting in enhanced caspase-1 recruitment and activation (270). In the present study, inhibition of K2P channels, non-selective K^+ channel inhibition, and K^+ efflux blockage, all inhibited caspase-1 activation without blocking the formation of NLRP3-dependent ASC specks in response to ATP. Furthermore, both inhibition of K^+ and Cl^- efflux together abolished ATP-induced speck formation. These data provide further evidence dissociating the impact of Cl^- and K^+ efflux on NLRP3 formation and activation with Cl^- driving ASC oligomerization and K^+ efflux dependent mechanism acting

potentially via K2P channels driving caspase-1 activation. These data suggest that K2P channels may be required to enable full activation of the inflammasome and caspase-1 in response to ATP.

Genetic ablation of THIK-1 and TWIK-2 has previously been shown to inhibit ATP-induced K^+ efflux in microglia and macrophages respectively suggesting K2P channels facilitate NLRP3 activation through regulating K^+ efflux (68, 78). However, in this study, both nonselective K^+ channel inhibition and K2P channel inhibition did not prevent a reduction in intracellular K^+ concentration induced by ATP in macrophages. Experiments were conducted in the presence of a caspase 1 inhibitor to prevent ATP-induced pyroptosis and therefore stop rupturing of the plasma membrane and passive release of K^+ form the cell. The data from this study would therefore suggest K2P channels are important in regulating NLRP3 activation but are not solely responsible for mediating the K^+ efflux induced by ATP. The contrasting results observed in this study could potentially be due to differences in methodology used. This study used pharmacological inhibitors to investigate the effect of reducing K2P channel activity on ATP-induced K^+ efflux, whereas previous studies used genetic knockdown and knockout approaches (68, 78). It is possible that pharmacological compounds do not completely inhibit K2P channel activity therefore allowing K^+ efflux through the remaining uninhibited channels. In support of this hypothesis, inhibiting K2P channels did not completely abolish IL-1β release in response to ATP. This would suggest K2P inhibitors do not completely block K^+ efflux as previous studies have demonstrated that preventing K^+ efflux results in a complete inhibition of ATP-induced NLRP3 activation (45). However, K2P inhibition did not even modestly reduce K^+ efflux in response to ATP treatment in this study. It is possible the ICP-MS technique used in this study to measure intracellular K^+ is not sensitive enough to record small differences in K^+ concentration therefore inhibition of K2P channels may reduce K^+ efflux but this is not picked up through ICP-MS.

The present study identifies K2P channels as potential regulators of NLRP3 activation in mouse macrophages and microglia in addition to human monocytes. Consistent with previous work (88) the study observed the formation of ASC specks can occur without downstream activation of caspase-1 and IL-1β cleavage. The study shows inhibition of K2P channels of which TWIK-2 and THIK-1 are expressed in BMDMs and microglia reduces caspase-1, IL-1β and GSDMD processing. These

results suggest K2P channels THIK-1 and TWIK-2 may regulate NLRP3 activation in both peripheral and CNS immune cells.

Chapter 4: Selective inhibition of the THIK-1 potassium channel blocks NLRP3 inflammasome activation.

4.1 Introduction

In the previous chapter, inhibition of K2P channels was found to inhibit NLRP3 activation in murine peripheral macrophages and CNS resident microglia in addition to human monocytes. These findings highlighted the K2P channel family as potential K^+ channels responsible for facilitating the K^+ efflux required for NLRP3 activation (45). However, in Chapter 3 the specific K2P channels regulating NLRP3 activation could not be distinguished due to the lack of commercially available selective inhibitors of individual K2P channels. The potential K2P channels involved in NLRP3 activation were narrowed down by investigating which K2P channels are expressed in cells demonstrating robust NLRP3 activation. Through analysing RNA-sequencing databases, only two K2P channels, THIK-1 and TWIK-2 were found to be expressed by both BMDMs and microglia (Fig. 1.1) suggesting these specific K2P channels may regulate NLRP3 inflammasome activation.

TWIK-2 has previously been shown to regulate NLRP3 inflammasome activation in BMDMs (78). However, the role of THIK-1 in NLRP3 activation remains unclear. Genetic knockdown of THIK-1 has previously been identified to inhibit ATP-induced IL-1β release in mouse hippocampal slices (68). However, whether inhibition of IL-1β release was due to THIK-1 regulation of NLRP3 inflammasome activation was undetermined in that study. Although in Chapter 3, Tpa inhibition of K2P channels identified a potential role of K2P channels in NLRP3 activation, Tpa is a non-selective blocker of K2P channels and therefore inhibits both TWIK-2 and THIK-1 simultaneously (259, 271). Therefore, Tpa could not be used to distinguish whether TWIK-2 and/or THIK-1 regulate NLRP3 activation. As TWIK-2 has already been shown to regulate NLRP3 activation, this chapter aimed to determine whether the K2P channel THIK-1 also regulates NLRP3 activation.

To investigate the role of THIK-1 in NLRP3 inflammasome activation, two selective THIK-1 inhibitors, CVN1 and CVN2 were provided as part of an ongoing collaboration with the biotechnology company Cerevance. Both CVN1 and CVN2 were screened by Cerevance for inhibitory activity against K^+ channels structurally similar to THIK-1, including TWIK-2 to determine the selectivity of the compounds to THIK-1. CVN1 and CVN2 were both found to selectively inhibit THIK-1 without inhibiting other structurally related K^+ channels including TWIK-2 (Cerevance personal

communication). Therefore, these compounds provide useful tools to study the specific role of THIK-1 in NLRP3 inflammasome activation.

To investigate whether THIK-1 plays a role in NLRP3 activation, THIK-1 inhibiting compounds CVN1 and CVN2 were tested in an array of NLRP3 inflammasome assays in both human and murine cells. The aim of this chapter was to determine whether selective THIK-1 inhibiting compounds inhibit activation of NLRP3 *in vitro.*

4.2 Results

4.2.1 THIK-1 inhibitors do not induce NLRP3 activation despite forming crystals within the media

Following on from findings in Chapter 3 which identified K2P channel inhibition to reduce NLRP3 inflammasome activation, the next study aimed to investigate the role of the THIK-1 K2P channel in NLRP3 activation. To investigate THIK-1's role in NLRP3 activation two THIK-1 inhibiting compounds CVN1 and CVN2 were provided by the biotechnology company Cerevance, as part of an ongoing collaboration. Due to the limited solubility of compound CVN2 in culture media, multiple 30 min sonication steps were required to remove crystals in the media formed from undissolved CVN2 compound. Crystalline structures are known to induce NLRP3 inflammasome activation and IL-1β release (272). Therefore, before testing the impact of these compounds in NLRP3 inflammasome assays, the compounds were screened to ensure CVN1 and CVN2 alone in the absence of an NLRP3 activating stimulus could not induce NLRP3 activation due to the potential formation of crystals in cell culture media.

To determine whether CVN1 or CVN2 alone could induce NLRP3 activation, iBMDMs were primed with LPS (1 μg mL^{-1}, 4 h) before incubation with a range of CVN1 and CVN2 concentrations (0.1 μM-10 μM) for 3 h. ATP treatment was used to stimulate NLRP3 activation as a control. Both CVN1 (Fig.4.1A) and CVN2 (Fig.4.1B) failed to induce NLRP3 activation at any of the concentrations tested. These data show that despite the potential to form crystals of undissolved in culture media, CVN1 and CVN2 alone are not capable of inducing NLRP3 activation.

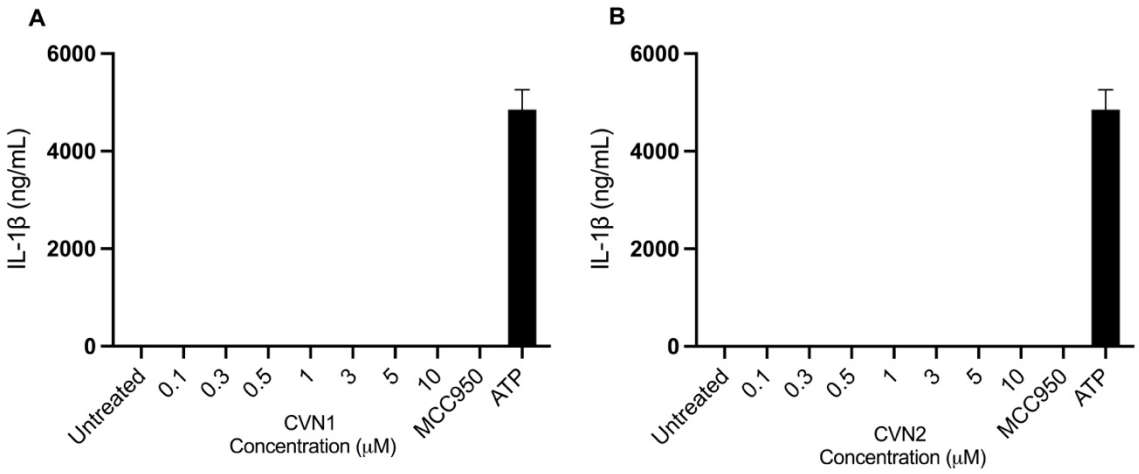

Figure 4.1 THIK-1 inhibitors CVN1 and CVN2 do not induce NLRP3 activation despite forming crystals of undissolved compound in cell culture media.
IL-1β ELISA of the supernatant of iBMDMs primed with LPS (1 μg mL^{-1}, 4 h) followed by treatment with CVN1 (0.1 μM-10 μM), CVN2 (0.1 μM-10 μM), MCC950 (10 μM) or ATP (5 mM, 1 h) (n=4). Statistical significance determined by one-way ANOVA with Dunnett's post hoc analysis. Values shown are the mean ± SEM.

4.2.2 Pharmacological inhibition of THIK-1 attenuates NLRP3 activation

Data collected in Chapter 3 suggested K2P channels regulate NLRP3 activation in both peripheral and CNS resident immune cells. Of the K2P channel family, RNA profiling of cultured BMDMs and microglia identified high expression of THIK-1 and TWIK-2 channels (Fig. 3.1) suggesting either THIK-1 and/or TWIK-2 can regulate NLRP3 activation. Previous research has already shown TWIK-2 to facilitate ATP-induced K^+ efflux and NLRP3 activation (78). However, the role of the K2P channel THIK-1 in NLRP3 activation remains unknown. This study utilized two selective THIK-1 inhibitors CVN1 and CVN2 provided by Cerevance to investigate the impact of selectively inhibiting THIK-1 on NLRP3 activation to determine whether THIK-1 in addition to TWIK-2 can also regulate NLRP3 activation. CVN1 and CVN2 are both selective THIK-1 inhibiting compounds but have significantly different core chemical structures.

To study the role of THIK-1 in NLRP3 activation, iBMDMs were primed with LPS (1 μg mL^{-1}) for 4 h, cells were then incubated with a range of concentrations (1 nM-10 μM) of CVN1 or CVN2 for 15 min and 30 min respectively. Incubation with MCC950 was used as a positive control (204). NLRP3 activation was then stimulated with ATP (5 mM) for 1 h. CVN1 began to significant inhibit ATP-induced IL-1β at 50 nM with the greatest inhibition observed at 100 nM (Fig. 4.2Ai). CVN1 failed to inhibit NLRP3 activation at concentrations lower than 50 nM. To determine whether 100 nM was the maximum effective concentration of CVN1, the impact of CVN1 concentrations above 100 nM on ATP-induced NLRP3 activation were tested. CVN1 also inhibited NLRP3 activation at higher concentrations ranging from 100 nM (0.1 μM) to 10 μM (Fig.4.2Aii). However, concentrations above 100 nM resulted in no greater NLRP3 inhibition in comparison to 100 nM CVN1 suggesting 100nM is the maximum effective NLRP3 inhibiting concentration of CVN1. At all concentrations tested (1 nM-10 μM) CVN1 failed to inhibit cell death in response to ATP, whereas MCC950 significantly inhibited ATP-induced cell death (Fig. 4.2B).

Having established the THIK-1 inhibitor CVN1 to attenuate NLRP3 activation in response to ATP, the impact of an additional THIK-1 inhibitor CVN2 was tested. In support of CVN1 findings, CVN2 also significantly inhibited ATP-induced IL-1β release (Fig. 4.3A). CVN2 was found to be a more potent NLRP3 inhibitor than CVN1, significantly inhibiting NLRP3 activation at 10 nM, with the

maximum inhibition observed at 100 nM (Fig. 4.3Ai). Increasing the concentration above 100 nM (0.1 μM) resulted in no greater inhibition suggesting as with CVN1, the maximum effective concentration of CVN2 is 100 nM (Fig. 4.3Aii). CVN2 failed to inhibit ATP-induced cell death at any of the concentrations used (Fig. 4.3B). These data show two THIK-1 inhibitors CVN1 and CVN2 both inhibit ATP-induced NLRP3 activation at nM concentrations. CVN2 was found to significantly inhibit NLRP3 at lower concentrations than CVN1, however, both compounds had the same maximum effective concentration of 100 nM. Therefore, suggesting the K2P channel THIK-1 regulates NLRP3 activation in addition to TWIK-2 previously shown to regulate NLRP3 activation (78).

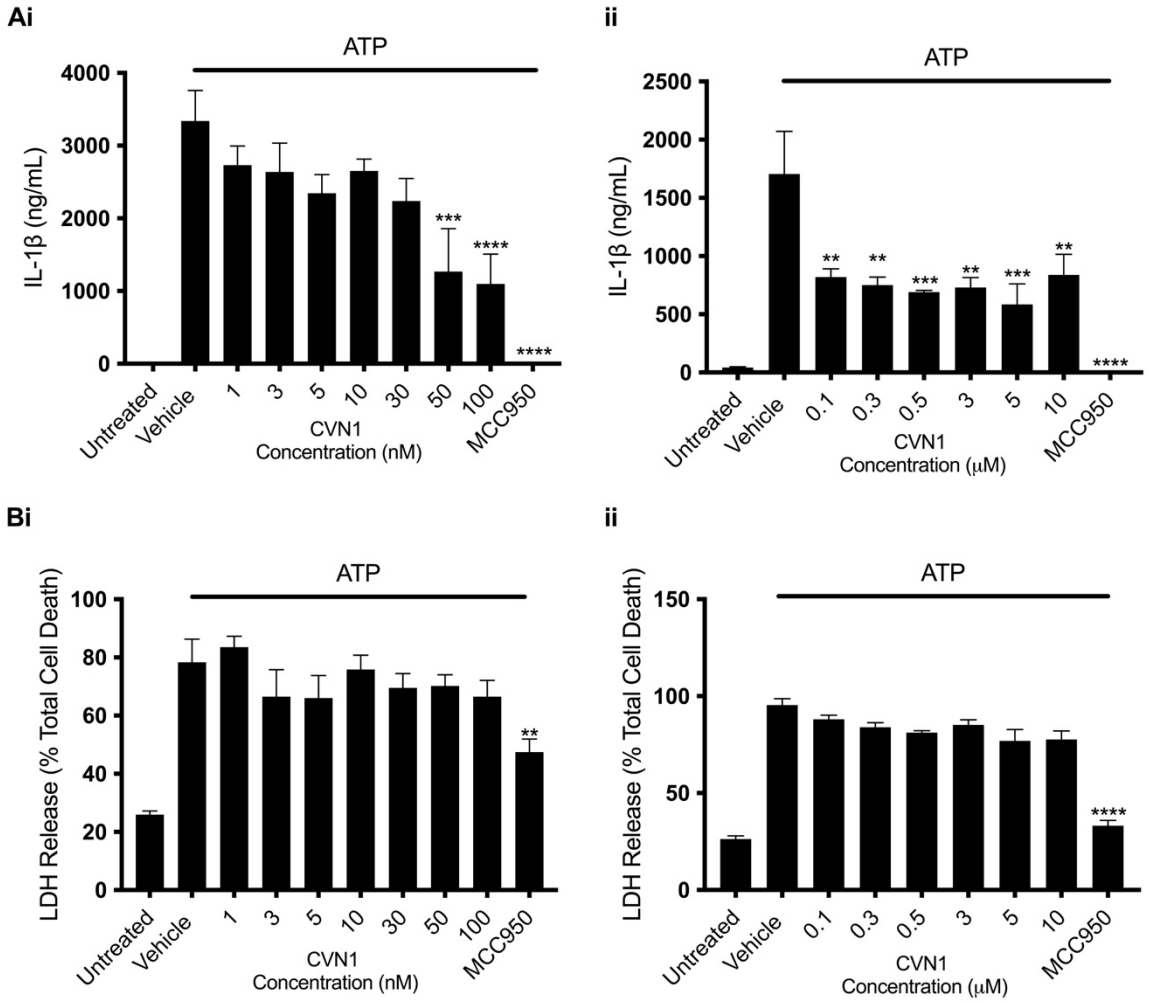

Figure 4.2 Pharmacological inhibition of THIK-1 with CVN1 blocks NLRP3 activation and IL-1β release in response to ATP.
A) IL-1β ELISA or **(B)** LDH release assay of the supernatant of iBMDMs primed with LPS (1 μg mL^{-1}, 4 h) followed by pretreatment with CVN1 (1 nM-10 μM) or MCC950 (10 μM) for 15 min before stimulation with ATP (5 mM, 1 h) (n=3-4). ****p<0.0001, ***p<0.001, **p<0.01 determined by one-way ANOVA with Dunnett's post hoc analysis. Values shown are the mean ± SEM.

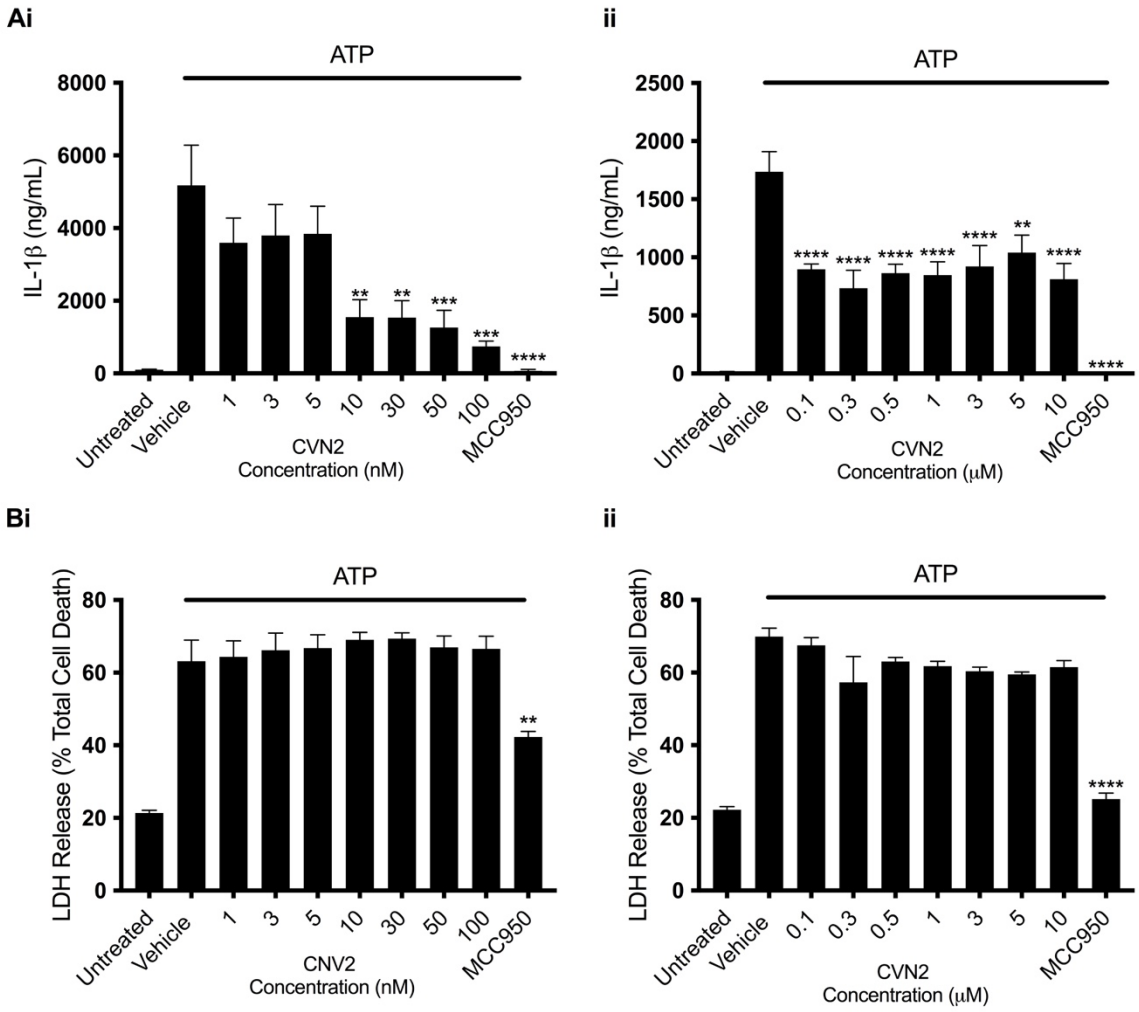

Figure 4.3 Pharmacological inhibition of THIK-1 with CVN2 blocks NLRP3 activation and IL-1β release in response to ATP.
(A) IL-1β ELISA or **(B)** LDH release assay of the supernatant of iBMDMs primed with LPS (1 μg mL^{-1}, 4 h) followed by pretreatment with CVN2 (1 nM-10 μM) for 30 min or MCC950 (10 μM) for 15 min before stimulation with ATP (5 mM, 1 h) (n=3-4). ****p<0.0001, ***p<0.001, **p<0.01 determined by one-way ANOVA with Dunnett's post hoc analysis. Values shown are the mean ± SEM.

Having established the maximum effective concentration of CVN1 and CVN2 to be 100 nM, the next study aimed to test the effect of 100 nM CVN1 and CVN2 on NLRP3 activation in response to additional canonical stimuli. Firstly, to determine whether THIK-1 inhibitors reduce NLRP3 activation in response to K^+ efflux dependent stimuli in addition to ATP, the impact of CVN1 and CVN2 on silica-induced activation was investigated. ATP-induced NLRP3 activation is dependent upon P2X7 receptor activation (55), whereas, silica induces activation through lysosomal destabilization (148). pBMDMs were primed with LPS for 4 h, cells were then incubated with 100 nM CVN1 or CVN2 for 15 and 30 min respectively, followed by NLRP3 stimulation with silica for 4 h. Both CVN1 and CVN2 significantly inhibited NLRP3 activation in response to silica (Fig. 4.4A) without inhibiting cell death (Fig. 4.4B). These data show CVN1 and CVN2 inhibit NLRP3 activation in response to silica in addition to ATP. This suggests CVN1 and CVN2 inhibit NLRP3 activation independently from directly blocking P2X7 receptor activation as silica-induced activation does not require P2X7 receptor activity.

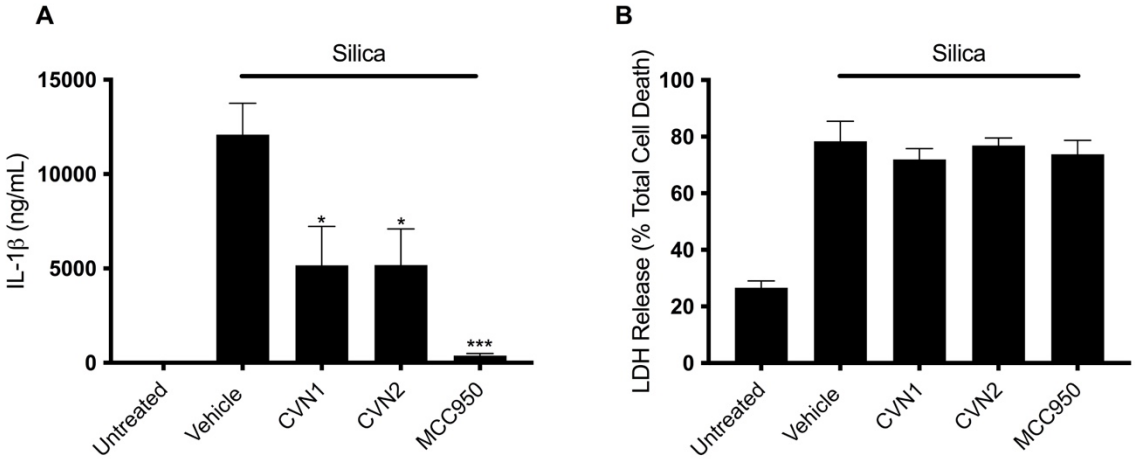

Figure 4.4 Pharmacological inhibition of THIK-1 with CVN1 or CVN2 blocks NLRP3 activation and IL-1β release in response to silica.
(A) IL-1β ELISA or **(B)** LDH release assay of the supernatant of pBMDMs primed with LPS (1 μg mL^{-1}, 4 h) followed by pretreatment with CVN1 (100 nM) for 15 min, CVN2 (100 nM) for 30 min or MCC950 (10 μM) for 15 min before stimulation with silica (300 μg mL^{-1}, 4 h) (n=4). ***p<0.001, *p<0.05 determined by one-way ANOVA with Dunnett's post hoc analysis. Values shown are the mean ± SEM.

The study next investigated the impact of CVN1 and CVN2 on K^+ channel independent NLRP3 activation. In order to determine whether the compounds had any K^+ channel independent "off-target" effects, the K^+ efflux independent stimuli imiquimod (21) and the K^+ channel independent stimuli nigericin were used (55). Stimulation of LPS primed pBMDMs with imiquimod induced IL-1β release which was inhibited by CVN1 but not CVN2 (Fig. 4.5Ai). In addition, CVN1 also inhibited imiquimod induced cell death, while CVN2 had no effect on cell death (Fig. 4.5Bi). Treatment with both CVN1 and CVN2 inhibited both nigericin-induced NLRP3 activation (Fig. 4.5Aii) and cell death (Fig. 4.5Bii). These data showing CVN1 inhibits both imiquimod and nigericin-induced NLRP3 activation suggest CVN1 inhibits canonical NLRP3 activation through inhibition of THIK-1 as well as potentially additional mechanisms independent of K^+ efflux modulation. However, it is possible THIK-1 is capable of regulating NLRP3 activation through additional mechanisms, in addition to facilitating K^+ efflux in response to certain NLRP3 stimuli. This would explain CVN1 inhibition of nigericin and imiquimod-induced NLRP3 activation. Although, CVN2 did not inhibit imiquimod-induced NLRP3 activation which would suggest CVN2 is inhibiting NLRP3 specifically through inhibiting K^+ efflux dependent mechanisms. Both CVN1 and CVN2 did inhibit nigericin-induced NLRP3 activation which suggests K^+ channels such as THIK-1 may play a role in nigericin-induced NLRP3 activation. The findings that both CVN1 and CVN2 inhibit nigericin-induced NLRP3 activation suggests THIK-1 and potentially other K^+ channels regulate NLRP3 activation in response to pore forming toxins. The observation that CVN1 and CVN2 have different effects on imiquimod-induced NLRP3 activation highlights the compounds differ slightly in activity profiles. Taken together, these data show THIK-1 inhibiting compounds CVN1 and CVN2 are effective inhibitors of canonical NLRP3 activation in BMDMs.

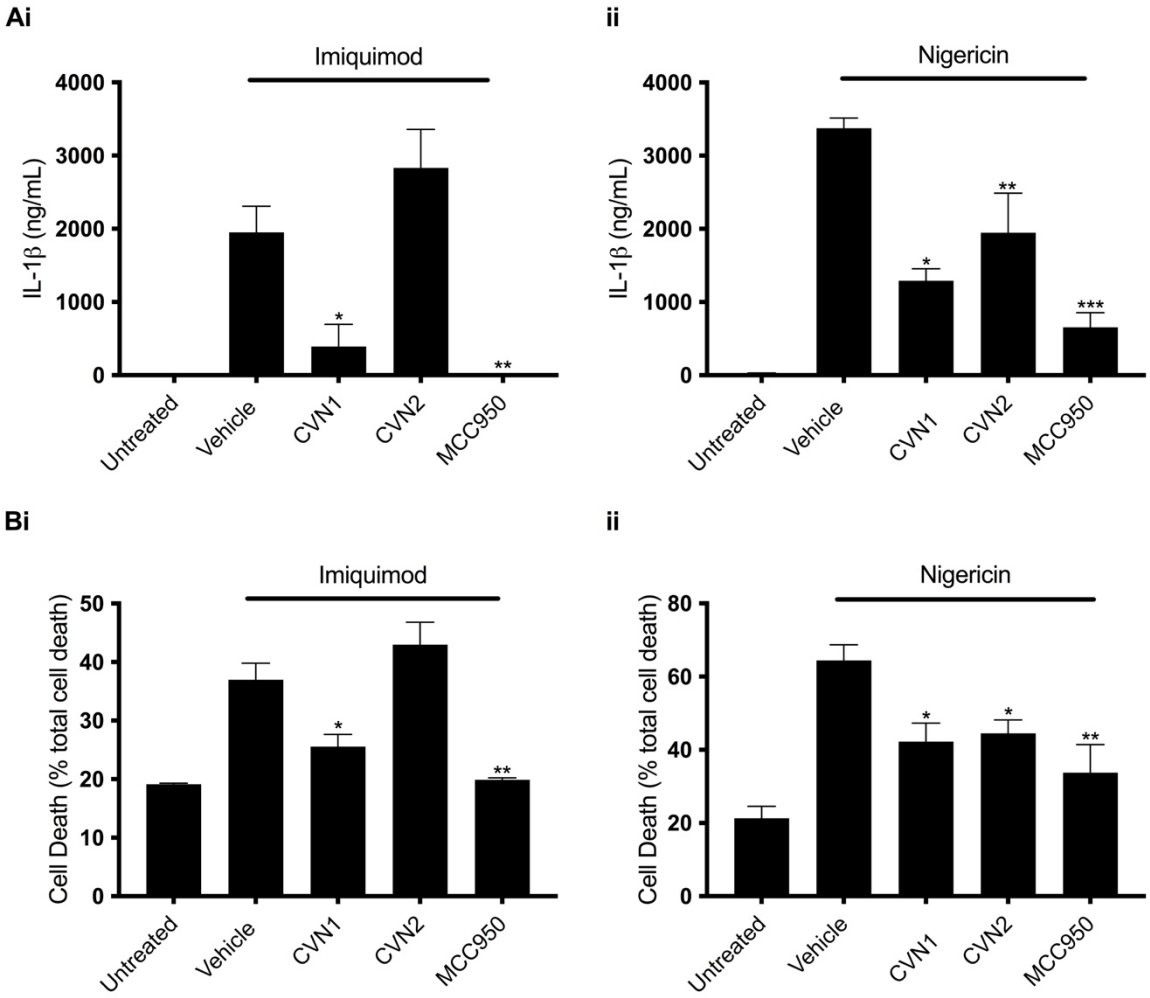

Figure 4.5 Pharmacological inhibition of THIK-1 with CVN1 or CVN2 blocks NLRP3 activation and IL-1β release in response to nigericin and imiquimod.
5 (A) IL-1β ELISA or **(B)** LDH release assay of the supernatant of pBMDMs primed with LPS (1 μg mL^{-1}, 4 h) followed by pretreatment with CVN1 (100 nM) for 15 min, CVN2 (100 nM) for 30 min or MCC950 (10 μM) for 15 min before stimulation with imiquimod (75 μM, 2 h) (n=4) or nigericin (10 μM, 1 h) (n=4) ***p<0.001, **p<0.01, *p<0.05 determined by one-way ANOVA with Dunnett's post hoc analysis. Values shown are the mean ± SEM.

As previously mentioned in Chapter 3, NLRP3 inflammasome activation results in caspase-1 activation and subsequent pro IL-1β and GSDMD cleavage (90, 116). To determine whether CVN1 and CVN2 inhibit downstream mediators of NLRP3 activation, western blotting was used to investigate the effect of CVN1 and CVN2 on ATP-induced caspase-1, IL-1β and GSDMD cleavage. Western blot analysis showed that ATP-induced caspase-1, IL-1β and GSDMD processing was inhibited by CVN1 and CVN2 (Fig. 4.6A, Fig. 4.6B) further indicating CVN1 and CVN2 as inhibitors of NLRP3 inflammasome activation. In addition to western blot experiments, the caspase Glo quantitative assay of caspase-1 enzymatic activity was used. In support of western blot experiments CVN1 inhibited caspase-1 activity in iBMDMs in response to ATP treatment (Fig. 4.6C). In contrast, CVN2 did not inhibit caspase-1 activity in in response to ATP in the caspase Glo assay (Fig. 4.6C), despite inhibiting caspase-1 cleavage and subsequent IL-1β and GSDMD processing (Fig. 4.6B). These contrasting results with CVN2 could be potentially caused by the limited solubility of the compound in cell culture media. As previously mentioned, CVN2 required two 30-minute sonication steps to ensure CVN2 dissolved in culture media and remove crystals of undissolved CVN2. The failure of CVN2 to inhibit caspase-1 activity in the caspase Glo assay is therefore likely due to CVN2 not dissolving fully into the culture media for these specific experiments. Taken together, these data suggest CVN1 and CVN2 inhibit of NLRP3 activation and downstream processing of caspase-1, IL-1β and GSDMD.

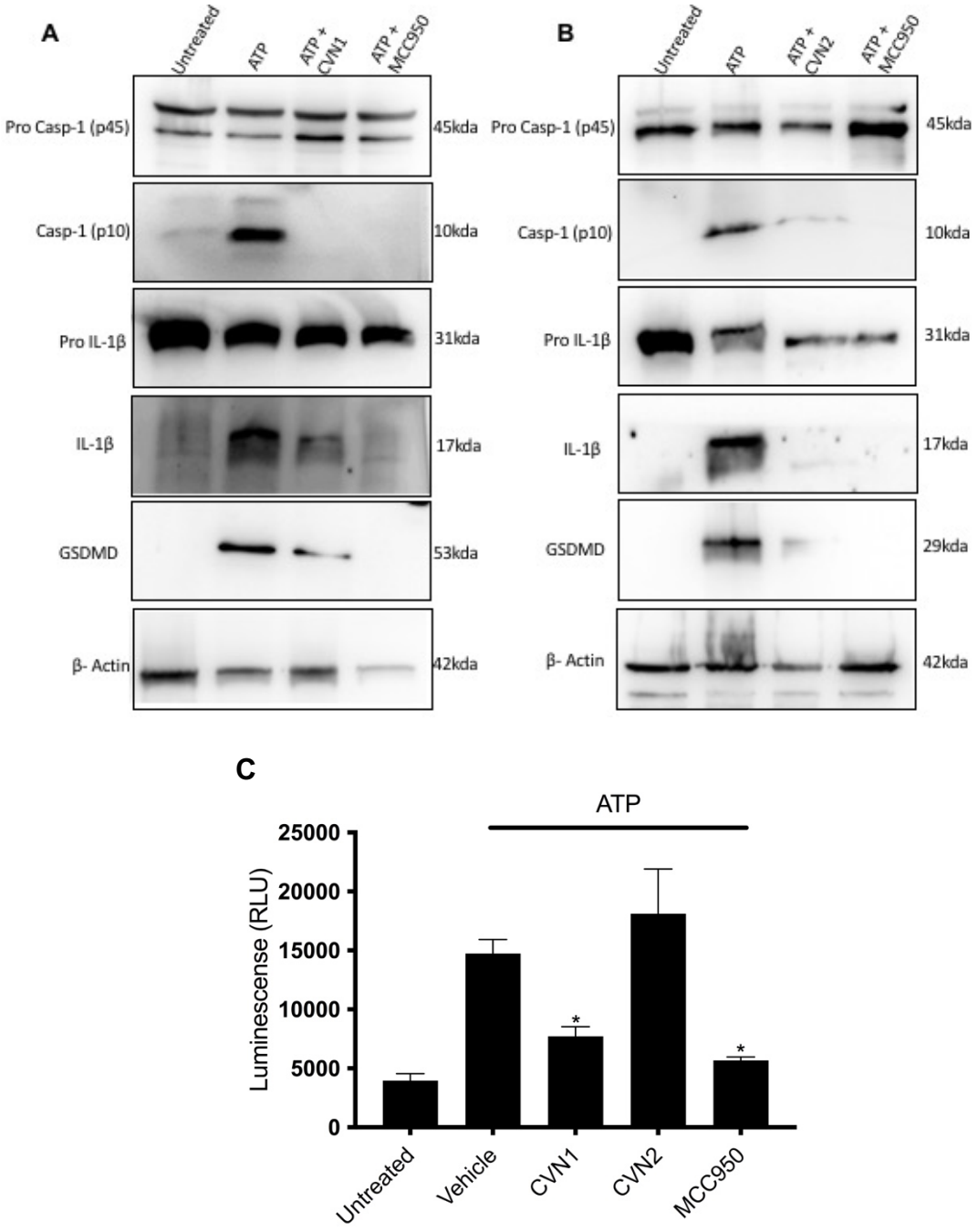

Figure 4.6 Pharmacological inhibition of THIK-1 potassium channels blocks caspase-1, IL-1β and GSDMD processing in response to ATP-induced NLRP3 activation.
(A, B) Caspase-1, IL- β and gasdermin D western blot of total cell lysates (cell lysate + supernatant) from LPS-primed (1 μg mL^{-1}, 4 h) iBMDMs pretreated with **(A)** vehicle control, CVN1 (100 nM) or MCC950 (10 μM) for 15 min then stimulated with ATP (5 mM, 1 h) or **(B)** vehicle control, CVN2 (100 nM) for 30 min or MCC950 (10 μM) for 15 min then stimulated with ATP (5 mM, 1 h). **(C)** Caspase-1 Glo assay to measure caspase-1 activity of LPS-primed (1 μg mL^{-1}, 4 h) iBMDMs pretreated with vehicle control, CVN1 (100 nM) for 15 min, CVN2 (100 nM) for 30 min or MCC950 (10 μM) for 15 min then stimulated with ATP (5 mM, 1 h) (n=4). *p<0.05 determined by one-way ANOVA with Dunnett's post hoc analysis. Values shown are the mean ± SEM.

4.2.3 Pharmacological blockade of THIK-1 potassium channels does not inhibit the AIM2 or NLRC4 inflammasome

As discussed in Chapter 3 section 3.2.3, in addition to NLRP3, other inflammasomes such as AIM2 and NLRC4 also drive caspase-1 activation and IL-1β release. However, dependence on K^+ efflux is a unique feature of the NLRP3 inflammasome as AIM2 and NLRC4 inflammasomes do not require K^+ efflux for activation (42, 43). In Chapter 3 section 3.2.3, non-selective K^+ channel inhibition and inhibition of K2P channels were found to inhibit NLRP3 activation but not AIM2 or NLRC4 inflammasomes suggesting K2P channels including THIK-1 do not regulate the AIM2 or NLRC4 inflammasome (Fig. 3.6). To determine the effect of THIK-1 inhibitors CVN1 and CVN2 on IL-1β release is selective to NLRP3 inflammasome activation, the impact of CVN1 and CVN2 on AIM2 and NLRC4 dependent IL-1β release was tested.

To test the impact of CVN1 and CVN2 on AIM2 and NLRC4 activation, pBMDMs were primed with LPS (1 μg mL^{-1}, 4 h). Cells were then incubated for 15 min with CVN1 or 30 min with CVN2. Incubation for 15 min with the caspase-1 inhibit Ac-YVAD-cmk was used as a positive control. pBMDMs were then transfected with poly(dA:dT) or flagellin to activate the AIM2 or NLRC4 inflammasome respectively. In support of the previous findings that K2P channel inhibition does not affect AIM2 or NLRC4 inflammasomes (Fig. 3.6), CVN1 and CVN2 had no effect on AIM2-induced IL-1β release (Fig.4.7Ai) or cell death (Fig. 4.7Bi). Furthermore, NLRC4 inflammasome activation was also unaffected by CVN1 or CVN2 (Fig. 4.7Aii). Cell death in response to NLRC4 activation was also unaffected by CVN1 or CVN2 (Fig. 4.7Bii). These data suggest CVN1 and CVN2 selectively inhibit the NLRP3 pathway, further suggesting THIK-1 K^+ channels do not regulate the AIM2 or NLRC4 inflammasome.

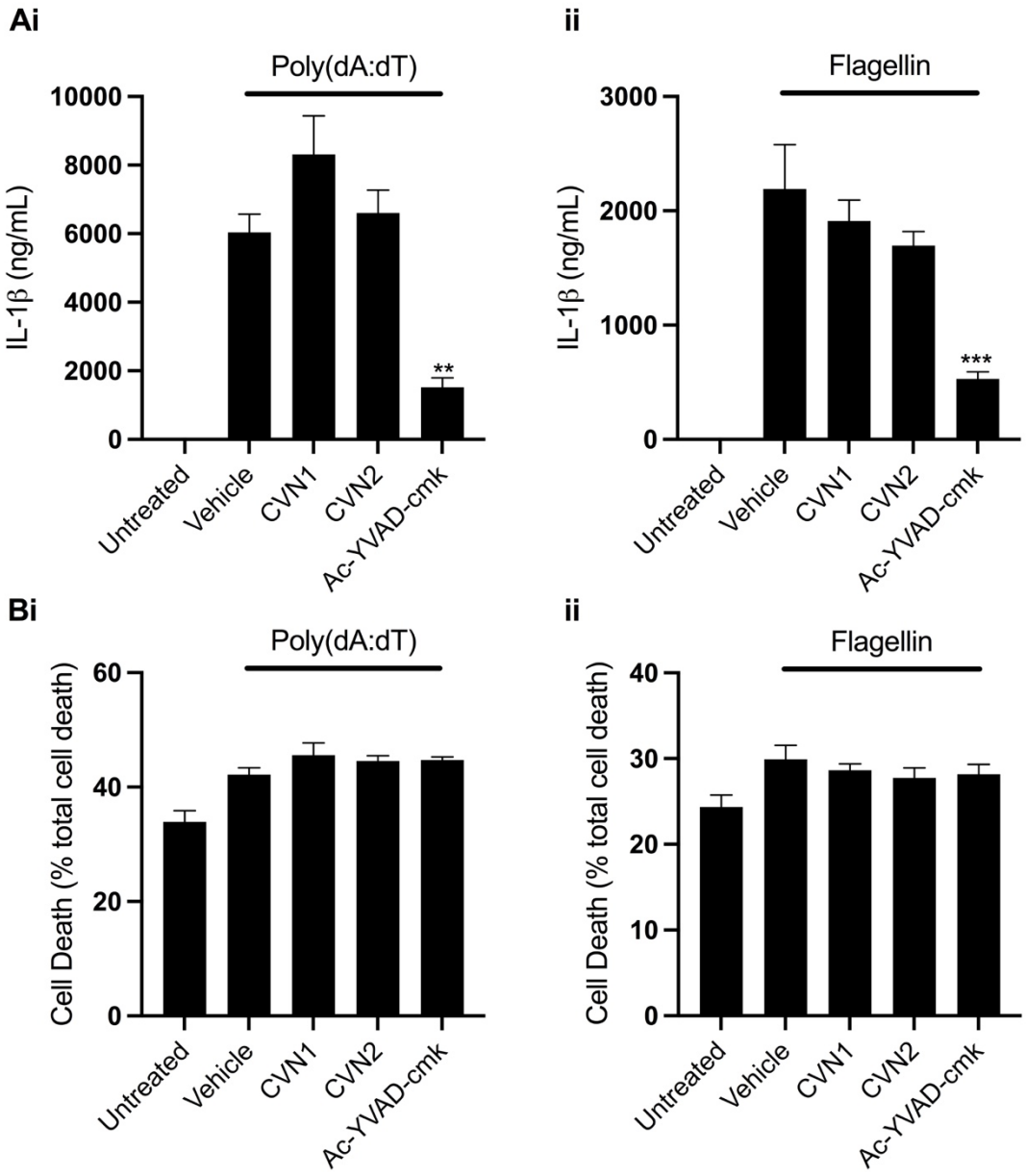

Figure 4.7 Pharmacological inhibition of THIK-1 potassium channels selectively regulates the NLRP3 inflammasome.
(A) IL-1β ELISA and **(B)** LDH release assay of the supernatant of pBMDMs primed with LPS (1 μg mL^{-1}, 4 h) followed by pretreatment with caspase 1 inhibitor Ac-YVAD-cmk (50 μM) or CVN1 (100 nM) for 15 min or CVN2 (100 nM) for 30 min before stimulation with transfected Poly(dA:dT) (1 μg mL^{-1}, 4 h) (n=4) or transfected ultrapure flagellin from Salmonella typhurium (1 μg mL^{-1}, 4 h) (n=4). ***p<0.001, **p<0.01 determined by one-way ANOVA with Dunnett's post hoc analysis. Values shown are the mean ± SEM.

4.2.4 Pharmacological inhibition of the THIK-1 potassium channel with CVN1 and CVN2 inhibits the NLRP3 priming step in iBMDMs

Previously, in Chapter 3, inhibition of K2P channels with Tpa was found to inhibit LPS-induced NLRP3 priming (Fig. 3.7). These findings suggest K2P channels of which TWIK-2 and THIK-1 are expressed in BMDMs (Fig.3.1) may regulate the NLRP3 priming step as well as activation. Following the observation that THIK-1 inhibitors CVN1 and CN2 reduce NLRP3 activation, the impact of both compounds on the initial priming step of canonical NLRP3 activation was investigated to determine whether THIK-1 regulates NLRP3 priming. As mentioned in section 3.2.4, LPS priming drives activation of the transcription factor NF-κB which upregulates NLRP3 and pro IL-1β expression, in addition to stimulating IL-6 and TNFα release (262, 263).

iBMDMs were incubated with THIK-1 inhibitors CVN1 and CVN2 in addition to the NF-κB inhibitor Bay11 as a positive control, prior to priming with LPS for 4 h. In support of previous findings that K2P channel inhibition reduced NLRP3 priming (Fig. 3.7), CVN1 significantly inhibited both IL-6 and TNFα release in response to LPS (Fig. 4.8A). CVN2 had no effect on IL-6 release but did significantly inhibit TNFα release in response to LPS (Fig. 4.8A). Both CVN1 and CVN2 had no effect on cell death in response to LPS suggesting at concentrations of 100nM the compounds are not cytotoxic (Fig. 4.8B). Western blot analysis was used to confirm the impact of CVN1 and CVN2 on NLRP3 priming. By western blot CVN1 and CVN2 were found to inhibit LPS-induced protein expression of NLRP3 and pro IL-1β (Fig. 4.8C). These results suggest THIK-1 may play a role in NLRP3 priming in addition to activation. However, THIK-1 inhibiting compounds CVN1 and CVN2 were found not to inhibit NLRP3 priming in primary BMDMs which will be discussed in Chapter 5. Therefore, suggesting the impact of CVN1, CVN2 and the K2P inhibiting compound Tpa on NLRP3 priming is an artefact only observed in this immortalized cell line and not primary cells.

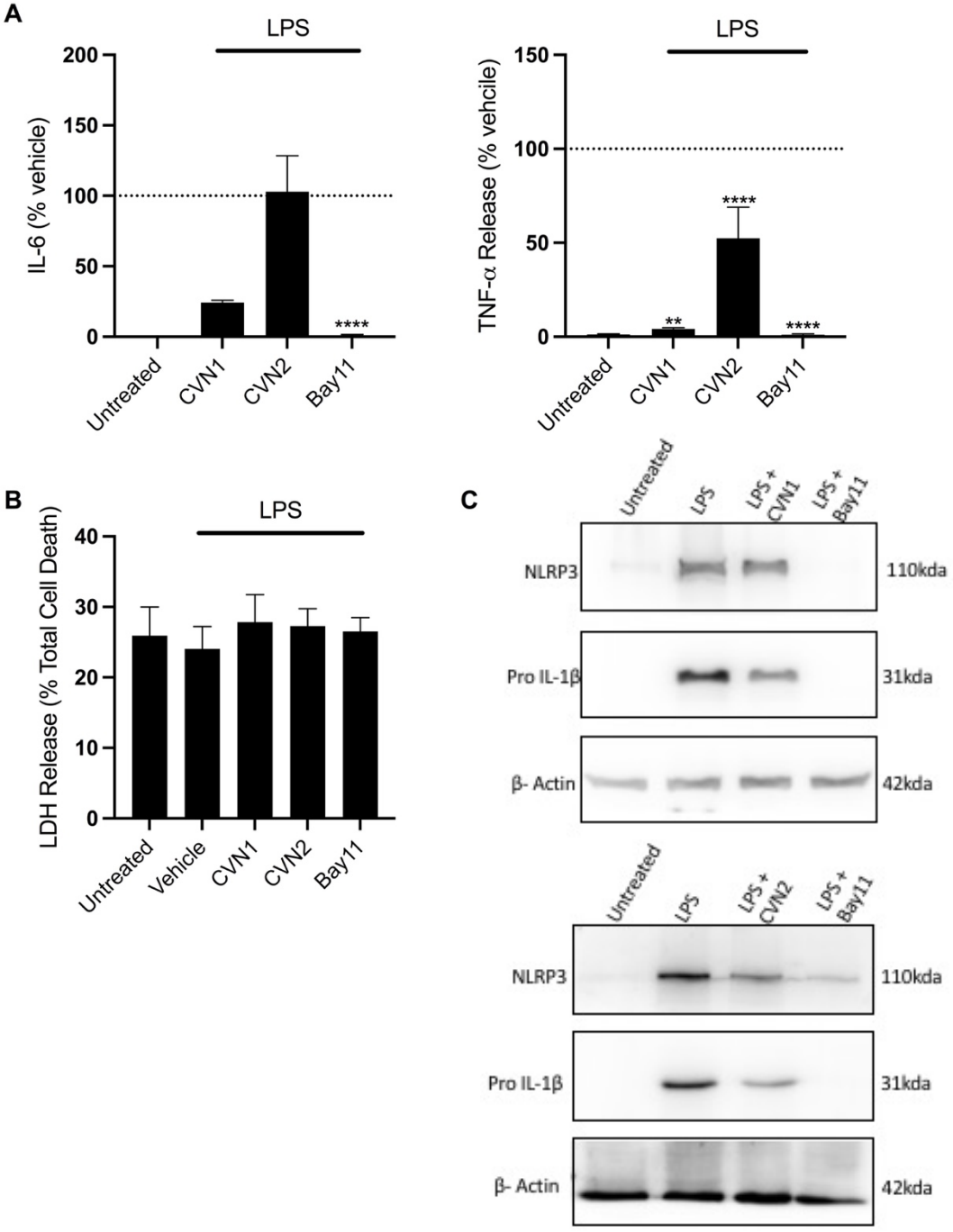

Figure 4.8 Pharmacological inhibition of THIK-1 potassium channels blocks priming of the NLRP3 inflammasome.
(A) IL-6 and TNFα ELISA and **(B)** LDH release assay of the supernatant of iBMDMs pretreated with Bay11(10 μM) or CVN1 (100 nM) for 15 min or CVN2 for 30 min before priming with LPS (1 μg mL^{-1}, 4h) (n=4). **(C)** NLRP3 and IL-1β western blot of the supernatant and total cell lysates respectively of iBMDMs pretreated with CVN1 (100 nM), CVN2 (100 nM) or Bay11(10 μM) for 15 min before priming with LPS (1 μg mL^{-1}, 4 h). ****p<0.0001, **p<0.01 determined by one-way ANOVA with Dunnett's post hoc analysis. Values shown are the mean ± SEM.

4.2.5 Blocking the THIK-1 potassium channel with CVN1 and CVN2 enhances ASC speck formation despite inhibiting NLRP3 inflammasome activation

As explained in section 3.2.5, activation of NLRP3 drives the recruitment and oligomerization of the adaptor protein ASC resulting in the formation of ASC specks (Fig. 3.8). The formed ASC speck then serves as a scaffold for caspase-1 recruitment and activation. Previously, blocking K2P channels or K^+ efflux was found to inhibit NLRP3 activation independently of preventing ASC speck formation (Fig.3.8, 3.9). These data suggest K^+ efflux, potentially via K2P channels is required for NLRP3 dependent caspase-1 activation but not ASC speck formation. To determine whether inhibition of THIK-1 also inhibited caspase-1 activation independently of preventing ASC oligomerization, the effects of CVN1 and CVN2 on speck formation were investigated.

Using the same protocol described in sections 3.2.5 and 3.2.6, iBMDMs stably expressing ASC-mCherry were used to study the impact of CVN1 and CVN2 on ASC speck formation over time. LPS-primed ASC-mCherry iBMDMs were incubated with a range of CVN1 or CVN2 concentrations (0.1 µM – 100 µM) previously shown to inhibit NLRP3 activation in response to ATP (Fig.4.2, 4.3). ASC speck formation was then induced by treatment with 5 mM ATP. ATP-induced ASC speck formation was again inhibited by MCC950 demonstrating speck formation was NLRP3 dependent (Fig.4.9). CVN1 at all concentrations was found to have no effect on ATP-induced ASC speck formation (Fig. 4.9Ai). At the maximum effective NLRP3 inhibiting concentration of 0.1 µM, CVN1 resulted in an increase in ASC speck formation, however, this difference was statistically insignificant (Fig.4.9Aii). In addition, CVN2 at NLRP3 inhibiting concentrations did not inhibit ASC speck formation (Fig.4.9Bi). In support of findings that blocking K2P channels with Tpa enhanced speck formation, the maximum effective concentration of CVN2 (0.1 µM) also induced an increase in ASC speck formation in response to ATP (Fig.4.9Bii). These data support the previous findings that K^+ efflux via K2P channels inhibits NLRP3 induced caspase-1 activation without inhibiting ASC speck formation (Fig.3.8, 3.9). Furthermore, the results imply that THIK-1 regulates NLRP3-dependent caspase-1 activation independently from inhibiting ASC speck formation. The observation that CVN2 enhances ASC speck formation in response to ATP is consistent with findings that Tpa enhances speck formation (Fig.3.8).

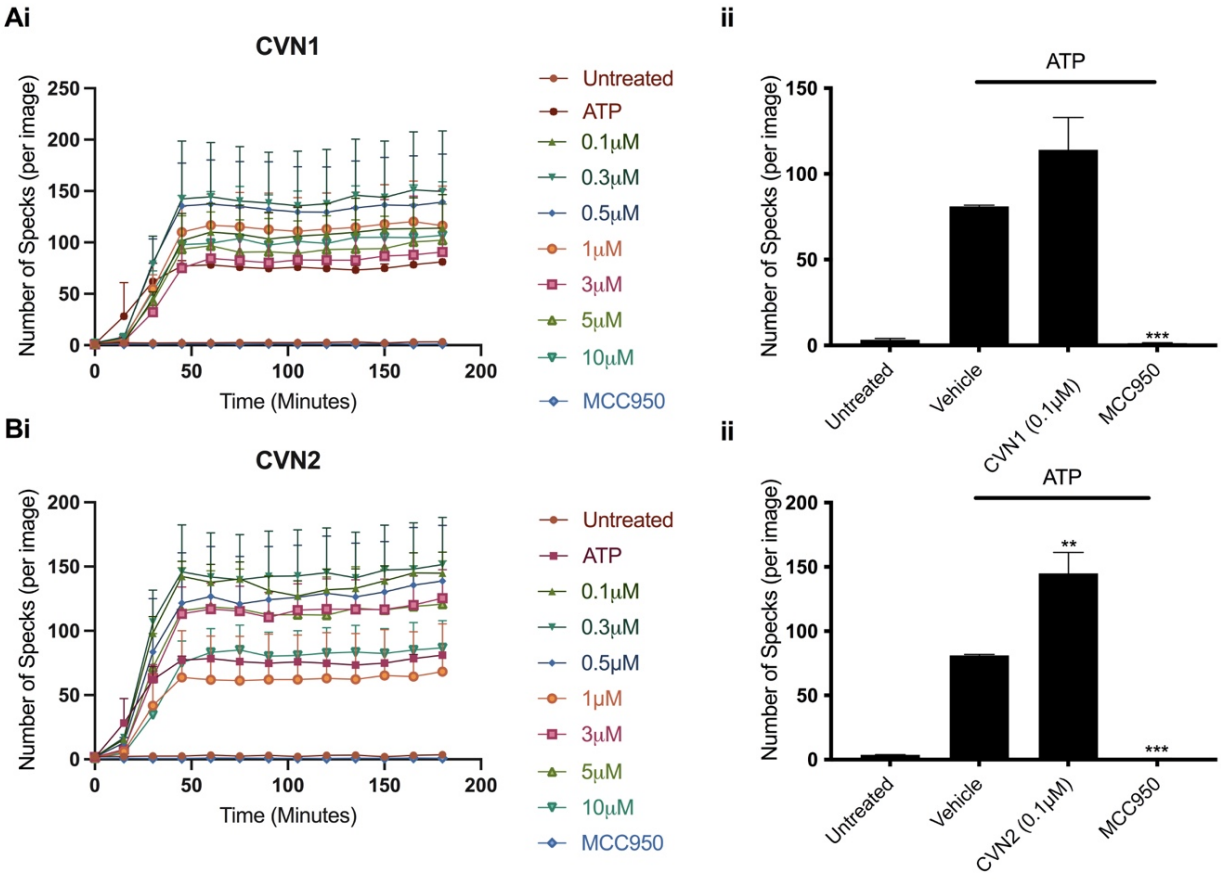

Figure 4.9 Inhibition of THIK-1 potassium channels inhibits NLRP3-dependent caspase-1 activation independently of inhibiting ASC speck formation.
(Ai,Bi) ASC speck formation measured in real time and **(Aii, Bii)** ASC speck formation after 165 min of ATP stimulation from ASC-mCherry iBMDMs primed with LPS (1 μg mL^{-1}, 4 h) followed by pretreatment with vehicle control,, **(A)** CVN1 (0.1 μM- 10 μM) for 15 min, **(B)** CVN2 (0.1 μM- 10 μM) for 30 min or MCC950 (10 μM) for 15 min before stimulation with ATP (5 mM) (n=3). ASC speck experiments were performed in the presence of Ac-YVAD-FMK (50 μM) to prevent pyroptosis and loss of ASC specks. ***p<0.001, **p<0.01 determined by one-way ANOVA with Dunnett's with Dunn's post hoc analysis. Values shown are the mean ± SEM.

4.2.6 Pharmacological inhibition of the THIK-1 potassium channel with CVN1 and CVN2 reduces NLRP3 activation in murine microglia

Having observed CVN1 and CVN2 to inhibit NLRP3 activation in BMDMs, the effect of THIK-1 inhibitors on microglial NLRP3 activation was investigated. Murine adult microglia were primed with LPS (1 μg mL^{-1}, 4 h) followed by incubation with a range of concentrations (1-1000 nM) of CVN1 or CVN2 for 15 and 30 min respectively. NLRP3 activation was then stimulated with ATP (5 mM, 1 h). In support of previous findings in BMDMs CVN1 significantly inhibited NLRP3 activation in adult microglia 1000nM (Fig. 4.10A). Despite CVN1 inhibiting ATP-induced NLRP3 activation in BMDMs at concentrations as low as 100 nM (Fig. 4.2), concentrations of 100 nM CVN1 and below had no inhibitory effect on microglial NLRP3 activation (Fig.4.10A). This data shows CVN1 inhibits microglial ATP-induced NLRP3 activation in addition to BMDMs yet is more effective at lower concentrations in BMDMs than microglia. Consistent with these findings CVN2 was also found to significantly inhibit NLRP3 activation in microglia (Fig. 4.10B). CVN2 inhibited ATP-induced NLRP3 activation in a concentration dependent manner with significant inhibition observed at 100 nM and completely abolished activation at 1000 nM (Fig. 4.10B). As with CVN1, higher concentrations of CVN2 were required to inhibit NLRP3 activation in microglia (100 nM) compared to BMDMs (10 nM) (Fig. 4.3). However, CVN1 and CVN2 had a larger inhibitory effect on microglial IL-1β activation in response to ATP when compared to BMDMs (Fig. 4.2, 4.3), suggesting THIK-1 plays a larger role in microglial NLRP3 activation compared to peripheral macrophages. These data demonstrate CVN1 and CVN2 inhibit ATP-induced NLRP3 activation in CNS resident microglia and peripheral macrophages potentially through inhibition of THIK-1. In addition, CVN1 and CVN2 were both found to be more potent inhibitors of NLRP3 activation in BMDMs than microglia. One potential explanation for the difference in potency of CVN1 and CVN2 in BMDMs and microglia is the difference in THIK-1 expression between the two cell types. THIK-1 appears to be more highly expressed in microglia and therefore higher concentration of THIK-1 inhibitor may be required to block sufficient THIK-1 K^+ channels to inhibit NLRP3 activation.

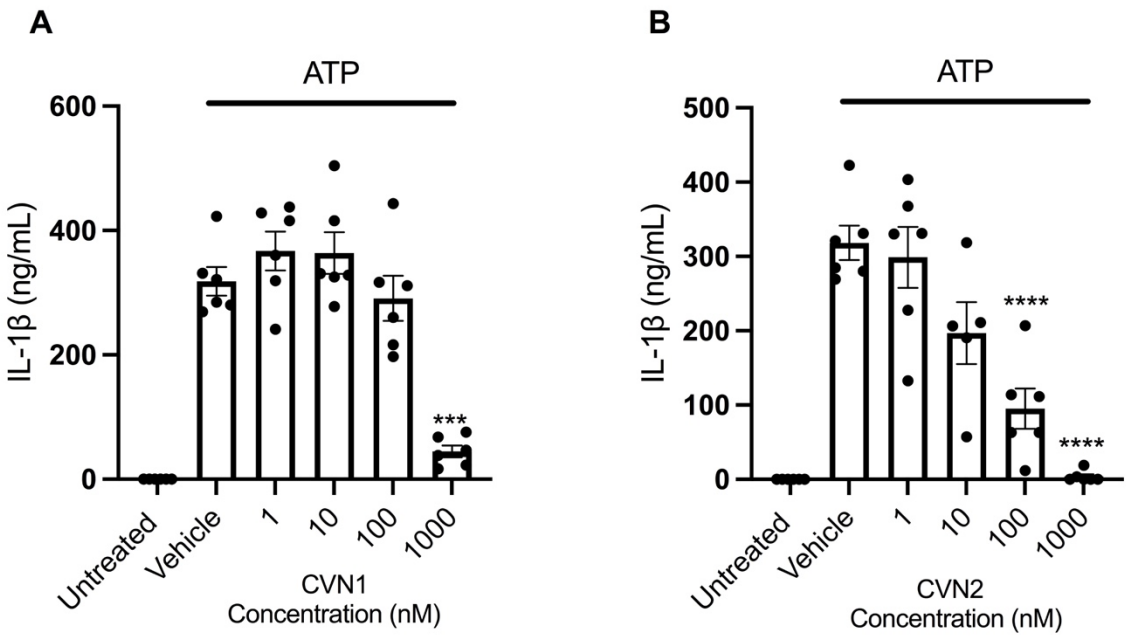

Figure 4.10 Pharmacological inhibition of THIK-1 with CVN1 and CVN2 blocks NLRP3 activation and IL-1β release in response to ATP in adult microglia.
IL-1β ELISA assay of the supernatant of mouse primary microglia primed with LPS (1 μg mL^{-1}, 4 h) followed by pretreatment with vehicle control, **(A)** CVN1 (1 nM-1000 nM) for 15 min or **(B)** CVN2 (1 nM- 1000 nM) for 30 min before stimulation with ATP (5 mM, 1 h) (n=4 or 6). ****p<0.0001, ***p<0.001 determined by one-way ANOVA with Dunnett's post hoc analysis. Values shown are the mean ± SEM.

4.2.7 Canonical and alternative NLRP3 activation in human monocytes is inhibited by THIK-1 inhibiting compounds CVN1 and CVN2

As discussed in section 3.2.8, LPS alone is known to stimulate K^+ efflux independent alternative NLRP3 activation in human monocytes (87, 104). Previously, K2P channel inhibition with Tpa was found to inhibit both canonical and alternative mechanisms of NLRP3 activation in human monocytes (Fig. 3.13). Therefore, the impact of THIK-1 inhibitors on canonical and alternative NLRP3 activation was tested in human monocyte THP-1 cell lines.

Stimulation of K^+-dependent canonical NLRP3 activation with LPS priming followed by silica treatment induced NLRP3 dependent IL-1β release in THP-1 cells (Fig. 4.11). In support of findings that K2P inhibition blocks canonical activation in human monocytes (Fig. 3.13), both CVN1 and CVN2 inhibited canonical activation in THP-1 cells. Alternative NLRP3 inflammasome activation was stimulated in THP-1 cells with 16 h LPS treatment. LPS-induced IL-1β release in a NLRP3 dependent manner which was also inhibited by CVN1 and CVN2 (Fig. 4.12A, 4.12B). These data are consistent with the findings that K2P channel inhibition blocks canonical and alternative NLRP3 activation in human monocytes (Fig. 3.13). These data suggest CVN1 and CVN2 inhibit canonical and alternative NLRP3 activation in human THP-1 cell lines via inhibition of THIK-1. Therefore, these findings suggest THIK-1 regulation of NLRP3 activation is conserved in human monocytes.

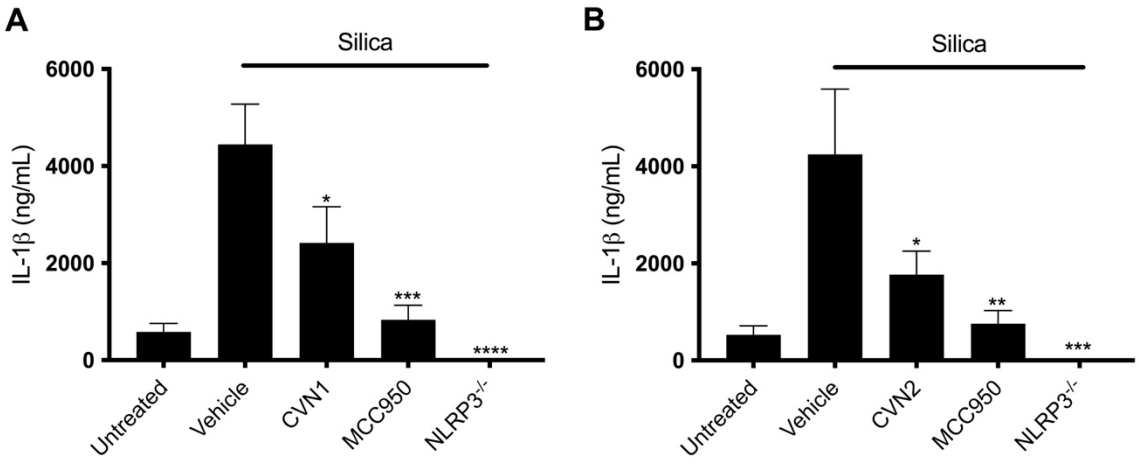

Figure 4.11 Pharmacological inhibition of THIK-1 potassium channels with CVN1 and CVN2 blocks canonical NLRP3 activation in THP-1 human monocytes.
IL-1β ELISA of the supernatant of WT and NLRP3 KO THP-1 monocytes primed with LPS (1 μg mL^{-1}, 4 h) followed by pretreatment with vehicle control, **(A)** CVN1 (100 nM) for 15 min, **(B)** CVN2 (100 nM) for 30 min or MCC950 (10 μM) for 15 min before stimulation with silica (300 μg mL^{-1}, 4 h) (n=4). ****p<0.0001, ***p<0.001, **p<0.01, *p<0.05 determined by one-way ANOVA with Dunnett's post hoc analysis. Values shown are the mean ± SEM.

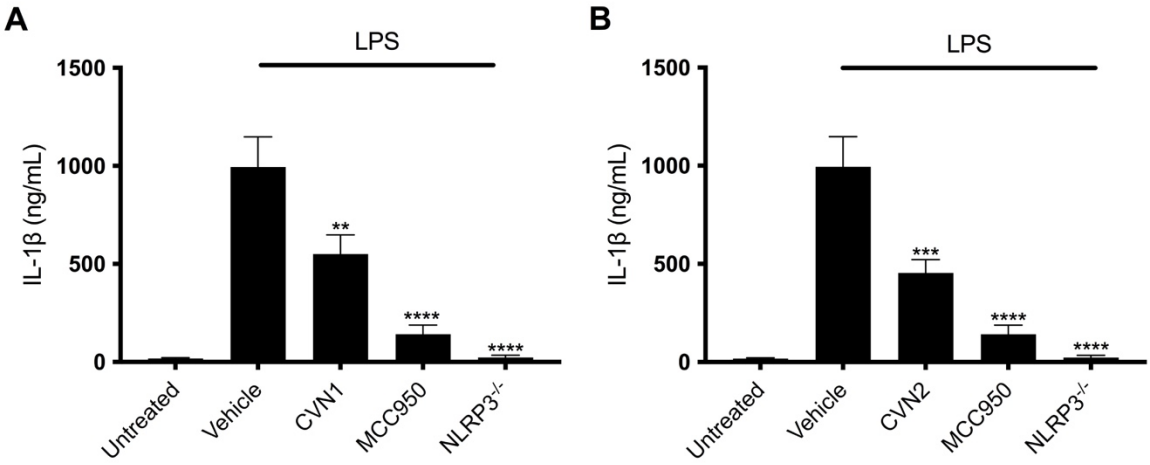

Figure 4.12 Pharmacological inhibition of THIK-1 potassium channels with CVN1 and CVN2 blocks canonical NLRP3 activation in THP-1 human monocytes.
A, B) IL -1β ELISA of the supernatant of WT and NLRP3 KO THP-1 monocytes pretreated with vehicle control, **(A)** CVN1 (100 nM) for 15 min, **(B)** CVN2 (100 nM) for 30 min or MCC950 (10 μM) for 15 min before stimulation with LPS (1 μg mL^{-1}, 16 h) (n=6). ****p<0.0001, ***p<0.001, **p<0.01 determined by one-way ANOVA with Dunnett's post hoc analysis. Values shown are the mean ± SEM.

4.2.8 THIK-1 inhibitor CVN1 and chloride channel inhibitor NS3728 have synergistic effect on NLRP3 inhibition

Although K^+ efflux is widely accepted as an essential second step required for NLRP3 activation (45), Cl^- channels have also been found to regulate NLRP3 activation (82, 86, 274). Previously, our group identified Cl^- efflux to facilitate NLRP3-dependent ASC oligomerization, while K^+ efflux was required for caspase-1 activation and IL-1β release (88). In support of these previous findings, this thesis identified inhibiting K^+ efflux, K2P channels and THIK-1 channels blocked NLRP3-dependent caspase-1 activation independently from inhibiting ASC oligomerization. These data together suggest Cl^- efflux via Cl^- channels is required for ASC oligomerization in response to NLRP3 activating stimuli, yet K^+ efflux, potentially via THIK-1 is required for ASC specks to recruit and activate caspase-1. This suggests Cl^- efflux and K^+ efflux both regulate NLRP3 activation of caspase-1 at different stages of the activation pathway, the formation of ASC specks and caspase-1 activation respectively. The study therefore aimed to determine whether simultaneously inhibiting both Cl^- and THIK-1 channels had a synergistic effect on NLRP3 inhibition.

To determine whether Cl^- and THIK-1 channel inhibition could have a synergistic effect, LPS-primed iBMDMs were incubated with both the Cl^- channel inhibitor NS3728 and the THIK-1 inhibitor CVN1. NS3728 has previously been shown to inhibit NLRP3 inflammasome activation (85). iBMDMs were co-incubated with a range of NS3728 (100 nM-10000 nM) and CVN1 (1 nM-100 nM) concentrations to determine which combination of concentrations display synergism. NLRP3 activation was then stimulated with 5 mM ATP treatment. Treatment with NS3728 or CVN1 alone inhibited NLRP3 activation in a concentration dependent manner (Fig. 4.13). Co-administration of both NS3728 and CVN1 at specific concentrations was found to induce greater percentage NLRP3 inhibition than the sum of individual effects of NS3728 and CVN1 (Fig. 4.14). An example of the synergistic effect can be observed at 1 nM CVN1 and 100nM NS3728, at which individually both compounds fail to inhibit NLRP3 activation (Fig. 4.14). However, simultaneous treatment with both 1 nM CVN1 and 100 nM NS3728 inhibits NLRP3 activation by 22.93%. (Fig. 4.14). To determine whether CVN1 and NS3728 were acting synergistically, the program SynergyFinder 2.0 was utilized to compute a synergy score using the Bliss independence model (275). A Bliss synergy score greater than 10 is considered to indicate that the interaction between two drugs is synergistic (275). CVN1 and NS3728 were found

to be acting synergistically at a number of concentrations (Fig. 4.15). The greatest synergy scores were found at 1 nM concentrations of CVN1 in combination with 100, 300 or 1000 nM NS2738 (Fig.4.15). The highest Bliss score was observed at 1 nM CVN1 and 300nM NS2738 suggesting these concentrations display the greatest synergism (Fig.4.15). These data show CVN1 and NS3728 can act synergistically to enhance NLRP3 inhibition in response to ATP. This suggests THIK-1 inhibition in combination with a Cl^- channel inhibitor can be combined to induce greater NLRP3 inhibition at lower concentrations than using each compound individually.

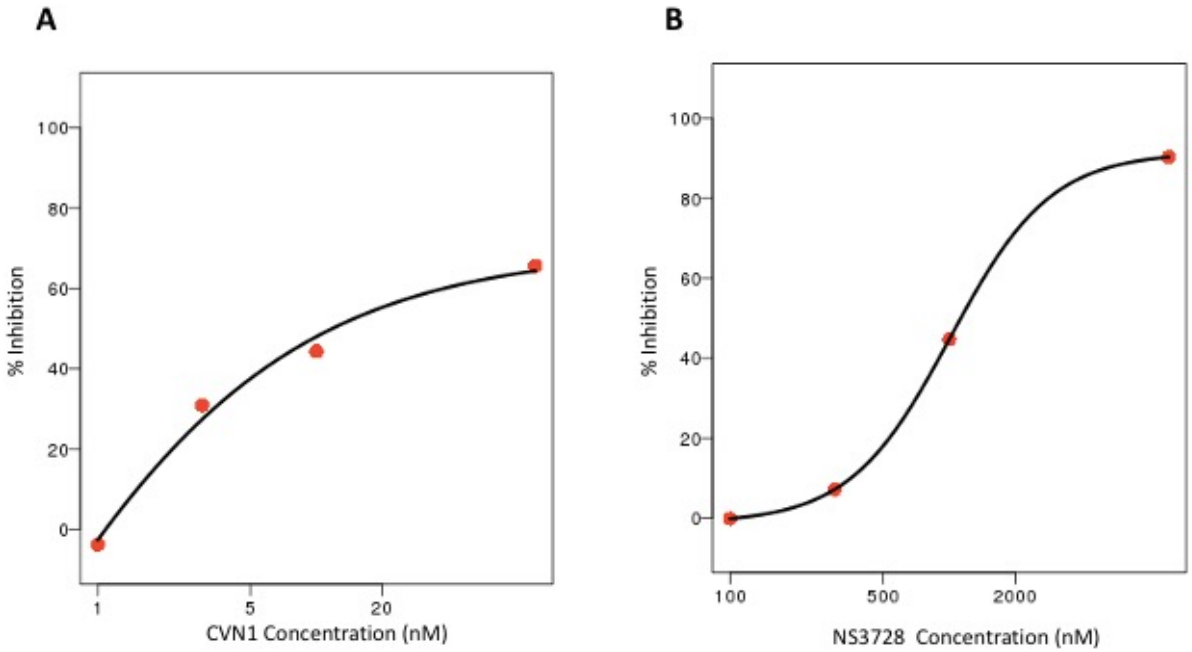

Figure 4.13 Pharmacological inhibition of THIK-1 with CVN1 or Cl^- channels with NS3728 inhibit NLRP3 activation and IL-1β release in a concentration dependent manner in response to ATP.
IL-1β ELISA assay of the supernatant of iBMDMs primed with LPS (1 μg mL^{-1}, 4 h) followed by pretreatment with vehicle control, **(A)** CVN1 (1 nM-100 nM) or **(B)** NS3728 (100 nM- 10000 nM) for 15 min stimulation with ATP (5 mM, 1 h) (n=4). Values shown are the mean % IL-1β inhibition.

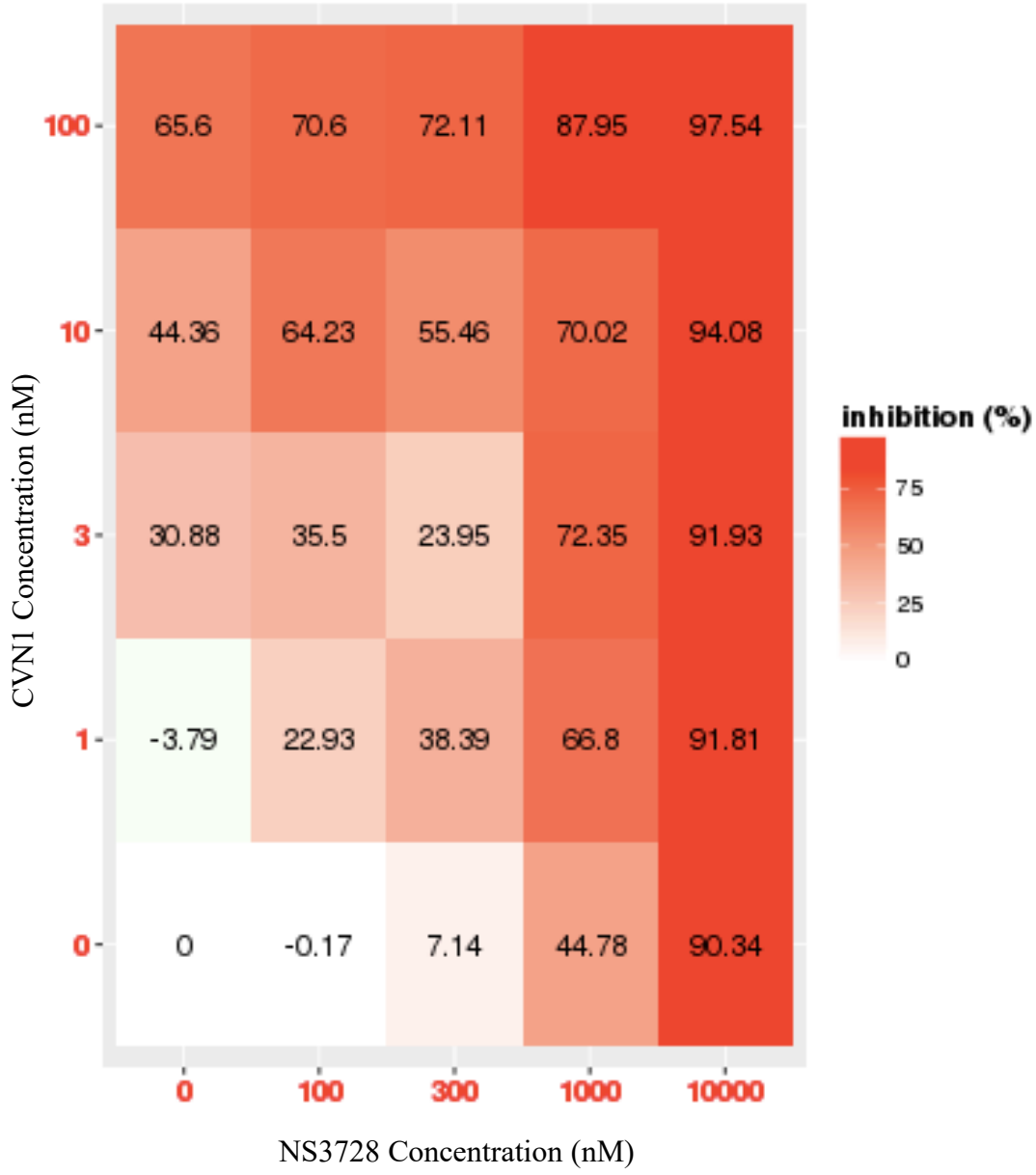

Figure 4.14 Co-administration of CVN1 and NS3728 enhance NLRP3 inhibition in response to ATP.
IL-1β ELISA assay of the supernatant of iBMDMs primed with LPS (1 μg mL^{-1}, 4 h) followed by pretreatment with vehicle control, CVN1 (1 nM-100 nM) and/or NS3728 (100 nM- 10000 nM) for 15 min stimulation with ATP (5 mM, 1 h) (n=4). Values shown are the mean % IL-1β inhibition.

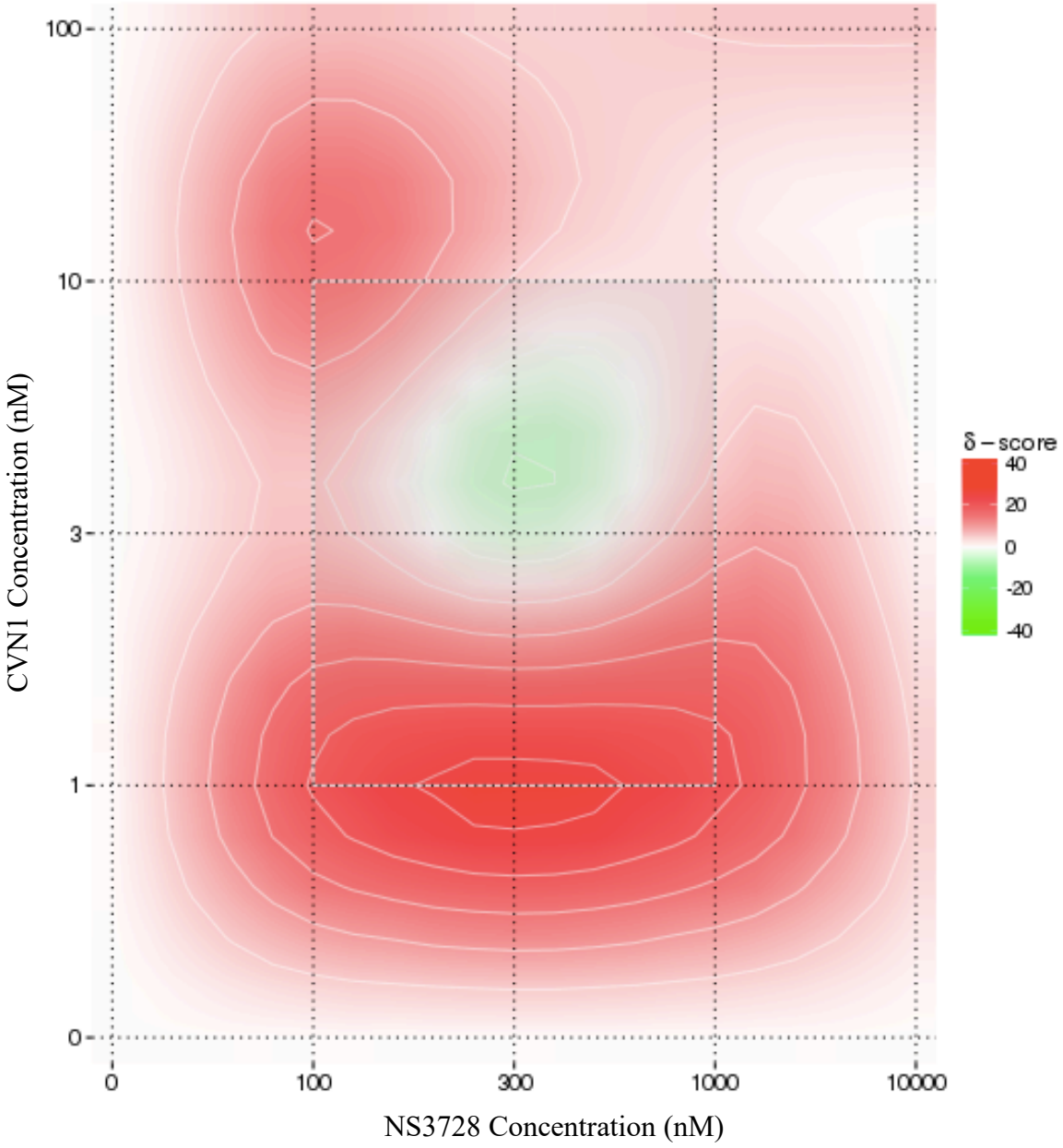

Figure 4.15 CVN1 and NS3728 act in synergy to inhibit ATP-induced NLRP3 activation. Heatmap displaying Bliss synergy scores of CVN1 and NS3728 from IL-1β ELISA assay of the supernatant of iBMDMs primed with LPS (1 μg mL^{-1}, 4 h) followed by pretreatment with vehicle control, CVN1 (1 nM-100 nM) and/or NS3728 (100 nM- 10000 nM) for 15 min stimulation with ATP (5 mM, 1 h) (n=4). Values shown are Bliss synergy scores. Heatmap represents Bliss synergy scored between -40 (green) and 40 (red).

4.3 Discussion

These data identify THIK-1 inhibiting compounds CVN1 and CVN2 as regulators of NLRP3 activation through a mechanism independent of ASC oligomerization. Therefore, suggesting THIK-1 is a potential drug target for limiting NLRP3 mediated activation of caspase-1.

Data gathered in Chapter 3 together with previous studies identified K2P channels TWIK-2 and THIK-1 as potential regulators of NLRP3 inflammasome activation in peripheral and CNS resident innate immune cells (68, 78). In support of this data, this chapter demonstrates pharmacological inhibition of THIK-1 attenuates NLRP3 activation in murine macrophages and CNS resident microglia in addition to human monocytes. However, previously in Chapter 3 the K2P channel inhibitor Tpa was observed to inhibit NLRP3 activation in response to ATP and silica, previously shown to be dependent on K^+ efflux (45). Tpa was found not to inhibit the K^+ efflux dependent stimuli imiquimod (51) or K^+ channel independent stimuli nigericin (55) suggesting Tpa inhibits NLRP3 through action specifically at K^+ channels. In contrast to data gathered with Tpa in Chapter 3, CVN1 and CVN2 inhibited K^+ channel independent NLRP3 stimuli imiquimod and/or nigericin. Both CVN1 and CVN2 were found to be selective inhibitors of THIK-1 in selectivity assays performed by Cerevance (Cerevance personal communication). As CVN1 and CVN2 both inhibited nigericin-induced NLRP3 activation in iBMDMs it is possible pore forming toxins such as nigericin still require the activation of K^+ channels such as THIK-1 in order to induce NLRP3 activation. Although speculated to be independent of K^+ channel activation. The findings that selective THIK-1 inhibiting compounds reduce nigericin induced NLRP3 activation suggest NLRP3 activation in response to pore forming toxins such as nigericin is potentially dependent on activation of K^+ channels such as THIK-1.

In response to K^+ efflux independent NLRP3 activation with imiquimod, contrasting results were obtained with CVN1 and CVN2. CVN1 was found to inhibit imiquimod-induced NLRP3 activation whereas CVN2 had no inhibitory effect. These results highlight potential differences in the activity of CVN1 and CVN2. The differences observed between the two THIK-1 inhibiting compounds could possibly be explained by the different structural backbones of the two compounds resulting in different biological activity. As imiquimod induced NLRP3 activation is independent of K^+ efflux, this suggests K^+ channel inhibition should have no impact on NLRP3 activation in response to imiquimod.

The findings that CVN1 inhibited imiquimod-induced activation suggests CVN1 may have unidentified activity beyond its ability to block THIK-1 which results in inhibition of K^+ efflux independent NLRP3 activation. However, as CVN2 had no effect on K^+ efflux independent NLRP3 activation this suggest CVN2 is exclusively inhibiting NLRP3 activation through blocking K^+ channels. These data show selective THIK-1 inhibitors CVN1 and CVN2 are effective inhibitors of canonical NLRP3 activation, suggesting THIK-1 is a regulator of NLRP3 activation. Furthermore, the data highlights potential differences in the activity of the CVN1 and CVN2 in murine BMDMs *in vitro* with CVN1 potentially having additional properties in addition to being an effective THIK-1 inhibitor.

Although the exact mechanism by which CVN1 and CVN2 inhibits imiquimod and/or nigericin induced IL-1β release remains unclear, direct inhibition of capase-1 can be ruled out as a potential mechanism of action. CVN1 and CVN2 failed to inhibit activation of AIM2 and NLRC4 inflammasomes which drive caspase-1 activation and subsequent IL-1β release (260, 261). Therefore, CVN1 and CVN2 selectively inhibit the NLRP3 inflammasome pathway and do not inhibit imiquimod or nigericin induced IL-1β release via direct inhibition of caspase-1.

Furthermore, as well as inhibiting NLRP3 activation, THIK-1 inhibiting compounds CVN1 and CVN2 also reduced transcriptional priming of the NLRP3 inflammasome. Pro IL-1β and NLRP3 protein levels in addition to the release of IL-6 and TNFα in response to LPS induced TLR4 signaling were reduced by CVN1 and CVN2 specifically in iBMDM cell lines. These data are consistent with findings in Chapter 3 which found K2P channel inhibition to dampen NLRP3 inflammasome priming. Together these data suggest K2P channels and particularly THIK-1 channels can regulate transcriptional NLRP3 priming in iBMDMs. However, as will be discussed in Chapter 5, CVN1 and CVN2 were found not to inhibit pro IL-1β or NLRP3 protein expression and failed to inhibit IL-6 and TNFα release in response to LPS in pBMDMs. Therefore, this suggests CVN1 and CVN2 inhibition of NLRP3 priming is only observed in iBMDM cell lines, indicating THIK-1 specifically regulates NLRP3 activation and not priming in primary cells. The contradicting results observed between primary cells and cell lines can be explained by the evolution of cell line populations. Cell lines are known to evolve in cell culture, regularly undergoing changes in gene expression resulting in functional differences between cell line populations. Previous research has shown spontaneous changes in cell line gene expression

impacts the functional response of cell line populations to pharmacological treatment (276). It is therefore possible that the accumulations of mutations in iBMDM cell populations has resulted functional changes resulting in different NLRP3 priming responses to CVN1 and CVN2 when compared with primary cells.

In addition, CVN1 and CVN2 inhibited canonical and K^+ efflux independent alternative inflammasome activation in THP-1 human monocytes. These data are consistent with findings in Chapter 3 which observed the K2P channel inhibitor Tpa to also inhibit canonical and alternative NLRP3 activation in human monocytes. Canonical activation of NLRP3 was stimulated in THP-1 cells using the K^+ efflux dependent stimuli, silica (45). CVN1 and CVN2 inhibition of silica induced NLRP3 activation in human monocytes may potentially be driven through THIK-1 inhibition and inhibition of K^+ efflux. However, alternative activation of NLRP3 occurs independently of K^+ efflux (104). Therefore, CVN1 and CVN2, in addition to Tpa, mediated inhibition of alternative NLRP3 activation is through a mechanism independent of blocking K^+ efflux and therefore likely to be independent of THIK-1 inhibition. As previously described in Chapter 3, both alternative NLRP3 activation and the priming step in canonical activation require TLR4 mediated cellular signaling (104). Therefore, as CVN1 and CVN2 were found to inhibit LPS mediated transcriptional priming of NLRP3, at least in iBMDMs and not in pBMDMs, they potentially also inhibit alternative activation through blocking TLR4 signaling pathways. CVN1 and CVN2 inhibition of alternative NLRP3 activation in THP-1 cells is therefore potentially driven through a mechanism downstream of TLR4 signaling, independent of K^+ efflux and THIK-1 inhibition.

As described in Chapter 3, a previously published study identified Cl^- efflux as a requirement for ASC speck formation in response to NLRP3 activation (88). K^+ efflux on the other hand was dispensable for ASC speck formation but required for caspase-1 activation following NLRP3 activation. In support of this work, in Chapter 3, K2P channel inhibition, in addition to blocking K^+ efflux was found to inhibit ATP induced caspase-1 activation independently from blocking ASC speck formation. These findings suggest K^+ efflux via K2P channels is required for caspase-1 activation in response to ATP induced NLRP3 activation but is dispensable for ASC speck formation. Providing further evidence to support this hypothesis, THIK-1 inhibitors were also found to inhibit ATP-induced NLRP3 activation

independently from blocking ASC speck formation. These findings suggest THIK-1 specifically regulates ATP induced caspase-1 activation without impacting ASC speck formation. This is the same response observed via blocking K2P channels or K^+ efflux. Moreover, THIK-1 inhibitors did not inhibit AIM2 or NLRC4 inflammasome activation, suggesting THIK-1 inhibitors do not directly inhibit caspase-1 activation. Together these data suggest THIK-1 inhibitors are blocking ASC mediated caspase-1 activation which the data collected in this thesis alongside previously published work indicate is dependent on K^+ efflux. THIK-1 inhibitors CVN1 and CVN2 may therefore inhibit ATP-induced NLRP3 activation through selective inhibition of THIK-1. Therefore, these data suggest THIK-1 regulates ATP-induced caspase-1 activation independently from regulating NLRP3 driven ASC speck formation. Indicating K^+ efflux via THIK-1 may be required for ATP-induced caspase-1 activation.

In addition to K^+ channels, Cl^- channels such as VRAC and CLICs have also been associated with regulation of the NLRP3 inflammasome (82, 86, 274). As such both K^+ and Cl^- channels represent potential therapeutic targets for limiting damaging NLRP3-mediated inflammation in a number of diseases (105). Traditional drug discovery methods have focused on the development of selective agents for a specific target able to modulate its activity and disease pathology. However, multitarget compounds able to modulate multiple interacting targets and show unique pharmacological profiles have been identified as important in the treatment of multifactorial pathologies such as CNS diseases (277). Advantages of multitarget therapies include improved efficacy due to additive or synergistic effects, lower incidence of molecular based side effects, lower risk of toxicity and lower incidence of target based resistance (277). Therefore, identifying interacting modulators of NLRP3 activation may potentially lead to the development of multitarget NLRP3 inhibitors which are more effective in limiting aberrant NLRP3 activation in disease. In this chapter, the THIK-1 inhibitor CVN1 and the Cl^- channel inhibitor NS3728 were found to have a synergetic effect on ATP-induced NLRP3 activation. These data demonstrated coadministration of CVN1 and NS3728 at individually ineffective concentrations, inhibit NLRP3 activation. Therefore, suggesting simultaneous targeting of both THIK-1 and Cl^- channels regulating NLRP3 activation may represent a more effective multitarget approach to limiting NLRP3 activation than selective K^+ or Cl^- channel inhibitors alone.

This chapter identifies the THIK-1 K^+ channel as a potential regulator of ATP induced NLRP3 activation in mouse macrophages and microglia. Consistent with previous work in Chapter 3, THIK-1 inhibition attenuated NLRP3 induced caspase-1 activation independently of preventing ASC speck formation, suggesting THIK-1 regulates caspase-1 activation following ASC speck formation. THIK-1 inhibition was also found to act in synergy with Cl^- channel inhibition to effectively inhibit ATP induced NLRP3 activation in macrophages. These data together suggest THIK-1 is a potential therapeutic target for limiting NLRP3 activation in disease and could be combined with other NLRP3 regulating compounds such as Cl^- channel inhibitors to improve efficacy of NLRP3 inhibition.

Chapter 5: Genetic knockout of THIK-1 inhibits NLRP3 inflammasome activation

5.1 Introduction

In previous chapters, pharmacological inhibition of K2P channels and more selective inhibition of the THIK-1 K^+ channel was found to inhibit both activation and priming of the NLRP3 inflammasome. Although THIK-1 inhibiting compounds were found to reduce NLRP3 activation and priming, the previous studies in Chapters 3 and 4 cannot rule out that NLRP3 inhibition is due to off-target effects of the compounds, independent of THIK-1 inhibition.

THIK-1 genetic ablation has been observed to reduce IL-1β release in response to ATP in mouse hippocampal slices supporting the hypothesis that THIK-1 regulates NLRP3 activation (68). However, this study did not investigate whether THIK-1 was regulating IL-1β release via facilitating NLRP3 inflammasome activation. This past study, together with data showing THIK-1 inhibiting compounds block NLRP3 activation in Chapters 3 and 4 suggest THIK-1 inhibitors reduced NLRP3 activation at least in part through THIK-1 inhibition. However, K^+ channel modulators are known to inhibit cellular signaling pathways independently from action at K^+ ion channels (267–269). It is therefore possible that the THIK-1 inhibitors used may inhibit NLRP3 activation independently from inhibiting THIK-1.

Due to the complex nature of signaling pathways responsible for NLRP3 activation, multiple biological mediators are likely to be involved in the regulation of NLRP3. Thus, the exact targets of NLRP3 inhibiting compounds can be difficult to distinguish. For example, fenamate NSAIDs were proposed to attenuate NLRP3 activation via inhibiting VRAC Cl^- channels (274). However, genetic ablation of VRAC was found to only inhibit hypotonicity-induced NLRP3 activation and not activation in response to other stimuli which were inhibited by the fenamates (85). These findings demonstrated fenamate NSAIDs can inhibit NLRP3 activation independently from VRAC inhibition. The targets of fenamate NSAIDs responsible for regulating NLRP3 activation remain unknown. These studies highlight the importance of genetic engineering studies in confirming results obtained using pharmacological inhibitors are due to inhibition of the desired target and not unidentified off-target effects.

To clarify the role of THIK-1 in NLRP3 activation and test the selectivity of THIK-1 inhibitors, genetic approaches were used to manipulate THIK-1 expression. Both siRNA-induced THIK-1 knockdown and cells from THIK-1 knockout (KO) mice were utilized to determine whether THIK-1 is a regulator of NLRP3 activation. The aim of this study was firstly to determine if THIK-1 is a regulator of NLRP3 activation and secondly investigate whether Tpa, CVN1, and CVN2 regulate NLRP3 activation through targeting THIK-1 and not an unidentified “off target” mechanism.

5.2 Results

5.2.1 THIK-1 specifically regulates ATP-induced NLRP3 inflammasome activation in macrophages

Although the use pharmacological inhibitors suggested THIK-1 K^+ channels played a role in NLRP3 activation, K^+ channel modulators are known to inhibit cellular signaling pathways independently from action at K^+ ion channels (267–269). Genetic approaches were therefore utilised to further determine which specific K^+ channel regulates NLRP3 activation. Of the K2P channel family, RNA profiling of cultured BMDMs and microglia identified high expression of THIK-1 and TWIK-2 channels (Fig. 3.1). In Chapter 4, selective THIK-1 inhibitors reduced NLRP3 activation suggesting THIK-1 as a potential regulator of the NLRP3 inflammasome. We therefore investigated the impact of THIK-1 knockdown and knockout on NLRP3 inflammasome activation to determine whether THIK-1 can regulate NLRP3 activation.

Firstly, to investigate the role of THIK-1 in macrophage NLRP3 activation, pBMDMs were transfected with control or THIK-1 small interfering RNA (siRNA) to knockdown the expression of THIK-1 within cells. Control and THIK-1 siRNA transfected cells were primed with LPS followed by NLRP3 stimulation with ATP, silica, imiquimod and nigericin. THIK-1 knockdown reduced NLRP3 activation in response to ATP (Fig. 5.1Ai) and had no effect on the response to silica (Fig. 5.1Aii). Pre-treatment of THIK-1 knockdown cells with Tpa resulted in no greater inhibition of IL-1β release when compared with THIK-1 knockdown cells in response to ATP stimulation (Fig. 5.1Ai). THIK-1 knockdown had no effect on cell death induced by ATP (Fig. 5.1Bi) or silica treatment (Fig. 5.1Bii). THIK-1 gene knockdown was confirmed by western blot (Fig. 5.1C). Furthermore, knocking down THIK-1 had no effect on imiquimod or nigericin-induced IL-1β release (Fig. 5.2A) or cell death (Fig. 5.2B). These data suggest THIK-1 specifically regulates NLRP3 activation in response to ATP and not other canonical stimuli.

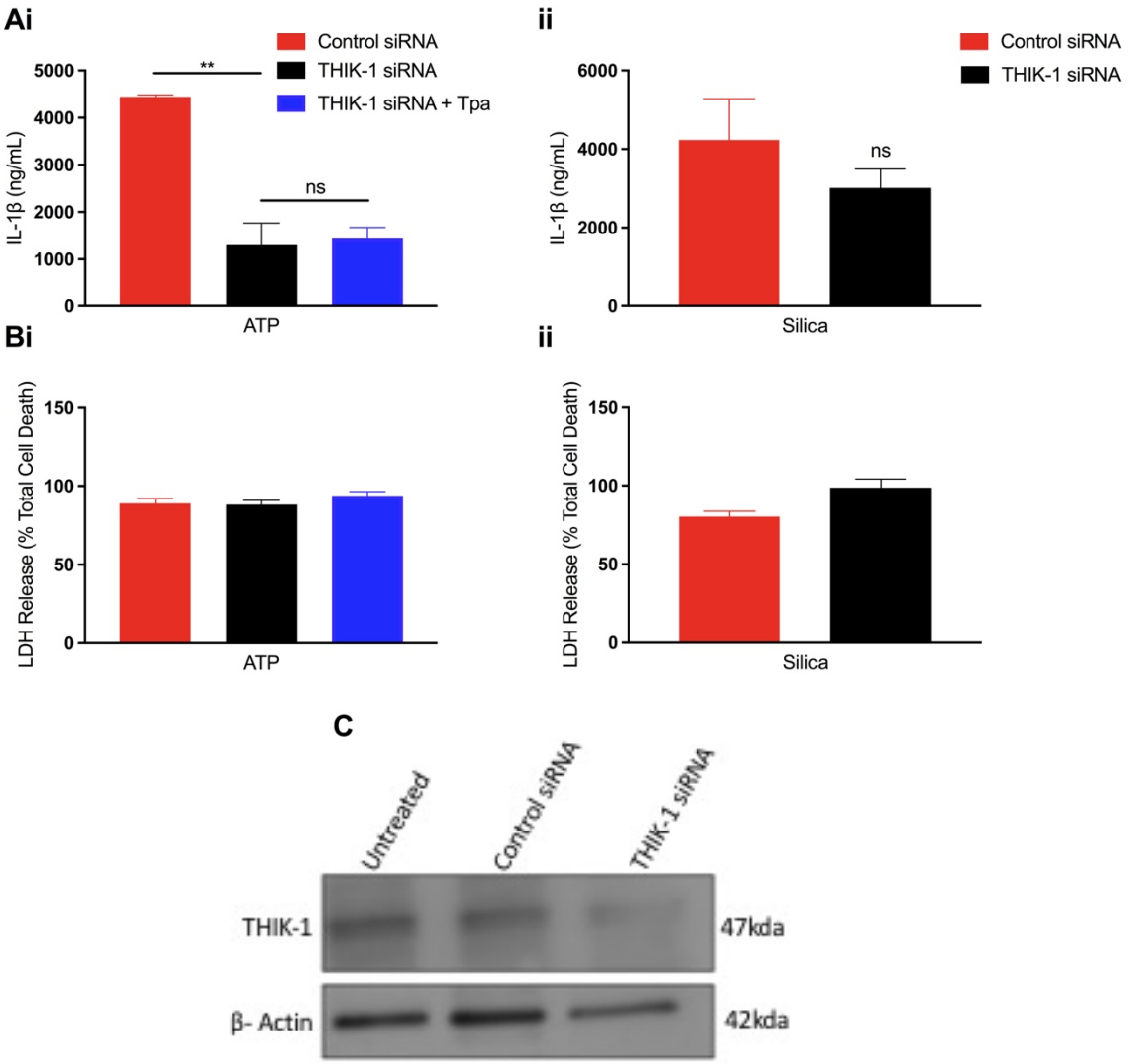

Figure 5.1 THIK-1 knockdown inhibits ATP-induced NLRP3 activation in bone-marrow-derived macrophages.
(A) IL-1β ELISA and **(B)** LDH release assay of the supernatant from pBMDM primed with LPS (1 μg mL^{-1}, 4 h) followed by pretreatment with vehicle control Tpa (50 μM) for 15 min before stimulation with ATP (5 mM, 1 h) (n=3) or silica (300 μg mL^{-1}, 4 h) (n=4). **(C)** THIK-1 western blot of cell lysates from untreated, control siRNA and THIK-1 siRNA pBMDMs. Prior to treatment pBMDMs were transfected with transfection media and 25 nM control non-targeting siRNA or 25 nM THIK-1 siRNA for 48 h. ***p*<0.01 determined by one-way ANOVA with Dunnett's post hoc analysis. Values shown are the mean ± SEM.

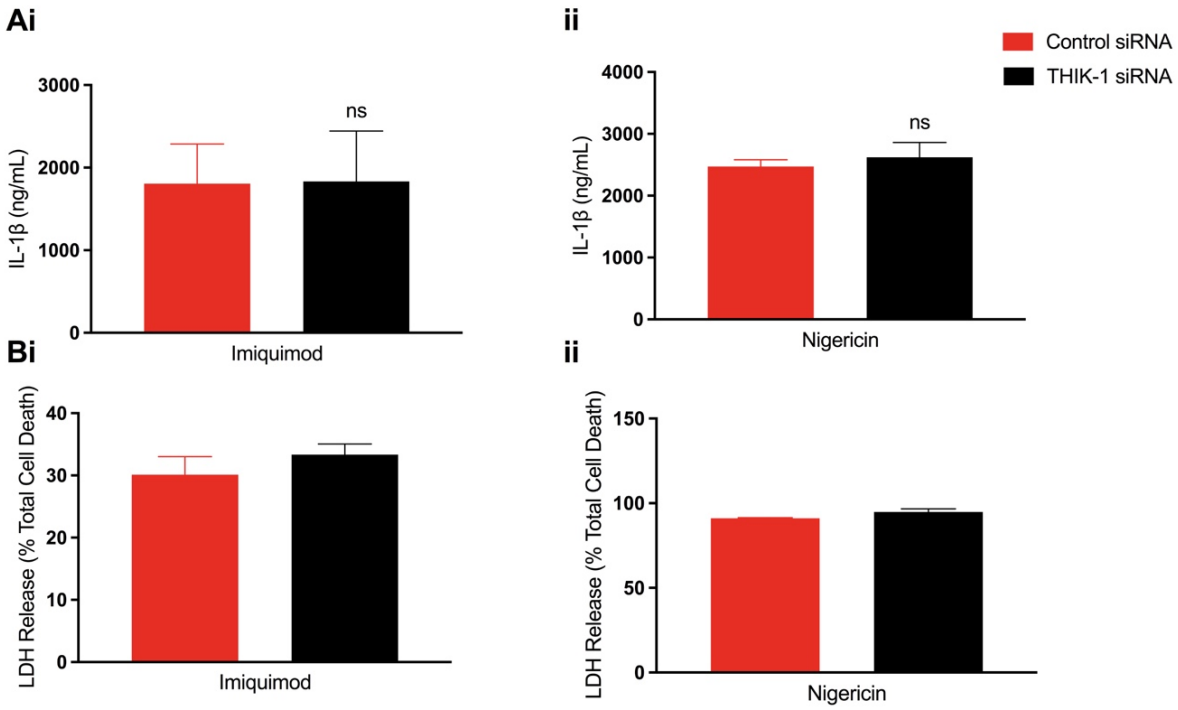

Figure 5.2 THIK-1 knockdown has no effect on imiquimod or nigericin-induced NLRP3 activation in bone-marrow-derived macrophages.
(A) IL-1β ELISA and **(B)** LDH release assay of the supernatant from pBMDMs primed with LPS (1 μg mL^{-1}, 4 h) before stimulation with imiquimod (75 μM, 2 h) (n=3) or nigericin (10 μM, 1 h) (n=4). Prior to treatment, pBMDMs were transfected with transfection media and 25nM control non-targeting siRNA or 25 nM THIK-1 siRNA for 48 h. Statistical significance determined by unpaired t-test. Values shown are the mean ± SEM.

To validate the results obtained in THIK-1 knockdown cells, pBMDMs were harvested from WT and THIK-1 KO mice. Genotype of WT and THIK-1 KO was confirmed by genotyping of mice following BMDM harvest. WT and THIK-1 KO BMDMs were primed with LPS and NLRP3 activation stimulated with ATP, silica, imiquimod and nigericin. Consistent with findings in THIK-1 siRNA transfected cells, knocking out THIK-1 specifically inhibited IL-1β release in response to ATP (Fig. 5.3Ai) and had no effect on the response to silica (Fig. 5.3Aii), imiquimod (Fig. 5.4Ai) or nigericin (Fig.5.4Aii) stimulation. THIK-1 KO had no effect on ATP (Fig. 5.3Bi), silica (Fig. 5.3Bii), imiquimod (Fig. 5.4Bi) or nigericin (Fig. 5.4Bii) induced cell death.

Furthermore, IL-1β release in response to ATP in KO BMDMs was not further inhibited by the THIK-1 inhibitors CVN1 or CVN2 (Fig. 5.3Ai). However, silica (Fig. 5.3Aii), imiquimod (Fig. 5.4Ai) and nigericin (Fig. 5.4Aii) induced IL-1β release was still inhibited by both CVN1 and CVN2 in THIK-1 KO BMDMs. These findings suggest that CVN1 and CVN2 inhibit ATP-induced NLRP3 activation specifically through inhibition of THIK-1. However, in response to other canonical stimuli such as silica, imiquimod and nigericin, CVN1 and CVN2 appear to inhibit activation of the NLRP3 inflammasome through an additional mechanism as well as inhibition of THIK-1 K^+ channels.

Western blotting was used to further characterise the effect of THIK-1 KO on the NLRP3 response. Caspase-1, IL-1β, and GSDMD processing, were reduced in THIK-1 KO BMDMs in comparison to WT in response to ATP (Fig. 5.5). Together these data show THIK-1 is specifically required for ATP-induced NLRP3 activation in BMDMs but is dispensable for activation in response to other canonical stimuli. Furthermore, these data suggest CVN1 and CVN2 inhibited NLRP3 activation independently from inhibiting THIK-1.

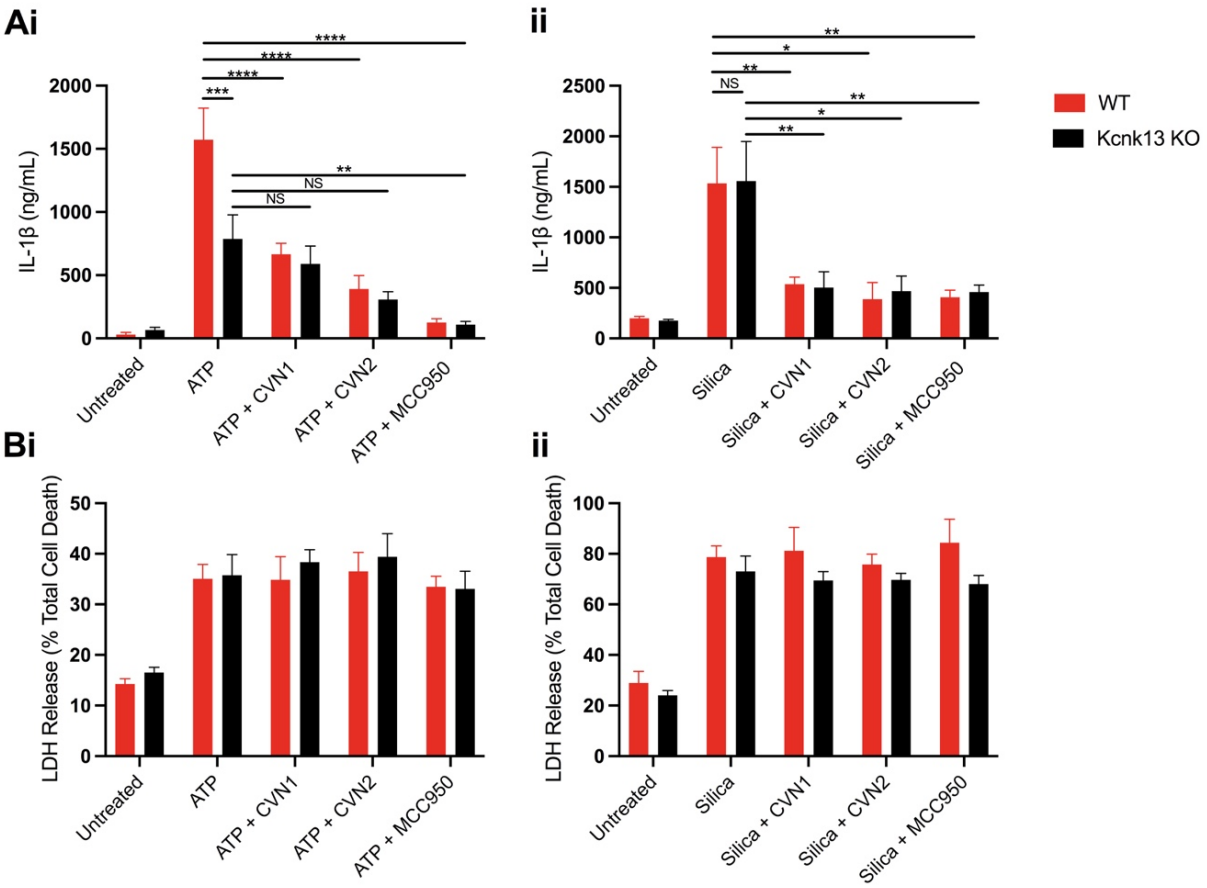

Figure 5.3 THIK-1 regulates ATP but not silica-induced NLRP3 activation in bone-marrow-derived macrophages.
(A) IL-1β ELISA and **(B)** LDH release assay of the supernatant of primary wild-type (WT) and Kcnk13 knockout (KO) BMDMs primed with LPS (1 μg mL^{-1}, 4 h) followed by pretreatment with CVN1 (100 nM), CVN2 (100 nM) or MCC950 (10 μM) for 15 min before stimulation with ATP (5 mM, 1 h) (n=7) or silica (300 μg mL^{-1},4 h) (n=7). ****p<0.0001, ***p<0.001, **p<0.01, *p<0.05 determined by two-way ANOVA with Bonferroni's post hoc analysis. Values shown are the mean ± SEM.

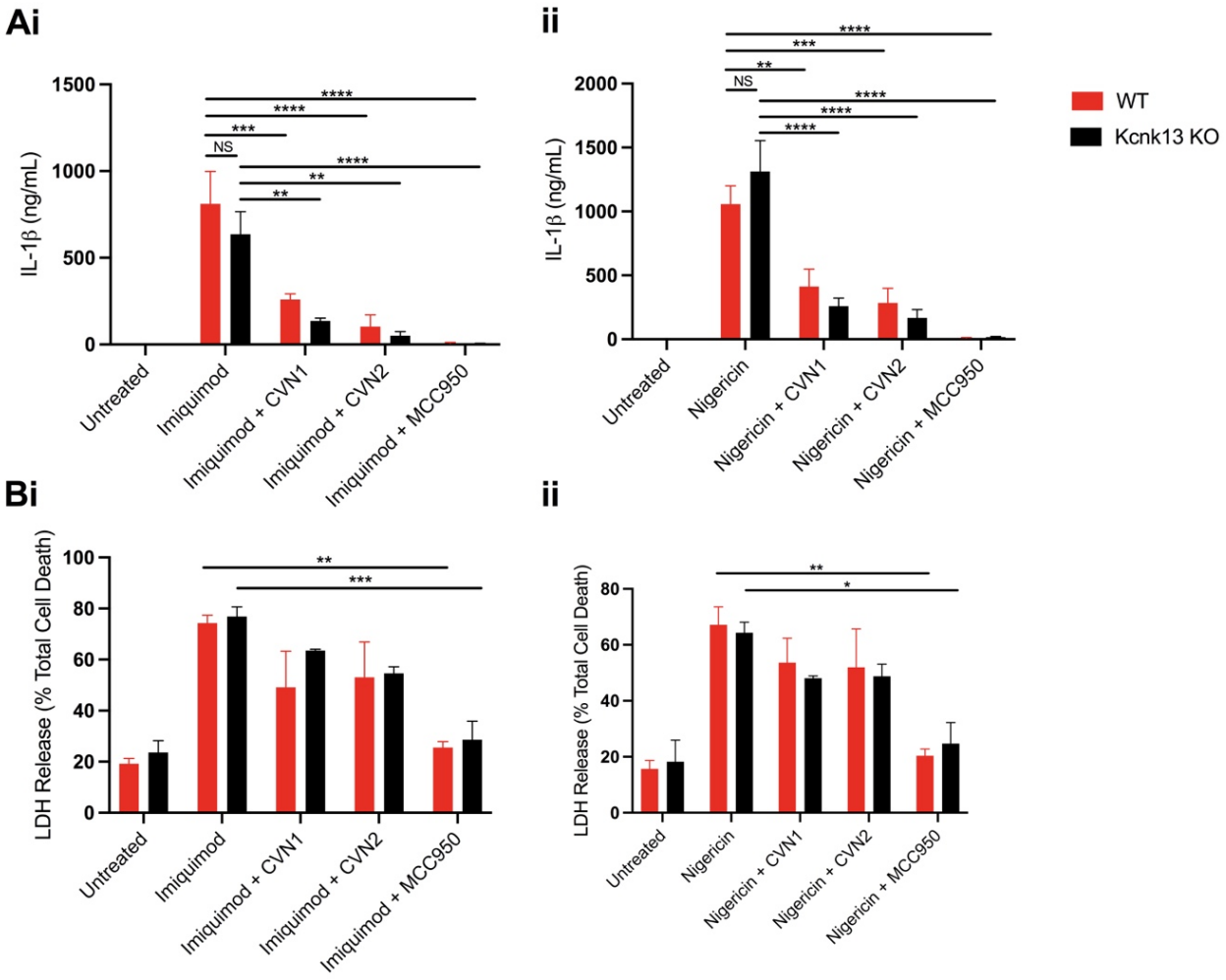

Figure 5.4 THIK-1 does not regulate imiquimod or nigericin-induced NLRP3 activation in bone-marrow-derived macrophages.
(A) IL-1β ELISA and **(B)** LDH release assay of the supernatant of primary wild-type (WT) and Kcnk13 knockout (KO) BMDMs primed with LPS (1 μg mL^{-1}, 4 h) followed by pre-treatment with CVN1 (100 nM), CVN2 (100 nM) or MCC950 (10 μM) for 15 min before stimulation with imiquimod (75 μM, 2 h) (n=4) or nigericin (10 μM, 1 h) (n=8). ****p<0.0001, ***p<0.001, **p<0.01, *p<0.05 determined by two-way ANOVA with Bonferroni's post hoc analysis. Values shown are the mean ± SEM.

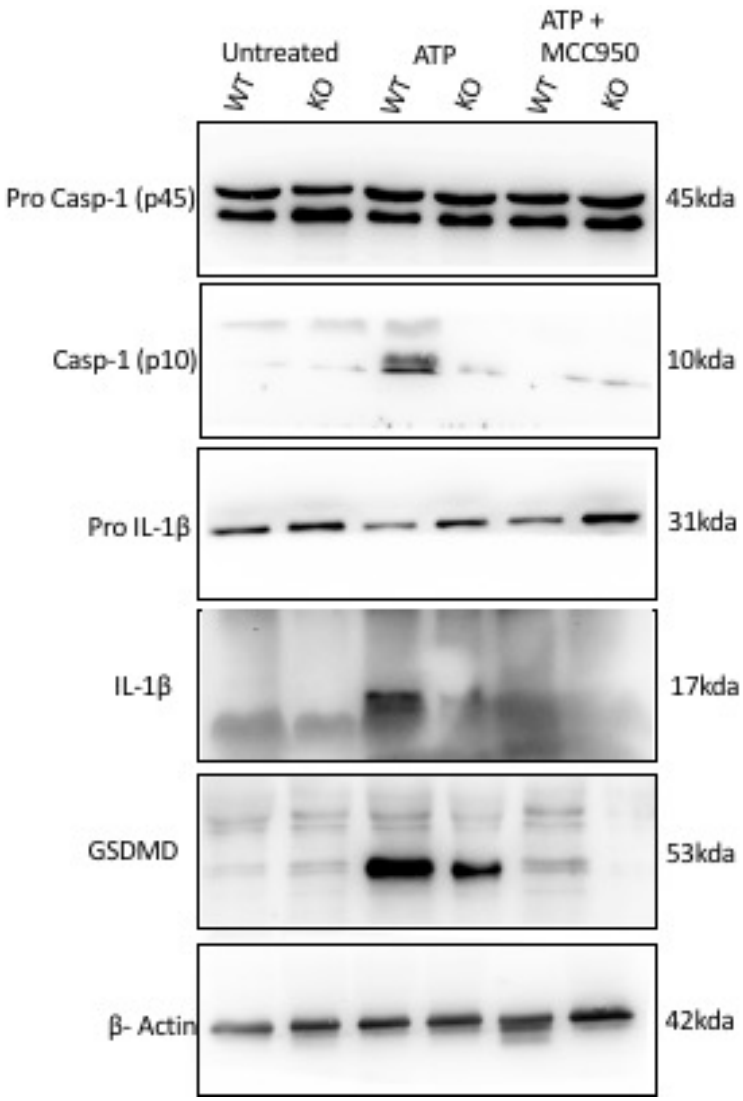

Figure 5.5 THIK-1 regulates caspase-1, IL-1β and GSDMD processing in response to ATP-induced NLRP3 activation.
Caspase-1, IL-1β and gasdermin D western blot of total cell lysates (cell lysate + supernatant) from LPS-primed WT and Kcnk13 KO pBMDMs pretreated with vehicle control or MCC950 (10 μM) for 15 min before stimulated with ATP (5 mM, 1 h).

To establish whether Tpa was reducing NLRP3 activation via inhibiting THIK-1, the impact of Tpa on NLRP3 activation in THIK-1 KO pBMDMs was investigated. Supporting previous findings (Fig. 5.3) THIK-1 KO inhibited ATP-induced NLRP3 activation (Fig. 5.6A) without inhibiting cell death (Fig. 5.6B). Tpa inhibited IL-1β release in response to ATP in WT pBMDMs but resulted in no greater inhibition in THIK-1 KO cells (Fig. 5.6A). This data suggests Tpa inhibits ATP-induced NLRP3 activation through inhibiting THIK-1. The effect of Tpa on imiquimod and nigericin in THIK-1 KO pBMDMs was also investigated. Replicating previous findings (Fig. 5.4) THIK-1 KO had no effect on imiquimod or nigericin-induced NLRP3 activation (Fig. 5.7A) or cell death (Fig. 5.7B). However, imiquimod and nigericin induced IL-1β release was still inhibited by Tpa in THIK-1 KO BMDMs, indicating that Tpa can also inhibit NLRP3 independently of THIK-1 inhibition (Fig. 5.7A). In support of these findings, Tpa was found in Chapter 3 (Fig. 3.2Aii) to inhibit silica-induced NLRP3 activation despite findings THIK-1 is dispensable for NLRP3 activation in response to silica (Fig. 5.3Aii). These results demonstrate that Tpa, in addition to CVN1 and CVN2 inhibit NLRP3 activation through inhibiting THIK-1 but may also inhibit NLRP3 activation in response to certain stimuli in BMDMs via additional modes of action.

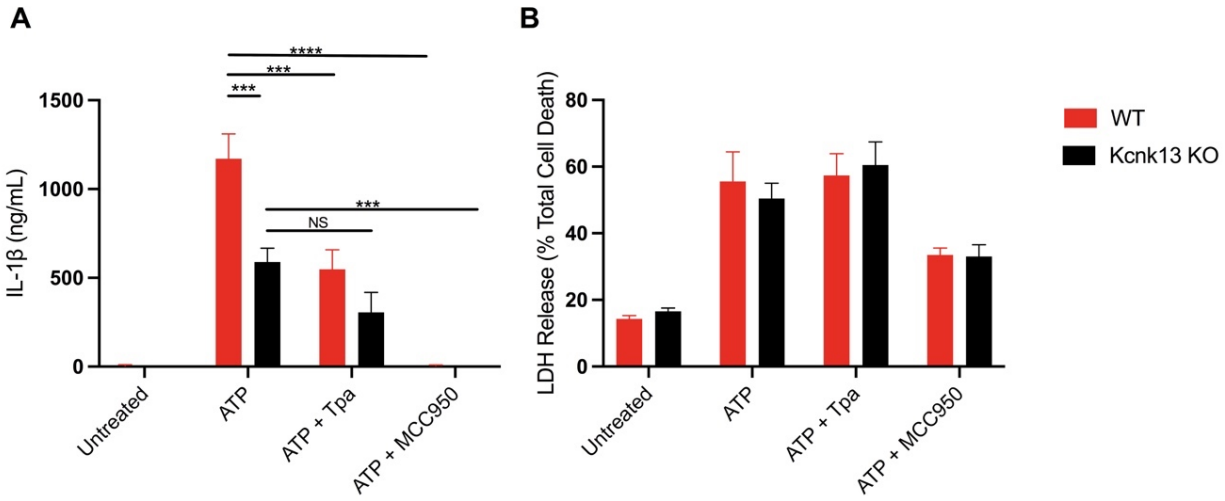

Figure 5.6 Tpa does not inhibit ATP-induced NLRP3 activation in THIK-1 knockout cells. **(A)** IL-1β ELISA and **(B)** LDH release assay of the supernatant of primary wild-type (WT) and Kcnk13 knockout (KO) BMDMs primed with LPS (1 μg mL^{-1}, 4 h) followed by pretreatment with vehicle control, Tpa (50 μM) or MCC950 (10 μM) for 15 minutes before stimulation with ATP (5 mM, 1 h) (n=4). ****p<0.0001, ***p<0.001 determined by two-way ANOVA with Bonferroni's post hoc analysis. Values shown are the mean ± SEM.

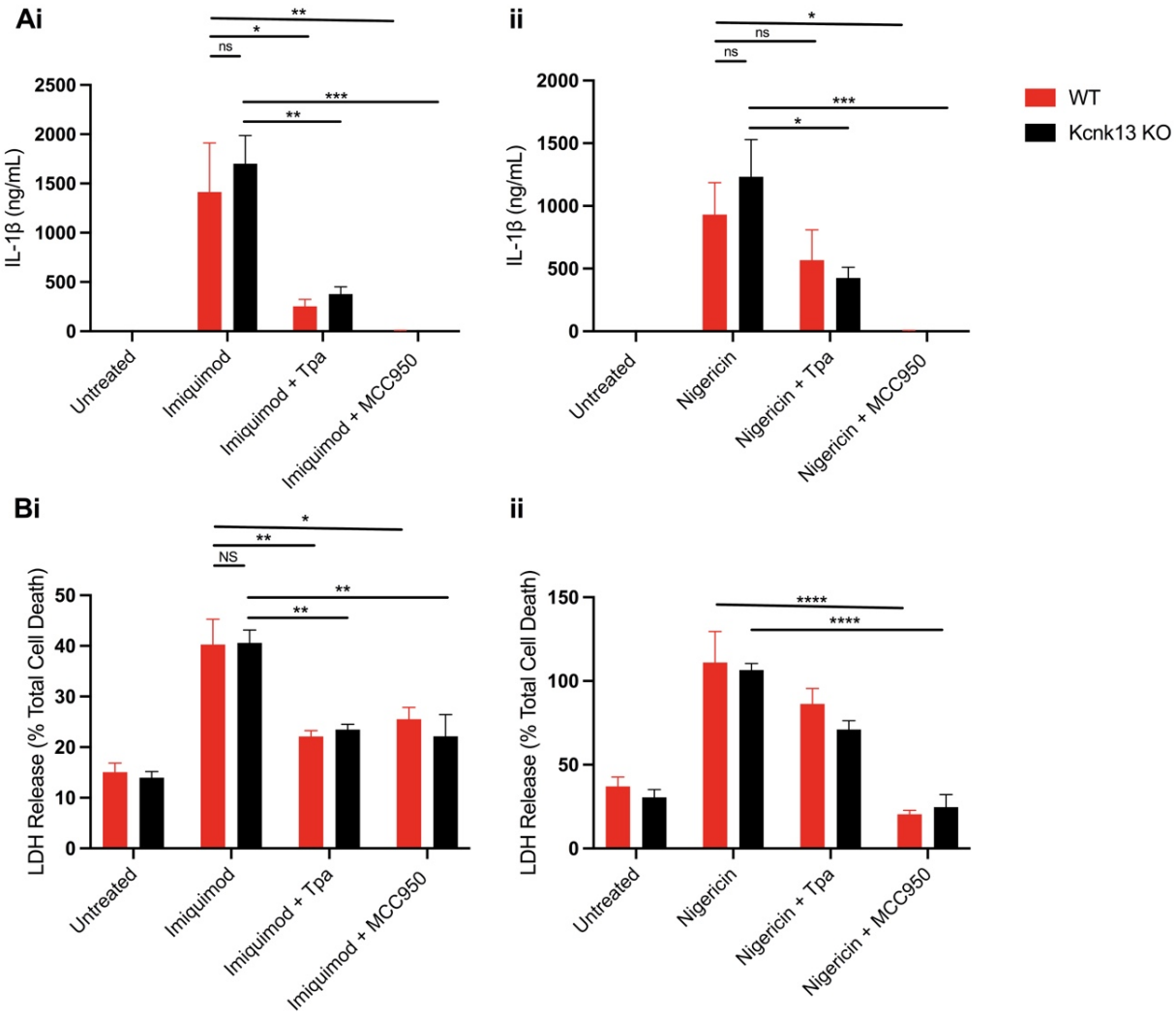

Figure 5.7 Tpa inhibits the NLRP3 inflammasome independently from inhibiting the THIK-1 K^+ channel.
(A) IL-1β ELISA and **(B)** LDH release assay of the supernatant of primary wild-type (WT) and Kcnk13 knockout (KO) BMDMs primed with LPS (1 μg mL^{-1}, 4 h) followed by pretreatment with vehicle control, Tpa (50 μM) or MCC950 (10 μM) for 15 minutes before stimulation with ATP (5 mM, 1 h) (n=4), imiquimod (75 μM, 2 h) (n=4) or nigericin (10 μM, 1 h) (n=4). ****p<0.0001, ***p<0.001, **p<0.01, *p<0.05 determined by two-way ANOVA with Bonferroni's post hoc analysis. Values shown are the mean ± SEM.

5.2.2 THIK-1 regulates ATP-induced NLRP3 activation independently of P2X7 receptor activation

ATP triggers NLRP3 inflammasome activation via activation of the P2X7 receptor (278). The study therefore next aimed to determine whether THIK-1 regulation of ATP-induced activation was occurring upstream or downstream of P2X7 receptor activation. Activation of the P2X7 receptor by ATP leads to the formation of a pore which permeabilises the plasma membrane to molecules up to 900 Da including the dye YO-PRO-1 (279, 280). YO-PRO-1 can be used as a readout of P2X7 receptor activation (245).

Control and THIK-1 siRNA transfected iBMDMs in addition non-transfected iBMDMs were primed with LPS and stimulated with ATP in the presence of the P2X7 permeable fluorescent stain YO-PRO-1. Transfection with THIK-1 siRNA had no effect on P2X7 receptor activation when compared to control siRNA treated cells in response to ATP (Fig. 5.8A). In addition, WT pBMDMs were primed with LPS and stimulated with ATP in the presence of YO-PRO-1. Pre-treatment with K2P inhibitor Tpa, and general K^+ channel inhibitor TEA, had no effect on P2X7-dependent pore formation, but the P2X7 inhibitor, oxidised ATP (oATP) inhibited YO-PRO-1 uptake (Fig. 5.8B). These data suggest that THIK-1 regulated ATP-induced NLRP3 activation downstream of P2X7 receptor activation.

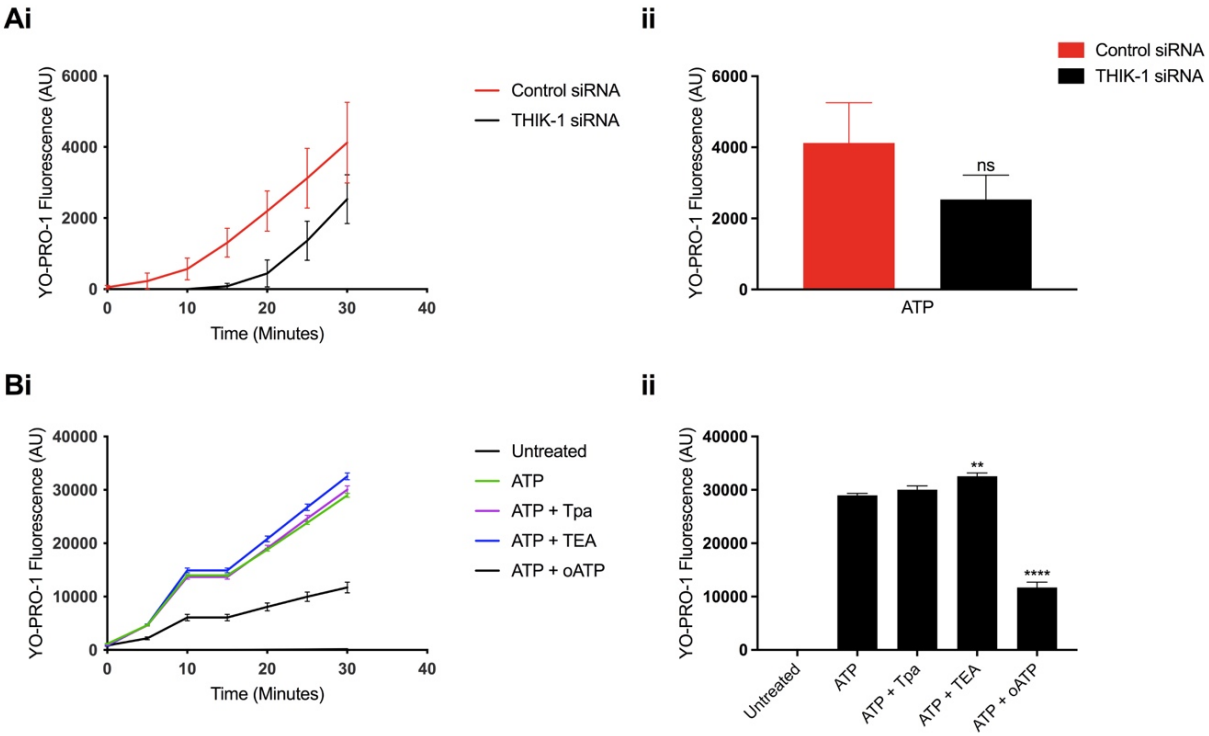

Figure 5.8 THIK-1 siRNA and pharmacological inhibition of THIK-1 has no effect on ATP-induced P2X7 receptor activation.
(A) YO-PRO-1 fluorescent P2X7 assay over 30 minutes of iBMDMs primed with LPS (1 µg mL^{-1}, 4 h) before stimulation with ATP (5 mM, 30 mins) (n=4). Prior to treatment, iBMDMs were transfected with transfection media and 25 nM control non-targeting siRNA or 25 nM THIK-1 siRNA for 48 h. **(B)** YO-PRO-1 fluorescent P2X7 assay over 30 minutes of pBMDMs primed with LPS (1µg mL^{-1}, 4 h) followed by pretreatment with TEA (50 mM), Tpa (50 µM) or oATP (5 mM) for 15 mins before stimulation with ATP (5 mM, 30 mins) (n=6), ****p<0.0001, **p<0.01 determined by t-test or one-way ANOVA with Dunnett's post hoc analysis. Values shown are the mean ± SEM.

5.2.3 THIK-1 does not regulate NLRP3 priming in murine macrophages

Following the observation that THIK-1 inhibiting compounds Tpa, CVN1 and CVN2 inhibited NLRP3 priming in Chapter 4 the next study sought to clarify whether THIK-1 also regulated the NLRP3 priming step in addition to activation. As previously mentioned above, THIK-1 siRNA transfection and pBMDMs harvested from THIK-1 KO mice were to study the role of THIK-1 in NLRP3 priming. THIK-1 siRNA had no effect on IL-6 or TNFα release in response to LPS treatment in pBMDMs when compared to control siRNA transfected cells (Fig. 5.9A). In addition, THIK-1 siRNA had no effect on cell death following LPS treatment (Fig. 5.9B).

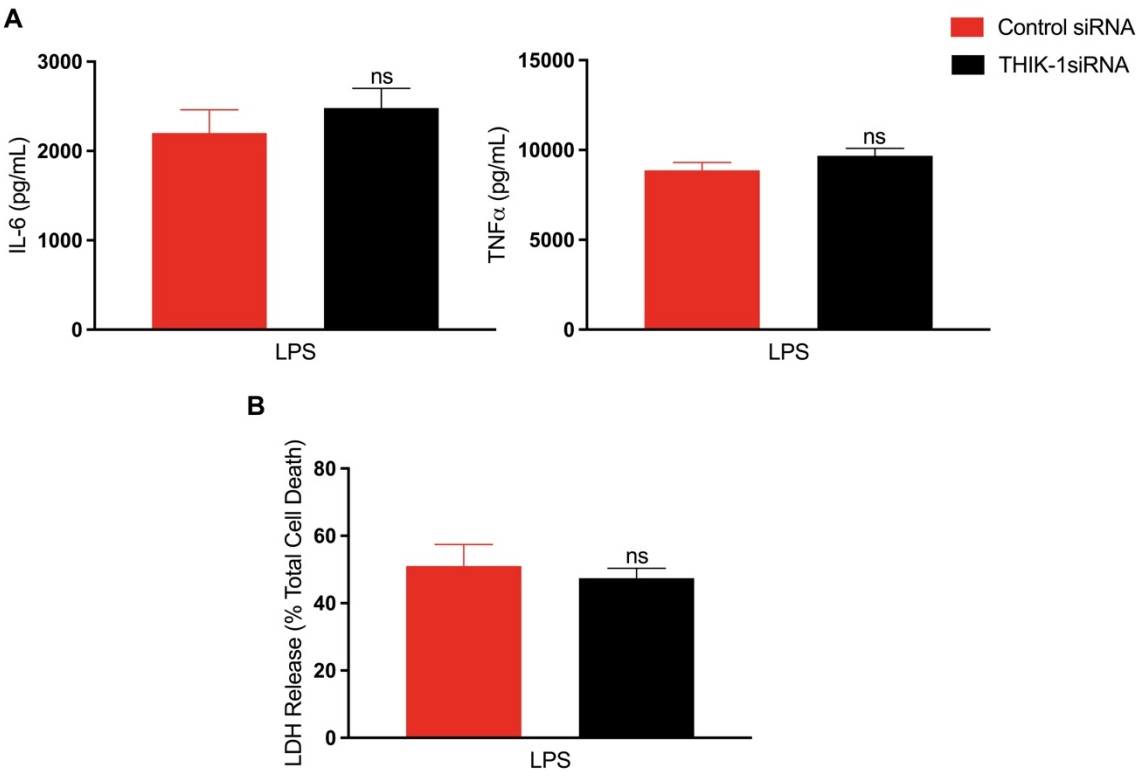

Figure 5.9 THIK-1 siRNA does not inhibit NLRP3 priming.
(A) IL-6 and TNFα ELISA and **(B)** LDH release assay of the supernatant from control and THIK-1 siRNA transfected iBMDM primed with LPS (1 μg mL^{-1}, 4 h). Prior to treatment, iBMDMs and pBMDMs were transfected with transfection media and 25 nM control non-targeting siRNA or 25 nM THIK-1 siRNA for 48 h. Statistical significance determined by one-way ANOVA with Dunnett's post hoc analysis. Values shown are the mean ± SEM.

In support of these findings THIK-1 KO had no effect on IL-6 or TNFα release in response to LPS (Fig. 5.10A). Furthermore, knocking out THIK-1 did not inhibit NLRP3 or pro-IL-1β protein expression stimulated by LPS (Fig. 10C). THIK-1 inhibitors CVN1 and CVN2 also did not inhibit IL-6 or TNFα release in WT or THIK-1 KO pBMDMs following LPS treatment (Fig. 5.10A). Also, THIK-1 KO, CVN1 or CVN2 had no impact on cell death in response to LPS (Fig. 10B). However, CVN1 and CVN2 were previously shown to inhibit NLRP3 priming in iBMDMs (Fig. 4.8), highlighting a potential mechanistic difference between NLRP3 activation in iBMDM cell lines and primary BMDMs. These data show THIK-1 is required for NLRP3 activation but is dispensable for NLRP3 priming.

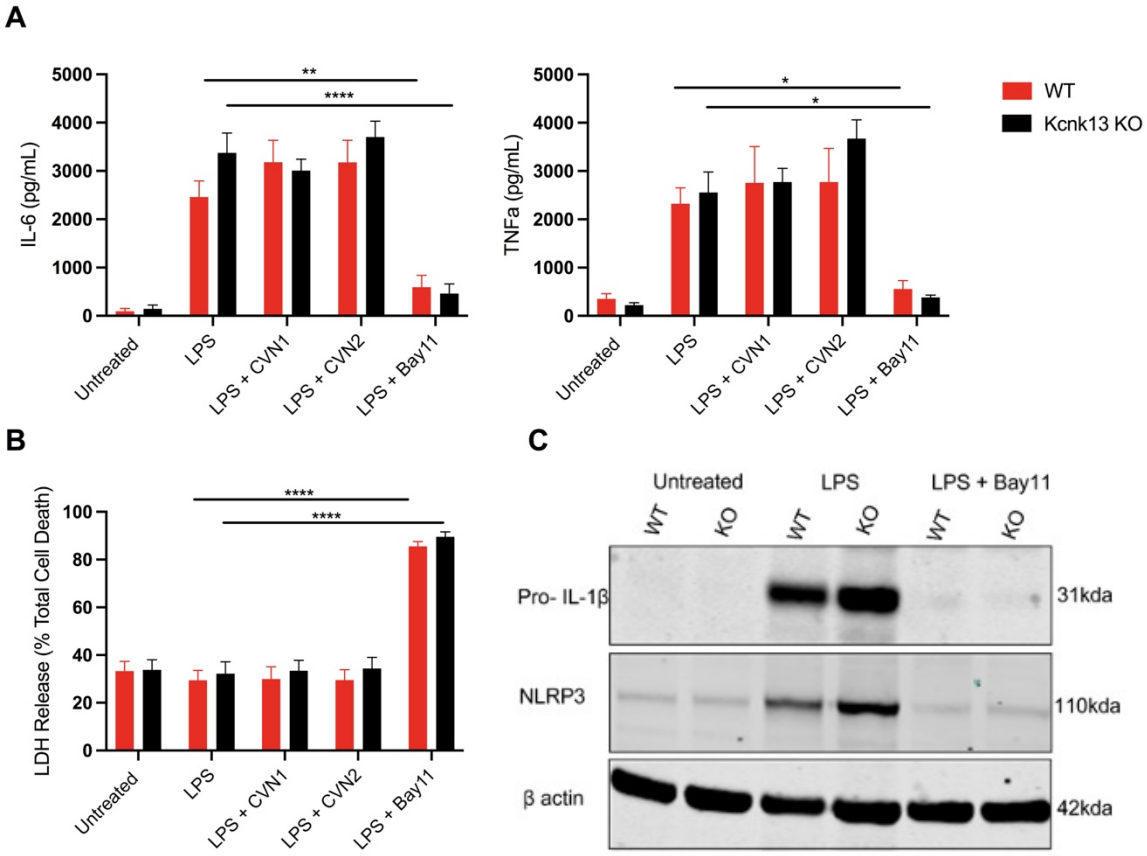

Figure 5.10 THIK-1 is dispensable for NLRP3 priming in bone marrow-derived macrophages.
(A) IL-6 and TNFα ELISA and **(B)** LDH release assay of the supernatant of primary wild-type (WT) and Kcnk13 knockout (KO) pBMDMs pretreated with CVN1 (100 nM), CVN2 (100 nM) or Bay11 (10 μM) for 15 min before priming with LPS (1 μg mL^{-1}, 4 h) (n=7). **(C)** NLRP3 and IL-1β western blot of the supernatant and total cell lysates respectively of primary wild-type (WT) and Kcnk13 knockout (KO) BMDMs pretreated with Bay11(10 μM) for 15 min before priming with LPS (1 μg mL^{-1}, 4 h). ****p<0.0001, **p<0.01, *p<0.05 determined by two-way ANOVA with Bonferroni's post hoc analysis. Values shown are the mean ± SEM.

Following the findings that THIK-1 is dispensable for priming of the NLRP3 inflammasome, the impact of Tpa on NLRP3 priming in THIK-1 KO pBMDMs was then investigated. Tpa was previously shown to inhibit NLRP3 priming in iBMDMs (Fig. 3.7), as THIK-1 KO does not impact priming this suggests Tpa can inhibit NLRP3 priming independently of inhibiting THIK-1. As previously observed THIK-1 KO had no effect on LPS-induced IL-6 or TNFα release (Fig. 5.11A). Pre-treatment with Tpa inhibited IL-6 release in both WT and THIK-1 KO pBMDMs but did not inhibit TNFα release (Fig. 5.11A). These findings confirm Tpa is capable of inhibiting NLRP3 priming independently from inhibiting THIK-1 K^+ channels. Taken together these studies show THIK-1 is not required for priming of the NLRP3 inflammasome. Furthermore, the data demonstrate Tpa can inhibit priming independently of its action at THIK-1 suggesting Tpa can regulate both NLRP3 priming in addition to activation independently from its THIK-1 inhibiting properties.

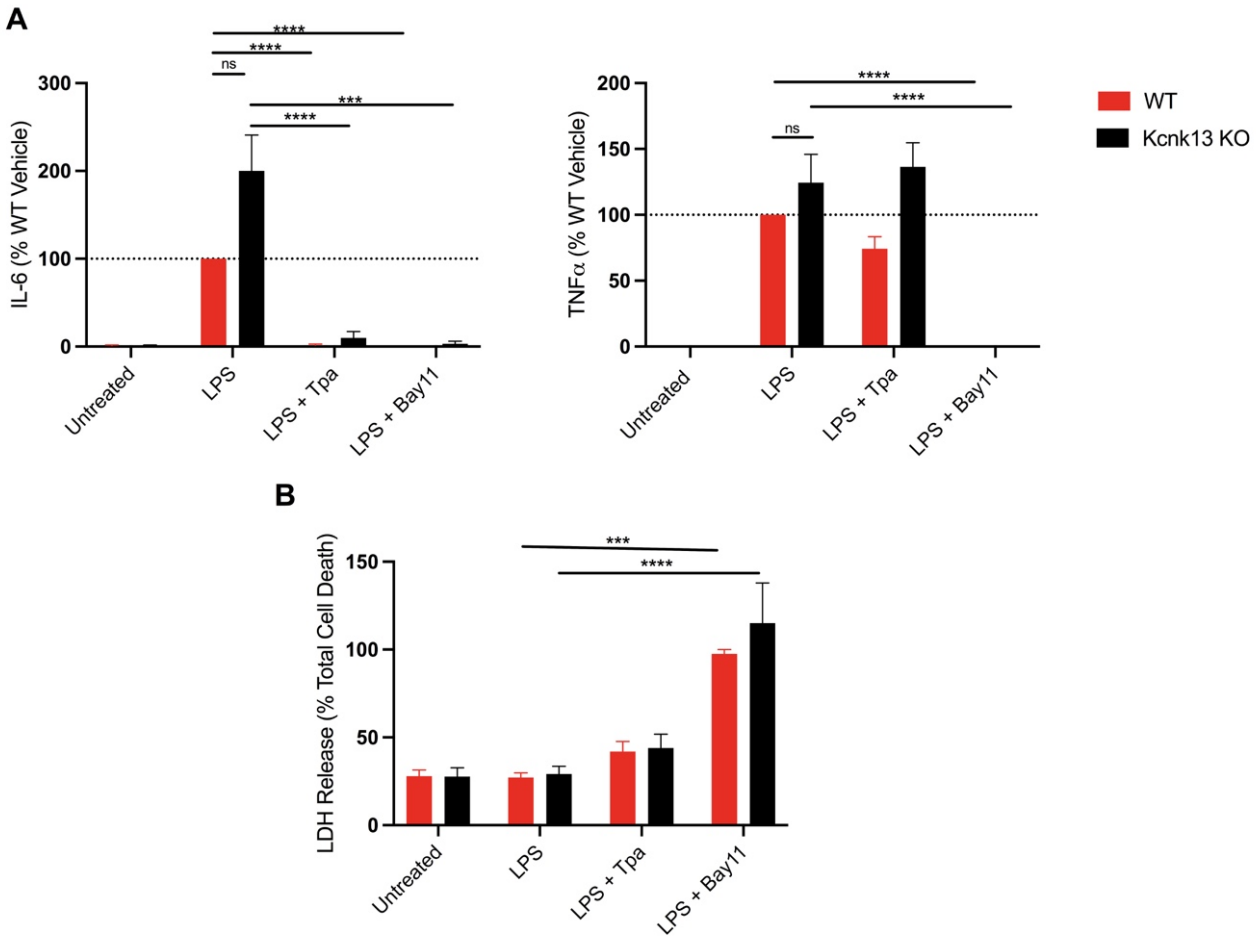

Figure 5.11 Tpa inhibits NLRP3 priming independently from THIK-1 inhibition.
(A) IL-6 and TNFα ELISA and **(B)** LDH release assay of the supernatant of primary wild-type (WT) and Kcnk13 knockout (KO) pBMDMs pretreated with Tpa (50 μM) or Bay11 (10 μM) for 15 min before priming with LPS (1 μg mL^{-1}, 4 h) (n=4). ****p<0.0001, ***p<0.001 determined by two-way ANOVA with Bonferroni's post hoc analysis. Values shown are the mean ± SEM.

5.2.4 THIK-1 antibody displays non-specific binding

Having confirmed THIK-1 depletion in THIK-1 KO BMDMs using cell genotyping, THIK-1 KO BMDMs were used to validate the selectivity of the THIK-1 antibody used to confirm THIK-1 knockdown. Four different THIK-1 antibody dilutions, 1/200, 1/400, 1/600 and 1/1000 were tested in BMDM cell lysates from WT (n=3) and THIK-1 KO (n=3) mice and western blotting used to investigate antibody selectivity. At each dilution, a band was observed at 47kda in the WT cells (Fig.5.8), which is the molecular weight of THIK-1 and the same molecular weight band observed in siRNA studies (Fig.5.1C). This data would suggest the band generated is due to the antibody binding the THIK-1 protein. However, in THIK-1 KO BMDMs, in which genotyping confirmed no THIK-1 expression, a strong band was still present (Fig.5.8). These findings show the THIK-1 antibody used in the confirmation of THIK-1 knockdown in siRNA experiments displays nonspecific binding. The band at 47kda in THIK-1 KO cells suggests the THIK-1 antibody binds to an additional protein of similar molecular weight to THIK-1. Therefore, this antibody is unsuitable for evaluating THIK-1 protein expression as the nonspecific band generated masks the band that should be present through antibody binding to THIK-1.

The finding that the THIK-1 antibody shows nonspecific binding suggests the western blot results confirming THIK-1 knockdown in Fig.5.1C are unreliable. Therefore, the study cannot confirm transfection of cells with THIK-1 siRNA was successful in knocking down protein expression of THIK-1. Despite THIK-1 siRNA treated cells displaying the same phenotypic responses to NLRP3 activators as THIK-1 KO cells, the study cannot conclude the observed results are due to THIK-1 knockdown. However, THIK-1 KO was confirmed without the need for a selective THIK-1 antibody by using qPCR. Thus, results obtained in THIK-1 KO cells can be concluded to be caused by depletion of THIK-1 expression. These results demonstrate the THIK-1 antibody used in these studies is not selective to THIK-1. The implications of this finding are that THIK-1 knockdown cannot be confirmed in siRNA studies and therefore data from THIK-1 knockdown experiments can no longer be used to support the findings in THIK-1 KO BMDMS.

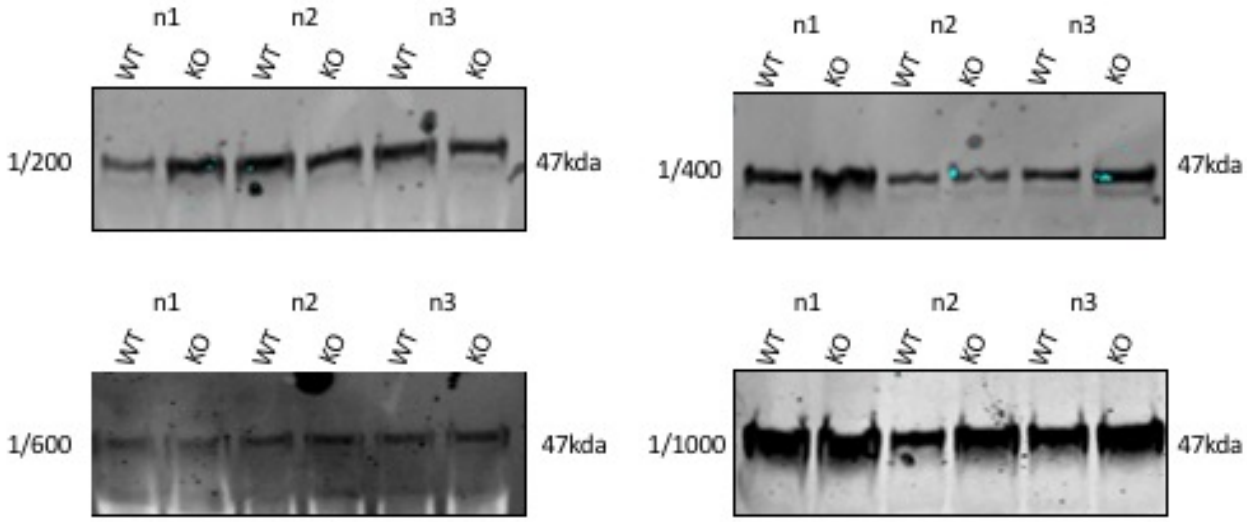

Figure 5.12 THIK-1 antibody is non-selective.
THIK-1 western blot of total cell lysates (cell lysate + supernatant) from WT and Kcnk13 KO pBMDMs to validate THIK-1 antibody. Four different THIK-1 antibody concentrations were used (1/200, 1/400, 1/600 and 1/1000).

5.2.5 THIK-1 regulates ATP and nigericin induced-NLRP3 inflammasome activation in microglia

To determine whether THIK-1 regulates NLRP3 activation in microglia in addition to peripheral macrophages, adult microglia from THIK-1 KO mice were harvested. WT and THIK-1 KO microglia were primed with LPS and NLRP3 activation stimulated with ATP, silica, imiquimod and nigericin. Knocking out THIK-1 inhibited NLRP3 activation in response to both ATP and nigericin but had no effect on silica or imiquimod-induced activation (Fig. 5.13A). One potential explanation for the different impact of THIK-1 KO in microglia versus BMDMs following nigericin-induced NLRP3 activation is the difference in THIK-1 expression between the two cell types. THIK-1 appears more highly expressed in microglia and may therefore play a broader role in NLRP3 activation when compared to BMDMs (Fig. 3.1). Further, THIK-1 KO had no effect on TNFα release from microglia in response to LPS treatment (Fig. 5.13B). These data suggest THIK-1 regulates NLRP3 activation in brain resident microglia in addition to peripheral macrophages.

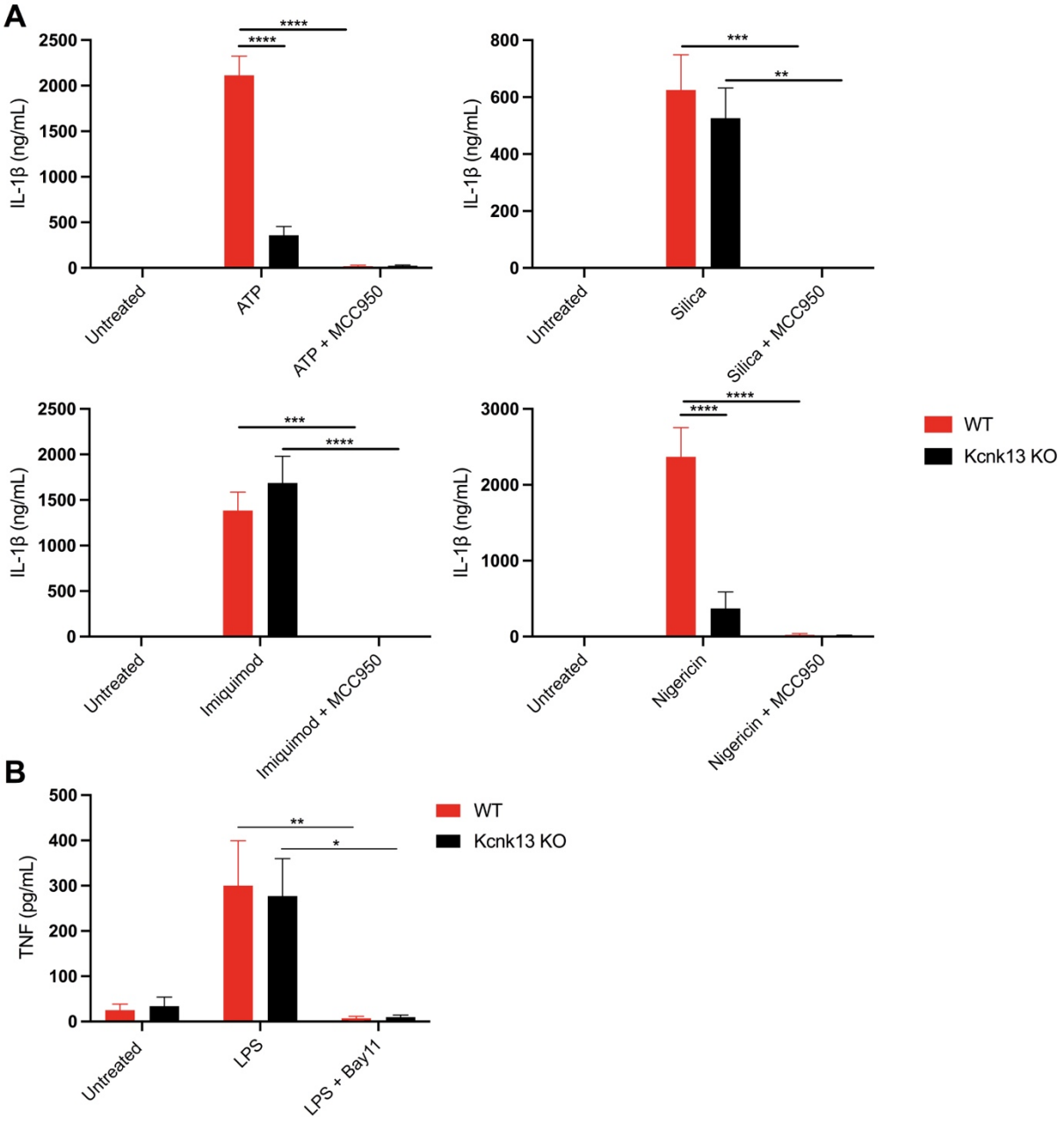

Figure 5.13 THIK-1 regulates NLRP3 activation in primary adult microglia.
(A) IL-1β ELISA of the supernatant of primary wild-type (WT) and Kcnk13 knockout (KO) adult microglia primed with LPS (1 μg mL^{-1}, 4h) followed by pretreatment with MCC950 (10 μM) for 15 min before stimulation with ATP (5 mM, 1h) (n=4), silica (300 μg mL^{-1},4 h) (n=3), imiquimod (75 μM, 2 h) (n=3) or nigericin (10 μM, 1 h) (n=4). **(B)** TNFα ELISA of the supernatant of primary wild-type (WT) and Kcnk13 knockout (KO) primary adult microglia pretreated with Bay11(10 μM) for 15 min before priming with LPS (1 μg mL^{-1}, 4 h) (n=5). ****p<0.0001, ***p<0.001, **p<0.01, *p<0.05 determined by two-way ANOVA with Bonferroni's post hoc analysis. Values shown are the mean ± SEM.

5.2.6 THIK-1 mRNA is upregulated in Alzheimer's and Parkinson's disease postmortem brain tissue

Neuroinflammation is heavily associated with the progression of neurodegenerative diseases like AD and PD, with previous studies suggesting NLRP3 is a key driver of pathogenic inflammation in both diseases (9, 281). Following the *in vitro* findings identifying THIK-1 as a regulator NLRP3 inflammasome activation the next study investigated whether THIK-1 mRNA expression was elevated in post-mortem brain tissue of AD and PD patients.

Using RT-qPCR, THIK-1 mRNA expression was quantified in human AD post-mortem temporal cortex tissue in addition to PD substantia nigra and frontal cortex tissue. Firstly, AD tissue was divided into age-matched groups based on the degree of AD pathology using Braak staging. The control non-AD group contained tissue with Braak staging 0-II, with the remaining tissue divided into two groups, Braak III-IV and V-VI. Following quantification of THIK-1 mRNA expression within each group we then calculated the fold-change in THIK-1 mRNA expression in comparison to the control group to evaluate how THIK-1 expression changed as a function of AD pathology. In comparison to control tissue, THIK-1-expression was found to be unchanged in Braak III-IV tissue (Fig. 5.14A). However, THIK-1 mRNA expression was significantly higher in Braak stage V-VI temporal cortex tissue in comparison to control tissue (Fig. 5.14A). Furthermore, THIK-1 expression did not increase with age in healthy control tissue suggesting increased THIK-1 expression is disease specific and not a result of ageing (data not shown). In support of these findings a recent study identified a rare variant in the *KCNK13* gene (encoding THIK-1) to be significantly associated with familial late onset AD further linking THIK-1 with AD pathology (282). The data in this study suggest THIK-1 expression is upregulated at later stages of AD progression which correlates with the greatest levels of neuroinflammation providing a causal link between THIK-1 mRNA expression and neuroinflammation in AD.

In addition to AD post-mortem tissue, THIK-1 mRNA expression was elevated in both substantia nigra and frontal cortex tissue from PD patients in comparison to age-matched healthy control tissue (Fig. 5.14B). These data demonstrate THIK-1 expression is elevated in NLRP3 associated neuroinflammatory diseases. Together with findings that THIK-1 regulates the NLRP3

inflammasome, it is possible that elevated THIK-1 expression in CNS enhances damaging NLRP3 mediated inflammation contributing to neurodegenerative disease progression.

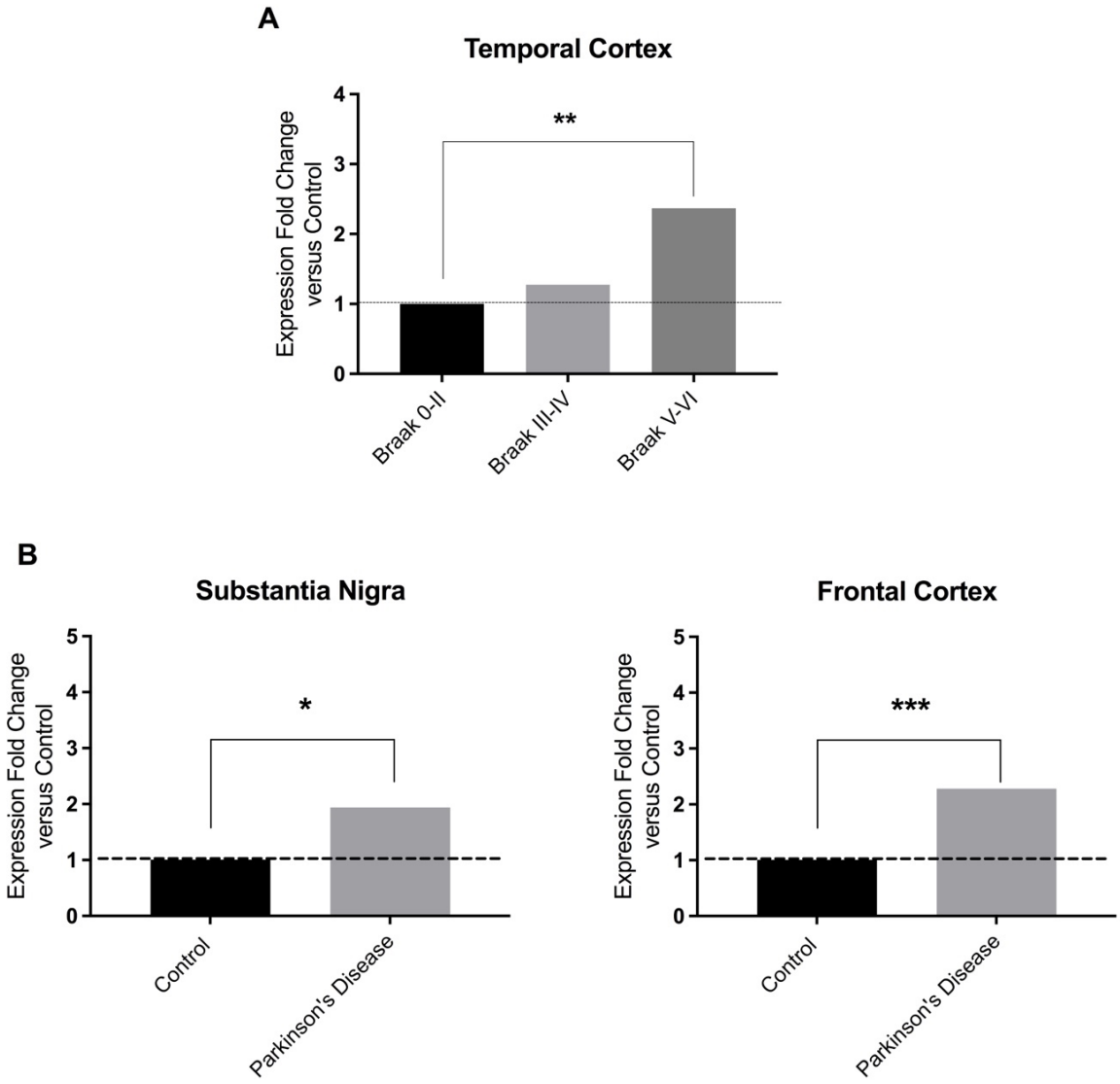

Figure 5.14 THIK-1 mRNA is upregulated in Alzheimer's and Parkinson's disease. **(A)** Data show expression fold change of THIK-1 mRNA in age-matched post-mortem temporal cortex tissue from Alzheimer's disease patients classified as Braak stages III-IV and Braak stages V-VI versus control non-Alzheimer's disease tissue (Braak stages 0-II) (n = 40, males = 20, females = 20, per group). **(B)** Data show expression fold change of THIK-1 mRNA in age-matched post-mortem substantia nigra and frontal cortex tissue from Parkinson's disease patients versus control non-Parkinson's disease tissue (n = 15, males = 6-8, females = 7-9, per group). Relative expression of THIK-1 mRNA in comparison to RPL13A and GAPDH mRNA was calculated using the 2-[delta][delta]Ct method. Data are presented as THIK-1 mRNA expression fold change versus control group. ***p<0.001, **p<0.01, *p<0.05 determined one-way ANOVA with Dunnett's post hoc analysis

5.3 Discussion

These data reveal THIK-1 as a specific regulator of ATP-induced NLRP3 activation and suggest that in response to extracellular ATP THIK-1 is required for the activation of caspase-1 and subsequent IL-1β processing and release. In addition, THIK-1 inhibitors Tpa, CVN1 and CVN2 were found to attenuate NLRP3 activation by an additional mechanism beyond THIK-1 inhibition in some cellular systems.

As previously mentioned, the K2P channels TWIK-2 and THIK-1 have been independently identified as potential regulators of ATP-induced NLRP3 activation (77, 78). Both studies suggest TWIK-2 and THIK-1 activation are regulated by purinergic receptors (P2X7 and P2Y12 respectively) (68, 78). TWIK-2 was conclusively demonstrated to be a positive regulator of NLRP3 activation and was the first study to highlight the involvement of K2P channels the regulation of the NLRP3 inflammasome (78). Although THIK-1 has been identified to regulate ATP-induced IL-1β release in hippocampal slices, whether this is mediated via regulation of NLRP3 was not determined (68). Consistent with prior studies (68) this present study demonstrates in THIK-1 KO macrophages that THIK-1 is required specifically for ATP-induced NLRP3 activation but is dispensable for activation in response to other canonical stimuli. These data together with previous work suggests THIK-1 and TWIK-2 K2P channels regulate NLRP3 activation downstream of ATP-induced activation of purinergic receptors

It is well established that purinergic receptors play a role in NLRP3 activation. ATP activation of the P2X7 receptor induces K^+ efflux and NLRP3 activation (283). Several studies suggest two complementing models for P2X7 cell permeabilization, the dilation of the P2X7 ionic pore and P2X7 mediated opening of additional large conductance channels such as hemichannels and K^+ channels (56, 78, 284–288). Prior research has also suggested other purinergic receptors other than P2X7 can influence NLRP3 activation (278). In particular, the P2Y family of G-protein coupled receptors which are also stimulated by nucleotides such as ATP and ADP have been associated with NLRP3 activation suggesting P2Y receptors may also regulate NLRP3 activation (66, 67). Pharmacological inhibition of P2Y1 reduces nano-particle-induced NLRP3 activation (66). ADP and UTP may also induce NLRP3 activation via P2Y receptor activation (67). It is therefore possible ATP and its metabolites stimulate purinergic receptors which indirectly induce K^+ efflux and NLRP3 activation

through downstream opening of K^+ channels. This present study observed transfection with THIK-1 siRNA and K2P channel inhibition to reduce ATP-induced NLRP3 activation without impacting P2X7 receptor activity suggesting THIK-1 regulates NLRP3 activation downstream of P2X7 receptor activation. P2X7 depletion blocks ATP-dependent NLRP3 activation and is thus fundamentally required for ATP-induced NLRP3 activation (54, 289, 290). However, deletion of P2Y12 also reduces NLRP3 activation in response to ATP (291). Together, previous findings and this study suggest P2X7 and P2Y12 may both be required for ATP-induced NLRP3 activation, potentially in part through regulation of K^+ currents through K2P channels such as THIK-1 and TWIK-2.

Despite THIK-1 being identified as a regulator of NLRP3 activation specifically in response to ATP in BMDMs, THIK-1 inhibitors were observed to still inhibit NLRP3 in THIK-1 KO cells. These findings show THIK-1 inhibitors Tpa, CVN1 and CVN2 are capable of inhibiting NLRP3 independently from their THIK-1 activity. The most likely explanation for these findings would be that these compounds also inhibit the only other K2P channel found in Chapter 1 to be expressed by BMDMS, TWIK-2, which is structurally similar to THIK-1 (69). However, TWIK-2 knockdown has previously been shown to have no effect on imiquimod or nigericin induced NLRP3 activation in BMDMs, showing TWIK-2 is dispensable for NLRP3 activation in response to these stimuli (78). The present study found Tpa, CVN1 and CVN2 to each inhibit either imiquimod and/or nigericin induced activation suggesting Tpa, CVN1 and CVN1 inhibit NLRP3 activation independently from inhibiting TWIK-2. Furthermore, the findings that THIK-1 inhibitors regulate NLRP3 activation in response to the K^+ efflux independent stimuli imiquimod suggests the inhibitors regulate NLRP3 activation independently from action at any K^+ channels in this system. In addition to K^+ channels, Cl^- channels have also been found to regulate NLRP3 activation (82, 86). Thus, THIK-1 inhibitors may also inhibit NLRP3 activation through inhibition of Cl^- channels such as the CLIC channels which are known to regulate NLRP3 activation in addition to inhibiting THIK-1 (82, 86). However, it was out of the scope of this thesis to identify the mechanism by which THIK-1 inhibitors attenuate NLRP3 activation in THIK-1 KO BMDMs in response to certain stimuli. Further work would need to be performed to fully elucidate any additional mechanisms that are contributing to the NLRP3 attenuating activity observed. The data gathered in this study suggests THIK-1 represents a viable target for limiting ATP-induced NLRP3 activation.

NLRP3 has been implicated in contributing to damaging neuroinflammation in a number of diseases including the neurodegenerative diseases AD and PD (9, 281). A recent association study used whole exome sequencing to identify gene variants associated with familial late onset AD (282). Of the several genetic variants found to significantly associate with AD was a rare variant in *KCNK13.* This finding provides the first genetic link between THIK-1 and AD suggesting THIK-1 may play a role in AD pathology. In support of these previous findings, the present study found THIK-1 mRNA expression to be upregulated in brain tissue from both AD and PD patients. Together these studies provide genetic evidence to suggest changes in THIK-1 expression or variations in the THIK-1 gene may play a role in neurodegenerative disease pathology. Taking into consideration the findings that THIK-1 regulates NLRP3 activation, NLRP3 is associated with AD and PD pathology and THIK-1 is genetically associated with AD it is possible THIK-1 contributes to AD and PD pathology through enhancing damaging NLRP3 mediated inflammation. Future studies should investigate the role of THIK-1 in animal models of AD and PD to fully establish the potential of THIK-1 as a therapeutic target for limiting pathological inflammation in neurodegenerative diseases. Given the limitations of available THIK-1 inhibitors due to lack of selectivity for THIK-1 the best approach would be to use THIK-1 KO mice for *in vivo* studies. Building on these findings, follow up studies could cross THIK-1 KO mice with APP/PS1 transgenic mouse AD models and evaluate how THIK-1 KO impacts markers of inflammation within the brain and cognitive deficits in the animals.

The present study identifies THIK-1 as a regulator of NLRP3 activation in mouse macrophages and microglia in response to the canonical stimuli ATP. Data show THIK-1 is required for NLRP3 dependent caspase-1 activation and IL-1β release in response to ATP. These results demonstrate that multiple K^+ channels may be involved in ATP driven NLRP3 activation and highlight the therapeutic potential of targeting K^+ channels to limit aberrant NLRP3-induced inflammation in disease. In support of this expression of THIK-1 was demonstrated to be elevated in both AD and PD. THIK-1 represents a viable therapeutic target for limiting NLRP3 inflammasome activation in peripheral and CNS diseases.

Chapter 6: General Discussion

6.1 Introduction

The NLRP3 inflammasome is a multi-protein complex which drives caspase-1-dependent processing and secretion of the pro-inflammatory cytokines IL-1β and IL-18, and pyroptotic cell death. A commonly reported mechanism contributing to NLRP3 inflammasome activation is potassium ion (K^+) efflux across the plasma membrane. Identification of K^+ channels involved in NLRP3 activation remains incomplete. The NLRP3 inflammasome contributes to inflammation in many diseases and thus understanding mechanisms regulating NLRP3 is an area of intense research interest. Identifying K^+ channels regulating NLRP3 inflammasome activation may provide effective therapeutic targets for liming NLRP3 induced inflammasome in disease.

The aim of this PhD was to identify K^+ channels regulating NLRP3 inflammasome activation. Firstly, genetic screening and pharmacological approaches were utilized to identify potential K^+ channels involved in regulation of NLRP3 activation. Secondly, following identification of potential NLRP3 regulating K^+ channels, the impact of selective K^+ channel inhibitors on NLRP3 activation were characterized. Finally, genetic engineering approaches were used to determine the selectivity of K^+ channel inhibitors used and confirm the role of an identified K^+ channel in NLRP3 activation.

6.2 THIK-1 is a target for limiting NLRP3 activation

NLRP3 has emerged as a key player in a wide range of inflammatory disease, ranging from peripheral diseases such as atherosclerosis, metabolic conditions including type-2 diabetes and even CNS diseases such as AD (292). As such understanding the mechanisms by which NLRP3 activation is regulated has become an area of intense research interest. Improving our understanding of NLRP3 regulatory mechanisms could potentially identify novel targets for manipulating NLRP3 activation in disease.

The association of NLRP3 with a diverse array of seemingly unrelated diseases has driven huge interest within the scientific community in discovering NLRP3 modulating compounds. In recent years, several inhibitors of the NLRP3 inflammasome pathway have been identified (293). However, no NLRP3 inhibitors are currently approved for clinical use. Current therapies for NLRP3 associated

diseases are limited IL-1β targeting compounds (294). However, IL-1β release can be driven by other inflammasomes and inflammasome independent pathways, therefore directly targeting IL-1β can have unwanted immunosuppressive effects. Therefore, developing NLRP3 specific inhibitors may provide therapeutic benefit to a wide-ranging number of patients with an array of different NLRP3-associated conditions.

Several studies have proposed mechanisms to explain how such a diverse range of stimuli converge on NLRP3 activation. One proposed mechanism is a decrease in intracellular K^+ which is important for multiple NLRP3 activating stimuli (44, 45). Therefore, suggesting the targeting of K^+ efflux may represent a pathway for limiting NLRP3 inflammasome activation. Recent findings have identified K2P channels as potential regulators of a K^+ sensitive process required for NLRP3 activation (68, 78). The K2P channel TWIK-2 has been shown to inhibit NLRP3 activation in peripheral macrophages in response to ATP (78). An additional K2P channel, THIK-1 has also been associated with IL-1β release in response to ATP in hippocampal slices but not conclusively shown to regulate NLRP3 activation (68). It was clear a more thorough characterization of the role of THIK-1 in NLRP3 activation was required.

In this work, evidence was gathered to support findings that K2P channels play an important role in regulating ATP-induced NLRP3 activation. Using RNA-sequencing databases, pharmacological K^+ channel inhibitors and genetic engineering techniques, the K^+ channel THIK-1 was identified as specific regulator of ATP-induced NLRP3 activation in peripheral macrophages and data gathered using THIK-1 inhibiting compounds suggest that this may occur through a mechanism independent of ASC oligomerization. THIK-1 was also found to selectively regulate the NLRP3 inflammasome pathway and did not impact the activation of other inflammasomes or NF-κB mediated NLRP3 priming. As discussed previously data in this thesis together with previous work suggest K2P channels THIK-1 and TWIK-2 regulate NLRP3 activation downstream of ATP-induced activation of purinergic receptors (Fig. 6.1). These data suggest THIK-1 may represent a novel therapeutic target for limiting ATP mediated NLRP3 inflammasome activation in peripheral inflammatory diseases without interfering with other inflammatory pathways. The ATP-P2X7-NLRP3 inflammasome activation pathway has been associated with a number of peripheral inflammatory diseases,

including diabetes, depression and cardiovascular disease (295, 296). Hence, THIK-1 may represent a potential therapeutic target for limiting inflammation in peripheral diseases in which ATP-P2X7-NLRP3 signaling is a contributor to pathology.

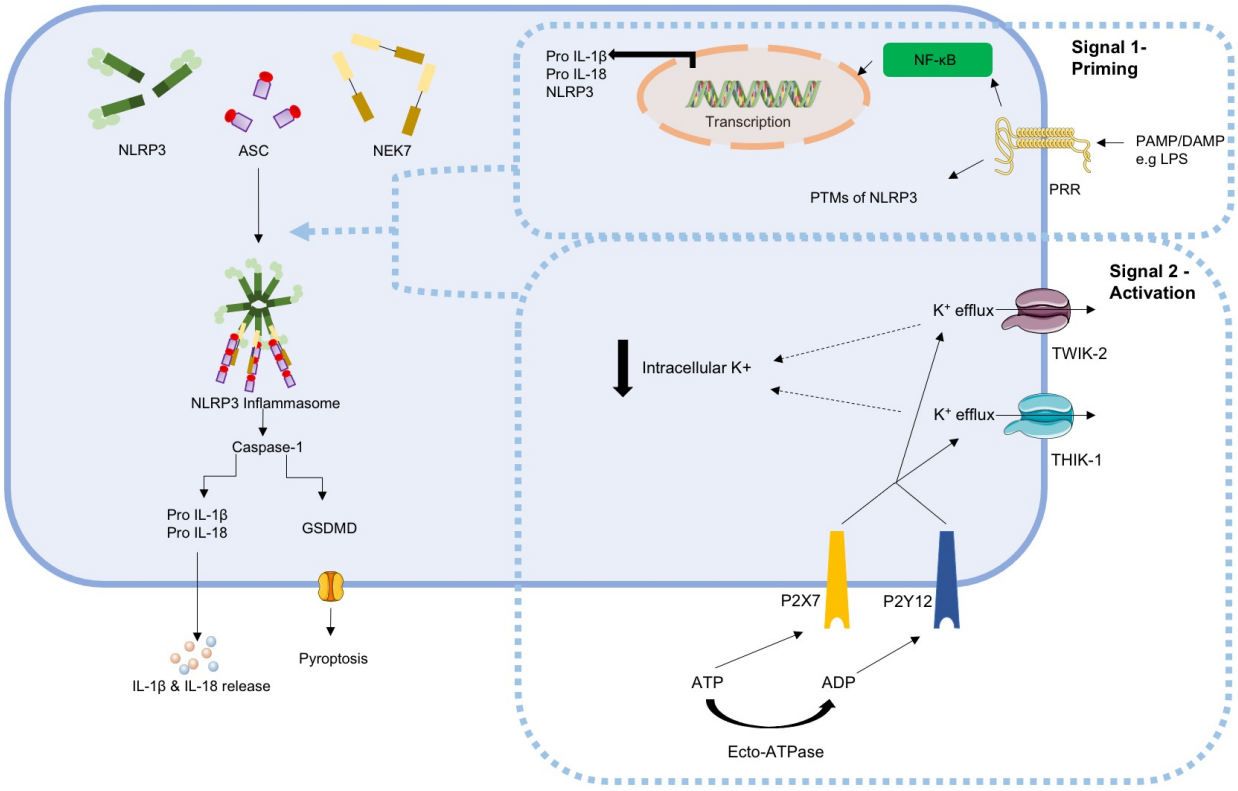

Figure 6.1 THIK-1 and TWIK2 regulation of NLRP3 activation.
Activation of NLRP3 requires an initial priming step which is triggered by the binding of PAMPs and DAMPs, such as LPS to PRRs, triggering NF-κB dependent transcription of NLRP3, pro IL-1β and pro IL-18. Priming also triggers PTMs of NLRP3 enabling rapid NLRP3 regulation. Following priming ATP can trigger NLRP3 activation through direct binding to and activating the P2X7 receptor. In addition, extracellular ATP can be converted to ADP by the ecto-ATPase CD39 which subsequently activates an additional purinergic receptor, P2Y12. Activation of purinergic receptors P2X7 and P2Y12 has been shown to induce activation of two-pore domain K^+ channels THIK-1 and TWIK-2. Activation of THIK-1 and TWIK-2 facilitates the efflux of K^+ from the cell, triggering a decrease in intracellular K^+ concentration which stimulates activation of the NLRP3 inflammasome.

Although, THIK-1 in this thesis and TWIK-2 in previously published work (78) were found to be specific regulators of ATP induced NLRP3 activation in peripheral macrophages, this thesis discovered THIK-1 to regulate ATP in addition to nigericin induced NLRP3 activation in CNS resident microglia. THIK-1 may therefore play a broader role in NLRP3 inflammasome regulation in microglial NLRP3 activation than peripheral macrophages. These findings could potentially be explained by the observation that THIK-1 mRNA expression appears to be higher in microglia when compared to peripheral macrophages. As THIK-1 regulates NLRP3 activation in response to multiple stimuli in microglia in comparison to just ATP in peripheral macrophages, targeting THIK-1 may be more effective at inhibiting NLRP3 activation in CNS inflammatory disease than peripheral disease.

Two examples of neurodegenerative diseases heavily associated with NLRP3 are AD and PD (292). Genetic depletion of NLRP3 in both AD and PD animal models has previously been demonstrated to protect against the development of disease pathology (7, 297). Thus indicating, inhibition of NLRP3 may be represent a viable treatment option for AD and PD patients. In this thesis, THIK-1 was identified as a novel regulator of the NLRP3 inflammasome in CNS resident microglial cells. THIK-1 could therefore represent a target to limit NLRP3 activation in NLRP3 associated CNS diseases such as AD and PD. In support of the potential of THIK-1 as a therapeutic target, this work demonstrated THIK-1 to be upregulated in the brains of AD and PD patients suggesting THIK-1 is associated with AD and PD pathology. A recent study provided further evidence that THIK-1 is involved in AD pathology. A rare variant in the *KCNK13* gene was associated with familial late onset AD (282). Together these data provide genetic evidence linking THIK-1 with AD and PD. Increased expression or variations in the THIK-1 gene may therefore contribute to neurodegenerative disease pathology through enhancing damaging NLRP3 mediated inflammation. Selective targeting of THIK-1 could therefore represent a mechanism by which to inhibit NLRP3 activity with the CNS without impacting other inflammasomes, or NF-κB, inflammatory signaling and therefore avoiding the immunosuppressive effects that may occur from other therapeutic interventions such as directly targeting IL-1β (298, 299).

Furthermore, within the CNS, THIK-1 is highly expressed in microglia, with low expression also observed in oligodendrocytes but no expression is found in neurons or astrocytes (300). Almost

exclusive expression of THIK-1 in microglia suggests selective inhibitors of THIK-1 will not bind to neuronal or astrocytic receptors which could promote unwanted side effects. THIK-1 therefore represents a target in which to exclusively inhibit microglial NLRP3 activation without impacting the function of other CNS cells.

However, although THIK-1 was found to regulate caspase-1 activation and IL-1β in response to NLRP3 activation in microglia, THIK-1 inhibiting compounds consistently enhanced ASC speck formation in peripheral macrophages. If inhibiting THIK-1 also enhances ASC speck formation in microglia as it does in peripheral macrophages this may pose a significant barrier in the effectiveness of THIK-1 inhibitors as a therapeutic intervention for neuroinflammatory diseases. A previous study identified ASC specks as potential drivers of Aβ pathology in AD (203). The study found that in AD, NLRP3 becomes activated in microglia resulting in the formation of ASC specks which are released into the extracellular space. In both AD patients and APP/PS1 transgenic mouse models of AD, ASC specks were observed to interact with Aβ within the brain (203). Furthermore, *in vitro* and *in vivo* studies in APP/PS1 mice observed ASC specks released from microglia in response to NLRP3 activation to contribute to the seeding and spreading of Aβ pathology. These data suggest ASC specks actively contribute to Aβ pathology in AD. Therefore, if inhibition of THIK-1 does enhance ASC speck formation in microglia in response to NLRP3 activation this may promote greater ASC speck release. Elevated extracellular ASC speck levels may then result in enhanced seeding and spreading of Aβ pathology in patients with AD. Despite THIK-1 inhibition enhancing ASC speck formation, it is unlikely these specks would firstly, be released from the cell and secondly, drive Aβ pathology. Although ASC specks were enhanced by THIK-1 inhibition, the specks formed were arrested in an inactive state, incapable of cleaving and activating caspase-1. This suggests these inactive ASC specks would not be released in response to NLRP3 activation as caspase-1 induction of GSDMD mediated pyroptosis would be inhibited. Therefore, enhancing intracellular ASC specks may not result in increased release of ASC specks. Furthermore, the specks formed during THIK-1 inhibition and blockage of K^+ efflux are functionally distinct from fully active ASC specks, suggesting these inactive specks may also lack the full pathological profile of active ASC specks and be unable to seed Aβ pathology. Together this suggests although ASC specks may be enhanced in microglia in response to THIK-1 inhibition and NLRP3 activation, these specks are unlikely to be released and

drive increased Aβ pathology in AD. Furthermore, ASC speck contribution to disease pathology was found to be a unique feature of AD, with ASC specks bound to Aβ undetected in post-mortem tissue from patients with other neurodegenerative diseases (203). In the unlikely event that enhanced formation of inactive ASC specks enhanced Aβ pathology in AD, THIK-1 inhibitors may be more effective in inhibiting NLRP3 activation in other NLRP3 associated neurodegenerative diseases such as PD.

Furthermore, it is worth noting that the benefits of reducing NLRP3 mediated inflammation in AD through attenuating NLRP3 inflammasome activation with THIK-1 inhibiting compounds may outweigh the potential detrimental impact of enhanced ASC speck driven Aβ pathology. Aβ burden within the brain has consistently been shown to poorly correlate with AD severity (301). This suggests Aβ plaques themselves are not intrinsically damaging in AD patients. Recent research suggests sustained neuroinflammatory responses in AD patients provides the missing link between Aβ deposition and AD pathogenesis (302). IL-1β is one inflammatory cytokine in particular that is heavily associated with AD progression (303). Therefore, it appears inflammatory responses such as NLRP3 driven IL-1β release are the drivers of AD pathology in response to Aβ deposits. Consequently, by inhibiting NLRP3 and IL-1β mediated neuroinflammation, THIK-1 inhibitors would remove the active driver of AD pathology and therefore potentially reduce cognitive deficits in AD patients. Finally, the assumption that inhibition of THIK-1 enhances ASC speck formation is based on the findings that THIK-1 inhibiting compounds enhances ASC speck formation in a macrophage cell line. THIK-1 regulation of NLRP3 activation was found to differ between peripheral macrophages and microglia. THIK-1 inhibition in microglial cells therefore may not result in increased ASC speck formation despite doing so in peripheral macrophages. It is possible that selective inhibition of THIK-1 may inhibit NLRP3 activation within the CNS without increasing ASC speck formation. In summary, this thesis provides data to suggest THIK-1 is a potential target for selectively limiting NLRP3 activation in diseases such as AD. However, more research is required to explore the limitation of THIK-1 as a therapeutic target, such as the effect of THIK-1 inhibition on ASC speck formation and the impact this has on Aβ pathology.

6.3 Limitations of THIK-1 inhibiting compounds

Genetic depletion studies confirmed THIK-1 as a regulator of NLRP3 inflammasome activation. The findings that THIK-1 inhibiting compounds also inhibited NLRP3 activation would suggest their inhibitory action is mediated through THIK-1. However, THIK-1 inhibitors used: Tpa, CVN1 and CVN2 were all found capable of inhibiting NLRP3 activation in the absence of THIK-1 in response to certain stimuli in BMDMs. These findings show these compounds are able to inhibit NLRP3 activation in response to particular stimuli via inhibiting THIK-1 in addition to other uncharacterised mechanisms of action. Yet, inhibitors did not further inhibit ATP induced NLRP3 activation in THIK-1 KO cells suggesting the inhibitors do inhibit NLRP3 activation in response to ATP via blocking THIK-1. Therefore, the THIK-1 inhibiting compounds used were useful tool compounds to initially identify potential K^+ channels regulating NLRP3 activation. Identification of potential K^+ channels involved in NLRP3 activation allowed for targeted KO studies to validate THIK-1 as a regulator of the NLRP3 inflammasome. However, the future use of the compounds in studying the specific role of THIK-1 in NLRP3 activation is however, limited. The inhibitors utilised were all shown as effective NLRP3 inhibiting compounds. These compounds do therefore demonstrate the potential in developing selective THIK-1 inhibiting compounds which could be used to regulate THIK-1 dependent NLRP3 activation in peripheral and CNS resident immune cells.

Development of more selective inhibitors will be critical in validating the potential of THIK-1 as a single therapeutic target for NLRP3 associated pathology. Testing currently available THIK-1 inhibitors in disease models could potentially lead to misleading results. Inhibitors used and particular Tpa was found to inhibit the NF-κB inflammatory signaling pathway which plays a critical role in inflammatory signaling in health and disease independently of THIK-1 inhibition. Inhibiting such a pivotal mediator of inflammatory signaling is likely to have an effect in inflammatory disease models. The current inhibitors could therefore have beneficial effects in disease models completely independent of THIK-1 inhibition. Generating selective, nontoxic THIK-1 inhibitors which regulate inflammatory pathways exclusively via THIK-1 inhibition will be fundamental in determining the prospective use of selective THIK-1 inhibitors in disease.

6.4 Future directions

The identification of THIK-1 as a specific regulator of ATP-induced NLRP3 activation suggest THIK-1 may represent a potential therapeutic target for limiting NLRP3 mediated inflammation in disease. However, further experimental work is required to determine whether THIK-1 regulates NLRP3 inflammasome activation *in vivo*. To first determine if THIK-1 regulates NLRP3 *in vivo* an LPS, ATP intraperitoneal injection model in mice could be used. Using THIK-1 KO and WT control mice, LPS followed by ATP could be injected interperitoneally to induce NLRP3 activation and IL-1β release as shown in previous studies (290). The peritoneal cavity could then be lavaged and tested by ELISA for the presence of cleaved IL-1β. Comparing IL-1β from WT and THIK-1 KO mice would identify whether THIK-1 regulates ATP-induced NLRP3 activation *in vivo* as well as *in vitro*.

If THIK-1 is found to regulate NLRP3 *in vivo,* following studies should investigate the relevance of THIK-1 to pathology in NLRP3 associated diseases. Following findings in this thesis that THIK-1 mRNA is upregulated in AD and that NLRP3 has previously been associated with AD pathology (7), the role of THIK-1 in AD mouse models could be investigated. The APP/PS1 transgenic mouse model of AD could be a potential model to investigate the role of THIK-1 in AD pathology. NLRP3 has been found to contribute to amyloid plaque burden, microglial activation and cognitive deficits APP/PS1 mice (7). To study the role of THIK-1 in AD pathology, APP/PS1 mice could be crossed with THIK-1 KO mice to generate APP/PS1/*kcnk13*$^{-/-}$ mice. The impact of THIK-1 on amyloid burden, microglial activation and cognitive deficits displayed by the APP/PS1 model could then be investigated. These experiments would determine whether THIK-1 contributes to NLRP3 associated disease pathology *in vivo*. In addition, these experiments would determine if THIK-1 depletion enhances ASC speck formation and release as well as the effect this has on Aβ pathology. The results of these studies would provide essential data to aid in determining whether THIK-1 is a viable therapeutic target for limiting NLRP3 inflammasome activation in disease.

Following these studies using THIK-1 KO mice, if THIK-1 is found to contribute to NLRP3 activation *in vivo*, selective THIK-1 inhibiting compounds could then be tested in these models. This would determine whether THIK-1 is a viable target for pharmaceutical intervention to reduce NLRP3 induced inflammation in disease.

6.5 Summary

This thesis identifies THIK-1 as a regulator of NLRP3 activation in mouse macrophages and microglia in response to the canonical stimuli ATP. Consistent with previous work (23) this work shows the formation of ASC specks can occur without downstream activation of caspase-1 and IL-1β cleavage. THIK-1 was found to be required for NLRP3 dependent caspase-1 activation and IL-1β release in response to ATP. These results demonstrate that multiple K^+ channels may be involved in P2X7 dependent NLRP3 activation and highlight the therapeutic potential of targeting K^+ channels to limit aberrant NLRP3-induced inflammation in disease. In addition, THIK-1 expression was found to be associated with the development of neurodegenerative disease. THIK-1 represents a viable therapeutic target for limiting NLRP3 inflammasome activation in peripheral and CNS diseases

Chapter 7: References

1. Medzhitov, R. (2010) Inflammation 2010: New Adventures of an Old Flame. *Cell*. 10.1016/j.cell.2010.03.006
2. Ferrero-Miliani, L., Nielsen, O. H., Andersen, P. S., and Girardin, S. E. (2007) Chronic inflammation: Importance of NOD2 and NALP3 in interleukin-1β generation. *Clin. Exp. Immunol.* 10.1111/j.1365-2249.2006.03261.x
3. Lamkanfi, M., and Dixit, V. M. (2012) Inflammasomes and Their Roles in Health and Disease. *Annu. Rev. Cell Dev. Biol.* 10.1146/annurev-cellbio-101011-155745
4. Latz, E., Xiao, T. S., and Stutz, A. (2013) Activation and regulation of the inflammasomes. *Nat. Rev. Immunol.* 10.1038/nri3452
5. Rock, K. L., Latz, E., Ontiveros, F., and Kono, H. (2010) The sterile inflammatory response. *Annu. Rev. Immunol.* 10.1146/annurev-immunol-030409-101311
6. Duewell, P., Kono, H., Rayner, K. J., Sirois, C. M., Vladimer, G., Bauernfeind, F. G., Abela, G. S., Franchi, L., Nũez, G., Schnurr, M., Espevik, T., Lien, E., Fitzgerald, K. A., Rock, K. L., Moore, K. J., Wright, S. D., Hornung, V., and Latz, E. (2010) NLRP3 inflammasomes are required for atherogenesis and activated by cholesterol crystals. *Nature*. 10.1038/nature08938
7. Heneka, M. T., Kummer, M. P., Stutz, A., Delekate, A., Schwartz, S., Vieira-Saecker, A., Griep, A., Axt, D., Remus, A., Tzeng, T. C., Gelpi, E., Halle, A., Korte, M., Latz, E., and Golenbock, D. T. (2013) NLRP3 is activated in Alzheimer's disease and contributes to pathology in APP/PS1 mice. *Nature*. 10.1038/nature11729
8. Masters, S. L., Dunne, A., Subramanian, S. L., Hull, R. L., Tannahill, G. M., Sharp, F. A., Becker, C., Franchi, L., Yoshihara, E., Chen, Z., Mullooly, N., Mielke, L. A., Harris, J., Coll, R. C., Mills, K. H. G., Mok, K. H., Newsholme, P., Nuñez, G., Yodoi, J., Kahn, S. E., Lavelle, E. C., and O'Neill, L. A. J. (2010) Activation of the NLRP3 inflammasome by islet amyloid polypeptide provides a mechanism for enhanced IL-1β 2 in type 2 diabetes. *Nat. Immunol.* 10.1038/ni.1935
9. Yan, Y. Q., Fang, Y., Zheng, R., Pu, J. L., and Zhang, B. R. (2020) NLRP3 Inflammasomes in Parkinson's disease and their Regulation by Parkin. *Neuroscience*. 10.1016/j.neuroscience.2020.08.004
10. Kumar, H., Kawai, T., and Akira, S. (2011) Pathogen recognition by the innate immune system. *Int. Rev. Immunol.* 10.3109/08830185.2010.529976
11. Drummond, R. A., and Brown, G. D. (2011) The role of Dectin-1 in the host defence against fungal infections. *Curr. Opin. Microbiol.* 10.1016/j.mib.2011.07.001
12. Deretic, V., Saitoh, T., and Akira, S. (2013) Autophagy in infection, inflammation and immunity. *Nat. Rev. Immunol.* 10.1038/nri3532
13. Lamkanfi, M., and Dixit, V. M. (2014) Mechanisms and functions of inflammasomes. *Cell*. 10.1016/j.cell.2014.04.007
14. Broz, P., and Dixit, V. M. (2016) Inflammasomes: Mechanism of assembly, regulation and signalling. *Nat. Rev. Immunol.* 10.1038/nri.2016.58
15. Martinon, F., Burns, K., and Tschopp, J. (2002) The Inflammasome: A molecular platform triggering activation of inflammatory caspases and processing of proIL-β. *Mol. Cell*. 10.1016/S1097-2765(02)00599-3
16. Von Moltke, J., Ayres, J. S., Kofoed, E. M., Chavarría-Smith, J., and Vance, R. E. (2013) Recognition of bacteria by inflammasomes. *Annu. Rev.*

Immunol. 10.1146/annurev-immunol-032712-095944
17. Hoffman, H. M., Mueller, J. L., Broide, D. H., Wanderer, A. A., and Kolodner, R. D. (2001) Mutation of a new gene encoding a putative pyrin-like protein causes familial cold autoinflammatory syndrome and Muckle-Wells syndrome. *Nat. Genet.* 10.1038/ng756
18. Aganna, E., Martinon, F., Hawkins, P. N., Ross, J. B., Swan, D. C., Booth, D. R., Lachmann, H. J., Gaudet, R., Woo, P., Feighery, C., Cotter, F. E., Thome, M., Hitman, G. A., Tschopp, J., and McDermott, M. F. (2002) Association of mutations in the NALP3/CIAS1/PYPAF1 gene with a broad phenotype including recurrent fever, cold sensitivity, sensorineural deafness, and AA amyloidosis. *Arthritis Rheum.* 10.1002/art.10509
19. Aksentijevich, I., Nowak, M., Mallah, M., Chae, J. J., Watford, W. T., Hofmann, S. R., Stein, L., Russo, R., Goldsmith, D., Dent, P., Rosenberg, H. F., Austin, F., Remmers, E. F., Balow, J. E., Rosenzweig, S., Komarow, H., Shoham, N. G., Wood, G., Jones, J., Mangra, N., Carrero, H., Adams, B. S., Moore, T. L., Schikler, K., Hoffman, H., Lovell, D. J., Lipnick, R., Barron, K., O'Shea, J. J., Kastner, D. L., and Goldbach-Mansky, R. (2002) De novo CIAS1 mutations, cytokine activation, and evidence for genetic heterogeneity in patients with neonatal-onset multisystem inflammatory disease (NOMID): A new member of the expanding family of pyrin-associated autoinflammatory diseases. *Arthritis Rheum.* 10.1002/art.10688
20. Kelley, N., Jeltema, D., Duan, Y., and He, Y. (2019) The NLRP3 inflammasome: An overview of mechanisms of activation and regulation. *Int. J. Mol. Sci.* 10.3390/ijms20133328
21. Bauernfeind, F. G., Horvath, G., Stutz, A., Alnemri, E. S., MacDonald, K., Speert, D., Fernandes-Alnemri, T., Wu, J., Monks, B. G., Fitzgerald, K. A., Hornung, V., and Latz, E. (2009) Cutting Edge: NF-κB Activating Pattern Recognition and Cytokine Receptors License NLRP3 Inflammasome Activation by Regulating NLRP3 Expression. *J. Immunol.* 10.4049/jimmunol.0901363
22. Franchi, L., Eigenbrod, T., and Núñez, G. (2009) Cutting Edge: TNF-α Mediates Sensitization to ATP and Silica via the NLRP3 Inflammasome in the Absence of Microbial Stimulation. *J. Immunol.* 10.4049/jimmunol.0900173
23. Hornung, V., and Latz, E. (2010) Critical functions of priming and lysosomal damage for NLRP3 activation. *Eur. J. Immunol.* 10.1002/eji.200940185
24. Franchi, L., Eigenbrod, T., and Nunez, G. (2009) Cutting Edge: TNF- Mediates Sensitization to ATP and Silica via the NLRP3 Inflammasome in the Absence of Microbial Stimulation. *J. Immunol.* 10.4049/jimmunol.0900173
25. Schroder, K., Sagulenko, V., Zamoshnikova, A., Richards, A. A., Cridland, J. A., Irvine, K. M., Stacey, K. J., and Sweet, M. J. (2012) Acute lipopolysaccharide priming boosts inflammasome activation independently of inflammasome sensor induction. *Immunobiology*. 10.1016/j.imbio.2012.07.020
26. Cogswell, J. P., Godlevski, M. M., Wisely, G. B., Clay, W. C., Leesnitzer, L. M., Ways, J. P., and Gray, J. G. (1994) NF-kappa B regulates IL-1 beta transcription through a consensus NF-kappa B binding site and a nonconsensus CRE-like site. *J. Immunol.*
27. Libermann, T. A., and Baltimore, D. (1990) Activation of interleukin-6 gene

expression through the NF-kappa B transcription factor. *Mol. Cell. Biol.* 10.1128/mcb.10.5.2327-2334.1990
28. Liu, H., Sidiropoulos, P., Song, G., Pagliari, L. J., Birrer, M. J., Stein, B., Anrather, J., and Pope, R. M. (2000) TNF-α Gene Expression in Macrophages: Regulation by NF-κB Is Independent of c-Jun or C/EBPβ. *J. Immunol.* 10.4049/jimmunol.164.8.4277
29. Juliana, C., Fernandes-Alnemri, T., Kang, S., Farias, A., Qin, F., and Alnemri, E. S. (2012) Non-transcriptional priming and deubiquitination regulate NLRP3 inflammasome activation. *J. Biol. Chem.* 10.1074/jbc.M112.407130
30. Bezbradica, J. S., Coll, R. C., and Schroder, K. (2017) Sterile signals generate weaker and delayed macrophage NLRP3 inflammasome responses relative to microbial signals. *Cell. Mol. Immunol.* 10.1038/cmi.2016.11
31. Fernandes-Alnemri, T., Kang, S., Anderson, C., Sagara, J., Fitzgerald, K. A., and Alnemri, E. S. (2013) Cutting Edge: TLR Signaling Licenses IRAK1 for Rapid Activation of the NLRP3 Inflammasome. *J. Immunol.* 10.4049/jimmunol.1301681
32. Condello, C., Yuan, P., Schain, A., and Grutzendler, J. (2015) Microglia constitute a barrier that prevents neurotoxic protofibrillar Aβ42 hotspots around plaques. *Nat. Commun.* 10.1038/ncomms7176
33. Lin, K. M., Hu, W., Troutman, T. D., Jennings, M., Brewer, T., Li, X., Nanda, S., Cohen, P., Thomas, J. A., and Pasare, C. (2014) IRAK-1 bypasses priming and directly links TLRs torapid NLRP3 inflammasome activation. *Proc. Natl. Acad. Sci. U. S. A.* 10.1073/pnas.1320294111
34. Lopez-Castejon, G. (2020) Control of the inflammasome by the ubiquitin system. *FEBS J.* 10.1111/febs.15118
35. Song, N., Liu, Z. S., Xue, W., Bai, Z. F., Wang, Q. Y., Dai, J., Liu, X., Huang, Y. J., Cai, H., Zhan, X. Y., Han, Q. Y., Wang, H., Chen, Y., Li, H. Y., Li, A. L., Zhang, X. M., Zhou, T., and Li, T. (2017) NLRP3 Phosphorylation Is an Essential Priming Event for Inflammasome Activation. *Mol. Cell*. 10.1016/j.molcel.2017.08.017
36. Palazón-Riquelme, P., Worboys, J. D., Green, J., Valera, A., Martín-Sánchez, F., Pellegrini, C., Brough, D., and López-Castejón, G. (2018) USP7 and USP47 deubiquitinases regulate NLRP3 inflammasome activation. *EMBO Rep.* 10.15252/embr.201744766
37. Barry, R., John, S. W., Liccardi, G., Tenev, T., Jaco, I., Chen, C. H., Choi, J., Kasperkiewicz, P., Fernandes-Alnemri, T., Alnemri, E., Drag, M., Chen, Y., and Meier, P. (2018) SUMO-mediated regulation of NLRP3 modulates inflammasome activity. *Nat. Commun.* 10.1038/s41467-018-05321-2
38. He, M., Chiang, H. H., Luo, H., Zheng, Z., Qiao, Q., Wang, L., Tan, M., Ohkubo, R., Mu, W. C., Zhao, S., Wu, H., and Chen, D. (2020) An Acetylation Switch of the NLRP3 Inflammasome Regulates Aging-Associated Chronic Inflammation and Insulin Resistance. *Cell Metab.* 10.1016/j.cmet.2020.01.009
39. Gritsenko, A., Yu, S., Martin-Sanchez, F., del Olmo, I. D., Nichols, E. M., Davis, D. M., Brough, D., and Lopez-Castejon, G. (2020) Priming is dispensable for NLRP3 inflammasome activation in human monocytes. *bioRxiv*. 10.1101/2020.01.30.925248
40. Dinarello, C. A. (2009) Immunological and inflammatory functions of the

interleukin-1 family. *Annu. Rev. Immunol.* 10.1146/annurev.immunol.021908.132612
41. Dinarello, C. A. (2018) Overview of the IL-1 family in innate inflammation and acquired immunity. *Immunol. Rev.* 10.1111/imr.12621
42. Thornberry, N. A., Bull, H. G., Calaycay, J. R., Chapman, K. T., Howard, A. D., Kostura, M. J., Miller, D. K., Molineaux, S. M., Weidner, J. R., Aunins, J., Elliston, K. O., Ayala, J. M., Casano, F. J., Chin, J., Ding, G. J. F., Egger, L. A., Gaffney, E. P., Limjuco, G., Palyha, O. C., Raju, S. M., Rolando, A. M., Salley, J. P., Yamin, T. T., Lee, T. D., Shively, J. E., MacCross, M., Mumford, R. A., Schmidt, J. A., and Tocci, M. J. (1992) A novel heterodimeric cysteine protease is required for interleukin-1βprocessing in monocytes. *Nature*. 10.1038/356768a0
43. Perregaux, D., and Gabel, C. A. (1994) Interleukin-1β maturation and release in response to ATP and nigericin. *J. Biol. Chem.*
44. Pétrilli, V., Papin, S., Dostert, C., Mayor, A., Martinon, F., and Tschopp, J. (2007) Activation of the NALP3 inflammasome is triggered by low intracellular potassium concentration. *Cell Death Differ.* 10.1038/sj.cdd.4402195
45. Muñoz-Planillo, R., Kuffa, P., Martínez-Colón, G., Smith, B. L., Rajendiran, T. M., and Núñez, G. (2013) K+ Efflux Is the Common Trigger of NLRP3 Inflammasome Activation by Bacterial Toxins and Particulate Matter. *Immunity*. 10.1016/j.immuni.2013.05.016
46. He, Y., Zeng, M. Y., Yang, D., Motro, B., and Núñez, G. (2016) NEK7 is an essential mediator of NLRP3 activation downstream of potassium efflux. *Nature*. 10.1038/nature16959
47. Schmid-Burgk, J. L., Chauhan, D., Schmidt, T., Ebert, T. S., Reinhardt, J., Endl, E., and Hornung, V. (2016) A genome-wide CRISPR (clustered regularly interspaced short palindromic repeats) screen identifies NEK7 as an essential component of NLRP3 inflammasome activation. *J. Biol. Chem.* 10.1074/jbc.C115.700492
48. Tapia-Abellán, A., Angosto-Bazarra, D., Alarcón-Vila, C., Baños, M. C., Hafner-Bratkovič, I., Oliva, B., and Pelegrín, P. (2021) Sensing low intracellular potassium by NLRP3 results in a stable open structure that promotes inflammasome activation. *Sci. Adv.* 10.1126/sciadv.abf4468
49. Hara, H., Seregin, S. S., Yang, D., Fukase, K., Chamaillard, M., Alnemri, E. S., Inohara, N., Chen, G. Y., and Núñez, G. (2018) The NLRP6 Inflammasome Recognizes Lipoteichoic Acid and Regulates Gram-Positive Pathogen Infection. *Cell*. 10.1016/j.cell.2018.09.047
50. Anand, P. K., Subbarao Malireddi, R. K., Lukens, J. R., Vogel, P., Bertin, J., Lamkanfi, M., and Kanneganti, T. D. (2012) NLRP6 negatively regulates innate immunity and host defence against bacterial pathogens. *Nature*. 10.1038/nature11250
51. Groß, C. J., Mishra, R., Schneider, K. S., Médard, G., Wettmarshausen, J., Dittlein, D. C., Shi, H., Gorka, O., Koenig, P. A., Fromm, S., Magnani, G., Ćiković, T., Hartjes, L., Smollich, J., Robertson, A. A. B., Cooper, M. A., Schmidt-Supprian, M., Schuster, M., Schroder, K., Broz, P., Traidl-Hoffmann, C., Beutler, B., Kuster, B., Ruland, J., Schneider, S., Perocchi, F., and Groß, O. (2016) K + Efflux-Independent NLRP3 Inflammasome Activation by Small Molecules Targeting Mitochondria. *Immunity*. 10.1016/j.immuni.2016.08.010

52. Meng, G., Zhang, F., Fuss, I., Kitani, A., and Strober, W. (2009) A Mutation in the Nlrp3 Gene Causing Inflammasome Hyperactivation Potentiates Th17 Cell-Dominant Immune Responses. *Immunity*. 10.1016/j.immuni.2009.04.012
53. Hogquist, K. A., Nett, M. A., Unanue, E. R., and Chaplin, D. D. (1991) Interleukin 1 is processed and released during apoptosis. *Proc. Natl. Acad. Sci. U. S. A.* 10.1073/pnas.88.19.8485
54. Ferrari, D., Chiozzi, P., Falzoni, S., Dal Susino, M., Melchiorri, L., Baricordi, O. R., and Di Virgilio, F. (1997) Extracellular ATP triggers IL-1 beta release by activating the purinergic P2Z receptor of human macrophages. *J. Immunol.*
55. Mariathasan, S., Weiss, D. S., Newton, K., McBride, J., O'Rourke, K., Roose-Girma, M., Lee, W. P., Weinrauch, Y., Monack, D. M., and Dixit, V. M. (2006) Cryopyrin activates the inflammasome in response to toxins and ATP. *Nature*. 10.1038/nature04515
56. Browne, L. E., Compan, V., Bragg, L., and North, R. A. (2013) P2X7 receptor channels allow direct permeation of nanometer-sized dyes. *J. Neurosci.* 10.1523/JNEUROSCI.2235-12.2013
57. North, R. A. (2002) Molecular physiology of P2X receptors. *Physiol. Rev.* 10.1152/physrev.00015.2002
58. Barberà-Cremades, M., Baroja-Mazo, A., Gomez, A. I., Machado, F., Di Virgilio, F., and Pelegrín, P. (2012) P2X7 receptor-stimulation causes fever via PGE2 and IL-1β release . *FASEB J.* 10.1096/fj.12-205765
59. Amores-Iniesta, J., Barberà-Cremades, M., Martínez, C. M., Pons, J. A., Revilla-Nuin, B., Martínez-Alarcón, L., Di Virgilio, F., Parrilla, P., Baroja-Mazo, A., and Pelegrín, P. (2017) Extracellular ATP Activates the NLRP3 Inflammasome and Is an Early Danger Signal of Skin Allograft Rejection. *Cell Rep.* 10.1016/j.celrep.2017.11.079
60. Hung, S. C., Choi, C. H., Said-Sadier, N., Johnson, L., Atanasova, K. R., Sellami, H., Yilmaz, Ö., and Ojcius, D. M. (2013) P2X4 Assembles with P2X7 and Pannexin-1 in Gingival Epithelial Cells and Modulates ATP-induced Reactive Oxygen Species Production and Inflammasome Activation. *PLoS One*. 10.1371/journal.pone.0070210
61. Sakaki, H., Fujiwaki, T., Tsukimoto, M., Kawano, A., Harada, H., and Kojima, S. (2013) P2X4 receptor regulates P2X7 receptor-dependent IL-1β and IL-18 release in mouse bone marrow-derived dendritic cells. *Biochem. Biophys. Res. Commun.* 10.1016/j.bbrc.2013.01.135
62. Chen, K., Zhang, J., Zhang, W., Zhang, J., Yang, J., Li, K., and He, Y. (2013) ATP-P2X4 signaling mediates NLRP3 inflammasome activation: A novel pathway of diabetic nephropathy. *Int. J. Biochem. Cell Biol.* 10.1016/j.biocel.2013.02.009
63. Zech, A., Wiesler, B., Ayata, C. K., Schlaich, T., Dürk, T., Hoßfeld, M., Ehrat, N., Cicko, S., and Idzko, M. (2016) P2rx4 deficiency in mice alleviates allergen-induced airway inflammation. *Oncotarget*. 10.18632/oncotarget.13375
64. Baroja-Mazo, A., Barberà-Cremades, M., and Pelegrín, P. (2013) The participation of plasma membrane hemichannels to purinergic signaling. *Biochim. Biophys. Acta - Biomembr.* 10.1016/j.bbamem.2012.01.002
65. Prager, P., Hollborn, M., Steffen, A., Wiedemann, P., Kohen, L., and Bringmann, A. (2016) P2Y1 receptor signaling contributes to high salt-

induced priming of the NLRP3 inflammasome in retinal pigment epithelial cells. *PLoS One*. 10.1371/journal.pone.0165653

66. Baron, L., Gombault, A., Fanny, M., Villeret, B., Savigny, F., Guillou, N., Panek, C., Le Bert, M., Lagente, V., Rassendren, F., Riteau, N., and Couillin, I. (2015) The NLRP3 inflammasome is activated by nanoparticles through ATP, ADP and adenosine. *Cell Death Dis.* 10.1038/cddis.2014.576
67. Riteau, N., Baron, L., Villeret, B., Guillou, N., Savigny, F., Ryffel, B., Rassendren, F., Le Bert, M., Gombault, A., and Couillin, I. (2012) ATP release and purinergic signaling: A common pathway for particle-mediated inflammasome activation. *Cell Death Dis.* 10.1038/cddis.2012.144
68. Madry, C., Kyrargyri, V., Arancibia-Cárcamo, I. L., Jolivet, R., Kohsaka, S., Bryan, R. M., and Attwell, D. (2018) Microglial Ramification, Surveillance, and Interleukin-1β Release Are Regulated by the Two-Pore Domain K+ Channel THIK-1. *Neuron*. 10.1016/j.neuron.2017.12.002
69. Lesage, F., and Lazdunski, M. (2000) Molecular and functional properties of two-pore-domain potassium channels. *Am. J. Physiol. - Ren. Physiol.* 10.1152/ajprenal.2000.279.5.f793
70. Patel, A. J., and Honoré, E. (2001) Properties and modulation of mammalian 2P domain K+ channels. *Trends Neurosci.* 10.1016/S0166-2236(00)01810-5
71. Lotshaw, D. P. (2007) Biophysical, pharmacological, and functional characteristics of cloned and native mammalian two-pore domain K+ channels. *Cell Biochem. Biophys.*
72. Kim, D. (2005) Physiology and Pharmacology of Two-Pore Domain Potassium Channels. *Curr. Pharm. Des.* 10.2174/1381612054546824
73. Goldstein, S. A. N., Bockenhauer, D., O'Kelly, I., and Zilberberg, N. (2001) Potassium leak channels and the KCNK family of two-p-domain subunits. *Nat. Rev. Neurosci.* 10.1038/35058574
74. Talley, E. M., Sirois, J. E., Lei, Q., and Bayliss, D. A. (2003) Two-pore-domain (KCNK) potassium channels: Dynamic roles in neuronal function. *Neuroscientist*. 10.1177/1073858402239590
75. Mathie, A. (2007) Neuronal two-pore-domain potassium channels and their regulation by G protein-coupled receptors. *J. Physiol.* 10.1113/jphysiol.2006.121582
76. Chemin, J., Patel, A., Duprat, F., Zanzouri, M., Lazdunski, M., and Honoré, E. (2005) Lysophosphatidic acid-operated K+ channels. *J. Biol. Chem.* 10.1074/jbc.M408246200
77. Ehling, P., Cerina, M., Budde, T., Meuth, S. G., and Bittner, S. (2015) The CNS under pathophysiologic attack—examining the role of K2P channels. *Pflugers Arch. Eur. J. Physiol.* 10.1007/s00424-014-1664-2
78. Di, A., Xiong, S., Ye, Z., Malireddi, R. K. S., Kometani, S., Zhong, M., Mittal, M., Hong, Z., Kanneganti, T. D., Rehman, J., and Malik, A. B. (2018) The TWIK2 Potassium Efflux Channel in Macrophages Mediates NLRP3 Inflammasome-Induced Inflammation. *Immunity*. 10.1016/j.immuni.2018.04.032
79. Patel, A. J., Maingret, F., Magnone, V., Fosset, M., Lazdunski, M., and Honore, E. (2000) TWIK-2, an inactivating 2P domain K+ channel. *J. Biol. Chem.* 10.1074/jbc.M003755200
80. Lloyd, E. E., Crossland, R. F., Phillips, S. C., Marrelli, S. P., Reddy, A. K., Taffet, G. E., Hartley, C. J., and Bryan, R. M. (2011) Disruption of K2P6.1 produces vascular dysfunction and hypertension in mice. *Hypertension*.

10.1161/HYPERTENSIONAHA.111.175349
81. Verhoef, P. A., Kertesy, S. B., Lundberg, K., Kahlenberg, J. M., and Dubyak, G. R. (2005) Inhibitory Effects of Chloride on the Activation of Caspase-1, IL-1β Secretion, and Cytolysis by the P2X7 Receptor. *J. Immunol.* 10.4049/jimmunol.175.11.7623
82. Tang, T., Lang, X., Xu, C., Wang, X., Gong, T., Yang, Y., Cui, J., Bai, L., Wang, J., Jiang, W., and Zhou, R. (2017) CLICs-dependent chloride efflux is an essential and proximal upstream event for NLRP3 inflammasome activation. *Nat. Commun.* 10.1038/s41467-017-00227-x
83. Compan, V., Baroja-Mazo, A., López-Castejón, G., Gomez, A. I., Martínez, C. M., Angosto, D., Montero, M. T., Herranz, A. S., Bazán, E., Reimers, D., Mulero, V., and Pelegrín, P. (2012) Cell Volume Regulation Modulates NLRP3 Inflammasome Activation. *Immunity*. 10.1016/j.immuni.2012.06.013
84. Daniels, M. J. D., Rivers-Auty, J., Schilling, T., Spencer, N. G., Watremez, W., Fasolino, V., Booth, S. J., White, C. S., Baldwin, A. G., Freeman, S., Wong, R., Latta, C., Yu, S., Jackson, J., Fischer, N., Koziel, V., Pillot, T., Bagnall, J., Allan, S. M., Paszek, P., Galea, J., Harte, M. K., Eder, C., Lawrence, C. B., and Brough, D. (2016) Fenamate NSAIDs inhibit the NLRP3 inflammasome and protect against Alzheimer's disease in rodent models. *Nat. Commun.* 10.1038/ncomms12504
85. Green, J. P., Swanton, T., Morris, L. V., El-Sharkawy, L. Y., Cook, J., Yu, S., Beswick, J., Adamson, A. D., Humphreys, N. E., Bryce, R., Freeman, S., Lawrence, C., and Brough, D. (2020) LRRC8A is essential for hypotonicity-, but not for damp-induced nlrp3 inflammasome activation. *Elife*. 10.7554/eLife.59704
86. Domingo-Fernández, R., Coll, R. C., Kearney, J., Breit, S., and O'Neill, L. A. J. (2017) The intracellular chloride channel proteins CLIC1 and CLIC4 induce IL-1β transcription and activate the NLRP3 inflammasome. *J. Biol. Chem.* 10.1074/jbc.M117.797126
87. Perregaux, D. G., Laliberte, R. E., and Gabel, C. A. (1996) Human monocyte interleukin-1β posttranslational processing. Evidence of a volume-regulated response. *J. Biol. Chem.* 10.1074/jbc.271.47.29830
88. Green, J. P., Yu, S., Martín-Sánchez, F., Pelegrin, P., Lopez-Castejon, G., Lawrence, C. B., and Brough, D. (2018) Chloride regulates dynamic NLRP3-dependent ASC oligomerization and inflammasome priming. *Proc. Natl. Acad. Sci.* 10.1073/pnas.1812744115
89. Chen, J., and Chen, Z. J. (2018) PtdIns4P on dispersed trans-Golgi network mediates NLRP3 inflammasome activation. *Nature*. 10.1038/s41586-018-0761-3
90. Lu, A., Magupalli, V. G., Ruan, J., Yin, Q., Atianand, M. K., Vos, M. R., Schröder, G. F., Fitzgerald, K. A., Wu, H., and Egelman, E. H. (2014) Unified polymerization mechanism for the assembly of asc-dependent inflammasomes. *Cell*. 10.1016/j.cell.2014.02.008
91. Manji, G. A., Wang, L., Geddes, B. J., Brown, M., Merriam, S., Al-Garawi, A., Mak, S., Lora, J. M., Briskin, M., Jurman, M., Cao, J., Distefano, P. S., and Bertin, J. (2002) PYPAF1, a PYRIN-containing Apaf1-like protein that assembles with ASC and regulates activation of NF-κB. *J. Biol. Chem.* 10.1074/jbc.M112208200
92. Masumoto, J., Taniguchi, S., Ayukawa, K., Sarvotham, H., Kishino, T., Niikawa, N., Hidaka, E., Katsuyama, T., Higuchi, T., and Sagara, J. (1999)

ASC, a novel 22-kDa protein, aggregates during apoptosis of human promyelocytic leukemia HL-60 cells. *J. Biol. Chem.* 10.1074/jbc.274.48.33835

93. Boucher, D., Monteleone, M., Coll, R. C., Chen, K. W., Ross, C. M., Teo, J. L., Gomez, G. A., Holley, C. L., Bierschenk, D., Stacey, K. J., Yap, A. S., Bezbradica, J. S., and Schroder, K. (2018) Caspase-1 self-cleavage is an intrinsic mechanism to terminate inflammasome activity. *J. Exp. Med.* 10.1084/jem.20172222
94. Kayagaki, N., Warming, S., Lamkanfi, M., Walle, L. Vande, Louie, S., Dong, J., Newton, K., Qu, Y., Liu, J., Heldens, S., Zhang, J., Lee, W. P., Roose-Girma, M., and Dixit, V. M. (2011) Non-canonical inflammasome activation targets caspase-11. *Nature*. 10.1038/nature10558
95. Russo, A. J., Behl, B., Banerjee, I., and Rathinam, V. A. K. (2018) Emerging Insights into Noncanonical Inflammasome Recognition of Microbes. *J. Mol. Biol.* 10.1016/j.jmb.2017.10.003
96. Kayagaki, N., Wong, M. T., Stowe, I. B., Ramani, S. R., Gonzalez, L. C., Akashi-Takamura, S., Miyake, K., Zhang, J., Lee, W. P., Muszyński, A., Forsberg, L. S., Carlson, R. W., and Dixit, V. M. (2013) Noncanonical inflammasome activation by intracellular LPS independent of TLR4. *Science (80-.).* 10.1126/science.1240248
97. Shi, J., Zhao, Y., Wang, Y., Gao, W., Ding, J., Li, P., Hu, L., and Shao, F. (2014) Inflammatory caspases are innate immune receptors for intracellular LPS. *Nature*. 10.1038/nature13683
98. Baker, P. J., Boucher, D., Bierschenk, D., Tebartz, C., Whitney, P. G., D'Silva, D. B., Tanzer, M. C., Monteleone, M., Robertson, A. A. B., Cooper, M. A., Alvarez-Diaz, S., Herold, M. J., Bedoui, S., Schroder, K., and Masters, S. L. (2015) NLRP3 inflammasome activation downstream of cytoplasmic LPS recognition by both caspase-4 and caspase-5. *Eur. J. Immunol.* 10.1002/eji.201545655
99. Kayagaki, N., Stowe, I. B., Lee, B. L., O'Rourke, K., Anderson, K., Warming, S., Cuellar, T., Haley, B., Roose-Girma, M., Phung, Q. T., Liu, P. S., Lill, J. R., Li, H., Wu, J., Kummerfeld, S., Zhang, J., Lee, W. P., Snipas, S. J., Salvesen, G. S., Morris, L. X., Fitzgerald, L., Zhang, Y., Bertram, E. M., Goodnow, C. C., and Dixit, V. M. (2015) Caspase-11 cleaves gasdermin D for non-canonical inflammasome signalling. *Nature*. 10.1038/nature15541
100. Rühl, S., and Broz, P. (2015) Caspase-11 activates a canonical NLRP3 inflammasome by promoting K+ efflux. *Eur. J. Immunol.* 10.1002/eji.201545772
101. Schmid-Burgk, J. L., Gaidt, M. M., Schmidt, T., Ebert, T. S., Bartok, E., and Hornung, V. (2015) Caspase-4 mediates non-canonical activation of the NLRP3 inflammasome in human myeloid cells. *Eur. J. Immunol.* 10.1002/eji.201545523
102. Rivers-Auty, J., and Brough, D. (2015) Potassium efflux fires the canon: Potassium efflux as a common trigger for canonical and noncanonical NLRP3 pathways. *Eur. J. Immunol.* 10.1002/eji.201545958
103. Netea, M. G., Nold-Petry, C. A., Nold, M. F., Joosten, L. A. B., Opitz, B., Van Der Meer, J. H. M., Van De Veerdonk, F. L., Ferwerda, G., Heinhuis, B., Devesa, I., Joel Funk, C., Mason, R. J., Kullberg, B. J., Rubartelli, A., Van Der Meer, J. W. M., and Dinarello, C. A. (2009) Differential requirement for the activation of the inflammasome for processing and release of IL-1β in

monocytes and macrophages. *Blood*. 10.1182/blood-2008-03-146720
104. Gaidt, M. M., Ebert, T. S., Chauhan, D., Schmidt, T., Schmid-Burgk, J. L., Rapino, F., Robertson, A. A. B., Cooper, M. A., Graf, T., and Hornung, V. (2016) Human Monocytes Engage an Alternative Inflammasome Pathway. *Immunity*. 10.1016/j.immuni.2016.01.012
105. Mangan, M. S. J., Olhava, E. J., Roush, W. R., Seidel, H. M., Glick, G. D., and Latz, E. (2018) Targeting the NLRP3 inflammasome in inflammatory diseases. *Nat. Rev. Drug Discov.* 10.1038/nrd.2018.97
106. Gaidt, M. M., and Hornung, V. (2017) Alternative inflammasome activation enables IL-1β release from living cells. *Curr. Opin. Immunol.* 10.1016/j.coi.2016.10.007
107. Awad, F., Assrawi, E., Louvrier, C., Jumeau, C., Georgin-Lavialle, S., Grateau, G., Amselem, S., Giurgea, I., and Karabina, S. A. (2018) Inflammasome biology, molecular pathology and therapeutic implications. *Pharmacol. Ther.* 10.1016/j.pharmthera.2018.02.011
108. Zewinger, S., Reiser, J., Jankowski, V., Alansary, D., Hahm, E., Triem, S., Klug, M., Schunk, S. J., Schmit, D., Kramann, R., Körbel, C., Ampofo, E., Laschke, M. W., Selejan, S. R., Paschen, A., Herter, T., Schuster, S., Silbernagel, G., Sester, M., Sester, U., Aßmann, G., Bals, R., Kostner, G., Jahnen-Dechent, W., Menger, M. D., Rohrer, L., März, W., Böhm, M., Jankowski, J., Kopf, M., Latz, E., Niemeyer, B. A., Fliser, D., Laufs, U., and Speer, T. (2020) Apolipoprotein C3 induces inflammation and organ damage by alternative inflammasome activation. *Nat. Immunol.* 10.1038/s41590-019-0548-1
109. Bergsbaken, T., Fink, S. L., and Cookson, B. T. (2009) Pyroptosis: Host cell death and inflammation. *Nat. Rev. Microbiol.* 10.1038/nrmicro2070
110. Cookson, B. T., and Brennan, M. A. (2001) Pro-inflammatory programmed cell death [2]. *Trends Microbiol.* 10.1016/s0966-842x(00)01936-3
111. Shi, J., Gao, W., and Shao, F. (2017) Pyroptosis: Gasdermin-Mediated Programmed Necrotic Cell Death. *Trends Biochem. Sci.* 10.1016/j.tibs.2016.10.004
112. Lamkanfi, M., Sarkar, A., Vande Walle, L., Vitari, A. C., Amer, A. O., Wewers, M. D., Tracey, K. J., Kanneganti, T.-D., and Dixit, V. M. (2010) Inflammasome-Dependent Release of the Alarmin HMGB1 in Endotoxemia. *J. Immunol.* 10.4049/jimmunol.1000803
113. Miao, E. A., Leaf, I. A., Treuting, P. M., Mao, D. P., Dors, M., Sarkar, A., Warren, S. E., Wewers, M. D., and Aderem, A. (2010) Caspase-1-induced pyroptosis is an innate immune effector mechanism against intracellular bacteria. *Nat. Immunol.* 10.1038/ni.1960
114. Stephenson, H. N., Herzig, A., and Zychlinsky, A. (2016) Beyond the grave: When is cell death critical for immunity to infection? *Curr. Opin. Immunol.* 10.1016/j.coi.2015.11.004
115. Jorgensen, I., Zhang, Y., Krantz, B. A., and Miao, E. A. (2016) Pyroptosis triggers pore-induced intracellular traps (PITs) that capture bacteria and lead to their clearance by efferocytosis. *J. Exp. Med.* 10.1084/jem.20151613
116. Shi, J., Zhao, Y., Wang, K., Shi, X., Wang, Y., Huang, H., Zhuang, Y., Cai, T., Wang, F., and Shao, F. (2015) Cleavage of GSDMD by inflammatory caspases determines pyroptotic cell death. *Nature*. 10.1038/nature15514
117. He, W. T., Wan, H., Hu, L., Chen, P., Wang, X., Huang, Z., Yang, Z. H., Zhong, C. Q., and Han, J. (2015) Gasdermin D is an executor of pyroptosis

and required for interleukin-1β secretion. *Cell Res.* 10.1038/cr.2015.139
118. Ding, J., Wang, K., Liu, W., She, Y., Sun, Q., Shi, J., Sun, H., Wang, D. C., and Shao, F. (2016) Pore-forming activity and structural autoinhibition of the gasdermin family. *Nature*. 10.1038/nature18590
119. Evavold, C. L., Ruan, J., Tan, Y., Xia, S., Wu, H., and Kagan, J. C. (2018) The Pore-Forming Protein Gasdermin D Regulates Interleukin-1 Secretion from Living Macrophages. *Immunity*. 10.1016/j.immuni.2017.11.013
120. Karmakar, M., Katsnelson, M., Malak, H. A., Greene, N. G., Howell, S. J., Hise, A. G., Camilli, A., Kadioglu, A., Dubyak, G. R., and Pearlman, E. (2015) Neutrophil IL-1β Processing Induced by Pneumolysin Is Mediated by the NLRP3/ASC Inflammasome and Caspase-1 Activation and Is Dependent on K + Efflux . *J. Immunol.* 10.4049/jimmunol.1401624
121. Heilig, R., Dick, M. S., Sborgi, L., Meunier, E., Hiller, S., and Broz, P. (2018) The Gasdermin-D pore acts as a conduit for IL-1β secretion in mice. *Eur. J. Immunol.* 10.1002/eji.201747404
122. Monteleone, M., Stanley, A. C., Chen, K. W., Brown, D. L., Bezbradica, J. S., von Pein, J. B., Holley, C. L., Boucher, D., Shakespear, M. R., Kapetanovic, R., Rolfes, V., Sweet, M. J., Stow, J. L., and Schroder, K. (2018) Interleukin-1β Maturation Triggers Its Relocation to the Plasma Membrane for Gasdermin-D-Dependent and -Independent Secretion. *Cell Rep.* 10.1016/j.celrep.2018.07.027
123. Kayagaki, N., Kornfeld, O. S., Lee, B. L., Stowe, I. B., O'Rourke, K., Li, Q., Sandoval, W., Yan, D., Kang, J., Xu, M., Zhang, J., Lee, W. P., McKenzie, B. S., Ulas, G., Payandeh, J., Roose-Girma, M., Modrusan, Z., Reja, R., Sagolla, M., Webster, J. D., Cho, V., Andrews, T. D., Morris, L. X., Miosge, L. A., Goodnow, C. C., Bertram, E. M., and Dixit, V. M. (2021) NINJ1 mediates plasma membrane rupture during lytic cell death. *Nature*. 10.1038/s41586-021-03218-7
124. Volchuk, A., Ye, A., Chi, L., Steinberg, B. E., and Goldenberg, N. M. (2020) Indirect regulation of HMGB1 release by gasdermin D. *Nat. Commun.* 10.1038/s41467-020-18443-3
125. de Vasconcelos, N. M., Van Opdenbosch, N., Van Gorp, H., Parthoens, E., and Lamkanfi, M. (2019) Single-cell analysis of pyroptosis dynamics reveals conserved GSDMD-mediated subcellular events that precede plasma membrane rupture. *Cell Death Differ.* 10.1038/s41418-018-0106-7
126. DiPeso, L., Ji, D. X., Vance, R. E., and Price, J. V. (2017) Cell death and cell lysis are separable events during pyroptosis. *Cell Death Discov.* 10.1038/cddiscovery.2017.70
127. Xia, S., Zhang, Z., Magupalli, V. G., Pablo, J. L., Dong, Y., Vora, S. M., Wang, L., Fu, T. M., Jacobson, M. P., Greka, A., Lieberman, J., Ruan, J., and Wu, H. (2021) Gasdermin D pore structure reveals preferential release of mature interleukin-1. *Nature*. 10.1038/s41586-021-03478-3
128. Broz, P., Pelegrín, P., and Shao, F. (2020) The gasdermins, a protein family executing cell death and inflammation. *Nat. Rev. Immunol.* 10.1038/s41577-019-0228-2
129. Rogers, C., Fernandes-Alnemri, T., Mayes, L., Alnemri, D., Cingolani, G., and Alnemri, E. S. (2017) Cleavage of DFNA5 by caspase-3 during apoptosis mediates progression to secondary necrotic/pyroptotic cell death. *Nat. Commun.* 10.1038/ncomms14128
130. Wang, Y., Gao, W., Shi, X., Ding, J., Liu, W., He, H., Wang, K., and Shao, F.

(2017) Chemotherapy drugs induce pyroptosis through caspase-3 cleavage of a gasdermin. *Nature*. 10.1038/nature22393

131. Baroja-Mazo, A., Martín-Sánchez, F., Gomez, A. I., Martínez, C. M., Amores-Iniesta, J., Compan, V., Barberà-Cremades, M., Yagüe, J., Ruiz-Ortiz, E., Antón, J., Buján, S., Couillin, I., Brough, D., Arostegui, J. I., and Pelegrín, P. (2014) The NLRP3 inflammasome is released as a particulate danger signal that amplifies the inflammatory response. *Nat. Immunol.* 10.1038/ni.2919
132. Agostini, L., Martinon, F., Burns, K., McDermott, M. F., Hawkins, P. N., and Tschopp, J. (2004) NALP3 forms an IL-1β-processing inflammasome with increased activity in Muckle-Wells autoinflammatory disorder. *Immunity*. 10.1016/S1074-7613(04)00046-9
133. Cordero, M. D., Alcocer-Gómez, E., and Ryffel, B. (2018) Gain of function mutation and inflammasome driven diseases in human and mouse models. *J. Autoimmun.* 10.1016/j.jaut.2018.03.002
134. Hawkins, P. N., Lachmann, H. J., and McDermott, M. F. (2003) Interleukin-1–Receptor Antagonist in the Muckle–Wells Syndrome. *N. Engl. J. Med.* 10.1056/nejm200306193482523
135. Lachmann, H. J., Kone-Paut, I., Kuemmerle-Deschner, J. B., Leslie, K. S., Hachulla, E., Quartier, P., Gitton, X., Widmer, A., Patel, N., and Hawkins, P. N. (2009) Use of Canakinumab in the Cryopyrin-Associated Periodic Syndrome. *N. Engl. J. Med.* 10.1056/nejmoa0810787
136. Hoffman, H. M., Throne, M. L., Amar, N. J., Sebai, M., Kivitz, A. J., Kavanaugh, A., Weinstein, S. P., Belomestnov, P., Yancopoulos, G. D., Stahl, N., and Mellis, S. J. (2008) Efficacy and safety of rilonacept (Interleukin-1 Trap) in patients with cryopyrin-associated periodic syndromes: Results from two sequential placebo-controlled studies. *Arthritis Rheum.* 10.1002/art.23687
137. Seoane, P. I., Lee, B., Hoyle, C., Yu, S., Lopez-Castejon, G., Lowe, M., and Brough, D. (2020) The NLRP3-inflammasome as a sensor of organelle dysfunction. *J. Cell Biol.* 10.1083/jcb.202006194
138. Wang, L., and Hauenstein, A. V. (2020) The NLRP3 inflammasome: Mechanism of action, role in disease and therapies. *Mol. Aspects Med.* 10.1016/j.mam.2020.100889
139. Heart Disease and Stroke Statistics-2021 Update A Report from the American Heart Association (2021) *Circulation*. 10.1161/CIR.0000000000000950
140. Shi, X., Xie, W. L., Kong, W. W., Chen, D., and Qu, P. (2015) Expression of the NLRP3 Inflammasome in Carotid Atherosclerosis. *J. Stroke Cerebrovasc. Dis.* 10.1016/j.jstrokecerebrovasdis.2015.03.024
141. Paramel Varghese, G., Folkersen, L., Strawbridge, R. J., Halvorsen, B., Yndestad, A., Ranheim, T., Krohg-Sørensen, K., Skjelland, M., Espevik, T., Aukrust, P., Lengquist, M., Hedin, U., Jansson, J. H., Fransén, K., Hansson, G. K., Eriksson, P., and Sirsjö, A. (2016) NLRP3 Inflammasome Expression and Activation in Human Atherosclerosis. *J. Am. Heart Assoc.* 10.1161/JAHA.115.003031
142. Rajaṁaki, K., Lappalainen, J., Öörni, K., Välimäki, E., Matikainen, S., Kovanen, P. T., and Kari, E. K. (2010) Cholesterol crystals activate the NLRP3 inflammasome in human macrophages: A novel link between cholesterol metabolism and inflammation. *PLoS One*.

10.1371/journal.pone.0011765
143. Stewart, C. R., Stuart, L. M., Wilkinson, K., Van Gils, J. M., Deng, J., Halle, A., Rayner, K. J., Boyer, L., Zhong, R., Frazier, W. A., Lacy-Hulbert, A., Khoury, J. El, Golenbock, D. T., and Moore, K. J. (2010) CD36 ligands promote sterile inflammation through assembly of a Toll-like receptor 4 and 6 heterodimer. *Nat. Immunol.* 10.1038/ni.1836
144. Zheng, F., Xing, S., Gong, Z., Mu, W., and Xing, Q. (2014) Silence of NLRP3 suppresses atherosclerosis and stabilizes plaques in apolipoprotein E-deficient mice. *Mediators Inflamm.* 10.1155/2014/507208
145. Christ, A., Günther, P., Lauterbach, M. A. R., Duewell, P., Biswas, D., Pelka, K., Scholz, C. J., Oosting, M., Haendler, K., Baßler, K., Klee, K., Schulte-Schrepping, J., Ulas, T., Moorlag, S. J. C. F. M., Kumar, V., Park, M. H., Joosten, L. A. B., Groh, L. A., Riksen, N. P., Espevik, T., Schlitzer, A., Li, Y., Fitzgerald, M. L., Netea, M. G., Schultze, J. L., and Latz, E. (2018) Western Diet Triggers NLRP3-Dependent Innate Immune Reprogramming. *Cell*. 10.1016/j.cell.2017.12.013
146. Zheng, F., Xing, S., Gong, Z., and Xing, Q. (2013) NLRP3 inflammasomes show high expression in Aorta of patients with atherosclerosis. *Hear. Lung Circ.* 10.1016/j.hlc.2013.01.012
147. So, A. (2008) Developments in the scientific and clinical understanding of gout. *Arthritis Res. Ther.* 10.1186/ar2509
148. Hornung, V., Bauernfeind, F., Halle, A., Samstad, E. O., Kono, H., Rock, K. L., Fitzgerald, K. A., and Latz, E. (2008) Silica crystals and aluminum salts activate the NALP3 inflammasome through phagosomal destabilization. *Nat. Immunol.* 10.1038/ni.1631
149. Chen, C. J., Shi, Y., Hearn, A., Fitzgerald, K., Golenbock, D., Reed, G., Akira, S., and Rock, K. L. (2006) MyD88-dependent IL-1 receptor signaling is essential for gouty inflammation stimulated by monosodium urate crystals. *J. Clin. Invest.* 10.1172/JCI28075
150. Martinon, F., Pétrilli, V., Mayor, A., Tardivel, A., and Tschopp, J. (2006) Gout-associated uric acid crystals activate the NALP3 inflammasome. *Nature*. 10.1038/nature04516
151. Hotamisligil, G. S. (2017) Inflammation, metaflammation and immunometabolic disorders. *Nature*. 10.1038/nature21363
152. Vandanmagsar, B., Youm, Y. H., Ravussin, A., Galgani, J. E., Stadler, K., Mynatt, R. L., Ravussin, E., Stephens, J. M., and Dixit, V. D. (2011) The NLRP3 inflammasome instigates obesity-induced inflammation and insulin resistance. *Nat. Med.* 10.1038/nm.2279
153. Fève, B., and Bastard, J. P. (2009) The role of interleukins in insulin resistance and type 2 diabetes mellitus. *Nat. Rev. Endocrinol.* 10.1038/nrendo.2009.62
154. Stienstra, R., Joosten, L. A. B., Koenen, T., Van Tits, B., Van Diepen, J. A., Van Den Berg, S. A. A., Rensen, P. C. N., Voshol, P. J., Fantuzzi, G., Hijmans, A., Kersten, S., Müller, M., Van Den Berg, W. B., Van Rooijen, N., Wabitsch, M., Kullberg, B. J., Van Der Meer, J. W. M., Kanneganti, T., Tack, C. J., and Netea, M. G. (2010) The inflammasome-mediated caspase-1 activation controls adipocyte differentiation and insulin sensitivity. *Cell Metab.* 10.1016/j.cmet.2010.11.011
155. Maedler, K., Sergeev, P., Ehses, J. A., Mathe, Z., Bosco, D., Berney, T., Dayer, J. M., Reinecke, M., Halban, P. A., and Donath, M. Y. (2004) Leptin

modulates β cell expression of IL-1 receptor antagonist and release of IL-1β in human islets. *Proc. Natl. Acad. Sci. U. S. A.* 10.1073/pnas.0305683101
156. Larsen, C. M., Faulenbach, M., Vaag, A., Vølund, A., Ehses, J. A., Seifert, B., Mandrup-Poulsen, T., and Donath, M. Y. (2007) Interleukin-1–Receptor Antagonist in Type 2 Diabetes Mellitus. *N. Engl. J. Med.* 10.1056/nejmoa065213
157. Miwa, T., Furukawa, S., Nakajima, K., Furukawa, Y., and Kohsaka, S. (1997) Lipopolysaccharide enhances synthesis of brain-derived neurotrophic factor in cultured rat microglia. *J. Neurosci. Res.* 10.1002/(sici)1097-4547(19971215)50:6<1023::aid-jnr13>3.3.co;2-s
158. Tahara, K., Kim, H. D., Jin, J. J., Maxwell, J. A., Li, L., and Fukuchi, K. I. (2006) Role of toll-like receptor signalling in Aβ uptake and clearance. *Brain*. 10.1093/brain/awl249
159. Ito, U., Nagasao, J., Kawakami, E., and Oyanagi, K. (2007) Fate of disseminated dead neurons in the cortical ischemic penumbra: Ultrastructure indicating a novel scavenger mechanism of microglia and astrocytes. *Stroke*. 10.1161/STROKEAHA.107.484394
160. Ribes, S., Ebert, S., Czesnik, D., Regen, T., Zeug, A., Bukowski, S., Mildner, A., Eiffert, H., Hanisch, U. K., Hammerschmidt, S., and Nau, R. (2009) Toll-like receptor prestimulation increases phagocytosis of Escherichia coli DH5α and Escherichia coli K1 strains by murine microglial cells. *Infect. Immun.* 10.1128/IAI.00903-08
161. Szretter, K. J., Samuel, M. A., Gilfillan, S., Fuchs, A., Colonna, M., and Diamond, M. S. (2009) The Immune Adaptor Molecule SARM Modulates Tumor Necrosis Factor Alpha Production and Microglia Activation in the Brainstem and Restricts West Nile Virus Pathogenesis. *J. Virol.* 10.1128/jvi.00836-09
162. Lazovic, J., Basu, A., Lin, H. W., Rothstein, R. P., Krady, J. K., Smith, M. B., and Levison, S. W. (2005) Neuroinflammation and both cytotoxic and vasogenic edema are reduced in interleukin-1 type 1 receptor-deficient mice conferring neuroprotection. *Stroke*. 10.1161/01.STR.0000182255.08162.6a
163. Choi, D. Y., Liu, M., Hunter, R. L., Cass, W. A., Pandya, J. D., Sullivan, P. G., Shin, E. J., Kim, H. C., Gash, D. M., and Bing, G. (2009) Striatal neuroinflammation promotes parkinsonism in rats. *PLoS One*. 10.1371/journal.pone.0005482
164. Abo-ouf, H., Hooper, A. W. M., White, E. J., Van Rensburg, H. J. J., Trigatti, B. L., and Igdoura, S. A. (2013) Deletion of tumor necrosis factor-α ameliorates neurodegeneration in sandhoff disease mice. *Hum. Mol. Genet.* 10.1093/hmg/ddt250
165. Karve, I. P., Taylor, J. M., and Crack, P. J. (2016) The contribution of astrocytes and microglia to traumatic brain injury. *Br. J. Pharmacol.* 10.1111/bph.13125
166. Shrivastava, S. K., Dalko, E., Delcroix-Genete, D., Herbert, F., Cazenave, P. A., and Pied, S. (2017) Uptake of parasite-derived vesicles by astrocytes and microglial phagocytosis of infected erythrocytes may drive neuroinflammation in cerebral malaria. *Glia*. 10.1002/glia.23075
167. Kierdorf, K., Erny, D., Goldmann, T., Sander, V., Schulz, C., Perdiguero, E. G., Wieghofer, P., Heinrich, A., Riemke, P., Hölscher, C., Müller, D. N., Luckow, B., Brocker, T., Debowski, K., Fritz, G., Opdenakker, G., Diefenbach, A., Biber, K., Heikenwalder, M., Geissmann, F., Rosenbauer,

F., and Prinz, M. (2013) Microglia emerge from erythromyeloid precursors via Pu.1-and Irf8-dependent pathways. *Nat. Neurosci.* 10.1038/nn.3318

168. Paolicelli, R. C., Bolasco, G., Pagani, F., Maggi, L., Scianni, M., Panzanelli, P., Giustetto, M., Ferreira, T. A., Guiducci, E., Dumas, L., Ragozzino, D., and Gross, C. T. (2011) Synaptic pruning by microglia is necessary for normal brain development. *Science (80-.).* 10.1126/science.1202529
169. Nayak, D., Roth, T. L., and McGavern, D. B. (2014) Microglia development and function. *Annu. Rev. Immunol.* 10.1146/annurev-immunol-032713-120240
170. Shah, V. B., Huang, Y., Keshwara, R., Ozment-Skelton, T., Williams, D. L., and Keshvara, L. (2008) β-Glucan Activates Microglia without Inducing Cytokine Production in Dectin-1-Dependent Manner. *J. Immunol.* 10.4049/jimmunol.180.5.2777
171. Hu, X., Liu, G., Hou, Y., Shi, J., Zhu, L., Jin, D., Peng, J., and Zhao, Y. (2012) Induction of M2-like macrophages in recipient NOD-scid mice by allogeneic donor CD4+ CD25+ regulatory T cells. *Cell. Mol. Immunol.* 10.1038/cmi.2012.47
172. Fu, R., Shen, Q., Xu, P., Luo, J. J., and Tang, Y. (2014) Phagocytosis of microglia in the central nervous system diseases. *Mol. Neurobiol.* 10.1007/s12035-013-8620-6
173. Becher, B., Prat, A., and Antel, J. P. (2000) Brain-immune connection: Immuno-regulatory properties of CNS-resident cells. *Glia*. 10.1002/(SICI)1098-1136(20000215)29:4<293::AID-GLIA1>3.0.CO;2-A
174. Saijo, K., Crotti, A., and Glass, C. K. (2013) Regulation of microglia activation and deactivation by nuclear receptors. *Glia*. 10.1002/glia.22423
175. Rock, R. B., Gekker, G., Hu, S., Sheng, W. S., Cheeran, M., Lokensgard, J. R., and Peterson, P. K. (2004) Role of microglia in central nervous system infections. *Clin. Microbiol. Rev.* 10.1128/CMR.17.4.942-964.2004
176. Kettenmann, H., Hanisch, U.-K., Noda, M., and Verkhratsky, A. (2011) Physiology of Microglia. *Physiol. Rev.* 10.1152/physrev.00011.2010
177. Byrnes, K. R., and Faden, A. I. (2007) Role of cell cycle proteins in CNS injury. *Neurochem. Res.* 10.1007/s11064-007-9312-2
178. Lalancette-Hébert, M., Gowing, G., Simard, A., Yuan, C. W., and Kriz, J. (2007) Selective ablation of proliferating microglial cells exacerbates ischemic injury in the brain. *J. Neurosci.* 10.1523/JNEUROSCI.5360-06.2007
179. Moss, D. W., and Bates, T. E. (2001) Activation of murine microglial cell lines by lipopolysaccharide and interferon-γ causes NO-mediated decreases in mitochondrial and cellular function. *Eur. J. Neurosci.* 10.1046/j.1460-9568.2001.01418.x
180. Heneka, M. T., and O'Banion, M. K. (2007) Inflammatory processes in Alzheimer's disease. *J. Neuroimmunol.* 10.1016/j.jneuroim.2006.11.017
181. Aoki, E., Yano, R., Yokoyama, H., Kato, H., and Araki, T. (2009) Role of nuclear transcription factor kappa B (NF-kappaB) for MPTP (1-methyl-4-phenyl-1,2,3,6-tetrahyropyridine)-induced apoptosis in nigral neurons of mice. *Exp. Mol. Pathol.* 10.1016/j.yexmp.2008.10.004
182. Fellner, L., Irschick, R., Schanda, K., Reindl, M., Klimaschewski, L., Poewe, W., Wenning, G. K., and Stefanova, N. (2013) Toll-like receptor 4 is required for α-synuclein dependent activation of microglia and astroglia. *Glia*. 10.1002/glia.22437

183. Elmore, M. R. P., Burton, M. D., Conrad, M. S., Rytych, J. L., Van Alstine, W. G., and Johnson, R. W. (2014) Respiratory viral infection in neonatal piglets causes marked microglia activation in the hippocampus and deficits in spatial learning. *J. Neurosci.* 10.1523/JNEUROSCI.2180-13.2014
184. Liu, B., Le, K. X., Park, M. A., Wang, S., Belanger, A. P., Dubey, S., Frost, J. L., Holton, P., Reiser, V., Jones, P. A., Trigg, W., Di Carli, M. F., and Lemere, C. A. (2015) In vivo detection of age-and disease-related increases in neuroinflammation by18F-GE180 TSPO microPET imaging in wild-type and alzheimer's transgenic mice. *J. Neurosci.* 10.1523/JNEUROSCI.0996-15.2015
185. Li, D., Wang, C., Yao, Y., Chen, L., Liu, G., Zhang, R., Liu, Q., Shi, F. D., and Hao, J. (2016) MTORC1 pathway disruption ameliorates brain inflammation following stroke via a shift in microglia phenotype from M1 type to M2 type. *FASEB J.* 10.1096/fj.201600495R
186. Kumar, A., Barrett, J. P., Alvarez-Croda, D. M., Stoica, B. A., Faden, A. I., and Loane, D. J. (2016) NOX2 drives M1-like microglial/macrophage activation and neurodegeneration following experimental traumatic brain injury. *Brain. Behav. Immun.* 10.1016/j.bbi.2016.07.158
187. Xian, W., Wu, Y., Xiong, W., Li, L., Li, T., Pan, S., Song, L., Hu, L., Pei, L., Yao, S., and Shang, Y. (2016) The pro-resolving lipid mediator Maresin 1 protects against cerebral ischemia/reperfusion injury by attenuating the pro-inflammatory response. *Biochem. Biophys. Res. Commun.* 10.1016/j.bbrc.2016.02.090
188. Wolf, S. A., Boddeke, H. W. G. M., and Kettenmann, H. (2017) Microglia in Physiology and Disease. *Annu. Rev. Physiol.* 10.1146/annurev-physiol-022516-034406
189. Schaum, N., Karkanias, J., Neff, N. F., May, A. P., Quake, S. R., Wyss-Coray, T., Darmanis, S., Batson, J., Botvinnik, O., Chen, M. B., Chen, S., Green, F., Jones, R. C., Maynard, A., Penland, L., Pisco, A. O., Sit, R. V., Stanley, G. M., Webber, J. T., Zanini, F., Baghel, A. S., Bakerman, I., Bansal, I., Berdnik, D., Bilen, B., Brownfield, D., Cain, C., Cho, M., Cirolia, G., Conley, S. D., Demers, A., Demir, K., de Morree, A., Divita, T., du Bois, H., Dulgeroff, L. B. T., Ebadi, H., Espinoza, F. H., Fish, M., Gan, Q., George, B. M., Gillich, A., Genetiano, G., Gu, X., Gulati, G. S., Hang, Y., Hosseinzadeh, S., Huang, A., Iram, T., Isobe, T., Ives, F., Kao, K. S., Karnam, G., Kershner, A. M., Kiss, B. M., Kong, W., Kumar, M. E., Lam, J. Y., Lee, D. P., Lee, S. E., Li, G., Li, Q., Liu, L., Lo, A., Lu, W. J., Manjunath, A., May, K. L., May, O. L., McKay, M., Metzger, R. J., Mignardi, M., Min, D., Nabhan, A. N., Ng, K. M., Noh, J., Patkar, R., Peng, W. C., Puccinelli, R., Rulifson, E. J., Sikandar, S. S., Sinha, R., Szade, K., Tan, W., Tato, C., Tellez, K., Travaglini, K. J., Tropini, C., Waldburger, L., van Weele, L. J., Wosczyna, M. N., Xiang, J., Xue, S., Youngyunpipatkul, J., Zardeneta, M. E., Zhang, F., Zhou, L., Castro, P., Croote, D., DeRisi, J. L., Kuo, C. S., Lehallier, B., Nguyen, P. K., Tan, S. Y., Wang, B. M., Yousef, H., Beachy, P. A., Chan, C. K. F., Huang, K. C., Weinberg, K., Wu, S. M., Barres, B. A., Clarke, M. F., Kim, S. K., Krasnow, M. A., Nusse, R., Rando, T. A., Sonnenburg, J., and Weissman, I. L. (2018) Single-cell transcriptomics of 20 mouse organs creates a Tabula Muris. *Nature*. 10.1038/s41586-018-0590-4
190. Zhang, Y., Chen, K., Sloan, S. A., Bennett, M. L., Scholze, A. R., O'Keeffe, S., Phatnani, H. P., Guarnieri, P., Caneda, C., Ruderisch, N., Deng, S.,

Liddelow, S. A., Zhang, C., Daneman, R., Maniatis, T., Barres, B. A., and Wu, J. Q. (2014) An RNA-Sequencing Transcriptome and Splicing Database of Glia, Neurons, and Vascular Cells of the Cerebral Cortex. *J. Neurosci.* 10.1523/JNEUROSCI.1860-14.2014

191. Heneka, M. T., McManus, R. M., and Latz, E. (2018) Inflammasome signalling in brain function and neurodegenerative disease. *Nat. Rev. Neurosci.* 10.1038/s41583-018-0055-7
192. Halle, A., Hornung, V., Petzold, G. C., Stewart, C. R., Monks, B. G., Reinheckel, T., Fitzgerald, K. A., Latz, E., Moore, K. J., and Golenbock, D. T. (2008) The NALP3 inflammasome is involved in the innate immune response to amyloid-β. *Nat. Immunol.* 10.1038/ni.1636
193. Burm, S. M., Zuiderwijk-Sick, E. A., T Jong, A. E. J., Van Der Putten, C., Veth, J., Kondova, I., and Bajramovic, J. J. (2015) Inflammasome-induced IL-1β secretion in microglia is characterized by delayed kinetics and is only partially dependent on inflammatory caspases. *J. Neurosci.* 10.1523/JNEUROSCI.2510-14.2015
194. Deora, V., Albornoz, E. A., Zhu, K., Woodruff, T. M., and Gordon, R. (2017) The Ketone Body β-Hydroxybutyrate Does Not Inhibit Synuclein Mediated Inflammasome Activation in Microglia. *J. Neuroimmune Pharmacol.* 10.1007/s11481-017-9754-5
195. Codolo, G., Plotegher, N., Pozzobon, T., Brucale, M., Tessari, I., Bubacco, L., and de Bernard, M. (2013) Triggering of Inflammasome by Aggregated α-Synuclein, an Inflammatory Response in Synucleinopathies. *PLoS One*. 10.1371/journal.pone.0055375
196. Zhou, Y., Lu, M., Du, R. H., Qiao, C., Jiang, C. Y., Zhang, K. Z., Ding, J. H., and Hu, G. (2016) MicroRNA-7 targets Nod-like receptor protein 3 inflammasome to modulate neuroinflammation in the pathogenesis of Parkinson's disease. *Mol. Neurodegener.* 10.1186/s13024-016-0094-3
197. Sims, R., Van Der Lee, S. J., Naj, A. C., Bellenguez, C., Badarinarayan, N., Jakobsdottir, J., Kunkle, B. W., Boland, A., Raybould, R., Bis, J. C., Martin, E. R., Grenier-Boley, B., Heilmann-Heimbach, S., Chouraki, V., Kuzma, A. B., Sleegers, K., Vronskaya, M., Ruiz, A., Graham, R. R., Olaso, R., Hoffmann, P., Grove, M. L., Vardarajan, B. N., Hiltunen, M., Nöthen, M. M., White, C. C., Hamilton-Nelson, K. L., Epelbaum, J., Maier, W., Choi, S. H., Beecham, G. W., Dulary, C., Herms, S., Smith, A. V., Funk, C. C., Derbois, C., Forstner, A. J., Ahmad, S., Li, H., Bacq, D., Harold, D., Satizabal, C. L., Valladares, O., Squassina, A., Thomas, R., Brody, J. A., Qu, L., Sánchez-Juan, P., Morgan, T., Wolters, F. J., Zhao, Y., Garcia, F. S., Denning, N., Fornage, M., Malamon, J., Naranjo, M. C. D., Majounie, E., Mosley, T. H., Dombroski, B., Wallon, D., Lupton, M. K., Dupuis, J., Whitehead, P., Fratiglioni, L., Medway, C., Jian, X., Mukherjee, S., Keller, L., Brown, K., Lin, H., Cantwell, L. B., Panza, F., McGuinness, B., Moreno-Grau, S., Burgess, J. D., Solfrizzi, V., Proitsi, P., Adams, H. H., Allen, M., Seripa, D., Pastor, P., Cupples, L. A., Price, N. D., Hannequin, D., Frank-García, A., Levy, D., Chakrabarty, P., Caffarra, P., Giegling, I., Beiser, A. S., Giedraitis, V., Hampel, H., Garcia, M. E., Wang, X., Lannfelt, L., Mecocci, P., Eiriksdottir, G., Crane, P. K., Pasquier, F., Boccardi, V., Henández, I., Barber, R. C., Scherer, M., Tarraga, L., Adams, P. M., Leber, M., Chen, Y., Albert, M. S., Riedel-Heller, S., Emilsson, V., Beekly, D., Braae, A., Schmidt, R., Blacker, D., Masullo, C., Schmidt, H., Doody, R. S., Spalletta, G., Jr, W. T. L.,

Fairchild, T. J., Bossù, P., Lopez, O. L., Frosch, M. P., Sacchinelli, E., Ghetti, B., Yang, Q., Huebinger, R. M., Jessen, F., Li, S., Kamboh, M. I., Morris, J. C., Sotolongo-Grau, O., Katz, M. J., Corcoran, C., Dunstan, M., Braddel, A., Thomas, C., Meggy, A., Marshall, R., Gerrish, A., Chapman, J., Aguilar, M., Taylor, S., Hill, M., Fairén, M. D., Hodges, A., Vellas, B., Soininen, H., Kloszewska, I., Daniilidou, M., Uphill, J., Patel, Y., Hughes, J. T., Lord, J., Turton, J., Hartmann, A. M., Cecchetti, R., Fenoglio, C., Serpente, M., Arcaro, M., Caltagirone, C., Orfei, M. D., Ciaramella, A., Pichler, S., Mayhaus, M., Gu, W., Lleó, A., Fortea, J., Blesa, R., Barber, I. S., Brookes, K., Cupidi, C., Maletta, R. G., Carrell, D., Sorbi, S., Moebus, S., Urbano, M., Pilotto, A., Kornhuber, J., Bosco, P., Todd, S., Craig, D., Johnston, J., Gill, M., Lawlor, B., Lynch, A., Fox, N. C., Hardy, J., Albin, R. L., Apostolova, L. G., Arnold, S. E., Asthana, S., Atwood, C. S., Baldwin, C. T., Barnes, L. L., Barral, S., Beach, T. G., Becker, J. T., Bigio, E. H., Bird, T. D., Boeve, B. F., Bowen, J. D., Boxer, A., Burke, J. R., Burns, J. M., Buxbaum, J. D., Cairns, N. J., Cao, C., Carlson, C. S., Carlsson, C. M., Carney, R. M., Carrasquillo, M. M., Carroll, S. L., Diaz, C. C., Chui, H. C., Clark, D. G., Cribbs, D. H., Crocco, E. A., Decarli, C., Dick, M., Duara, R., Evans, D. A., Faber, K. M., Fallon, K. B., Fardo, D. W., Farlow, M. R., Ferris, S., Foroud, T. M., Galasko, D. R., Gearing, M., Geschwind, D. H., Gilbert, J. R., Graff-Radford, N. R., Green, R. C., Growdon, J. H., Hamilton, R. L., Harrell, L. E., Honig, L. S., Huentelman, M. J., Hulette, C. M., Hyman, B. T., Jarvik, G. P., Abner, E., Jin, L. W., Jun, G., Karydas, A., Kaye, J. A., Kim, R., Kowall, N. W., Kramer, J. H., Laferla, F. M., Lah, J. J., Leverenz, J. B., Levey, A. I., Li, G., Lieberman, A. P., Lunetta, K. L., Lyketsos, C. G., Marson, D. C., Martiniuk, F., Mash, D. C., Masliah, E., McCormick, W. C., McCurry, S. M., McDavid, A. N., McKee, A. C., Mesulam, M., Miller, B. L., Miller, C. A., Miller, J. W., Murrell, J. R., Myers, A. J., O'Bryant, S., Olichney, J. M., Pankratz, V. S., Parisi, J. E., Paulson, H. L., Perry, W., Peskind, E., Pierce, A., Poon, W. W., Potter, H., Quinn, J. F., Raj, A., Raskind, M., Reisberg, B., Reitz, C., Ringman, J. M., Roberson, E. D., Rogaeva, E., Rosen, H. J., Rosenberg, R. N., Sager, M. A., Saykin, A. J., Schneider, J. A., Schneider, L. S., Seeley, W. W., Smith, A. G., Sonnen, J. A., Spina, S., Stern, R. A., Swerdlow, R. H., Tanzi, R. E., Thornton-Wells, T. A., Trojanowski, J. Q., Troncoso, J. C., Van Deerlin, V. M., Van Eldik, L. J., Vinters, H. V., Vonsattel, J. P., Weintraub, S., Welsh-Bohmer, K. A., Wilhelmsen, K. C., Williamson, J., Wingo, T. S., Woltjer, R. L., Wright, C. B., Yu, C. E., Yu, L., Garzia, F., Golamaully, F., Septier, G., Engelborghs, S., Vandenberghe, R., De Deyn, P. P., Fernadez, C. M., Benito, Y. A., Thonberg, H., Forsell, C., Lilius, L., Kinhult-Stählbom, A., Kilander, L., Brundin, R., Concari, L., Helisalmi, S., Koivisto, A. M., Haapasalo, A., Dermecourt, V., Fievet, N., Hanon, O., Dufouil, C., Brice, A., Ritchie, K., Dubois, B., Himali, J. J., Keene, C. D., Tschanz, J., Fitzpatrick, A. L., Kukull, W. A., Norton, M., Aspelund, T., Larson, E. B., Munger, R., Rotter, J. I., Lipton, R. B., Bullido, M. J., Hofman, A., Montine, T. J., Coto, E., Boerwinkle, E., Petersen, R. C., Alvarez, V., Rivadeneira, F., Reiman, E. M., Gallo, M., O'Donnell, C. J., Reisch, J. S., Bruni, A. C., Royall, D. R., Dichgans, M., Sano, M., Galimberti, D., St George-Hyslop, P., Scarpini, E., Tsuang, D. W., Mancuso, M., Bonuccelli, U., Winslow, A. R., Daniele, A., Wu, C. K., Peters, O., Nacmias, B., Riemenschneider, M., Heun, R., Brayne, C., Rubinsztein,

D. C., Bras, J., Guerreiro, R., Al-Chalabi, A., Shaw, C. E., Collinge, J., Tsolaki, M., Clarimón, J., Sussams, R., Lovestone, S., O'Donovan, M. C., Owen, M. J., Behrens, T. W., Mead, S., Uitterlinden, A. G., Holmes, C., Cruchaga, C., Ingelsson, M., Bennett, D. A., Powell, J., Golde, T. E., Graff, C., De Jager, P. L., Morgan, K., Ertekin-Taner, N., Combarros, O., Psaty, B. M., Passmore, P., Younkin, S. G., Berr, C., Gudnason, V., Rujescu, D., Dickson, D. W., Dartigues, J. F., Destefano, A. L., Ortega-Cubero, S., Hakonarson, H., Campion, D., Boada, M., Kauwe, J. K., Farrer, L. A., Van Broeckhoven, C., Ikram, M. A., Jones, L., Haines, J. L., Tzourio, C., Tzourio, C., Escott-Price, V., Mayeux, R., Deleuze, J. F., Amin, N., Goate, A. M., Pericak-Vance, M. A., Amouyel, P., Van Duijn, C. M., Ramirez, A., Wang, L. S., Lambert, J. C., Seshadri, S., Williams, J., and Schellenberg, G. D. (2017) Rare coding variants in PLCG2, ABI3, and TREM2 implicate microglial-mediated innate immunity in Alzheimer's disease. *Nat. Genet.* 10.1038/ng.3916

198. Griciuc, A., Serrano-Pozo, A., Parrado, A. R., Lesinski, A. N., Asselin, C. N., Mullin, K., Hooli, B., Choi, S. H., Hyman, B. T., and Tanzi, R. E. (2013) Alzheimer's disease risk gene cd33 inhibits microglial uptake of amyloid beta. *Neuron*. 10.1016/j.neuron.2013.04.014
199. Morales, I., Jiménez, J. M., Mancilla, M., and Maccioni, R. B. (2013) Tau oligomers and fibrils induce activation of microglial cells. *J. Alzheimer's Dis.* 10.3233/JAD-131843
200. Sanchez-Mejias, E., Navarro, V., Jimenez, S., Sanchez-Mico, M., Sanchez-Varo, R., Nuñez-Diaz, C., Trujillo-Estrada, L., Davila, J. C., Vizuete, M., Gutierrez, A., and Vitorica, J. (2016) Soluble phospho-tau from Alzheimer's disease hippocampus drives microglial degeneration. *Acta Neuropathol.* 10.1007/s00401-016-1630-5
201. Heneka, M. T., Golenbock, D. T., and Latz, E. (2015) Innate immunity in Alzheimer's disease. *Nat. Immunol.* 10.1038/ni.3102
202. Heneka, M. T., Kummer, M. P., Stutz, A., Delekate, A., Schwartz, S., Vieira-Saecker, A., Griep, A., Axt, D., Remus, A., Tzeng, T. C., Gelpi, E., Halle, A., Korte, M., Latz, E., and Golenbock, D. T. (2013) NLRP3 is activated in Alzheimer's disease and contributes to pathology in APP/PS1 mice. *Nature*. 10.1038/nature11729
203. Venegas, C., Kumar, S., Franklin, B. S., Dierkes, T., Brinkschulte, R., Tejera, D., Vieira-Saecker, A., Schwartz, S., Santarelli, F., Kummer, M. P., Griep, A., Gelpi, E., Beilharz, M., Riedel, D., Golenbock, D. T., Geyer, M., Walter, J., Latz, E., and Heneka, M. T. (2017) Microglia-derived ASC specks crossseed amyloid-β in Alzheimer's disease. *Nature*. 10.1038/nature25158
204. Coll, R. C., Robertson, A. A. B., Chae, J. J., Higgins, S. C., Muñoz-Planillo, R., Inserra, M. C., Vetter, I., Dungan, L. S., Monks, B. G., Stutz, A., Croker, D. E., Butler, M. S., Haneklaus, M., Sutton, C. E., Núñez, G., Latz, E., Kastner, D. L., Mills, K. H. G., Masters, S. L., Schroder, K., Cooper, M. A., and O'Neill, L. A. J. (2015) A small-molecule inhibitor of the NLRP3 inflammasome for the treatment of inflammatory diseases. *Nat. Med.* 10.1038/nm.3806
205. Dempsey, C., Rubio Araiz, A., Bryson, K. J., Finucane, O., Larkin, C., Mills, E. L., Robertson, A. A. B., Cooper, M. A., O'Neill, L. A. J., and Lynch, M. A. (2017) Inhibiting the NLRP3 inflammasome with MCC950 promotes non-phlogistic clearance of amyloid-β and cognitive function in APP/PS1 mice.

Brain. Behav. Immun. 10.1016/j.bbi.2016.12.014

206. Lonnemann, N., Hosseini, S., Marchetti, C., Skouras, D. B., Stefanoni, D., D'Alessandro, A., Dinarello, C. A., and Korte, M. (2020) The NLRP3 inflammasome inhibitor OLT1177 rescues cognitive impairment in a mouse model of Alzheimer's disease. *Proc. Natl. Acad. Sci. U. S. A.* 10.1073/pnas.2009680117
207. Ising, C., Venegas, C., Zhang, S., Scheiblich, H., Schmidt, S. V., Vieira-Saecker, A., Schwartz, S., Albasset, S., McManus, R. M., Tejera, D., Griep, A., Santarelli, F., Brosseron, F., Opitz, S., Stunden, J., Merten, M., Kayed, R., Golenbock, D. T., Blum, D., Latz, E., Buée, L., and Heneka, M. T. (2019) NLRP3 inflammasome activation drives tau pathology. *Nature*. 10.1038/s41586-019-1769-z
208. Stancu, I. C., Cremers, N., Vanrusselt, H., Couturier, J., Vanoosthuyse, A., Kessels, S., Lodder, C., Brône, B., Huaux, F., Octave, J. N., Terwel, D., and Dewachter, I. (2019) Aggregated Tau activates NLRP3–ASC inflammasome exacerbating exogenously seeded and non-exogenously seeded Tau pathology in vivo. *Acta Neuropathol.* 10.1007/s00401-018-01957-y
209. Gordon, R., Albornoz, E. A., Christie, D. C., Langley, M. R., Kumar, V., Mantovani, S., Robertson, A. A. B., Butler, M. S., Rowe, D. B., O'Neill, L. A., Kanthasamy, A. G., Schroder, K., Cooper, M. A., and Woodruff, T. M. (2018) Inflammasome inhibition prevents -synuclein pathology and dopaminergic neurodegeneration in mice. *Sci. Transl. Med.* 10.1126/scitranslmed.aah4066
210. Gustot, A., Gallea, J. I., Sarroukh, R., Celej, M. S., Ruysschaert, J. M., and Raussens, V. (2015) Amyloid fibrils are the molecular trigger of inflammation in Parkinson's disease. *Biochem. J.* 10.1042/BJ20150617
211. Mogi, M., Harada, M., Kondo, T., Riederer, P., Inagaki, H., Minami, M., and Nagatsu, T. (1994) Interleukin-1β, interleukin-6, epidermal growth factor and transforming growth factor-α are elevated in the brain from parkinsonian patients. *Neurosci. Lett.* 10.1016/0304-3940(94)90508-8
212. von Herrmann, K. M., Salas, L. A., Martinez, E. M., Young, A. L., Howard, J. M., Feldman, M. S., Christensen, B. C., Wilkins, O. M., Lee, S. L., Hickey, W. F., and Havrda, M. C. (2018) NLRP3 expression in mesencephalic neurons and characterization of a rare NLRP3 polymorphism associated with decreased risk of Parkinson's disease. *npj Park. Dis.* 10.1038/s41531-018-0061-5
213. Barrett, P. J., and Timothy Greenamyre, J. (2015) Post-translational modification of α-synuclein in Parkinson's disease. *Brain Res.* 10.1016/j.brainres.2015.06.002
214. Chamorro, Á., Meisel, A., Planas, A. M., Urra, X., Van De Beek, D., and Veltkamp, R. (2012) The immunology of acute stroke. *Nat. Rev. Neurol.* 10.1038/nrneurol.2012.98
215. Sobowale, O. A., Parry-Jones, A. R., Smith, C. J., Tyrrell, P. J., Rothwell, N. J., and Allan, S. M. (2016) Interleukin-1 in Stroke: From Bench to Bedside. *Stroke*. 10.1161/STROKEAHA.115.010001
216. Relton, J. K., and Rothwell, N. J. (1992) Interleukin-1 receptor antagonist inhibits ischaemic and excitotoxic neuronal damage in the rat. *Brain Res. Bull.* 10.1016/0361-9230(92)90033-T
217. Garcia, J. H., Liu, K. F., and Relton, J. K. (1995) Interleukin-1 receptor antagonist decreases the number of necrotic neurons in rats with middle cerebral artery occlusion. *Am. J. Pathol.*

218. Yamasaki, Y., Matsuura, N., Shozuhara, H., Onodera, H., Itoyama, Y., and Kogure, K. (1995) Interleukin-1 as a pathogenetic mediator of ischemic brain damage in rats. *Stroke*. 10.1161/01.str.26.4.676
219. Boutin, H., LeFeuvre, R. A., Horai, R., Asano, M., Iwakura, Y., and Rothwell, N. J. (2001) Role of IL-1alpha and IL-1beta in ischemic brain damage. *J. Neurosci.*
220. Ohtaki, H., Funahashi, H., Dohi, K., Oguro, T., Horai, R., Asano, M., Iwakura, Y., Yin, L., Matsunaga, M., Goto, N., and Shioda, S. (2003) Suppression of oxidative neuronal damage after transient middle cerebral artery occlusion in mice lacking interleukin-1. *Neurosci. Res.* 10.1016/S0168-0102(02)00238-9
221. Barrington, J., Lemarchand, E., and Allan, S. M. (2017) A brain in flame; do inflammasomes and pyroptosis influence stroke pathology? *Brain Pathol.* 10.1111/bpa.12476
222. Yang, F., Wang, Z., Wei, X., Han, H., Meng, X., Zhang, Y., Shi, W., Li, F., Xin, T., Pang, Q., and Yi, F. (2014) NLRP3 deficiency ameliorates neurovascular damage in experimental ischemic stroke. *J. Cereb. Blood Flow Metab.* 10.1038/jcbfm.2013.242
223. Yang-Wei Fann, D., Lee, S. Y., Manzanero, S., Tang, S. C., Gelderblom, M., Chunduri, P., Bernreuther, C., Glatzel, M., Cheng, Y. L., Thundyil, J., Widiapradja, A., Lok, K. Z., Foo, S. L., Wang, Y. C., Li, Y. I., Drummond, G. R., Basta, M., Magnus, T., Jo, D. G., Mattson, M. P., Sobey, C. G., and Arumugam, T. V. (2013) Intravenous immunoglobulin suppresses NLRP1 and NLRP3 inflammasome-mediated neuronal death in ischemic stroke. *Cell Death Dis.* 10.1038/cddis.2013.326
224. Ismael, S., Zhao, L., Nasoohi, S., and Ishrat, T. (2018) Inhibition of the NLRP3-inflammasome as a potential approach for neuroprotection after stroke. *Sci. Rep.* 10.1038/s41598-018-24350-x
225. McColl, B. W., Allan, S. M., and Rothwell, N. J. (2009) Systemic infection, inflammation and acute ischemic stroke. *Neuroscience*. 10.1016/j.neuroscience.2008.08.019
226. Denes, A., Coutts, G., Lénárt, N., Cruickshank, S. M., Pelegrin, P., Skinner, J., Rothwell, N., Allan, S. M., and Brough, D. (2015) AIM2 and NLRC4 inflammasomes contribute with ASC to acute brain injury independently of NLRP3. *Proc. Natl. Acad. Sci. U. S. A.* 10.1073/pnas.1419090112
227. Lemarchand, E., Barrington, J., Chenery, A., Haley, M., Coutts, G., Allen, J. E., Allan, S. M., and Brough, D. (2019) Extent of Ischemic Brain Injury After Thrombotic Stroke Is Independent of the NLRP3 (NACHT, LRR and PYD Domains-Containing Protein 3) Inflammasome. *Stroke*. 10.1161/STROKEAHA.118.023620
228. Grebe, A., Hoss, F., and Latz, E. (2018) NLRP3 inflammasome and the IL-1 pathway in atherosclerosis. *Circ. Res.* 10.1161/CIRCRESAHA.118.311362
229. Ridker, P. M., MacFadyen, J. G., Thuren, T., Everett, B., Libby, P., Glynn, R., Ridker, P., Lorenzatti, A., Krum, H., Varigos, J., Siostrzonek, P., Sinnaeve, P., Fonseca, F., Nicolau, J., Gotcheva, N., Genest, J., Yong, H., Urina-Triana, M., Milicic, D., Cifkova, R., Vettus, R., Koenig, W., Anker, S. D., Manolis, A. J., Wyss, F., Forster, T., Sigurdsson, A., Pais, P., Fucili, A., Ogawa, H., Shimokawa, H., Veze, I., Petrauskiene, B., Salvador, L., Kastelein, J., Cornel, J. H., Klemsdal, T. O., Medina, F., Budaj, A., Vida-Simiti, L., Kobalava, Z., Otasevic, P., Pella, D., Lainscak, M., Seung, K. B.,

Commerford, P., Dellborg, M., Donath, M., Hwang, J. J., Kultursay, H., Flather, M., Ballantyne, C., Bilazarian, S., Chang, W., East, C., Forgosh, L., Harris, B., Ligueros, M., Bohula, E., Charmarthi, B., Cheng, S., Chou, S., Danik, J., McMahon, G., Maron, B., Ning, M. M., Olenchock, B., Pande, R., Perlstein, T., Pradhan, A., Rost, N., Singhal, A., Taqueti, V., Wei, N., Burris, H., Cioffi, A., Dalseg, A. M., Ghosh, N., Gralow, J., Mayer, T., Rugo, H., Fowler, V., Limaye, A. P., Cosgrove, S., Levine, D., Lopes, R., Scott, J., Hilkert, R., Tamesby, G., Mickel, C., Manning, B., Woelcke, J., Tan, M., Manfreda, S., Ponce, T., Kam, J., Saini, R., Banker, K., Salko, T., Nandy, P., Tawfik, R., O'Neil, G., Manne, S., Jirvankar, P., Lal, S., Nema, D., Jose, J., Collins, R., Bailey, K., Blumenthal, R., Colhoun, H., and Gersh, B. (2017) Effect of interleukin-1β inhibition with canakinumab on incident lung cancer in patients with atherosclerosis: exploratory results from a randomised, double-blind, placebo-controlled trial. *Lancet*. 10.1016/S0140-6736(17)32247-X

230. Perregaux, D. G., Mcniff, P., Laliberte, R., Hawryluk, N., Peurano, H., Stam, E., Eggler, J., Griffiths, R., Dombroski, M. A., and Gabel, C. A. (2001) Identification and characterization of a novel class of interleukin-1 post-translational processing inhibitors. *J. Pharmacol. Exp. Ther.*
231. Van Der Heijden, T., Kritikou, E., Venema, W., Van Duijn, J., Van Santbrink, P. J., Slütter, B., Foks, A. C., Bot, I., and Kuiper, J. (2017) NLRP3 Inflammasome Inhibition by MCC950 Reduces Atherosclerotic Lesion Development in Apolipoprotein E-Deficient Mice - Brief Report. *Arterioscler. Thromb. Vasc. Biol.* 10.1161/ATVBAHA.117.309575
232. Perregaux, D. G., Svensson, L., and Gabel, C. A. (1996) Tenidap and other anion transport inhibitors disrupt cytolytic T lymphocyte-mediated IL-1β post-translational processing. *J. Immunol.*
233. Hamon, Y., Luciani, M. F., Becq, F., Verrier, B., Rubartelli, A., and Chimini, G. (1997) Interleukin-1β secretion is impaired by inhibitors of the Atp binding cassette transporter, ABC1. *Blood*. 10.1182/blood.v90.8.2911
234. Lamkanfi, M., Mueller, J. L., Vitari, A. C., Misaghi, S., Fedorova, A., Deshayes, K., Lee, W. P., Hoffman, H. M., and Dixit, V. M. (2009) Glyburide inhibits the Cryopyrin/Nalp3 inflammasome. *J. Cell Biol.* 10.1083/jcb.200903124
235. Youm, Y. H., Nguyen, K. Y., Grant, R. W., Goldberg, E. L., Bodogai, M., Kim, D., D'Agostino, D., Planavsky, N., Lupfer, C., Kanneganti, T. D., Kang, S., Horvath, T. L., Fahmy, T. M., Crawford, P. A., Biragyn, A., Alnemri, E., and Dixit, V. D. (2015) The ketone metabolite β-hydroxybutyrate blocks NLRP3 inflammasome-mediated inflammatory disease. *Nat. Med.* 10.1038/nm.3804
236. Jiang, H., He, H., Chen, Y., Huang, W., Cheng, J., Ye, J., Wang, A., Tao, J., Wang, C., Liu, Q., Jin, T., Jiang, W., Deng, X., and Zhou, R. (2017) Identification of a selective and direct NLRP3 inhibitor to treat inflammatory disorders. *J. Exp. Med.* 10.1084/jem.20171419
237. Baldwin, A. G., Rivers-Auty, J., Daniels, M. J. D., White, C. S., Schwalbe, C. H., Schilling, T., Hammadi, H., Jaiyong, P., Spencer, N. G., England, H., Luheshi, N. M., Kadirvel, M., Lawrence, C. B., Rothwell, N. J., Harte, M. K., Bryce, R. A., Allan, S. M., Eder, C., Freeman, S., and Brough, D. (2017) Boron-Based Inhibitors of the NLRP3 Inflammasome. *Cell Chem. Biol.* 10.1016/j.chembiol.2017.08.011

238. Guo, C., Fulp, J. W., Jiang, Y., Li, X., Chojnacki, J. E., Wu, J., Wang, X. Y., and Zhang, S. (2017) Development and Characterization of a Hydroxyl-Sulfonamide Analogue, 5-Chloro-N-[2-(4-hydroxysulfamoyl-phenyl)-ethyl]-2-methoxy-benzamide, as a Novel NLRP3 Inflammasome Inhibitor for Potential Treatment of Multiple Sclerosis. *ACS Chem. Neurosci.* 10.1021/acschemneuro.7b00124
239. He, Y., Varadarajan, S., Muñoz-Planillo, R., Burberry, A., Nakamura, Y., and Núñez, G. (2014) 3,4-Methylenedioxy-β'-nitrostyrene inhibits NLRP3 inflammasome activation by blocking assembly of the inflammasome. *J. Biol. Chem.* 10.1074/jbc.M113.515080
240. Marchetti, C., Swartzwelter, B., Gamboni, F., Neff, C. P., Richter, K., Azam, T., Carta, S., Tengesdal, I., Nemkov, T., D'Alessandro, A., Henry, C., Jones, G. S., Goodrich, S. A., St. Laurent, J. P., Jones, T. M., Scribner, C. L., Barrow, R. B., Altman, R. D., Skouras, D. B., Gattorno, M., Grau, V., Janciauskiene, S., Rubartelli, A., Joosten, L. A. B., and Dinarello, C. A. (2018) OLT1177, a β-sulfonyl nitrile compound, safe in humans, inhibits the NLRP3 inflammasome and reverses the metabolic cost of inflammation. *Proc. Natl. Acad. Sci. U. S. A.* 10.1073/pnas.1716095115
241. Brown, S. D. M., and Moore, M. W. (2012) The International Mouse Phenotyping Consortium: Past and future perspectives on mouse phenotyping. *Mamm. Genome*. 10.1007/s00335-012-9427-x
242. Bradley, A., Anastassiadis, K., Ayadi, A., Battey, J. F., Bell, C., Birling, M. C., Bottomley, J., Brown, S. D., Bürger, A., Bult, C. J., Bushell, W., Collins, F. S., Desaintes, C., Doe, B., Aris, E., Eppig, J. T., Finnell, R. H., Fletcher, C., Fray, M., Frendewey, D., Friedel, R. H., Grosveld, F. G., Hansen, J., Hérault, Y., Hicks, G., Hörlein, A., Houghton, R., Hrabé De Angelis, M., Huylebroeck, D., Iyer, V., De Jong, P. J., Kadin, J. A., Kaloff, C., Kennedy, K., Koutsourakis, M., Kent Lloyd, K. C., Marschall, S., Mason, J., McKerlie, C., McLeod, M. P., Von Melchner, H., Moore, M., Mujica, A. O., Nagy, A., Nefedov, M., Nutter, L. M., Pavlovic, G., Peterson, J. L., Pollock, J., Ramirez-Solis, R., Rancourt, D. E., Raspa, M., Remacle, J. E., Ringwald, M., Rosen, B., Rosenthal, N., Rossant, J., Ruiz Noppinger, P., Ryder, E., Schick, J. Z., Schnütgen, F., Schofield, P., Seisenberger, C., Selloum, M., Simpson, E. M., Skarnes, W. C., Smedley, D., Stanford, W. L., Francis Stewart, A., Stone, K., Swan, K., Tadepally, H., Teboul, L., Tocchini-Valentini, G. P., Valenzuela, D., West, A. P., Yamamura, K. I., Yoshinaga, Y., and Wurst, W. (2012) The mammalian gene function resource: The International Knockout Mouse Consortium. *Mamm. Genome*. 10.1007/s00335-012-9422-2
243. Pettitt, S. J., Liang, Q., Rairdan, X. Y., Moran, J. L., Prosser, H. M., Beier, D. R., Lloyd, K. C., Bradley, A., and Skarnes, W. C. (2009) Agouti C57BL/6N embryonic stem cells for mouse genetic resources. *Nat. Methods*. 10.1038/nmeth.1342
244. Hoyle, C., Redondo-Castro, E., Cook, J., Tzeng, T. C., Allan, S. M., Brough, D., and Lemarchand, E. (2020) Hallmarks of NLRP3 inflammasome activation are observed in organotypic hippocampal slice culture. *Immunology*. 10.1111/imm.13221
245. RAT, P., OLIVIER, E., TANTER, C., WAKX, A., and Dutot, M. (2017) A fast and reproducible cell- and 96-well plate-based method for the evaluation of P2X7 receptor activation using YO-PRO-1 fluorescent dye. *J. Biol. Methods*.

10.14440/jbm.2017.136
246. Hornung, V., Bauernfeind, F., Halle, A., Samstad, E. O., Kono, H., Rock, K. L., Fitzgerald, K. A., and Latz, E. (2008) Silica crystals and aluminum salts activate the NALP3 inflammasome through phagosomal destabilization. *Nat. Immunol.* 10.1038/ni.1631
247. Franchi, L., Kanneganti, T. D., Dubyak, G. R., and Núñez, G. (2007) Differential requirement of P2X7 receptor and intracellular K+ for caspase-1 activation induced by intracellular and extracellular bacteria. *J. Biol. Chem.* 10.1074/jbc.M610762200
248. Meuth, S. G., Bittner, S., Meuth, P., Simon, O. J., Budde, T., and Wiendl, H. (2008) TWIK-related acid-sensitive K+ channel 1 (TASK1) and TASK3 critically influence T lymphocyte effector functions. *J. Biol. Chem.* 10.1074/jbc.M800637200
249. Bittner, S., Bobak, N., Herrmann, A. M., Göbel, K., Meuth, P., Höhn, K. G., Stenner, M. P., Budde, T., Wiendl, H., and Meuth, S. G. (2010) Upregulation of K2P5.1 potassium channels in multiple sclerosis. *Ann. Neurol.* 10.1002/ana.22010
250. Bobak, N., Bittner, S., Andronic, J., Hartmann, S., Mühlpfordt, F., Schneider-Hohendorf, T., Wolf, K., Schmelter, C., Göbel, K., Meuth, P., Zimmermann, H., Döring, F., Wischmeyer, E., Budde, T., Wiendl, H., Meuth, S. G., and Sukhorukov, V. L. (2011) Volume regulation of murine T lymphocytes relies on voltage-dependent and two-pore domain potassium channels. *Biochim. Biophys. Acta - Biomembr.* 10.1016/j.bbamem.2011.04.013
251. Hoyle, C., Rivers-Auty, J., Lemarchand, E., Vranic, S., Wang, E., Buggio, M., Rothwell, N. J., Allan, S. M., Kostarelos, K., and Brough, D. (2018) Small, Thin Graphene Oxide Is Anti-inflammatory Activating Nuclear Factor Erythroid 2-Related Factor 2 via Metabolic Reprogramming. *ACS Nano*. 10.1021/acsnano.8b03642
252. Coll, R. C., Robertson, A. A. B., Chae, J. J., Higgins, S. C., Muñoz-, R., Inserra, M. C., Vetter, I., Dungan, L. S., Monks, B. G., Croker, D. E., Butler, M. S., Haneklaus, M., Sutton, C. E., Latz, E., Kastner, D. L., Mills, K. H. G., Masters, S. L., Cooper, M. A., and Neill, L. A. J. O. (2015) A small molecule inhibitior of the NLRP3 inflammasome is a potential therapeutic for inflammatory diseases. *Nat. Med.*
253. Schaarschmidt, G., Wegner, F., Schwarz, S. C., Schmidt, H., and Schwarz, J. (2009) Characterization of voltage-gated potassium channels in human neural progenitor cells. *PLoS One*. 10.1371/journal.pone.0006168
254. Roy, J. W., Cowley, E. A., Blay, J., and Linsdell, P. (2010) The intermediate conductance Ca 2+-activated K + channel inhibitor TRAM-34 stimulates proliferation of breast cancer cells via activation of oestrogen receptors. *Br. J. Pharmacol.* 10.1111/j.1476-5381.2009.00557.x
255. Nguyen, H. M., Grössinger, E. M., Horiuchi, M., Davis, K. W., Jin, L. W., Maezawa, I., and Wulff, H. (2017) Differential Kv1.3, KCa3.1, and Kir2.1 expression in “classically” and “alternatively” activated microglia. *Glia*. 10.1002/glia.23078
256. Schmalhofer, W. A., Ratliff, K. S., Weinglass, A. B., Kaczorowski, G. J., Garcia, M. L., and Herrington, J. (2009) A KV2.1 gating modifier binding assay suitable for highthroughput screening. *Channels*. 10.4161/chan.3.6.10201
257. Schmitz, A. (2005) Design of PAP-1, a Selective Small Molecule Kv1.3

Blocker, for the Suppression of Effector Memory T Cells in Autoimmune Diseases. *Mol. Pharmacol.* 10.1124/mol.105.015669
258. Paul, A. A., Leishman, D. J., Witchel, H. J., and Hancox, J. C. (2001) Effects of the Class III antiarrhythmic agent dofetilide (UK-68,798) on L-type calcium current from rabbit ventricular myocytes. *J. Pharm. Pharmacol.* 10.1211/0022357011778061
259. Piechotta, P. L., Rapedius, M., Stansfeld, P. J., Bollepalli, M. K., Erhlich, G., Andres-Enguix, I., Fritzenschaft, H., Decher, N., Sansom, M. S. P., Tucker, S. J., and Baukrowitz, T. (2011) The pore structure and gating mechanism of K2P channels. *EMBO J.* 10.1038/emboj.2011.268
260. Schroder, K., and Tschopp, J. (2010) The Inflammasomes. *Cell*. 10.1016/j.cell.2010.01.040
261. Fernandes-Alnemri, T., Yu, J. W., Datta, P., Wu, J., and Alnemri, E. S. (2009) AIM2 activates the inflammasome and cell death in response to cytoplasmic DNA. *Nature*. 10.1038/nature07710
262. Bauernfeind, F., Horvath, G., Stutz, A., Alnemri, E. S., Speert, D., Fernandes-alnemri, T., Wu, J., Brian, G., Fitzgerald, K. A., Hornung, V., and Latz, E. (2010) NF-kB activating pattern recognition and cytokine receptors license NLRP3 inflammasome activation by regulating NLRP3 expression. *J. Immunol.* 10.4049/jimmunol.0901363.NF-kB
263. Liu, T., Zhang, L., Joo, D., and Sun, S. C. (2017) NF-κB signaling in inflammation. *Signal Transduct. Target. Ther.* 10.1038/sigtrans.2017.23
264. Franklin, B. S., Bossaller, L., De Nardo, D., Ratter, J. M., Stutz, A., Engels, G., Brenker, C., Nordhoff, M., Mirandola, S. R., Al-Amoudi, A., Mangan, M. S., Zimmer, S., Monks, B. G., Fricke, M., Schmidt, R. E., Espevik, T., Jones, B., Jarnicki, A. G., Hansbro, P. M., Busto, P., Marshak-Rothstein, A., Hornemann, S., Aguzzi, A., Kastenmüller, W., and Latz, E. (2014) The adaptor ASC has extracellular and “prionoid” activities that propagate inflammation. *Nat. Immunol.* 10.1038/ni.2913
265. Schell, J. B., Crane, C. A., Smith, M. F., and Roberts, M. R. (2007) Differential ex vivo nitric oxide production by acutely isolated neonatal and adult microglia. *J. Neuroimmunol.* 10.1016/j.jneuroim.2007.07.004
266. Brannan, C. A., and Roberts, M. R. (2004) Resident microglia from adult mice are refractory to nitric oxide-inducing stimuli due to impaired NOS2 gene expression. *Glia*. 10.1002/glia.20066
267. Humphries, E. S. A., and Dart, C. (2015) Neuronal and cardiovascular potassium channels as therapeutic drug targets: Promise and pitfalls. *J. Biomol. Screen.* 10.1177/1087057115601677
268. Akopova, O. V (2017) Direct and Off-Target Effects of ATP-Sensitive Potassium Channels Opener Diazoxide. *J. Drug Metab. Toxicol.* 10.4172/2157-7609.1000227
269. Kravenska, Y., Checchetto, V., and Szabo, I. (2021) Routes for potassium ions across mitochondrial membranes: A biophysical point of view with special focus on the atp-sensitive k+ channel. *Biomolecules*. 10.3390/biom11081172
270. Martín-Sánchez, F., Compan, V., Tapia-Abellán, A., Gómez-Sánchez, A. I., Baños, M. C., Schmidt, F. I., and Pelegrín, P. (2020) ASC oligomer favor caspase-1CARD domain recruitment after intracellular potassium efflux. *bioRxiv*. 10.1101/2020.01.27.921239
271. Lotshaw, D. P. (2007) Biophysical, pharmacological, and functional

characteristics of cloned and native mammalian two-pore domain K+ channels. *Cell Biochem. Biophys.* 10.1007/s12013-007-0007-8

272. Hari, A., Zhang, Y., Tu, Z., Detampel, P., Stenner, M., Ganguly, A., and Shi, Y. (2014) Activation of NLRP3 inflammasome by crystalline structures via cell surface contact. *Sci. Rep.* 10.1038/srep07281
273. Groß, C. J., Mishra, R., Schneider, K. S., Médard, G., Wettmarshausen, J., Dittlein, D. C., Shi, H., Gorka, O., Koenig, P. A., Fromm, S., Magnani, G., Ćiković, T., Hartjes, L., Smollich, J., Robertson, A. A. B., Cooper, M. A., Schmidt-Supprian, M., Schuster, M., Schroder, K., Broz, P., Traidl-Hoffmann, C., Beutler, B., Kuster, B., Ruland, J., Schneider, S., Perocchi, F., and Groß, O. (2016) K+ Efflux-Independent NLRP3 Inflammasome Activation by Small Molecules Targeting Mitochondria. *Immunity*. 10.1016/j.immuni.2016.08.010
274. Daniels, M. J. D., Rivers-Auty, J., Schilling, T., Spencer, N. G., Watremez, W., Fasolino, V., Booth, S. J., White, C. S., Baldwin, A. G., Freeman, S., Wong, R., Latta, C., Yu, S., Jackson, J., Fischer, N., Koziel, V., Pillot, T., Bagnall, J., Allan, S. M., Paszek, P., Galea, J., Harte, M. K., Eder, C., Lawrence, C. B., and Brough, D. (2016) Fenamate NSAIDs inhibit the NLRP3 inflammasome and protect against Alzheimer's disease in rodent models. *Nat. Commun.* 10.1038/ncomms12504
275. Ianevski, A., Giri, A. K., and Aittokallio, T. (2021) SynergyFinder 2.0: Visual analytics of multi-drug combination synergies. *Nucleic Acids Res.* 10.1093/NAR/GKAA216
276. Ben-David, U., Siranosian, B., Ha, G., Tang, H., Oren, Y., Hinohara, K., Strathdee, C. A., Dempster, J., Lyons, N. J., Burns, R., Nag, A., Kugener, G., Cimini, B., Tsvetkov, P., Maruvka, Y. E., O'Rourke, R., Garrity, A., Tubelli, A. A., Bandopadhayay, P., Tsherniak, A., Vazquez, F., Wong, B., Birger, C., Ghandi, M., Thorner, A. R., Bittker, J. A., Meyerson, M., Getz, G., Beroukhim, R., and Golub, T. R. (2018) Genetic and transcriptional evolution alters cancer cell line drug response. *Nature*. 10.1038/s41586-018-0409-3
277. Anighoro, A., Bajorath, J., and Rastelli, G. (2014) Polypharmacology: Challenges and opportunities in drug discovery. *J. Med. Chem.* 10.1021/jm5006463
278. Gombault, A., Baron, L., and Couillin, I. (2012) ATP release and purinergic signaling in NLRP3 inflammasome activation. *Front. Immunol.* 10.3389/fimmu.2012.00414
279. Steinberg, T. H., Newman, A. S., Swanson, J. A., and Silverstein, S. C. (1987) ATP4- permeabilizes the plasma membrane of mouse macrophages to fluorescent dyes. *J. Biol. Chem.* 10.1016/s0021-9258(18)47497-2
280. Rassendren, F., Buell, G. N., Virginio, C., Collo, G., North, R. A., and Surprenant, A. (1997) The permeabilizing ATP receptor, P2X7. Cloning and expression of a human cDNA. *J. Biol. Chem.* 10.1074/jbc.272.9.5482
281. Hanslik, K. L., and Ulland, T. K. (2020) The Role of Microglia and the Nlrp3 Inflammasome in Alzheimer's Disease. *Front. Neurol.* 10.3389/fneur.2020.570711
282. Zhang, X., Zhu, C., Beecham, G., Vardarajan, B. N., Ma, Y., Lancour, D., Farrell, J. J., Chung, J., Bellair, M., Dinh, H., Doddapeneni, H., Dugan-Perez, S., English, A., Gibbs, R. A., Han, Y., Hu, J., Jayaseelan, J., Kalra, D., Khan, Z., Korchina, V., Lee, S., Liu, Y., Liu, X., Muzny, D., Nasser, W., Salerno, W., Santibanez, J., Skinner, E., White, S., Worley, K., Zhu, Y.,

Beiser, A., Chen, Y., Cupples, L. A., DeStefano, A., Dupuis, J., Farrell, J., Farrer, L., Lin, H., Liu, C. T., Lunetta, K., Patel, D., Sarnowski, C., Satizabal, C., Seshadri, S., Sun, F. J., Choi, S. H., Banks, E., Gabriel, S., Gupta, N., Bush, W., Butkiewicz, M., Haines, J., Smieszek, S., Song, Y., Barral, S., De Jager, P. L., Mayeux, R., Reitz, C., Reyes, D., Tosto, G., Vardarajan, B., Amad, S., Amin, N., Ikram, M. A., van der Lee, S., van Duijn, C., Vanderspek, A., Schmidt, H., Schmidt, R., Goate, A., Kapoor, M., Marcora, E., Renton, A., Faber, K., Foroud, T., Feolo, M., Stine, A., Launer, L. J., Bennett, D. A., Xia, L. C., Hamilton-Nelson, K., Jaworski, J., Kunkle, B., Martin, E., Pericak-Vance, M., Rajabli, F., Schmidt, M., Mosley, T. H., Cantwell, L., Childress, M., Chou, Y. F., Cweibel, R., Gangadharan, P., Kuzma, A., Leung, Y. Y., Lin, H. J., Malamon, J., Mlynarski, E., Naj, A., Qu, L., Schellenberg, G., Valladares, O., Wang, L. S., Wang, W., Zhang, N., Below, J. E., Boerwinkle, E., Bressler, J., Fornage, M., Jian, X., Liu, X., Bis, J. C., Blue, E., Brown, L., Day, T., Dorschner, M., Horimoto, A. R., Nafikov, R., Nato, A. Q., Navas, P., Nguyen, H., Psaty, B., Rice, K., Saad, M., Sohi, H., Thornton, T., Tsuang, D., Wang, B., Wijsman, E., Witten, D., Antonacci-Fulton, L., Appelbaum, E., Cruchaga, C., Fulton, R. S., Koboldt, D. C., Larson, D. E., Waligorski, J., Wilson, R. K., Schellenberg, G. D., Pericak-Vance, M. A., Lunetta, K. L., and Farrer, L. A. (2019) A rare missense variant of CASP7 is associated with familial late-onset Alzheimer's disease. *Alzheimer's Dement.* 10.1016/j.jalz.2018.10.005

283. Hafner-Bratkovič, I., and Pelegrín, P. (2018) Ion homeostasis and ion channels in NLRP3 inflammasome activation and regulation. *Curr. Opin. Immunol.* 10.1016/j.coi.2018.03.010
284. Pelegrín, P. (2011) Many ways to dilate the P2X7 receptor pore. *Br. J. Pharmacol.* 10.1111/j.1476-5381.2011.01325.x
285. Marques-Da-Silva, C., Chaves, M. M., Castro, N. G., Coutinho-Silva, R., and Guimaraes, M. Z. P. (2011) Colchicine inhibits cationic dye uptake induced by ATP in P2X2 and P2X7 receptor-expressing cells: Implications for its therapeutic action. *Br. J. Pharmacol.* 10.1111/j.1476-5381.2011.01254.x
286. Cankurtaran-Sayar, S., Sayar, K., and Ugur, M. (2009) P2X7 receptor activates multiple selective dye-permeation pathways in RAW 264.7 and human embryonic kidney 293 cells. *Mol. Pharmacol.* 10.1124/mol.109.059923
287. Schachter, J., Motta, A. P., Zamorano, A. de S., da Silva-Souza, H. A., Guimarães, M. Z. P., and Persechini, P. M. (2008) ATP-induced P2X7-associated uptake of large molecules involves distinct mechanisms for cations and anions in macrophages. *J. Cell Sci.* 10.1242/jcs.029991
288. Jiang, L. H., Rassendren, F., Mackenzie, A., Zhang, Y. H., Surprenant, A., and North, R. A. (2005) N-methyl-D-glucamine and propidium dyes utilize different permeation pathways at rat P2X7 receptors. *Am. J. Physiol. - Cell Physiol.* 10.1152/ajpcell.00253.2005
289. Ferrari, D., Villalba, M., Chiozzi, P., Falzoni, S., Ricciardi-Castagnoli, P., and Di Virgilio, F. (1996) Mouse microglial cells express a plasma membrane pore gated by extracellular ATP. *J. Immunol.*
290. Solle, M., Labasi, J., Perregaux, D. G., Stam, E., Petrushova, N., Koller, B. H., Griffiths, R. J., and Gabel, C. A. (2001) Altered cytokine production in mice lacking P2X7 receptors. *J. Biol. Chem.* 10.1074/jbc.M006781200
291. Suzuki, T., Kohyama, K., Moriyama, K., Ozaki, M., Hasegawa, S., Ueno, T.,

Saitoe, M., Morio, T., Hayashi, M., and Sakuma, H. (2020) Extracellular ADP augments microglial inflammasome and NF-κB activation via the P2Y12 receptor. *Eur. J. Immunol.* 10.1002/eji.201848013

292. Wang, Z., Zhang, S., Xiao, Y., Zhang, W., Wu, S., Qin, T., Yue, Y., Qian, W., and Li, L. (2020) NLRP3 Inflammasome and Inflammatory Diseases. *Oxid. Med. Cell. Longev.* 10.1155/2020/4063562
293. Zahid, A., Li, B., Kombe, A. J. K., Jin, T., and Tao, J. (2019) Pharmacological inhibitors of the nlrp3 inflammasome. *Front. Immunol.* 10.3389/fimmu.2019.02538
294. Dinarello, C. A., and van der Meer, J. W. M. (2013) Treating inflammation by blocking interleukin-1 in humans. *Semin. Immunol.* 10.1016/j.smim.2013.10.008
295. Wang, D., Wang, H., Gao, H., Zhang, H., Zhang, H., Wang, Q., and Sun, Z. (2020) P2X7 receptor mediates NLRP3 inflammasome activation in depression and diabetes. *Cell Biosci.* 10.1186/s13578-020-00388-1
296. Zhou, J., Zhou, Z., Liu, X., Yin, H. Y., Tang, Y., and Cao, X. (2021) P2X7 Receptor–Mediated Inflammation in Cardiovascular Disease. *Front. Pharmacol.* 10.3389/fphar.2021.654425
297. Ou, Z., Zhou, Y., Wang, L., Xue, L., Zheng, J., Chen, L., and Tong, Q. (2021) NLRP3 Inflammasome Inhibition Prevents α-Synuclein Pathology by Relieving Autophagy Dysfunction in Chronic MPTP–Treated NLRP3 Knockout Mice. *Mol. Neurobiol.* 10.1007/s12035-020-02198-5
298. Salliot, C., Dougados, M., and Gossec, L. (2009) Risk of serious infections during rituximab, abatacept and anakinra treatments for rheumatoid arthritis: Meta-analyses of randomised placebo-controlled trials. *Ann. Rheum. Dis.* 10.1136/ard.2007.083188
299. Kullenberg, T., Löfqvist, M., Leinonen, M., Goldbach-Mansky, R., and Olivecrona, H. (2016) Long-term safety profile of anakinra in patients with severe cryopyrin-associated periodic syndromes. *Rheumatol. (United Kingdom)*. 10.1093/rheumatology/kew208
300. Zhang, Y., Chen, K., Sloan, S. A., Bennett, M. L., Scholze, A. R., O'Keeffe, S., Phatnani, H. P., Guarnieri, P., Caneda, C., Ruderisch, N., Deng, S., Liddelow, S. A., Zhang, C., Daneman, R., Maniatis, T., Barres, B. A., and Wu, J. Q. (2014) An RNA-sequencing transcriptome and splicing database of glia, neurons, and vascular cells of the cerebral cortex. *J. Neurosci.* 10.1523/JNEUROSCI.1860-14.2014
301. Kametani, F., and Hasegawa, M. (2018) Reconsideration of amyloid hypothesis and tau hypothesis in Alzheimer's disease. *Front. Neurosci.* 10.3389/fnins.2018.00025
302. Kinney, J. W., Bemiller, S. M., Murtishaw, A. S., Leisgang, A. M., Salazar, A. M., and Lamb, B. T. (2018) Inflammation as a central mechanism in Alzheimer's disease. *Alzheimer's Dement. Transl. Res. Clin. Interv.* 10.1016/j.trci.2018.06.014
303. Forlenza, O. V., Diniz, B. S., Talib, L. L., Mendonça, V. A., Ojopi, E. B., Gattaz, W. F., and Teixeira, A. L. (2009) Increased serum IL-1beta level in Alzheimer's disease and mild cognitive impairment. *Dement. Geriatr. Cogn. Disord.* 10.1159/000255051